Universidad Michoacana de San Nicolás de Hidalgo

Facultad de Ingeniería Química
División de Estudios de Posgrado
Doctorado en Ciencias en Ingeniería Química
Línea de Ingeniería de Procesos Sustentables

Diseño Óptimo de Sistemas de Desalinización Integrados Térmicamente

TESIS DOCTORAL

Que para obtener el grado de Doctor en Ciencias en Ingeniería Química presenta:

M. C. Ramón González-Bravo

Asesor:

Dr. José María Ponce Ortega

Co – asesor:

Dr. Fabricio Nápoles Rivera

Morelia Michoacán, Agosto 2017

Universidad Michoacana de San Nicolás de Hidalgo

Faculty of Chemical Engineering
PhD in Chemical Engineering
PSE Process System Engineering

Optimal Design of Desalination Systems Thermally Coupled

PhD THESIS

Presented by:

M. C. Ramón González-Bravo

Advisor:

Dr. José María Ponce Ortega

j

Co – Advisor:

Dr. Fabricio Nápoles Rivera

Morelia Michoacán, August 2017

DEDICATORIA

A mi madre Rosalinda

Por haberme apoyado en todo momento, por sus valores, por la motivación constante que me ha permitido ser una persona de bien

A mi padre Ramón

Por los ejemplos de trabajo, perseverancia y constancia que lo caracterizan y que me ha enseñado siempre, por el valor mostrado para salir adelante

A mis hermanas Mary, Claudia y Gaby

Por estar conmigo y apoyarme siempre, las quiero mucho

AGRADECIMIENTOS

A la Universidad Michoacana de San Nicolás de Hidalgo, en especial a los profesores del Posgrado de Ingeniería Química por su tiempo compartido y por impulsar el desarrollo de mi formación profesional

A mi asesor el Dr. José María Ponce Ortega por creer en mí, por su persistente guía, su gran apoyo y motivación para la culminación de mis estudios y para la elaboración de esta tesis.

Un agradecimiento especial al Dr. Fabricio Nápoles Rivera por sus constantes aportes en la finalización de este trabajo.

A los miembros de la mesa el Dr. Agustín Jaime Castro Montoya, el Dr. Medardo Serna González y el Dr. Arturo Jiménez Gutiérrez por sus observaciones y comentarios positivos hacia el trabajo, así como el apoyo brindado y la disposición en la realización de este trabajo.

Al Consejo Nacional de Ciencia y Tecnología por el apoyo económico brindado a través del programa de becas.

Al Banco Mundial por el apoyo otorgado durante mi estancia de investigación en la Ciudad de College Station, Texas.

A mis amigos Ilse, Karla, Magda, Martha, Marce, Rosita, Abimael, Fabian, Juan, Martín y Ramón, por su compañía, tiempo, apoyo, consejos y sobre todo su gran y valiosa amistad.

Diseño Óptimo de Sistemas de Desalinización Integrados Térmicamente

Presentada por:

Ramón González-Bravo

Facultad de Ingeniería Química
División de Estudios de Posgrado
Doctorado en Ciencias en Ingeniería Química
Linea de Ingeniería de Procesos Sustentables

Resumen

El consumo de agua y energía ha aumentado considerablemente en las últimas décadas. La escasez de agua ha llevado a un aumento en la extracción de agua en acuíferos, ríos y lagos, esto ha generado serios problemas de sobreexplotación de los recursos hídricos. Además, el crecimiento de la población en las zonas urbanizadas, así como el aumento de las demandas de agua y energía en la industria, la agricultura y los hogares han intensificado este problema. Como consecuencia, hay varias regiones donde es casi imposible satisfacer las demandas de agua utilizando los recursos hídricos disponibles. En este contexto, estrategias alternativas como el tratamiento de aguas negras, la recolección de agua de lluvia y el uso potencial de agua desalinizada puede ser una opción. Sin embargo, procesos como la desalinización de agua de mar son altamente costosos, principalmente por el alto consumo de energético, en este sentido, la integración térmica involucrando los sistemas de desalinización de agua de mar aparece como una opción viable para la reducción de los costos de producción. En esta tesis de investigación se presentan tres estrategias de integración térmica enfocadas a la reducción de los costos de desalación, así como la integración a sistemas macroscópicos de distribución de agua de mar involucrando sistemas de desalinización acoplados a sistemas de producción de energía eléctrica. En los capítulos de esta tesis se presentan diversos modelos de optimización matemática desarrollados para evaluar la viabilidad económica, ambiental y social de las diferentes estrategias presentadas en este trabajo de investigación.

En el capítulo uno se presenta una visión general de los sistemas de desalinización más utilizados y su relación con las estrategias propuestas en este trabajo de investigación. El capítulo dos presenta un modelo sistemático para obtener la optimización simultanea de una unidad de desalinización TMD acoplada con las corrientes frías y calientes de un proceso existente, los resultados muestran que con la estrategia propuesta se logra reducir el costo unitario de agua desalinizada (USD$/m^3). La sección tres presenta la síntesis de una red de desalinización utilizando módulos individuales de desalinización por TMD, en esta metodología se utilizan estrategias de integración térmica y másica para reducir los costos totales anuales de producción. En el capítulo cuatro se presenta un modelo matemático para la elección óptima de un sistema de desalinización basado en los requerimientos de calentamiento y enfriamiento incorporando sistemas de recuperación de calor residual, los resultados muestran beneficios importantes en términos económicos y ambientales basados en las ventas de agua desalada y producción de energía eléctrica. Los capítulos cinco y seis presentan modelos de distribución, a nivel macroscópico, de agua y energía eléctrica considerando el acoplamiento de un sistema de desalinización con una planta de generación de energía eléctrica para satisfacer las demandas en el sector doméstico, agrícola e industrial, en ambos capítulos se consideran modelos multi-objetivo considerando el impacto económico, social y ambiental.

Palabras clave: Desalinización; Optimización; Manejo adecuado del agua; Integracion térmica.

Dirigido por:

Dr. José María Ponce Ortega

Dr. Fabricio Nápoles Rivera

Optimal Design of Desalination Systems Thermally Coupled

Presented by:

Ramón Gonzalez-Bravo

Faculty of Chemical Engineering
PhD in Chemical Engineering
PSE: Process System Engineering

Abstract

Water and energy consumption has increased substantially over the last decades. Water scarcity has led to an increase in the extraction of fresh water from aquifers, dams, and lakes, and it has produced serious overexploitation problems. Furthermore, the population growth in urbanized areas and the increase in water and energy demands in the industry, agriculture, and households have amplified this problem. As consequence, there are several regions where is almost impossible to satisfy the water demands using the available water resources. In this context, the use of alternative water resources such as reclaimed water, rainwater harvesting and the potential use of desalinated water can be an option. However, desalinated seawater is very expensive because the high energy consumption and this way to integrate a seawater desalination plant to a power plant to simultaneously produce clean water and power can be an attractive option.

This thesis presents three strategies of thermal integration focused on the reduction of desalination costs, as well as the integration of power-desalination plants into macroscopic water and power distribution networks. In the following chapters, a series of mathematical optimization models are presented in order to evaluate either economic, environmental or social viability. Chapter one presents an overview of the most used desalination systems and their relationship with the strategies proposed in this thesis. Chapter two presents a systematic optimization model to obtain the simultaneous optimization of a TMD desalination unit coupled with hot and cold process streams of an existing process, the results show that the proposed strategy can reduce the unitary water cost (USD$/m^3). Section three presents the synthesis of a seawater desalination network using individual TMD modules. In this approach, thermal and mass integration strategies are used in order to reduce the total annual

costs. In Chapter 4, a mathematical optimization model for the optimal selection of a desalination system based on heating and cooling requirements are presented incorporating waste heat recovery systems, the results show important economic and environmental benefits based on total annual sales. Chapters five and six present optimization approaches for water and power distribution networks into a macroscopic scheme, the optimization model considers power-desalination plants to satisfy water and power demands of domestic, agricultural and industrial users. In both chapters are considered multi-objective optimization models considering economic, social and environmental points of view.

Keywords: Desalination; Optimization; Water Resource Management; Heat Integration.

Directed by:

Dr. José María Ponce Ortega

Dr. Fabricio Nápoles Rivera

CONTENT

CHAPTER I

Introduction

This chapter provides a general overview of the main seawater desalination technologies and the endeavors proposed in this thesis to reduce energy consumption, incorporating optimization tools to increase system productivity.

1.1 Overview of water desalination systems

The accelerated population growth and the negative effects of the global warming have increased the global water and energy consumption. The increased water and energy consumption in industry, agriculture, and households have been intensified this issue.[1] This problem has been getting worse in certain regions where water availability is low, in which the extraction of fresh water from aquifers, dams, and lakes has carried to serious problems of overexploitation of groundwater and surface water resources. In this framework, water desalination has become one of the most important water sources in regions with high water stress worldwide. However, this process is very expensive due to high energy consumption. In addition to the depletion of non-renewable energy sources, the use of large quantities of fossil fuels has negative environmental implications.

Since conventional desalination technologies typically consume high levels of energy, it is important to incorporate heat integration techniques, renewable energy sources and to develop efficient desalination technologies. Nonetheless, cost and performance continue to be challenging issues.[2] In order to constantly improve the technologies and reduce the cost of desalination, extensive research and development activities have been carried out. **Figure 1.1** shows an overview of the main desalination process categories and the various technologies within each category. Desalination system is classified according to the energy source such as thermal, mechanical, electrical and chemical energy sources; also, desalination systems can be classified depending on the desalination process: evaporation-condensation, filtration and crystallization technique. Reverse osmosis (RO) followed by multi-stage flash (MSF) and multi-effect distillation (MED) systems are the most worldwide

implemented desalination technologies, emerging technologies such as membrane distillation and thermal vapor compression are gaining more attention and potential application. **Figure 1.2** shows the contribution of each desalination technology to the world water production. **Table 1.1** presents a summary of characteristics of major desalination technologies.[3]

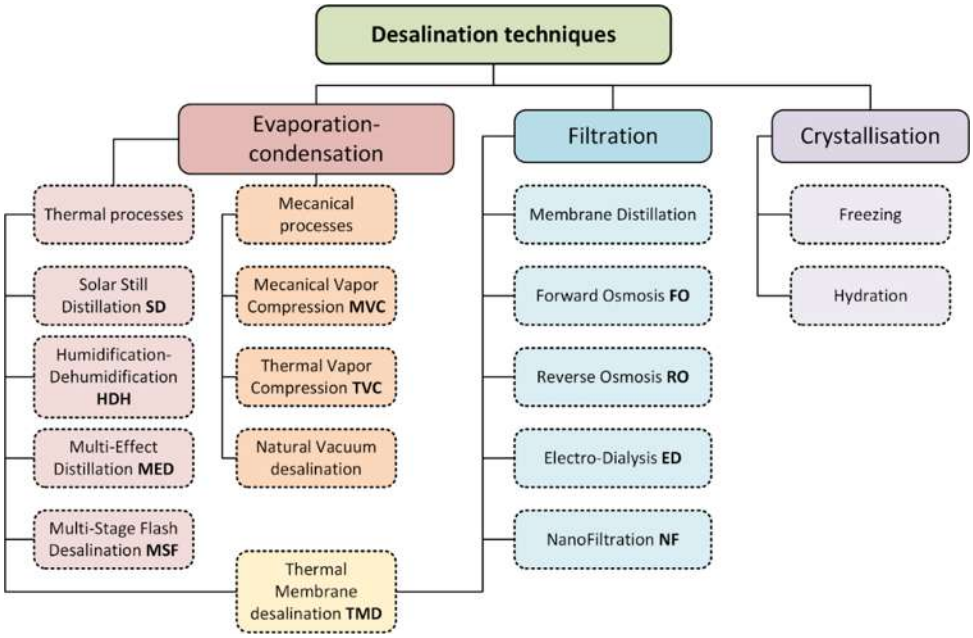

Figure 1.1 Overview of the main desalination technologies.[3]

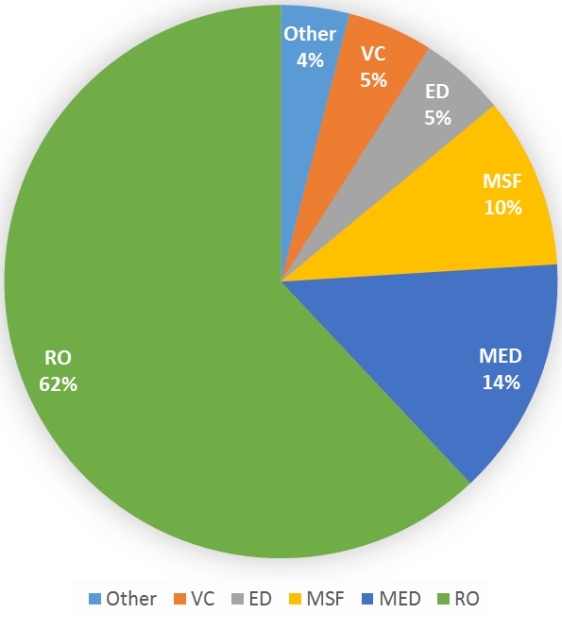

Figure 1.2. Global Use of Desalination Technologies.[3]

Table 1.1. Characteristics of Major Desalination Technologies (adapted with revision from Nicot et al., 2006).[4]

Technology Characteristics	**Reverse Osmosis (RO)**	**Electrodialysis Reversal (EDR)**	**Vapor Compression**	**Multistage Flash (MSF)**	**Multiple-Effect Distillation (MED)**	**Thermal Membrane Distillation**
Energy usage	Moderate	High	High (Moderate in the case of advanced vapor compression)	High	Very high	Moderate
Salinity Level of Feed Water	Broad range	Brackish	Broad range	Broad range	Broad range	Broad range
Configuration/Scale	Modular	Modular	Large	Large	Large	Modular
Bacterial contamination	Possible	Post-treatment always needed	Unlikely	Unlikely	Unlikely	Unlikely
Final product salinity	On demand	On demand	On demand	Can be <10 mg/L TDS	Can be <10 mg/L TDS	Low
Susceptibility to scaling	High	Low	Low	Low	Low	High
Water recovery	30-50% for seawater (up to 90% for brackish water)	High	High	Low (10-25%)	Low (but higher than MSF)	Medium

According to the International Desalination Association, nowadays there are more than 18,426 desalination plants around the world providing more than 86.8 million cubic meters per day, in which more than 300 million persons depend on the water produced by these plants.[3]

Water and energy are closely linked, energy production uses large amounts of water resources, and providing freshwater requires energy for pumping, treating and transporting water to the consumers.[5] In most of the power production plants, water is used as cooling utility (hydroelectric, nuclear and refining), because of that, many desalination plants around the world are coupled with power production plants, employing this form of cogeneration can significantly reduce desalinated water cost and investment and it has become the main model for existing large desalination projects. The integration of desalination with power plants presents mutual benefits such as higher energy efficiency, in some cases the energy improvement can be 10-20% or better, also, the greenhouse gas emissions are reduced significantly with the coupling of water desalination and power production, however, water

management, water, and energy distribution networks represent major challenges in power-desalination schemes.[6]

Furthermore, water desalination still requires major improvements in all aspects, in this way, this thesis is aimed at developing systematic optimization strategies and demonstrating proof of concepts for integrating desalination systems with the simultaneous consideration of energy and desalination issues. First, the chapter three includes energy and mass integration strategies to reduce water desalination cost, while chapters four and five present strategies of power desalination plants (dual purpose power plants) in a macroscopic water distribution network. On this basis, every chapter presents highly efficient approaches which provide answers to the desalination issues nowadays.

1.2 References

1. WWAP (World Water Assessment Programme), The United Nations World Water Development Report 2017: The untapped resource, Paris, France, UNESCO, 1, 2017.
2. Shahzad, M. W.; Burhan, M.; Ang, L.; Ng, K. C., Energy-water-environment nexus underpinning future desalination sustainability, *Desalination*, 2017, 413, 52-64.
3. Alkaisi, A., Mossad, R.; Sharifian-Barforoush, A., A review of the water desalination system integrated with renewable energy, *Energy Procedia*, 2017, 110, 268-274.
4. J. P. Nicot, S. Walden, L. Greenlee, and J. Els, A Desalination Database for Texas, the University of Texas at Austin, Bureau of Economic Geology, 2005.
5. WWAP (World Water Assessment Programme), UN-Water GLAAS 2017: Financing universal water, sanitation and hygiene under the Sustainable Development Goals, Paris, France, UNESCO, 2, 2012.
6. Averyt, K.; Fisher, J., Huber-Lee, A.; Lewis, A.; Macknick, J.; Madden, N.; Rogers, J.; Tellinghuisen, S., Freshwater use by U.S. power plants: Electricity's thirst for a precious resource. A report of the Energy and Water in a Warming World initiative, Cambridge, MA: Union of Concerned Scientists, November.

CHAPTER II

Optimal Design of Thermal Membrane Distillation Systems with Heat Integration with Process Plants

This chapter presents an optimization approach for the design of thermal membrane distillation (TMD) systems that are thermally coupled with processing facilities. A superstructure representation and an optimization formulation are introduced to obtain simultaneously the optimization of the TMD unit and a heat-exchange network (HEN) that integrates heating and cooling in the processing facility. The superstructure and associated optimization formulation seek to identify the system configuration along with design and operating variables such as heat-exchanger areas, membrane area, the extent of thermal coupling between the process and TMD, and the TMD feed-preheating temperature. The objective function maximizes the net annual profit which accounts for the revenues from the sales of purified water, the avoided cost of the treated wastewater, and the total annualized costs accounting for the capital investment of the added heat transfer units and the TMD network, the operating costs for the heating and cooling utilities and the operating expenses for the TMD system. The proposed optimization formulation is applied to a case study where a TMD system is integrated with a methanol plant and the results show significant economic benefits for the implementation of the proposed methodology.

2.1 Introduction

The limited supplies of fresh water coupled with the overexploitation of the available fresh water bodies represent major challenges for the sustainable development and call for cost-effective strategies for water management.[1] There are several regions around the world where desalination is the main source of freshwater.[2] Treatment and recycle/reuse of industrial wastewater can also play a key role in managing water resources. There are several technologies for the industrial wastewater treatment and seawater desalination. **Figure 2.1** shows common categories and technologies. Thermal processes include vapor compression, multistage flash, multi-effect distillation, humidification/dehumidification, and freeze concentration.[3] Membrane systems include reverse osmosis,[4] ultrafiltration,[5] and pervaporation.[6]

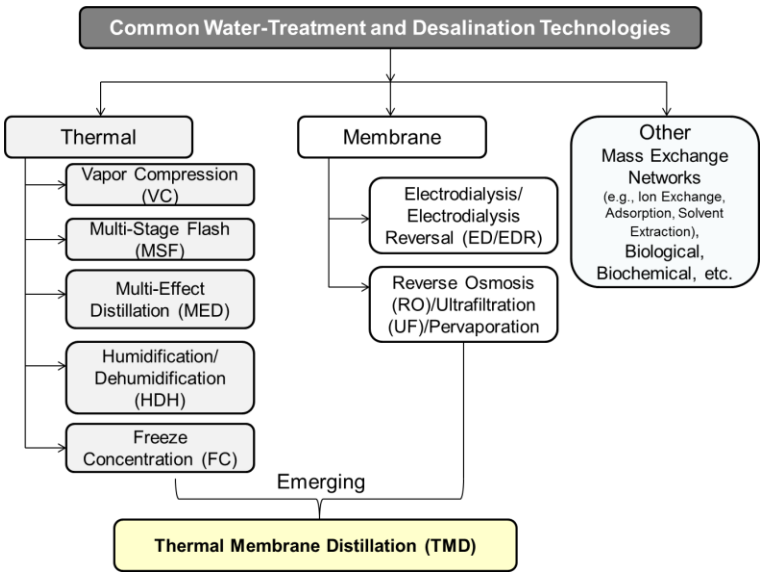

Figure 2.1. Common water treatment and desalination technologies.

Thermal membrane distillation (TMD) is a new technology that lies at the interface between thermal and membrane technologies. It is a non-isothermal separation process that is based on heating up the feed solution to be distilled to some moderate temperature to create partial evaporation of water. The produced water vapor passes preferentially through a hydrophobic - microporous membrane. The vapor that permeates through the membrane is condensed and collected as a highly pure liquid on the permeate side. The driving force in this process is the difference in chemical potential across the membrane, which is strongly

dependent on the vapor pressure difference between the feed and the permeate sides.[7] **Figure 2.2** shows a representation of a direct contact TMD module. Seawater or wastewater is preheated to induce some evaporation but not to completely evaporate the feed. The water vapor travels through the membrane and is condensed on the permeate side using a recirculating permeate-sweeping liquid.[8] Different configurations can be found in recent literature.[9] Recent advances in membrane development have led to improved performance and enhanced mass and heat transfer rates and have paved the way for the potential of cost-effective commercialization.[10]

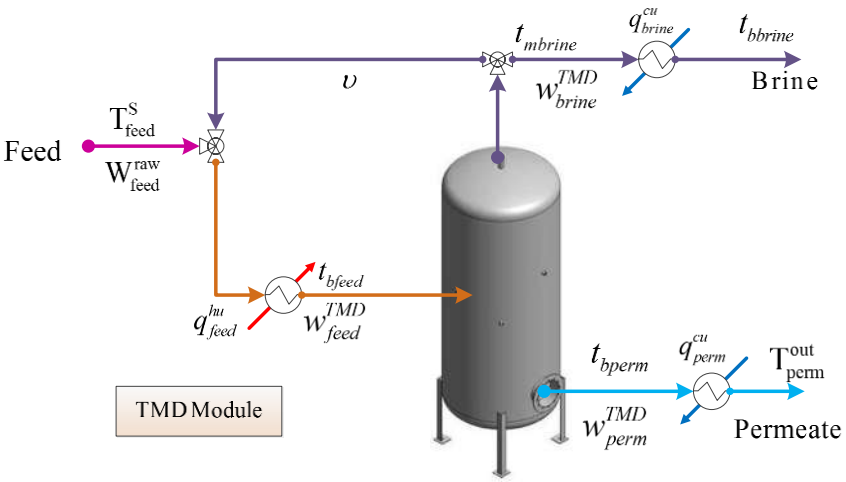

Figure 2.2. TMD direct contact configuration.

In spite of the important advances in the design of seawater-desalination and wastewater-treatment systems through TMD modules, one of the primary drawbacks is still the one associated to the high energy consumption to vaporizing the permeate. Elsayed et al.[8] proposed a sequential process integration framework to extract excess heat from industrial facilities and use it to drive TMD without taking into account the design for the associated heat exchanger network. Proper extraction of heat should involve the simultaneous synthesis of process heat-exchange networks (HENs) and the TMD network as well as the related capital costs. In this context, several approaches have been reported for the synthesis of process HENs by transferring heat from the hot process streams to the cold process streams,[11] furthermore, the sustainable development has been highlighted in the application of thermal engineering.[12] In this context, several methodologies for energy integration in the process industry have been reported, including deterministic and stochastic optimization

approaches,[13] computer fluid dynamic models,[14] heuristic rules[15] and thermo-hydraulic models.[16] Moreover, these methodologies have been applied to several cases, involving biogas production,[17] batch processes,[18] absorption refrigeration cycles,[19] eco-industrial parks,[20] retrofitting existing processes,[21] Kraft pulp mills,[22] desalination,[23] across different plants,[24] involving multi-purpose heat transfer units,[25] considering optimal cleaning,[26] scheduling,[27] for retrofitting large scale processes,[28] involving different costs[29] and temperature progression.[30]

For the specific case of TMD, Dotremont et al.[31] proposed a desalination system as a sustainable solution for the industry. Lee et al.[32] presented a mathematical model that integrates a membrane distillation system with a heat exchanger network. Qtaishat and Banat[33] proposed an integrated TMD system to be run by solar energy. Elsayed et al.[8] presented a systematic approach for integrating a TMD module with excess heat from industrial processes. In this chapter, there was proposed a systematic sequential approach for integrating processing facilities with TMD networks, in the first stage the targets for energy integration in the processing facility were determined and in the second stage there is applied an optimization model for designing the TMD module. However, in this chapter the heat exchanger network was not designed, the capital costs for the heat transfer units were not determined and the simultaneous optimization for the HEN and the TMD was not considered. Furthermore, there was not proposed any superstructure.

Notwithstanding the value of the aforementioned approaches, they suffer from at least one of the following limitations:

- No optimization of the design and operating variables of the TMD system (e.g., membrane area, feed temperature).
- No simultaneous consideration of the combined economic functions of the process and the TMD system.
- No simultaneous synthesis of the TMD network and the HEN (only HEN utility targets were considered without network configuration).
- The capital costs have not been properly considered.

In this chapter, an optimization approach is proposed for the simultaneous energy integration, HEN synthesis, and TMD system design. The proposed approach accounts for

the simultaneous structural and operational optimization of the system through a new superstructure that is modeled with a mixed-integer nonlinear programming (MINLP) model. The objective function consists of the overall profit that accounts for the value obtained from the sale of the permeate as well as the possible value obtained for wastewater treatment in the same industry. The objective function also involves the total annualized costs associated with the HEN and the TMD system. It should be noted that the proposal in this chapter is an extension of the superstructure by Yee and Grossmann[34] for HEN synthesis including the TMD model proposed by Elsayed.[8]

2.2 Problem statement

The problem addressed in this chapter can be described as follows.

Given are the following:

- An industrial process with:
  - A set of process hot stream (HS) and a set of process cold streams (CS) with known inlet (supply) and outlet (target) temperatures as well as the heat to be removed from/added to the hot/cold streams, respectively. The minimum temperature difference for heat transfer between streams is designated as (ΔT_{min}). Available for service is a set of cooling and heating utilities to satisfy the energy demands that are not met through heat integration among the hot and cold process streams.
  - Specific demands for fresh water that are characterized in terms of required flow rate and composition.
  - Discharge of wastewater that is described in terms of flow rate, inlet composition, and temperature, and desired treatment objective (e.g., outlet composition).
- A source of saline water that may be desalinated to provide fresh water.
- A set of TMD modules that can be used for wastewater treatment and seawater desalination. The number, size and operating conditions of the TMD network are to be determined via optimization.

The design problem consists of finding the optimal integrated system to satisfy the energy and fresh water demands as well as the wastewater treatment requirements for the process. Key design questions to be answered include:

- How should heat be integrated within the industrial process and with the TMD network?
- What is the optimal configuration of the HEN for matching the hot and cold streams? What are the sizes of the heat exchangers?
- How should the heat be provided to the TMD network? (e.g., how much heat from external heating sources versus excess process heat).
- What is the optimal TMD-feed pre-heating temperature?
- What is the optimal design of the TMD network?
- How much of the fresh water supplied to the process should come from external sources versus through TMD?
- What is the cost for the needed heat exchanger units?

In the next section, a structural representation and an optimization formulation will be developed to address the aforementioned design challenges.

2.3 Design approach

Figure 2.3 shows the proposed superstructure for the optimal design of the integrated TMD module with a process industry. First, the heat-exchange tasks for TMD system are represented as hot and cold streams. It should be noted that the design of the TMD module is to be simultaneously optimized along with the design of the HEN. Flows and temperatures common to the TMD and the HEN are set as optimization variables. In the representation, the hot process streams flow from left to right and the cold process streams flow from right to left. The network is decomposed into stages. Within a stage, each hot stream is split into a number of streams that may be matched with split cold streams. In the inner stages of the superstructure, it is possible to have heat exchange between the process streams and TMD feed. At the right and left extremes of the superstructure, the cooling and heating utilities are placed. It is worth noting that the inner temperatures in the superstructure are optimization variables and also the heat load and the existence of the heat transfer units are optimization variables used for the structural optimization. The number of stages of the superstructure

corresponds to the maximum of hot or cold streams involved (i.e., NOK). The simultaneous optimization of the TMD and HEN allows for tradeoffs of tasks and costs and leads to the optimization of the desired economic objective function. The following section presents the mathematical formulation for the optimization problem associated with this superstructure.

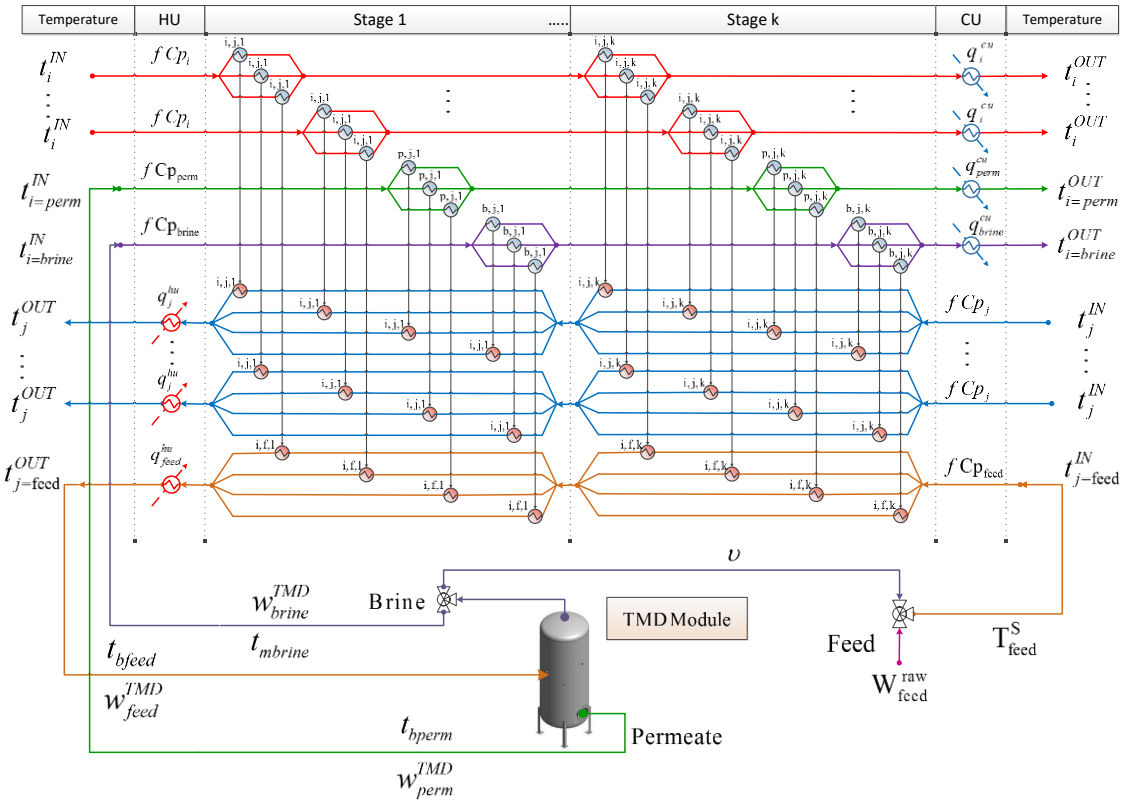

Figure 2.3. Proposed superstructure for energy integration between a TMD module associated with a process industry.

2.3.1 Model for TMD system

The TMD model is taken from Elsayed et al.[8] The following are the key equations of the model. For the details and background of this model, the reader is referred to Elsayed et al.[8] The permeate flux passing through the membrane (j_w) is calculated using the following equation:

$$j_w = b_w \left(p^{vap}_{wfeed} \gamma_{wfeed} x_{wfeed} - p^{vap}_{wperm} \right) \tag{2.1}$$

where x_{wfeed} is the mole fraction of water in feed, p_{wfeed}^{vap} is the vapor pressure in the feed side and p_{wperm}^{vap} is the vapor pressure in the permeate side of the membrane, these vapor pressures are a function of the temperature and these are calculated by the Antoine equation as follows:

$$P_{wfeed}^{vap} = \exp\left(23.1964 - \frac{3816.44}{t_{mfeed} - 46.13}\right) \tag{2.2}$$

$$P_{wperm}^{vap} = \exp\left(23.1964 - \frac{3816.44}{t_{mperm} - 46.13}\right) \tag{2.3}$$

b_w is a parameter for the molecular diffusion of water in the air,[35] and it depends on the parameter $\mathrm{B_{wB}}$ and the average temperature (t_m) in the TMD module ($t_m = (t_{bfeed} + \mathrm{T_{bperm}})/2$) as follows:

$$b_w = \mathrm{B_{wB}} t_m^{1.334} \tag{2.4}$$

where $\mathrm{B_{wB}}$ is a temperature independent base value used for evaluating the molecular diffusion of water in the air and it is defined as $\mathrm{B_{wB}} = \frac{4.46\times10^{-6}\pi \mathrm{r}^2}{\mathrm{R}P_m \tau\delta}$, where r is the pore radius, R is the universal gas constant, P_m is the air pressure in the membrane pores, τ is the pore tortuosity, δ is the thickness of the membrane. It should be noted that t_m is evaluated for the temperatures t_{bfeed} and $\mathrm{T_{bperm}}$ because there is easier to have experimental data for these temperatures.

The activity coefficient is a function of the concentration. In the case of NaCl removal, it can be calculated as follows:

$$\gamma_{wfeed} = 1 - 0.5x_{NaCl} - 10x_{NaCl}^2 \tag{2.5}$$

where x_{NaCl} is the mole fraction of NaCl in the feed.

The membrane area can be calculated by dividing the desired permeate flow rate (w_{perm}^{TMD}) by the water flux:

$$A_m = \frac{w_{perm}^{TMD}}{j_w} \tag{2.6}$$

The heat transfer through the boundary layers on the two sides of the membrane is a function of the temperature gradient between the bulk and the membrane temperatures for the feed and the permeate as shown in **Figure 2.4**.

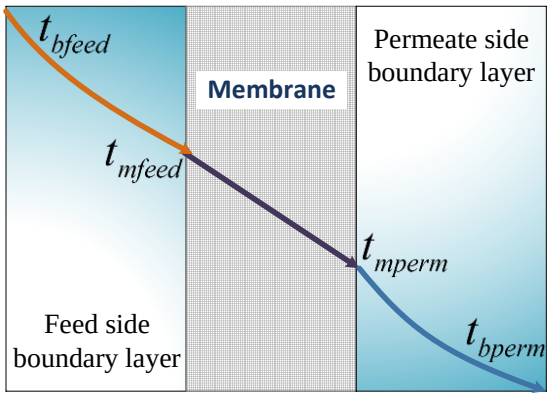

Figure 2.4. Temperature profile for the boundary layers and the membrane.[8]

The temperature polarization coefficient is defined as follows:

$$\theta = \frac{t_{mfeed} - t_{mperm}}{t_{bfeed} - t_{bperm}} \tag{2.7}$$

The vaporization of water (Δh_{vw}) in the feed side of the membrane is calculated from the correlation suggested by Elsayed et al.:[8]

$$\Delta h_{vw} = 3190 - 2.5009 t_{mfeed} \tag{2.8}$$

The conduction losses in the membrane (q_{Cond}) can be calculated as follows:[36]

$$q_{Cond} = \frac{K_m}{\delta}\left(t_{mfeed} - t_{mperm}\right) \tag{2.9}$$

where K_m is the thermal conductivity of the membrane[37] and δ is the membrane thickness.

The heat lost to vaporize the liquid (q_{Vap}) is a function of the total flux passed through the membrane (j_w) and the enthalpy of water vaporization (Δh_{vw}) and it is calculated as follows:

$$q_{Vap} = j_w \Delta h_{vw} \tag{2.10}$$

The heat loss due to conduction in the membrane ($\eta_{Conduction}$) is defined as follows:

$$\eta_{Conduction} = \frac{\frac{K_m}{\delta}\left(t_{mfeed} - t_{mperm}\right)}{j_w \Delta h_{vw} + \frac{K_m}{\delta}\left(t_{mfeed} - t_{mperm}\right)} \tag{2.11}$$

The thermal efficiency for vaporization in TMD units ($\eta_{Thermal}$) is defined as follows: $\eta_{Thermal} = \frac{heat\,used\,in\,flux\,vaporizaton}{total\,heat\,provided\,to\,TMD\,feed}$. Considering that the heat losses are 50% of the conduction losses, the overall thermal efficiency of TMD module is given by the following relationship:[38]

$$\eta_{Thermal} = 1 - 1.5 \cdot \eta_{Conduction} \tag{2.12}$$

The TMD feed flow rate (w_{feed}^{TMD}) is the sum the total flow rate of the raw water to be treated (W_{feed}^{raw}) and the recycled flow rate (υW_{feed}^{raw}). The energy balance for the entire TMD unit is given as follows:

$$\eta_{Thermal} w_{feed}^{TMD} Cp_{feed}\left(t_{bfeed} - T_{feed}^{S}\right) = w_{perm}^{TMD} \Delta h_{vw} \tag{2.13}$$

The energy balance in the mixer is given as follows:

$$\upsilon W_{feed}^{raw} Cp_{feed} t_{mbrine} + W_{feed}^{raw} Cp_{feed} T_{feed}^{S} = w_{feed}^{TMD} t_{feed}^{TMD} Cp_{feed} \tag{2.14}$$

For the case of a highly rejecting membrane (i.e., permeate is virtually pure water), the reject concentration (y_{brine}) can be calculated through a source material balance for the

whole system ($y_{brine} = y_{feed}^{raw} / (1-\xi)$), where y_{feed}^{raw} is the concentration of impurities in raw water, and ξ is the water recovered for the TMD unit ($\xi = w_{perm}^{TMD} / W_{feed}^{raw}$). The mass concentration around the mixing point of the raw feed and the recycled stream (y_{feed}^{TMD}) is calculated as follows:

$$y_{feed}^{TMD} = \frac{y_{feed}^{raw} + \upsilon y_{brine}}{1+\upsilon} \tag{2.15}$$

Then, the molar fraction of NaCl in the feed (x_{NaCl}) is a function of the mass concentration in the feed of TMD (y_{feed}^{TMD}), the atomic weight of the water and the atomic weight of NaCl as follows:

$$x_{NaCl} = \frac{\left(y_{feed}^{TMD} / PM_{NaCl} \right)}{\left(y_{feed}^{TMD} / PM_{NaCl} \right) + \left(1 - y_{feed}^{TMD} / PM_{wt} \right)} \tag{2.16}$$

Finally, the mole fraction of the water in the feed is:

$$x_{wfeed} = 1 - x_{NaCl} \tag{2.17}$$

For a TMD module with laminar flows and comparable flows of the feed and the sweeping liquid, the absolute value of temperature difference (*deltat*) between the bulk and the membrane on each side of the membrane is assumed to be roughly the same:

$$t_{bfeed} - t_{mfeed} = deltat \tag{2.18}$$

$$t_{mperm} - t_{bperm} = deltat \tag{2.19}$$

2.3.2 Model for heat integration

In the model formulation, HS, CS, SN represent the hot streams, cold streams and the number of stages in the superstructure, respectively.[34] The index *i* is used for hot streams, *j* represents cold streams, *k* represents the stages in the superstructure and *NOK* is the cardinal of the total number of stages. To model the proposed superstructure, the following relationships are required.

2.3.3 Total energy balance for process streams

The total energy for the hot stream i is equal to the sum of the energy exchanged with any cold process stream j in any stage of the superstructure ($q_{i,j,k}$) and the heat exchanged with the cooling utilities (q_i^{cu}):

$$\left(t_i^{IN} - t_i^{OUT}\right) fCp_i = \sum_{k \in SN} \sum_{j \in CS} q_{i,j,k} + q_i^{cu} \qquad \forall i \tag{2.20}$$

The total energy for any cold stream j is equal to the sum of the energy exchanged with any hot stream i in any stage of the superstructure ($q_{i,j,k}$) and the heat exchanged with the heating utility (q_j^{hu}):

$$\left(t_j^{OUT} - t_j^{IN}\right) fCp_j = \sum_{k \in SN} \sum_{j \in HS} q_{i,j,k} + q_j^{hu} \qquad \forall j \tag{2.21}$$

2.3.4 Energy balance for each intermediate stages of the superstructure

To determine the intermediate temperatures of the superstructure, energy balances for each stage *k* are required. This way, for hot streams:

$$(t_{i,k} - t_{i,k+1})\, fCp_i = \sum_{j \in CS} q_{i,j,k} \qquad \forall i, \forall k \tag{2.22}$$

For cold streams:

$$(t_{j,k} - t_{j,k+1})\, fCp_j = \sum_{i \in HS} q_{i,j,k} \qquad \forall j, \forall k \tag{2.23}$$

2.3.5 Balances for heating and cooling utilities

After heat exchanging between hot and cold process streams through the stages of the superstructure, hot process streams must be cooled using cooling utility at the right end of the superstructure:

$$(t_{i,NOK+1} - t_i^{OUT})\, fCp_i = q_i^{cu} \qquad \forall i \tag{2.24}$$

And the cold streams can be heated using heating utility at the left end of the superstructure:

$$(t_j^{OUT} - t_{j,1})\, fCp_j = q_j^{hu} \qquad \forall j \tag{2.25}$$

2.3.6 Constraints for the feasibility of temperatures in the superstructure

There is required a set of constraints for the temperature of the process streams to ensure a monotonic decrement from the left to the right-hand side of the superstructure:

$$t_{i,k} \geq t_{i,k+1} \qquad \forall i, \forall k \tag{2.26}$$

$$t_{\mathrm{i,NOK+1}} \geq T_i^{OUT} \qquad \forall i \tag{2.27}$$

$$t_{j,k} \geq t_{j,k+1} \qquad \forall j, \forall k \tag{2.28}$$

$$T_{\mathrm{j}}^{\mathrm{OUT}} \geq t_{j,1} \qquad \forall j \tag{2.29}$$

2.3.7 Assignment of temperatures

First, the inlet temperature for the hot process streams (i' corresponds to hot process streams not associated to the TMD module) must be equal to the temperature at the first border of the superstructure:

$$t_{i'}^{IN} = t_{i',1} \qquad \forall i' \tag{2.30}$$

For the permeate stream, the inlet temperature to the superstructure is given as follows:

$$t_{mperm} = t_{i=perm,1}^{IN} \tag{2.31}$$

Whereas the outlet temperature for the permeate side is equal to the temperature of the last border of the superstructure for this stream:

$$\mathrm{T}_{\mathrm{perm}}^{\mathrm{out}} = t_{i=perm}^{OUT} \tag{2.32}$$

For the brine, the inlet temperature to the superstructure is given as follows:

$$t_{mbrine} = t_{i=brine,1}^{IN} \tag{2.33}$$

And the outlet temperature for the brine is equal to the temperature at the last border of the superstructure:

$$\mathrm{T}_{\mathrm{bbrine}} = t_{i=brine}^{OUT} \tag{2.34}$$

The inlet temperature for the cold process streams (*j'* corresponds to cold process streams not associated to the TMD module) must be equal to the temperature at the first border of the superstructure:

$$t_{j'}^{IN} = t_{j',NOK+1} \qquad \forall j' \tag{2.35}$$

The inlet temperature of the feed stream is given as follows:

$$\mathrm{T}_{\mathrm{feed}}^{\mathrm{S}} = t_{i=feed}^{IN} \tag{2.36}$$

The outlet temperature of the feed stream is equal to the temperature at the first border of the superstructure as follows:

$$t_{bfeed} = t_{j=feed,1}^{OUT} \tag{2.37}$$

2.3.8 Assignment of flow rates

The inlet heat capacity flow rate for the hot process streams must be equal to the heat capacity flow rate known for these streams and given from the process conditions:

$$fCp_{i'} = \mathrm{FCp}_{\mathrm{i'}} \qquad \forall i' \tag{2.38}$$

For the permeate side, the inlet heat capacity flow rate to the superstructure is given from the conditions in the thermal membrane desalination unit as follows:

$$fCp_{i=perm} = w_{perm}\,\mathrm{Cp}_{\mathrm{perm}} \tag{2.39}$$

For the rejected brine, the inlet heat capacity flow rate to the superstructure also depends on the thermal membrane distillation units as follows:

$$fCp_{i=brine} = (\mathrm{W}_{\mathrm{feed}}^{\mathrm{raw}} - w_{perm})\,\mathrm{Cp}_{\mathrm{brine}} \tag{2.40}$$

The inlet heat capacity flow rate for the cold process streams given by the process condition must be equal to the heat capacity flow rate at the first border of the superstructure:

$$fCp_{j'} = \mathrm{F}\,\mathrm{Cp}_{j'} \qquad \forall j' \tag{2.41}$$

The inlet heat capacity flow rate of the feed stream is given as follows:

$$fCp_{j=feed} = w_{feed}^{TMD}\,\mathrm{Cp}_{\mathrm{feed}} \tag{2.42}$$

2.3.9 Existence of heat exchanger units

Binary variables are used to activate the existence for the heat transfer units of the superstructure, and these are activated through big-M formulation as follows.

For the heat exchangers units between streams through the stages in the superstructure:

$$q_{i,j,k} - \mathrm{Q}_{\mathrm{i,j}}^{\mathrm{MAX}} z_{i,j,k} \le 0 \qquad \forall i, \forall j, \forall k \tag{2.43}$$

For the coolers that use cooling water:

$$q_i^{cu} - \mathrm{Q}_{\mathrm{i}}^{\mathrm{MAX}} z_i^{cu} \le 0 \qquad \forall i \tag{2.44}$$

For the heaters that use heating utility:

$$q_j^{hu} - \mathrm{Q}_{\mathrm{j}}^{\mathrm{MAX}} z_j^{hu} \le 0 \qquad \forall j \tag{2.45}$$

2.3.10 Feasibilities for the temperature differences

If a heat exchanger exists, then the temperature differences for the hot and the cold ends between the hot and the cold streams must be greater than a minimum value; on the other hand, when a heat exchanger unit does not exist, these constraints are not required. These constraints are formulated as big-M formulations as follows.

For the heat exchangers units between process streams in the stages of the superstructure, the following mixed integer relationships are used:

$$dt_{i,j,k} \le t_{i,k} - t_{j,k} + \Delta\mathrm{T}_{\mathrm{i,j}}^{\mathrm{MAX}}(1 - z_{i,j,k}) \qquad \forall i, \forall j, \forall k \tag{2.46}$$

$$dt_{i,j,k+1} \le t_{i,k+1} - t_{j,k+1} + \Delta\mathrm{T}_{\mathrm{i,j}}^{\mathrm{MAX}}(1 - z_{i,j,k}) \qquad \forall i, \forall j, \forall k \tag{2.47}$$

For the coolers that use cooling water:

$$dt_i^{cu} \le t_{i,k+1} - \mathrm{T}_{\mathrm{OUT}}^{\mathrm{cu}} + \Delta\mathrm{T}_{\mathrm{i}}^{\mathrm{MAX}}(1 - z_i^{cu}) \qquad \forall i \tag{2.48}$$

For the heaters using hot utility:

$$dt_j^{hu} \le \mathrm{T}_{\mathrm{OUT}}^{\mathrm{hu}} - t_{j,1} + \Delta\mathrm{T}_{\mathrm{j}}^{\mathrm{MAX}}(1 - z_i^{hu}) \qquad \forall j \tag{2.49}$$

Finally, to ensure a feasible heat exchange, the following constraints must be included:

$$\Delta\mathrm{T}_{\min} \le dt_{i,j,k} \qquad \forall i, \forall j, \forall k \tag{2.50}$$

$$\Delta\mathrm{T}_{\min} \le dt_i^{cu} \qquad \forall i \tag{2.51}$$

$$\Delta\mathrm{T}_{\min} \le dt_j^{hu} \qquad \forall j \tag{2.52}$$

2.3.11 Objective function

The objective function consists in maximizing the net profit, which is stated as follows:

$$Max\,Profit = V_{perm}^{Annual} + \mathrm{V}_{\mathrm{ww}}^{\mathrm{Annual}} - TAC \tag{2.53}$$

The profit (*Profit*) is the sum of the revenue from the sale of the permeate (V_{perm}^{Annual}) and the income from the wastewater treatment ($\mathrm{V}_{\mathrm{ww}}^{\mathrm{Annual}}$) minus the total annual cost (*TAC*).

The income from the sales of the permeate (V_{perm}^{Annual}) as fresh water is given as follows:

$$V_{perm}^{Annual} = \mathrm{H}_{\mathrm{Y}}\ w_{perm} \cdot \mathrm{V}_{\mathrm{perm}} \tag{2.54}$$

where w_{perm} is the flow rate for the permeate, $\mathrm{V}_{\mathrm{perm}}$ is the value per kg of permeate and $\mathrm{H_Y}$ corresponds to the operating time per year.

The income from the wastewater treatment of the process industry ($\mathrm{V}_{\mathrm{ww}}^{\mathrm{Annual}}$) is obtained as follows:

$$V_{ww}^{Annual} = H_Y \, W_{ww} \, V_{ww} \tag{2.55}$$

where W_{ww} is the wastewater flow rate and V_{ww} is the income for wastewater treatment.

The total annual cost (TAC) is described as follows:

$$\begin{aligned} TAC = & \\ & \sum_{i\in HS}\sum_{j\in CS}\sum_{k\in SN} C_{F_{i,j,k}}^{exc} \, z_{i,j,k} + \sum_{i\in HS} C_{F_i}^{cu} \, z_i^{cu} + \sum_{j\in CS} C_{F_j}^{hu} \, z_j^{hu} \\ & + \sum_{i\in HS}\sum_{j\in CS}\sum_{k\in SN} C_{i,j}^{exc} \left\{ \frac{q_{i,j,k}\left(\frac{1}{H_i}+\frac{1}{H_j}\right)}{\left[\left(dt_{i,j,k}\right)\left(dt_{i,j,k+1}\right)\left(\frac{dt_{i,j,k}+dt_{i,j,k+1}}{2}\right)+\varphi\right]^{1/3}} \right\}^{\beta} \\ & + K_F \left[+ \sum_{i\in HS} C_i^{cu} \left\{ \frac{q_i^{cu}\left(\frac{1}{H_i}+\frac{1}{H_{cu}}\right)}{\left[\left(T_i^{OUT}-t_{i,NOK+1}\right)\left(dt_i^{cu}\right)\left(\frac{\left(T_i^{OUT}-t_{i,NOK+1}\right)+\left(dt_i^{cu}\right)}{2}\right)+\varphi\right]^{1/3}} \right\}^{\beta} \right. \\ & \left. + \sum_{j\in CS} C_j^{hu} \left\{ \frac{q_j^{hu}\left(\frac{1}{H_j}+\frac{1}{H_{hu}}\right)}{\left[\left(t_{j,1}-T_j^{OUT}\right)\left(dt_j^{hu}\right)\left(\frac{\left(t_{j,1}-T_j^{OUT}\right)+\left(dt_j^{hu}\right)}{2}\right)+\varphi\right]^{1/3}} \right\}^{\beta} \right] \\ & + K_F \, AFC^{TMD} \\ & + H_Y \, AOC^{TMD} \\ & + H_Y \sum_{i\in HS} CCU \, q_i^{cu} + H_Y \sum_{j\in CS} CHU \, q_j^{hu} \end{aligned} \tag{2.56}$$

It should be noted that the previous relationships include the capital costs for the heat transfer units, these costs are divided into fixed terms, for units between process streams ($C_{F_{i,j,k}}^{exc}$), for coolers ($C_{F_i}^{cu}$) and heaters ($C_{F_j}^{hu}$), and area dependent terms, for heating utilities (C_j^{hu}), cooling utilities (C_i^{cu}) and intermediate heat exchangers($C_{i,j}^{exc}$), also the equation includes the fouling heat transfer coefficient (H), the capital cost (AFC^{TMD}) and operating

cost ($AOC_{No\,H}^{TMD}$) for the TMD module in addition to the cooling (CCU) and heating costs (CHU). The term $q_{i,j,k}$ is the heat exchanged between process streams, q_i^{cu} is the heat exchanged with the cooling utilities, q_j^{hu} is the heat exchanged with the heating utilities. The logarithmic mean temperature differences in the objective function are estimated using Chen's approximation.[39]

The capital cost (AFC^{TMD}) for the TMD unit is stated as follows:

$$AFC^{TMD} = \mathrm{C}_{\mathrm{F}}^{\mathrm{TMD}} A_m + \mathrm{C}_{\mathrm{nm}}^{\mathrm{TMD}} w_{feed}^{TMD} \tag{2.57}$$

where $\mathrm{C}_{\mathrm{F}}^{\mathrm{TMD}}$ is the unit capital cost of the membrane, A_m is the membrane area, $\mathrm{C}_{\mathrm{nm}}^{\mathrm{TMD}}$ is the unit non-membrane capital cost.

The operating cost of the TMD module (excluding heating) (AOC^{TMD}) is given by the following relationship:

$$AOC^{TMD} = \left[\mathrm{C}_{\mathrm{Op1}}^{\mathrm{TMD}} + \mathrm{C}_{\mathrm{Op2}}^{\mathrm{TMD}} \left(1-\xi\right) + \mathrm{C}_{\mathrm{Op3}}^{\mathrm{TMD}} \left(1+\upsilon\right) \right] \mathrm{W}_{\mathrm{feed}}^{\mathrm{raw}} \tag{2.58}$$

where $\mathrm{C}_{\mathrm{Op1}}^{\mathrm{TMD}}$, $\mathrm{C}_{\mathrm{Op2}}^{\mathrm{TMD}}$ and $\mathrm{C}_{\mathrm{Op3}}^{\mathrm{TMD}}$ are unit operating costs for the TMD unit.

2.4 Case study

The case study is based on the process for converting shale gas (156 MMSCF/d) to methanol (5,000 tons/d) described by Ehlinger et al.[40] The hot and cold stream data for the methanol plant are given in **Table 2.1**.

Table 2.1. Hot and cold stream data for the gas-to-methanol process.[40]

Stream Number	Supply Temperature, K	Target Temperature, K	Heat Duty, kW
Hot streams			
1	1,544	313	-283,206
2	597	313	-51,008
3	513	423	-42,389
4	420	318	-37,093
Cold streams			
1	299	473	7,614
2	313	573	45,129

The problem is to integrate the thermal and water aspects of the methanol process with a TMD network. The TMD network has a raw feed flow of 174.0 kg/s. The feed is predominantly brackish water (162.0 kg/s), which is mixed with a small waste water stream from a methanol plant (12.0 kg/s). The primary solute in the raw feed stream is NaCl (0.77 wt %). The feed has specific heat Cp_{feed} = 4.0 kJ/kg K and temperature T_f^S = 293 K. A water recovery from the raw feed (ξ) of 0.8 was considered (i.e., w_{perm} = 139.2 kg/s). The value of the produced permeate is \$8.00/m^3. The TMD network also receives \$5.00/m^3 for wastewater treatment from the methanol plant.

The considered TMD module uses a polypropylene hollow-fiber membrane MD020CP2N (Manufactured by Microdyn) with a membrane thickness of 0.65 mm. The TMD data and modeling equations are given by Elsayed et al.[8] The maximum allowable temperature for heating the feed stream is 363 K.

Table 2.2. TMD unit operating costs.

Cost item	Value	Characteristic
Pretreatment	0.0190	\$/m^3 of raw feed
Labor	0.0300	\$/m^3 of raw feed
Brine disposal	0.0015	\$/m^3 of brine
Pumping	0.0560	\$/m^3 of total feed (raw feed and recycled reject) to the TMD
Heating utilities	5.00	\$/10^9 J heating utility
Cooling utilities	4.00	\$/10^9 J cooling water

For the cost calculation, Al-Obaidani et al.[41] estimated the cost of the membranes to be \$90/m^2. Therefore, using a Lang factor of 5.0, a 10-year linear depreciation scheme with no salvage value, and assuming that the membrane lifetime is 4 years, the unit fixed cost of the membrane modules is estimated to be as follows: C_F^{TMD}=58.8 \$/(m^2 y). The unit non-membrane capital cost (that includes the units involved in the TMD module; i.e. pumps, pipes, instrumentation, electrical subsystems, and installation) is estimated as follows: C_{nm}^{TMD} =11,150 \$/(kg/s y). Considering an annual operation of 8,000 h and according to the basis of the data presented in **Table 2.2**, the unit operating costs are C_{Op1}^{TMD}=1,411 \$/(kg/s y), C_{Op2}^{TMD}=43 \$/(kg/s y) and C_{Op3}^{TMD}=1,613 \$/(kg/s y). For the unit fixed capital costs for the heat exchanger

units, the following unit costs were used $C^{exc}_{F_{i,j,k}} = 5,500\ \$/y$, $C^{cu}_{F_i} = C^{hu}_{Fj} = 150\ \$/y$, and $C^{exc}_{i,j} = C^{cu}_{i} = C^{hu}_{j} = 150\ \$/y \cdot m^2$. It should be noticed that that for this case study the unit capital costs have been annualized as previous reports, this way the coded model uses a value for K_F of 1. Finally, the used film heat transfer coefficients are $H_i = H_j = H_{cu} = H_{hu} = 0.1 kW/m^2K$.

2.5 Results and discussion

The problem was coded in the software GAMS,[42] where the solvers DICOPT, CONOPT, and CPLEX were used to solve the associated mixed-integer nonlinear programming, nonlinear programming and linear programming problems, respectively. For solving this problem, a computer with an Intel® Core ™ i7-4700MQ processor at 2.40 GHz and 8 GB of RAM was used. The problem statistics are shown in **Table 2.3**.

Three scenarios are analyzed. The first one (Scenario 1) considers that there is not energy interaction between the TMD unit and the methanol plant. The second scenario (Scenario 2) considers only the heat integration among the process streams within the methanol plant (no heat integration with TMD). The third scenario (Scenario 3) involves the heat integration between the methanol plant and the TMD unit. This also includes heat integration within the methanol plant.

Table 2.3. Problem statistics.

Concept	Value
Number of continuous variables	314
Number of binary variables	68
Number of constraints	39
CPU time (s)	5.94

First, the optimization problem for Scenario 1 was solved. The optimal solution is shown in **Figure 2.5**. **Table 2.4** shows the optimal operating conditions for the TMD module. For this case, the feed preheating temperature for the TMD system is 359 K and the permeate temperature after the TMD unit reaches 299 K. The temperature after the mixing of the raw feed and the reject is 344 K. The membrane area needed to operate the TMD module is 19,950

m^2. Without heat integration, the needed heat-exchange area to the heating utilities is 10,470 m^2 with a transferred heating rate of 131,012 kW. The heat-exchange area for the cooling utilities is 60,920 m^2 with a transferred cooling rate of 420,570 kW. **Table 2.5** shows the main economic results for three scenarios.

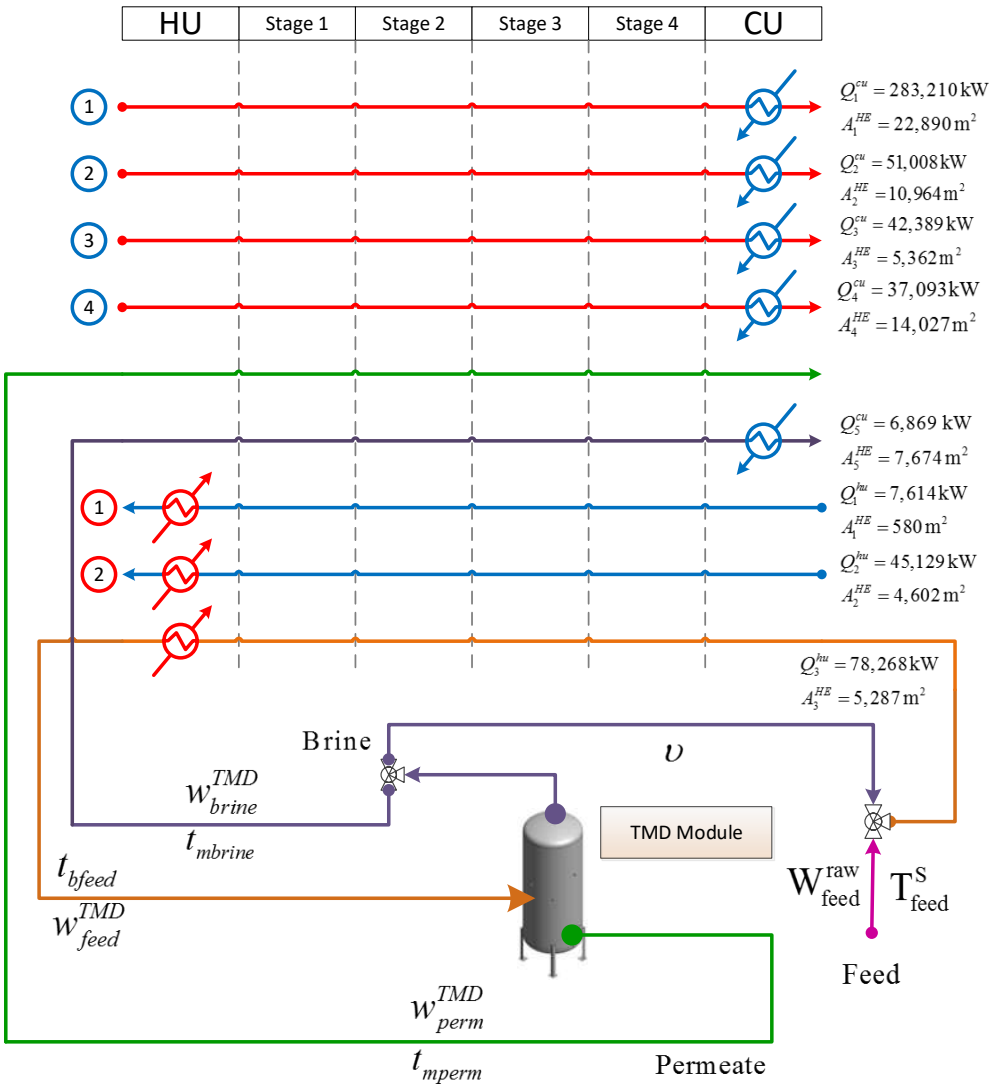

Figure 2.5. TMD module without heat integration with the methanol plant (Scenario 1).

The total annual cost for this solution without energy integration (Scenario 1) is $MM 23.292/y. In should be noticed that for this case the capital cost for the coolers CU is the main contribution to the total annual cost, which represents the 39.2%, the second contribution is related to the cooling cost (22.9%), followed by the annual fixed cost for the TMD unit (11.6%), the annual operating cost for the TMD unit represents the 10.5%, the annual heating

cost is 9%, and finally the capital cost for the heaters (6.7%). It is worth noting that the TMD heating cost represents 59.7% of the combined heating cost for the methanol plant and the TMD system. On the other hand, the TMD cooling cost is 1.7% of the combined cost of cooling for the methanol plant and the TMD system. The intermediate heat exchangers are the units needed to integrate heat between the methanol plant and the TMD system. Therefore, for Scenario 1, the area of the intermediate heat exchangers is zero. The total gross profit is $MM 33.863/y, which is composed of 95% from the sales of permeate and 5% for wastewater treatment from the methanol plant. The total annual profit for this solution without energy integration is $MM 10.571/y.

Table 2.4. Key results for the three scenarios of the case study

Variable	Unit	(Scenario 1)	(Scenario 2)	(Scenario 3)
Membrane area	m^2	19,950	19,950	19,950
Raw feed flow	kg/s	174	174	174
Flow rate of the permeate	kg/s	139	139	139
Intermediate heat exchangers area	m^2	0	1,737	3,089
Heat exchanged in intermediate stages	kW	0	52,743	131,012
Heaters area (HU)	m^2	10,470	5,287	0
Total heat exchanged (HU)	kW	131,012	78,269	0
Coolers area (CU)	m^2	60,920	59,060	56,641
Total heat exchanged (CU)	kW	420,570	367,826	289,553

Figure 2.6 shows the optimal configuration of the heat exchanger network considering only the heat integration between the hot streams and the cold streams within the methanol plant (Scenario 2), notice that hot streams and cold streams from the TMD unit cannot be integrated because the temperatures for these streams do not satisfy the ΔT_{min} (344 K for the cold stream and 359 for the hot stream).

In this case of Scenario 2, considering only the heat integration in the methanol plant, the annual cost is $MM 20.031/y. Key cost items include the annualized capital cost of the coolers, annual cooling cost and the capital cost for intermediate heat exchangers which

account for 44.2%, 18.5%, and 1.4%, respectively, of the total annualized cost. The annual profit is $MM 13.832/y which is 1.3 times the annual profit for Scenario 1.

Figure 2.7 shows the optimal configuration of the heat exchanger network considering the heat integration between the TMD unit and the methanol process (Scenario 3), it should be noticed that in this case heating utilities are not needed due to the energy integration between the process streams and the streams associated with the TMD module in addition to the simultaneous optimization for the temperatures and flow rates of the TMD module. First, for this energetically integrated scenario, the TMD module presents the configuration described in **Table 2.4**. It should be noticed that the main difference between this case and the "no energy integration" case is the heating cost.

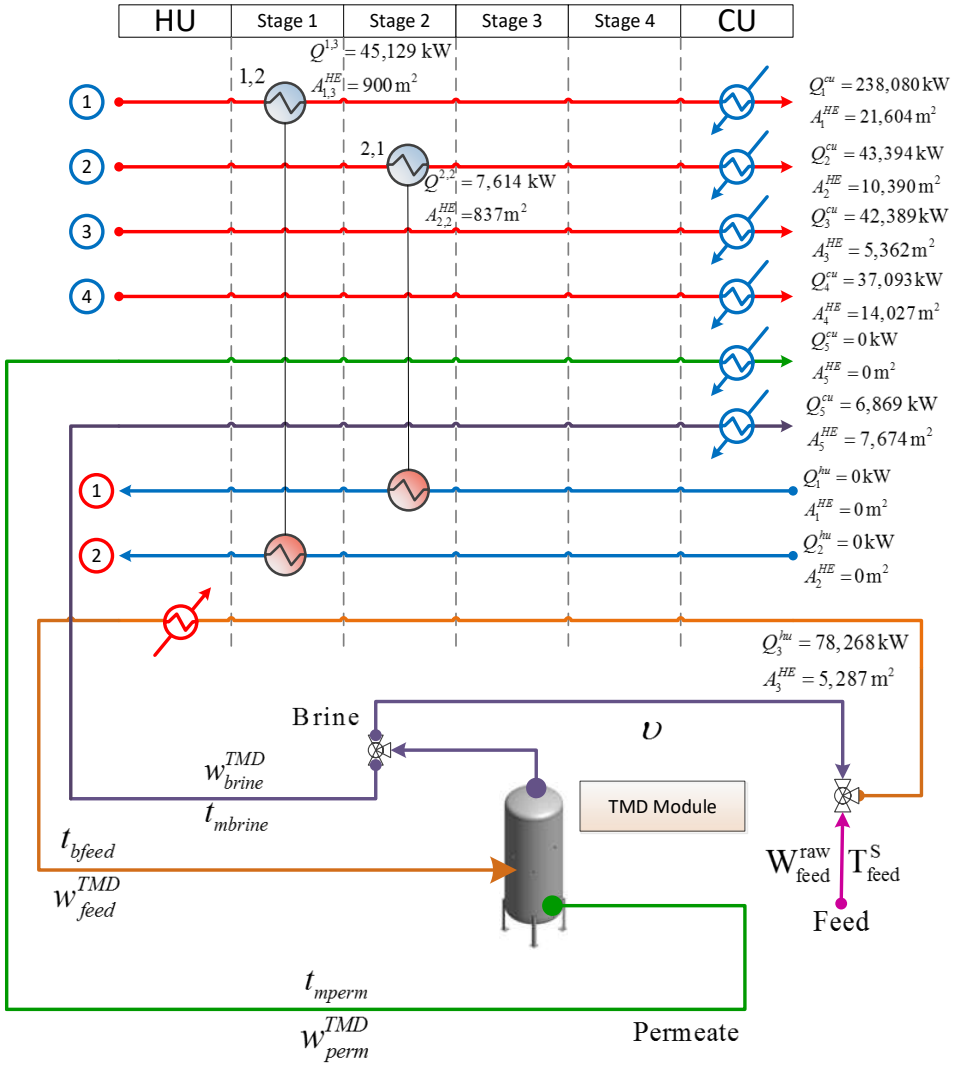

Figure 2.6. Optimal HEN for Scenario 2.

For this case including energy integration, the total annual cost is $MM 17.808/y. Key cost items include the annualized fixed cost of the coolers , the annual cooling cost and the capital cost for intermediate heat exchanger, 47.7 %, 20.7 % and 2.8 %, respectively, of the total annualized cost, notice that the annual heating and capital costs for heaters are zero. The total heat in the cooling utilities is reduced by 31 % and the area for the coolers is reduced by 7% from Scenario 1. Then, gross profit is $MM 33.863/y, which yields a total annual profit of $MM 16.055/y which is 50% more of the annual profit for Scenario 1. **Table 2.5** shows the comparison between the three analyzed scenarios.

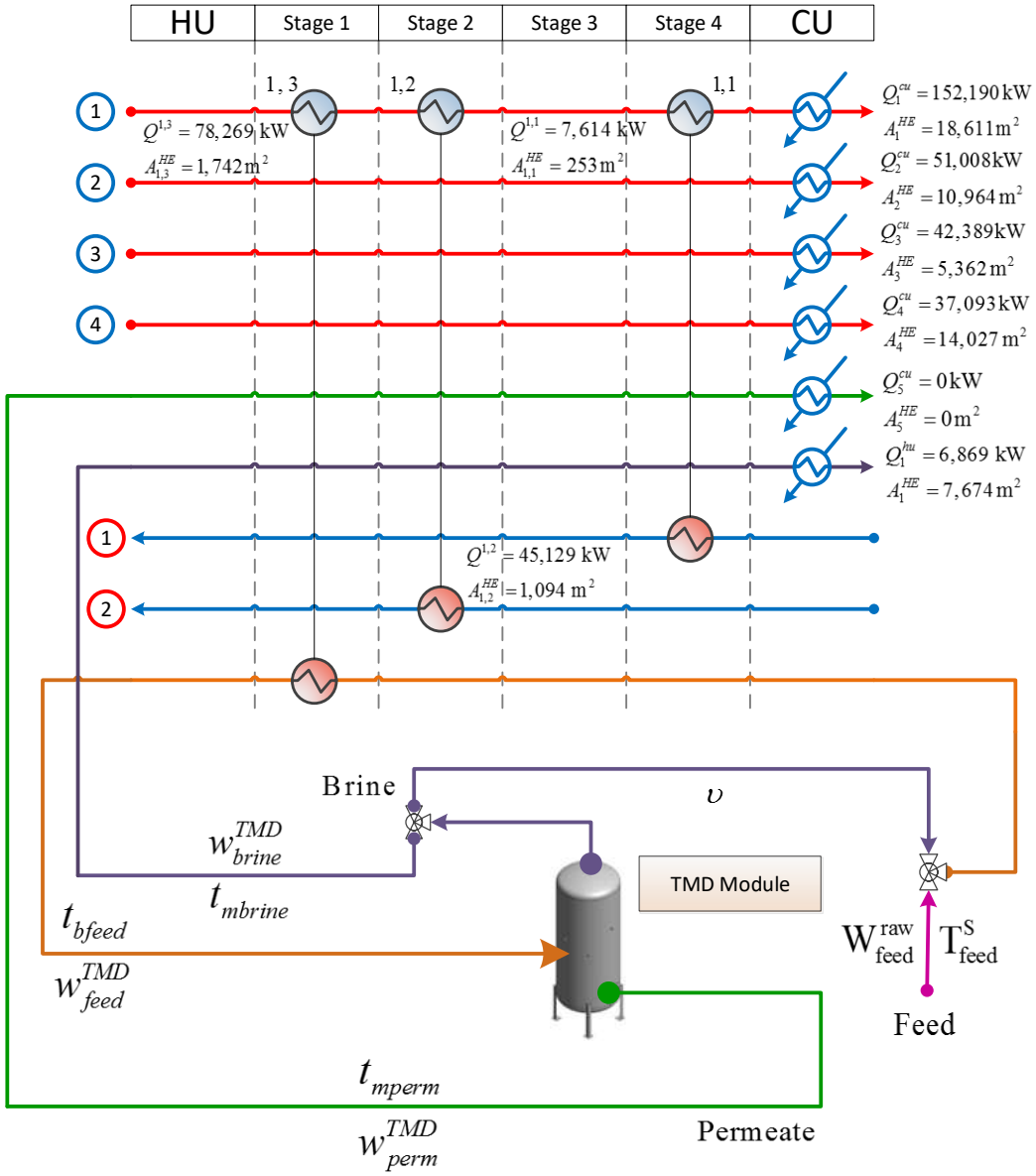

Figure 2.7. TMD module with heat integration with the methanol plant (Scenario 3).

Table 2.5. Economic results.

Concept	Scenario 1 ($MM/y)	Scenario 2 ($MM/y)	Scenario 3 ($MM/y)
Annual fixed cost for TMD	2.691	2.691	2.691
Annual operating cost of TMD	2.453	2.453	2.453
Annual heating cost for TMD	1.252	1.252	0
Annual cooling cost for TMD	0.088	0.088	0.088
Annual heating cost for Methanol plant	0.845	0	0
Annual cooling cost for Methanol plant	2.254	3.610	3.589
Annualized capital cost for heat exchangers HU	1.571	0.793	0
Annualized capital cost for heat exchangers CU	9.138	8.860	8.496
Annualized capital cost for intermediate heat exchangers	0	0.283	0.491
Annual cooling cost	5.342	3.698	3.677
Annual heating cost	2.097	1.252	0
Total annual cost	23.292	20.031	17.808
Gross revenue for TMD (value of permeate)	32.143	32.143	32.143
Gross revenue for waste treatment	1.720	1.720	1.720
Total annual profit	10.571	13.832	16.055

2.6 Conclusions

This chapter has presented a mathematical programing model for the optimal thermal integration between a TMD network and a processing facility. The configuration of the heat-exchange network is optimized simultaneously with the design of the TMD network. The optimization approach also accounts for the synergistic effects of reducing energy requirements for the TMD network and the processing plant and enabling cost-effective treatment of wastewater and saline water. Three scenarios have been studied in this chapter: no heat integration, heat integration within the process, and thermal coupling between the process and the TMD network. The results show that substantial benefits can accrue as a result of the coupling between the process and the TMD network through the synergistic effects of thermal coupling and water integration. Additionally, the results have shown that the capital costs for heat exchangers (heaters, coolers and intermediate exchangers) represent

a significant contribution, which must be taken into account to obtain the optimal solution, which was not considered by previously reported approaches.

2.7 References

1. WWAP (World Water Assessment Programme), The United Nations World Water Development Report 4: Managing Water under Uncertainty and Risk, Paris, France, UNESCO, 1, 2012.
2. WWAP (World Water Assessment Programme), The United Nations World Water Development Report 4: Knowledge Base, Paris, France, UNESCO, 2, 2012.
3. Li, C.; Goswami, Y.; Stefanakos, E. Solar assisted sea water desalination: A review, *Renewable and Sustainable Energy Reviews*, 2013, 19, 136-163.
4. Alnouri, S. Y.; Linke P. Optimal SWRO desalination network synthesis using multiple water quality parameters, *Journal of Membrane Science*, 2013, 444, 493-512.
5. Charcosset, C. A review of membrane processes and renewable energies for desalination, *Desalination*, 2009, 245, 214-231.
6. Srinivas, B. K.; El-Halwagi, M. M. Optimal design of pervaporation systems for waste reduction, *Computers and Chemical Engineering*, 1993, 17 (10), 957-970.
7. Adham, S.; Hussain, A.; Matar, J. M.; Dores, R.; Jason A. Application of membrane distillation for desalting brines from thermal desalination plants, *Desalination*, 2013, 314, 101-108.
8. Elsayed, N. A.; Barrufet, M. A.; El-Halwagi, M. M. Integration of thermal membrane distillation networks with processing facilities, *Industrial and Engineering Chemistry*, 2014: 53, 5284-5298.
9. Camacho, L. M.; Dumée, L.; Zhang, J.; Li, J.-d.; Duke, M.; Gomez, J.; Gray, S. Advances in membrane distillation for water desalination and purification application, *Water*, 2013, 5, 94-196.
10. Khayet, M. Membranes and theoretical modeling of membrane distillation: A review, *Advances in Colloid and Interface Science*, 2011, 164, 56-88.
11. Morari, M.; Agachi, P. S. Review: Important contributions in development and improvement of the heat integration techniques, *Computers and Chemical Engineering*, 2010, 34, 1171-1179.
12. Lam, H. L.; Varvanov, P. S.; Klemes, J. J. Applied Thermal Engineering towards sustainable development, *Applied Thermal Engineering*, 2014, 70 (2), 1051-1055.
13. Gorji-Bandpy, M.; Yahyazadeh-Jelodar, H.; Khalili, M., Optimization of heat exchanger network, *Applied Thermal Engineering*, 2011, 31, 779-784.
14. Selma, B.; Desilets, M.; Proulx, P., Optimization of an industrial heat exchanger using an open-source CFD code, *Applied Thermal Engineering*, 2014, 69, 241-250.
15. Goncalves, C. O.; Queiroz, E. M.; Pessoa, F. L. P.; Liporace, F. S.; Oliveira, S. G.; Costa, A. L. H., Heuristic optimization of the cleaning schedule of crude preheat trains, *Applied Thermal Engineering*, 2014, 73 (1), 3-14.
16. Polley, G. T.; Tamakloe, E.; Picon-Nuñez, M.; Ishiyama, E. M.; Wilson, D. I., Applying thermo-hydraulic simulation and heat exchanger analysis to the retrofit of heat recovery systems, *Applied Thermal Engineering*, 2013, 51, 137-143.
17. Drobež, R.; Pintarič, Z. N.; Pahor, B.; Kravanja, Z.; Simultaneous synthesis of a biogas process and heat exchanger network, *Applied thermal Engineering*, 2012, 43, 91-100.

18. Yang, P.; Liu, L. L.; Du, J.; Li, J. L.; Meng, Q. W., Heat exchanger network for batch processes by involving heat storages with cost targets, *Applied thermal Engineering*, 2014, 70 (2), 1276-1282.
19. Lira-Barragán, L. F.; Ponce-Ortega, J. M.; Serna-González, M.; El-Halwagi, M. M. Synthesis of integrated absorption refrigeration systems involving economic and quantifying social benefits, *Applied Thermal Engineering*, 2013, 52, 402-419.
20. Hipólito-Valencia, B. J.; Rubio-Castro, E.; Ponce-Ortega, J. M.; Serna-González, M.; Nápoles-Rivera, F.; El-Halwagi, M. M., Optimal design of inter-plant waste energy integration, *Applied Thermal Engineering*, 2014, 62, 633-652.
21. Bonhivers, J. C., Srinivasan, B.; Stuart, P. R., New analysis method to reduce the industrial energy requirements by heat-exchanger network retrofit: Par 1 – Concepts, *Applied Thermal Engineering*, 2017, 119, 659-669.
22. Bonhivers, J. C.; Svensson, E.; Berntsson, T.; Stuart, P. R., Comparison between pinch analysis and bridge analysis to retrofit the heat exchanger network of a kraft pulp mill, *Applied Thermal Engineering*, 2014, 70, 369-379.
23. Ammar, Y.; Li, H.; Walsh, C.; Thornley, P.; Sharifi, V.; Roskilly, A. P., Reprint of "Desalination using low grade heat in the process industry: Challenges and perspectives", *Applied Thermal Engineering*, 2013, 53, 217-225.
24. Wang, Y.; Feng, X.; Chu, K. H., Trade-off between energy and distance related costs for different connection patterns in heat integration across plants, *Applied Thermal Engineering*, 2014, 70, 857-866.
25. Anastasovki, A., Design of common heat exchanger network for batch processes, *Applied Thermal Engineering*, 2014, 65,458-468.
26. Lee, J. Y.; Chen, C. L.; Wen, T. L.; Ng, D. K. S.; Foo, D. C. Y.; Wang, T. C., Synthesis and design of chilled water networks using mathematical optimization, *Applied Thermal Engineering*, 2013, 58, 638-649.
27. Assis, B. C. G.; Lemons, J. C.; Queiroz, E. M.; Pessoa, F. L. P.; Liporace, F. S.; Oliveira, S. G.; Costa, A. L- H., Optimal allocation of cleanings in heat exchanger networks, *Applied Thermal Engineering*, 2013, 58, 605-614.
28. Pan, M.; Bulatov, I.; Smith, R.; Kim, J. K., Optimization for the retrofit of large scale heat exchanger networks with different intensified heat transfer techniques, *Applied Thermal Engineering*, 2013, 53, 373-386.
29. Escobar, M.; Trierweiler, J. O., Optimal heat exchanger network synthesis: A case study comparison, *Applied Thermal Engineering*, 2013, 51, 801-826.
30. Dowidat, C.; Ulonska, K.; Bramsiepe, C.; Schembecker, G., Heat integration in batch processes including heat streams with time-dependent temperature progression, *Applied Thermal Engineering*, 2014, 70, 321-327.
31. Dotremont, C.; Kregersman, B.; Sih, R.; Lai, C. K.; Koh, K.; Seah, H., Seawater desalination with Memstill technology – A sustainable solution for the industry, *Water Practice and Technology*, 2010, 5 (2), 1-14.
32. Lee, H.; He, F.; Song, L.; Gilron, J.; Sirkar, K. K., Desalination with a cascade of cross-flow hollow fiber membrane distillation devices integrated with a heat exchanger, *AIChE Journal*, 2011, 57 (7), 1780-1795.
33. Qtaishat, M. R.; Banat, F., Desalination by solar-powered membrane distillation systems, *Desalination*, 2012, 308, 186-197.

34. Yee, T. F.; Grossmann, I. E., Simultaneous optimization models for heat integration-II, Heat exchanger network synthesis, *Computers and Chemical Engineering*, 1990, 14 (10), 1165-1184.
35. Lawson, K. W.; Lloyd, D. R., Membrane distillation II: Direct contact MD, *Journal of Membrane Science*, 1996, 120, 13-133.
36. Lawson, K. W.; Lloyd, D. R., Review: Membrane distillation, *Journal of Membrane Science*, 1997, 124, 1-25.
37. Khayet, M.; Matsuura, T., Membrane distillation: Principles and applications, Elsevier, Amsterdam, Netherlands, 2011.
38. Fane, A. G.; Fell, C. J. D., A review of fouling and fouling control in ultrafiltration, *Desalination*, 1987, 62, 117-136.
39. Chen, J. J. J., Comments on improvements on a replacement for the logarithmic mean, *Chemical Engineering Science*, 1987, 42 (10), 2488-2489.
40. Ehlinger, V. M.,; Gabriel, K. J.; Noureldin, M. M. B.; El-Halwagi, M. M., Process design and integration of shale gas to methanol, *ACS Sustainable Chemistry and Engineering*, 2013, 2 (1), 30-37.
41. Al-Obaidani, S.; Curcio, E.; Macedonio, F.; Di-Profio, G.; Al-Hinai, H.; Drioli, E., Potential of membrane distillation in seawater desalination: Thermal efficiency, sensitivity study, and cost estimation, *Journal of Membrane Science*, 2008, 323, 85-98.
42. Brooke, A.; Kendrik, D.; Meeruas, A.; Raman, R., GAMS-language guide, GAMS Development Corporation, Washington D. C., USA. 2014.

CHAPTER III

Synthesis of Optimal Thermal Membrane Distillation Networks

Thermal membrane distillation (TMD) is an emerging separation method which involves simultaneous heat and mass transfer through a hydrophobic semi-permeable membrane. Traditionally, studies of this technology have focused on the performance of individual modules. Because of purity and recovery requirements, multiple TMD modules may be used in various configurations including series, parallel, and combinations. Furthermore, there may be a need to reroute streams from one module to another or to recycle a stream to the same unit. The objective of this chapter is to develop a systematic approach to synthesize an optimal TMD network. A structural representation is developed to embed potential configurations of interest. A mathematical formulation is developed to transform the design problem into an optimization task that seeks to minimize the cost of the system. Two case studies are presented to illustrate the applicability of the developed approach and its merit over conventional design scenarios.

3.1 Introduction

Thermal membrane distillation (TMD) is emerging as a promising technology that can achieve high levels of separation. TMD has similarities to both membrane separation and distillation. Separation is based on the difference in vapor-liquid equilibrium and preferential permeation through a membrane. The driving force is the difference in the partial vapor pressure across a microporous hydrophobic membrane.[1,2] The feed is preheated to a temperature below boiling point. Then, the vapor diffuses through the membrane and is condensed and collected as permeate.

TMD offers several benefits over other existing desalination technologies including very high theoretical rejection of ions, macro molecules, colloids, cells, and other non-volatiles, low-level heating and moderate operating temperature and pressure, compact size, ability to handle concentrated feeds and it is relatively simple to increase capacity by adding TMD modules.[3,4] Membrane distillation systems may be classified into four configurations, a brief description can be found in literature.[4,5]

Many studies have shown the applicability of the TMD technology to produce ultrapure water and to remove non-volatile solutes in aqueous solutions such as salts, sugar, fruit juices and blood.[6-8] Furthermore, TMD has been shown to work well in water-treatment applications such as desalination and water purification.[9-12] Elsayed et al. (2014) developed an approach for modeling TMD units and thermal coupling with industrial facilities, which has the potential to decrease the unit cost of desalination from 7.56 \$/m^3 to 1.05 \$/m^3.[13]

It is worth noting that although TMD units offer high separation levels, there are several applications where a single stage is not sufficient to reach the desired purity levels. In such cases, permeate staging through layers of TMD units in series may be required. Furthermore, if the desired recovery of permeate is not achieved in one stage, reject (brine or retentate) staging may be required. Also, when brine discharge is limited or when levels approaching zero-liquid discharge (ZLD) are needed, there may be a need for reject staging. When the high-concentration reject is fed to a TMD unit, the concentration of permeate may be too high. This, in turn, requires further permeate staging. All of these issues call for the need to design networks of TMD units involving configurations in series and parallel. This

issue has not been addressed in the literature. The current work is aimed at synthesizing networks of TMD units.

While there has been no prior work on the synthesis of integrated TMD networks, several papers have been published in the area of synthesizing other types of membrane networks. El-Halwagi introduced a technique for synthesizing reverse osmosis networks (RONs) that account for network configuration and integration of multiple types of units.[14,15] Srinivas and El-Halwagi addressed the problem of synthesizing pervaporation networks using mixed-integer programming techniques.[16] Crabtree et al. developed an optimization procedure for synthesizing gas-permeation networks.[17] Zhu et al. proposed a multi-period approach to the design and scheduling of flexible RONs.[18] See et al. presented an optimization model for reverse osmosis (RO) desalination where the effect of the network configuration on the optimal cleaning schedule and total cost of a membrane desalination plant was considered.[19] An optimal design strategy was proposed by Qi and Henson for membrane networks for separating multicomponent gas mixtures.[20] Maskan et al. presented a model using individual reverse osmosis units to optimal configuration network configurations.[21] Kookos presented an approach for optimizing the selection of membrane material along with the structure of the membrane network.[22] Marriott and Sorensen introduced a design procedure using genetic algorithms for membrane systems such as pervaporation.[23] Uppaluri et al. proposed a robust stochastic technique using a simulated annealing procedure for minimizing the annualized cost of gas permeation networks.[24] Karuppiah et al. presented an optimization approach for synthesizing water treatment systems accounting for RO units,[25] whereas Abejón et al. considering RO units for ultra-purification of chemicals.[26] Alnouri and Linke proposed a systematic process synthesis and optimization approach that takes into consideration multiple water quality parameters in synthesizing RO desalination networks.[27,28] Du et al. proposes a multi-objective optimization approach for synthesizing RO networks for seawater desalination.[29] Almansoori and Saif presented an optimal integrated RO system and a pressure retarded osmosis (PRO) for seawater desalination and power generation.[30] Saif et al. presented an approach for the optimal design of RO networks considering variations in the stream properties.[31] Dahdah and Mitsos introduced a methodology to identify improved thermal-based desalination structures, the

model considers either a multi-effect distillation system (MED) or a stage in a multi-stage flash system (MSF) to determine the best configuration.[32]

As discussed earlier, several applications require the use of multiple TMD modules that may be arranged in series, parallel, or a combination. In addition to the configuration of the TMD units, the use of heaters and coolers throughout the network is an important design variable. In order to enhance the permeation flux, the feed to each TMD may be heated to some optimal temperature. The vapor permeate has to be condensed. Therefore, the placement and duties of heaters, coolers, and heat exchangers (integrating heat transfer) must be considered. Furthermore, because of the relatively low water recover per pass of TMD, it may be necessary to increase the feed flow rate to each stage through recycling the reject stream. The extent and allocation of reject recycle are optimization variables. These issues contribute to the complexity of synthesizing an optimal TMD networks (TMDN). A TMDN is composed of multiple TMD modules, pumps, heaters, condensers, mixers, and splitters. This chapter first describes the problem of synthesizing a system of TMD modules and then presents a systematic procedure for designing an optimal TMDN based on a new superstructure and a mathematical programming formulation.

3.2 Problem statement

The synthesis of a TMDN can be stated as follows: Given a feed flow rate Q_F and feed concentration C_F, it is desired to synthesize a TMDN to obtain a permeate stream (e.g., clean water) with targeted flow rate and purity at minimum cost. The TMDN consists of several interconnected TMD modules, pumps, heaters, and condensers, whose structure, interconnection, configuration, sizes, and operating conditions which must be optimized. The total annual cost includes the capital costs for the units (fixed and variable costs) as well as the operating cost minus the revenues obtained from the sale of the permeate and/or the concentrated retentate.

The TMDN synthesis problem involves addressing several design challenges. The first issue is the need to consider many configurations of the system. Some common configurations for TMDN are in series, parallel and combined arrangements. **Figures 3.1 and 3.2** illustrate examples of potential configurations for TMDN. The series arrangement (see **Figure 3.1a**) is the one typically used when the desired extent of separation exceeds the

maximum ability of one stage. TMD modules are arranged in parallel (**Figure 3.1b**) when the flow rate of the feed to the network exceeds the capacity of an individual module. The tapered arrangement (**Figure 3.2**) of TMD units (sometimes referred to as the "Christmas tree" arrangement) is a hybrid of the series and parallel configurations to address the need for permeate recovery and purity as well as constraints on liquid discharge.

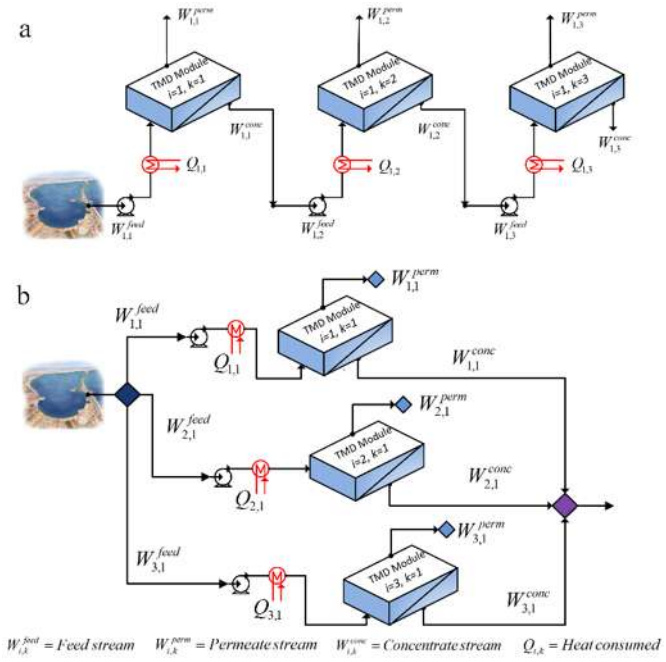

Figure 3.1. Schematic representation of TMD modules in (a) series arrangement and (b) parallel arrangement.

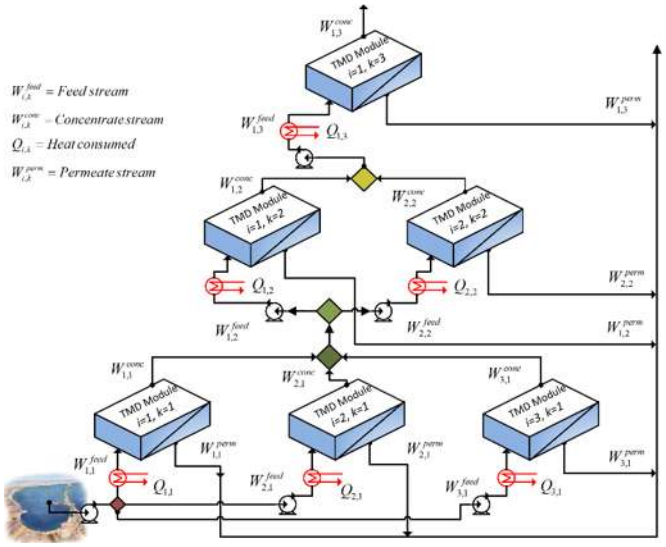

Figure 3.2. Tapered TMDN configuration.

In addition to the design challenges associated with the selection of the system configuration, there are several other design decisions that must be included:

- The number of modules to be used.
- The total membrane area for the network.
- The configuration for the modules (e.g., in series, parallel, combination).
- The optimal values of heating and cooling duties.
- The extent and allocation of reject recycle.
- The optimal values of operating variables for each module (temperature and concentration).

The aforementioned challenges call for the development of a systematic procedure and a mathematical formulation that can address these design tasks and provide optimal solutions to the synthesis of the TMDN problem. This is presented in the next section.

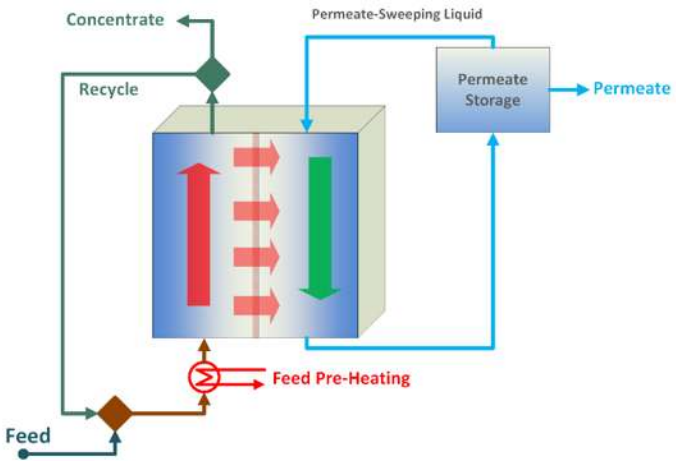

Figure 3.3. TMD scheme with reject recycle and permeate sweeping liquid.

3.3 Design approach

A source-sink approach presented by El-Halwagi et al. was employed to represent the network configuration.[33] A source is a process stream that is rich in the constituent(s) that has to be removed in the separation task. For this case, we propose a building block consisting of a TMD module (see **Figure 3.3**). The TMD module offers advantages of simplicity of construction, operation, and maintenance as well as consistent performance. In the TMD

module, the feed water is preheated. Enough heat should be provided to induce the evaporation at a moderate temperature. The heat to be supplied and the temperature of the stream fed to the TMD unit are optimization variables. The water vapor travels through the membrane and is condensed on the permeate side using a recirculating permeate-sweeping liquid which is colder than the feed. The size of each element is an optimization variable (including a zero size, which indicates that the element does not exist). Each TMD unit produces two sources (permeate and reject). Either one or both may be rerouted back to the network to be assigned to new sinks.

Figure 3.4 shows the proposed superstructure for designing an integrated TMDN. The feed may be split into several fractions assigned to the TMD units. In turn, each unit produces two sources (permeate and reject) that may be recycled or fed to another unit. The problem consists of determining the optimum network configuration, unit sizes, stream allocation, and operating conditions. In formulating the program, the following assumptions were used:

- Separation performance of the thermal membrane distillation modules is a function of temperature. This is due to the fact that the flux of permeate is a function of temperature.
- Temperature at a module is independent of that at other modules.
- Specific heat of the mixture does not vary with the temperature.
- Only a single component is considered in the total feed concentration.

This section presents the proposed optimization model for designing the TMDN based on the superstructure shown in **Figure 3.4**. The indexes used in this model are the following: i represents the number of TMD units connected in a parallel arrangement, k indicates the number of units connected in series, and i' is used to indicate a subsequent line of TMD modules. For better understanding of the model the super indexes are also defined: $feed$ is the raw feed stream from initial or previous stage , TMD represents the streams that feed the TMD unit, $conc$ is the stream that leaves the TMD unit before the recycle divisor, $recycle$ is a recycle process stream, rej is the rejected stream from TMD process which is sent to another stage and $perm$ is the permeate stream.

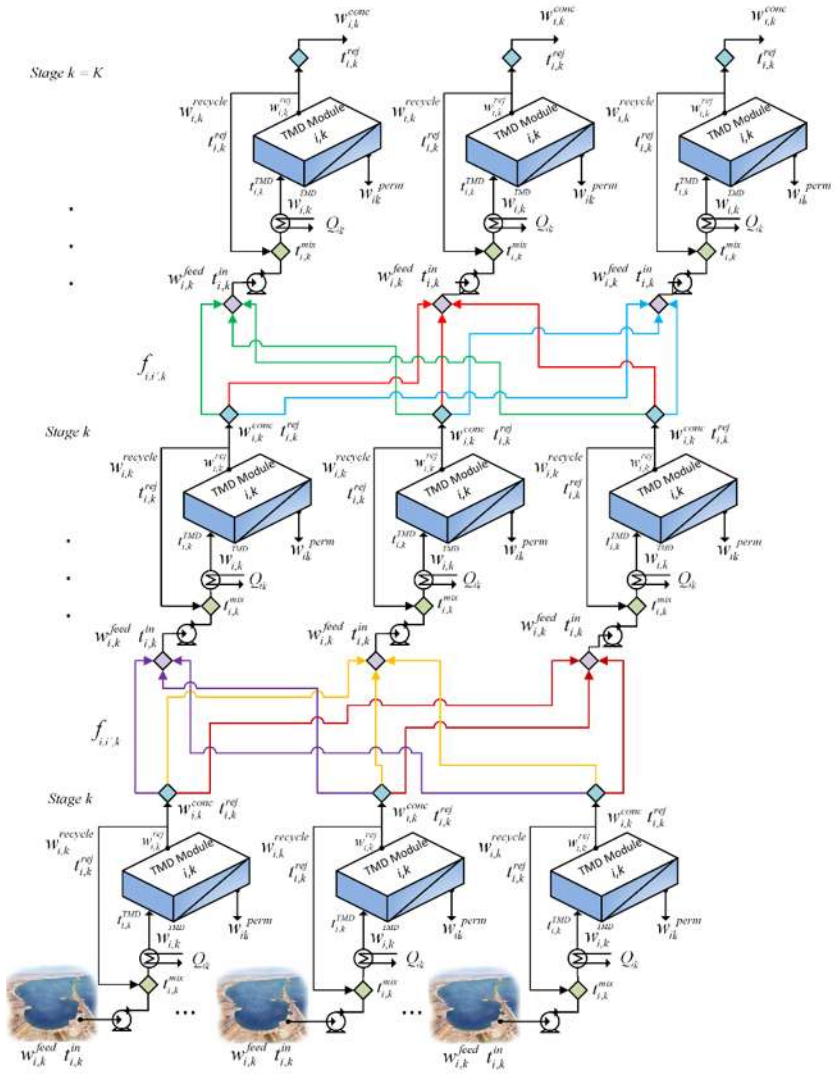

Figure 3.4. The proposed superstructure for synthesizing an integrated TMDN.

3.3.1 Mass balance, salt balance and energy balance in the recycle mixers

A feed stream (e.g., seawater) is transported directly from the origin (e.g., sea) to the storage units. The main process starts with a stream mixer for which the mass balance in this unit is the sum of the feed flow rate ($w_{i,k}^{feed}$) plus the recycle stream ($w_{i,k}^{recycle}$) to give the feed flow rate to the TMD unit ($w_{i,k}^{TMD}$).

$$w_{i,k}^{TMD} = w_{i,k}^{feed} + w_{i,k}^{recycle}, \quad \forall i \in I, \forall k \in K \tag{3.1}$$

Then, the solute balance for the recycle mixer is given as follows:

$$w_{i,k}^{TMD} z_{i,k}^{TMD} = w_{i,k}^{feed} z_{i,k}^{feed} + w_{i,k}^{recycle} z_{i,k}^{rej}, \quad \forall i \in I, \forall k \in K \tag{3.2}$$

Where $z_{i,k}^{TMD}$ is the concentration of the stream ($w_{i,k}^{TMD}$) to be fed into the TMD unit, $z_{i,k}^{feed}$ is the concentration of the raw feed ($w_{i,k}^{feed}$) and $z_{i,k}^{rej}$ is the concentration in the recycled stream from the concentrate ($w_{i,k}^{recycle}$).

The energy balance in the mixer can be stated as follows:

$$w_{i,k}^{TMD} \mathrm{Cp}_{i,k}^{TMD}(t_{i,k}^{mix}) = w_{i,k}^{feed} \mathrm{Cp}_{i,k}^{feed}(t_{i,k}^{in}) + w_{i,k}^{recycle} \mathrm{Cp}_{i,k}^{rej}(t_{i,k}^{rej}), \quad \forall i \in I, \forall k \in K \tag{3.3}$$

where the temperature $t_{i,k}^{mix}$ is the result of the temperatures from the mixed streams $w_{i,k}^{feed}$ and $w_{i,k}^{recycle}$, and $t_{i,k}^{in}$ and $t_{i,k}^{rej}$ are the temperatures of the raw feed and the recycled stream, respectively.

3.3.2 Energy balance in the heaters

The mixed stream is pre-heated using heating utilities, the energy balance in the heater can be described by the following equation:

$$w_{i,k}^{TMD} \mathrm{Cp}_{i,k}^{TMD}(t_{i,k}^{TMD} - t_{i,k}^{mix}) = Q_{i,k}^{Heating}, \quad \forall i \in I, \forall k \in K \tag{3.4}$$

The total water flow rate ($w_{i,k}^{TMD}$) is heated from a temperature $t_{i,k}^{mix}$ to the operating temperature in the TMD unit ($t_{i,k}^{TMD}$), where $Q_{i,k}^{Heating}$ is the heat required to reach the TMD operating temperature.

3.3.3 Mass balance and salt balance for TMD units

For the process, the amount of feed assigned to the TMD unit ($w_{i,k}^{TMD}$) is equal to the permeate ($w_{i,k}^{perm}$) plus the rejected stream ($w_{i,k}^{rej}$).

$$w_{i,k}^{TMD} = w_{i,k}^{perm} + w_{i,k}^{rej}, \quad \forall i \in I, \forall k \in K \tag{3.5}$$

In the case of desalination, the salinity of seawater or brackish water depends on the region and affects the amount of the obtained permeate at the end of the treatment stages ($w_{i,k}^{perm}$).

$$z_{i,k}^{TMD}\, w_{i,k}^{TMD} = \mathrm{z}_{\mathrm{i,k}}^{\mathrm{perm}}\, w_{i,k}^{perm} + z_{i,k}^{rej}\, w_{i,k}^{rej}, \qquad \forall i \in I, \forall k \in K \tag{3.6}$$

3.3.4 Mass balance around the recycle splitters

The stream that leaves the TMD unit ($w_{i,k}^{rej}$) is divided into two streams: $w_{i,k}^{recycle}$ that is returned to the main process and $w_{i,k}^{conc}$ that can be sent to another TMD unit:

$$w_{i,k}^{rej} = w_{i,k}^{recycle} + w_{i,k}^{conc}, \qquad \forall i \in I, \forall k \in K \tag{3.7}$$

Notice that because of splitting, $w_{i,k}^{recycle}$ and $w_{i,k}^{conc}$ have the same concentration ($z_{i,k}^{rej}$), temperature ($t_{i,k}^{rej}$) and specific heat capacity ($\mathrm{Cp}_{\mathrm{i,k}}^{\mathrm{rej}}$) as the original stream $w_{i,k}^{rej}$.

3.3.5 Mass balance for splitters

The concentrated water obtained from each TMD unit from each stage *k* ($w_{i,k}^{conc}$) is segregated to be sent to the next stage through the flows $f_{i,i',k}$:

$$w_{i,k}^{conc} = \sum_{i'} f_{i,i',k}, \quad \forall i \in I, \forall k \in K, k \neq NOK \tag{3.8}$$

Notice that previous relationship is not valid for the last stage of the superstructure because this concentrated water from the last stage is not used. In this case, *NOK* is the total number of stages. Also, $f_{i,i',k}$ has the same concentration ($z_{i,k}^{rej}$), temperature ($t_{i,k}^{rej}$) and specific heat capacity ($\mathrm{Cp}_{\mathrm{i,k}}^{\mathrm{rej}}$) as the original stream $w_{i,k}^{conc}$.

3.3.6 Mass balance, solute (or pollutant) balance and energy balance for mixers

The sum of the concentrated water from the stage *k* from any TMD unit *i* ($f_{i,i',k}$) can be fed to the TMD units of the next stage ($w_{i',\mathrm{k+1}}^{feed}$):

$$\sum_{i} f_{i,i',k} = w_{i',\mathrm{k+1}}^{feed}, \qquad \forall i' \in I', \forall \mathrm{k} \in K, k \neq NOK \tag{3.9}$$

The previous relationship is not valid for the last stage because the last concentrated water is not fed to any other TMD unit.

The concentration in the mixer ($z_{i',k}^{feed}$) is a function of the concentration of the reject from the preceding stage from any unit *i* ($z_{i,k}^{rej}$):

$$\sum_i z_{i,k}^{rej} \; f_{i,i',k} = z_{i',k+1}^{feed} \; w_{i',k+1}^{feed}, \qquad \forall i' \in I', \forall k \in K, k \neq NOK \tag{3.10}$$

To determine the temperature of the stream entering the TMD unit for stages other than the first, an energy balance is used for the mixer before any TMD unit. This way, the sum of the heat inlet from the streams from the previous stage ($\sum_i f_{i,i',k-1} \, \mathrm{Cp}_{i,k-1}^{rej}(t_{i,k-1}^{rej})$) is equal to the heat inlet to the TMD unit ($w_{i',k+1}^{feed} \mathrm{Cp}_{i',k+1}^{feed}(t_{i',k+1}^{in})$) for each TMD unit *i'* in any stage *k*, and this is stated as follows:

$$\sum_i f_{i,i',k} \mathrm{Cp}_{i,k}^{rej}(t_{i,k}^{rej}) = w_{i',k+1}^{feed} \mathrm{Cp}_{i',k+1}^{feed}(t_{i',k+1}^{in}), \quad \forall i' \in I', \forall k \in K, k \neq NOK \tag{3.11}$$

where $\mathrm{Cp}_{i,k-1}^{rej}$ and $\mathrm{Cp}_{i',k}^{feed}$ are the heat capacities for streams of the previous stage and the one for the streams entering the TMD unit *i'* of the stage *k*, respectively. It should be noted that previous balance is not valid for the first stage because the inlet temperature is known for the feed of the network (e.g., seawater).

3.3.7 Design equations for each TMD unit

For modeling the required TMD units (see **Figure 3.4**), the amount of permeated water is strongly influenced by the energy provided to the unit. In this context, the heating for each TMD unit is provided by external utilities and this is equal to the feed flow rate ($w_{i,k}^{TMD}$) times the heat capacity of this stream ($\mathrm{Cp}_{i,k}^{TMD}$) and the temperature difference ($t_{i,k}^{TMD} - t_{i,k}^{mix}$). Only a fraction of this added heat is used in vaporizing the permeate. The fraction is given by the efficiency factor ($\eta_{i,k}$). Hence, the heat balance for the TMD unit is given by:

$$\eta_{i,k} Q_{i,k}^{heating} = w_{i,k}^{perm} \Delta h_{vw_{i,k}}, \qquad \forall i \in I, \forall k \in K \tag{3.12}$$

Where $w_{i,k}^{perm}$ is the permeate flow rate and Δh_{vw} is the latent heat of vaporization. Experimental data may be used to measure the thermal efficiency. Alternatively, semi-empirical expressions may be used. For instance, Elsayed et al. proposed the following

expression for certain TMD modules (a polypropylene hollow-fiber membrane MD020CP2N manufactured by Microdyn):[13]

$$\eta_{i,k} = 1 - \frac{1.5 \cdot \frac{k_{m_{i,k}}}{\delta}(t_{mfeed_{i,k}} - t_{mperm_{i,k}})}{j_{w_{i,k}} \Delta h_{vw_{i,k}} + \frac{k_{m_{i,k}}}{\delta}(t_{mfeed_{i,k}} - t_{mperm_{i,k}})} \qquad \forall i \in I, \forall k \in K \tag{3.13}$$

Where, $k_{m_{i,k}}$ is the thermal conductivity of the membrane, δ is the membrane thickness, $j_{w_{i,k}}$ is the permeate flux passing through the membrane, $t_{mfeed_{i,k}}$ is the temperature at the membrane on the feed side and $t_{mperm_{i,k}}$ is the temperature at the membrane on the permeate side. An example of an expression for calculating the thermal conductivity of a certain membrane is the correlation given by Elsayed et al.[13]

$$k_{m_{i,k}} = 1.7 \times 10^{-7} t_{m_{i,k}} - 4.0 \times 10^{-5} \qquad \forall i \in I, \forall k \in K \tag{3.14}$$

3.3.8 Flux modeling equations

The TMD unit is described using the modeling equations given by Elsayed et al. (2014).[13] Permeate flux passing through the membrane ($j_{w_{i,k}}$) is calculated using the following expression:

$$j_{w_{i,k}} = b_{w_{i,k}} \left(p^{vap}_{wfeed_{i,k}} \gamma_{wfeed_{i,k}} x_{wfeed_{i,k}} - p^{vap}_{wperm_{i,k}} \right), \quad \forall i \in I, \forall k \in K \tag{3.15}$$

where $x_{wfeed_{i,k}}$ is the mole fraction of water in feed, $p^{vap}_{wfeed_{i,k}}$ is the vapor pressure in the feed side and $p^{vap}_{wperm_{i,k}}$ is the vapor pressure in the permeate side of the membrane, these vapor pressures are a function of the temperature and these are calculated by Antoine's equation as follows:

$$P^{vap}_{wfeed_{i,k}} = \exp\left(23.1964 - \frac{3816.44}{t_{mfeed_{i,k}} - 46.13} \right), \qquad \forall i \in I, \forall k \in K \tag{3.16}$$

$$P^{vap}_{wperm_{i,k}} = \exp\left(23.1964 - \frac{3816.44}{t_{mperm_{i,k}} - 46.13} \right), \qquad \forall i \in I, \forall k \in K \tag{3.17}$$

$b_{w_{i,k}}$ is a parameter for the molecular diffusion of water in the air, and it can be calculated by multiplying the membrane permeability (B_{wB}) by the average temperature:[34]

$$b_{w_{i,k}} = B_{wB} t_{m_{i,k}}^{1.334}, \qquad \forall i \in I, \forall k \in K \tag{3.18}$$

$t_{m_{i,k}}$ is the average temperature in the TMD module determined as follows:

$$t_{m_{i,k}} = \frac{t_{i,k}^{TMD} + t_{i,k}^{perm}}{2}, \qquad \forall i \in I, \forall k \in K \tag{3.19}$$

$\gamma_{wfeed_{i,k}}$ is the activity coefficient that is a function of the concentration. In the case of NaCl removal, it can be calculated as follows:

$$\gamma_{wfeed_{i,k}} = 1 - 0.5 x_{NaCl_{i,k}} - 10 x_{NaCl_{i,k}}^2, \qquad \forall i \in I, \forall k \in K \tag{3.20}$$

Where $x_{NaCl_{i,k}}$ is the mole fraction of NaCl in the feed.

Then, the molar fraction of NaCl in the feed ($x_{NaCl_{i,k}}$) is a function of the mass concentration in the feed of the TMD unit ($z_{i,k}^{TMD}$), the molecular weight of the water and the atomic weight of NaCl, and can be calculated with the next equation:

$$x_{NaCl_{i,k}} \cdot \left[\left(z_{i,k}^{TMD} / PM_{NaCl} \right) + \left(1 - z_{i,k}^{TMD} / PM_{wt} \right) \right] = \left(z_{i,k}^{TMD} / PM_{NaCl} \right) \qquad \forall i \in I, \forall k \in K \tag{3.21}$$

Finally, the mole fraction of the water in the feed is given as follows:

$$x_{wfeed_{i,k}} = 1 - x_{NaCl_{i,k}} \qquad \forall i \in I, \forall k \in K \tag{3.22}$$

3.3.9 Membrane area and temperature profile

The membrane area can be calculated by dividing the permeate water flow rate ($w_{i,k}^{perm}$) by the water flux:

$$A_{m_{i,k}} = \frac{w_{i,k}^{perm}}{j_{w_{i,k}}}, \qquad \forall i \in I, \forall k \in K \tag{3.23}$$

The temperature profile in the membrane can be calculated through the use of the temperature polarization coefficient given by the next equation:[35]

$$\theta_{i,k} = \frac{t_{mfeed_{i,k}} - t_{mperm_{i,k}}}{t_{i,k}^{TMD} - t_{i,k}^{perm}}, \qquad \forall i \in I, \forall k \in K \tag{3.24}$$

Where $\theta_{i,k}$ is the temperature polarization coefficient and $t_{i,k}^{TMD}$ is the temperature of the feed in the bulk in the feed side, $t_{mfeed_{i,k}}$ is the temperature of the feed at the membrane, $t_{i,k}^{perm}$ is the temperature of permeate in the bulk, $t_{mperm_{i,k}}$ is the temperature of permeate at the membrane, as shown in **Figure 3.5**.

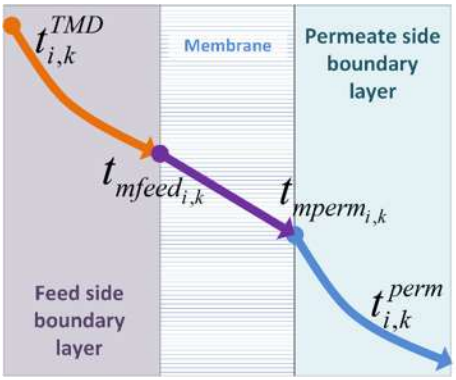

Figure 3.5. Temperature profile for the boundary layers at the membrane.[36]

The temperature polarization coefficient ($\theta_{i,k}$) may be evaluated from experimental data. Alternatively, correlations may be used for certain membranes. For instance, Elsayed et al. showed a linear behavior as a function of the temperature according to the next expression:[13]

$$\theta_{i,k} = 1.104 - 0.00086 \cdot t_{i,k}^{TMD} \qquad \forall i \in I, \forall k \in K \tag{3.25}$$

The temperature for the reject stream ($t_{i,k}^{rej}$) is an average between the temperature in the bulk ($t_{i,k}^{TMD}$) and the temperature at the membrane boundary layer ($t_{mfeed_{i,k}}$), as shows in the next expression:

$$t_{i,k}^{rej} = \frac{t_{i,k}^{TMD} + t_{mfeed_{i,k}}}{2} \qquad \forall i \in I, \forall k \in K \tag{3.26}$$

The vaporization of water ($\Delta h_{vw_{i,k}}$) in the feed side is calculated from the next correlation:[13]

$$\Delta h_{vw_{i,k}} = 3190 - 2.5009 t_{mfeed_{i,k}} \qquad \forall i \in I, \forall k \in K \tag{3.27}$$

3.3.10 Logical relationships

Logical relationships are required to determine if a potential unit from the superstructure is required in the optimal solution. This depends on the amount of water that is recovered, the final concentration of permeate, and the impact on the total cost (capital and operating). Therefore, binary variables are used to indicate the existence or absence of such units (i.e., the binary variable associated with a given TMD unit is one when the unit exists, otherwise it is zero, $y_{i,k} = Unit\ existance, \{0,1\}$). This is modeled through the following relationship:

$$\mathrm{W}^{\min} \cdot y_{i,k} \le w_{i,k}^{feed} \le \mathrm{W}^{\max} \cdot y_{i,k}, \qquad \forall i \in I, \forall k \in K \tag{3.28}$$

Where $\mathrm{W}^{\max}$ and $\mathrm{W}^{\min}$ are upper and lower limits for the flow rate of the feed that can be used in a TMD unit. When the inlet flow rate to the unit *i* in the stage *k* ($w_{i,k}^{feed}$) is greater than zero then the associated binary variable ($y_{i,k}$) must be one. On the other hand, when the binary variable $y_{i,k}$ is zero (i.e., the associated TMD unit does not exist), the treated flow rate ($w_{i,k}^{feed}$) must be zero.

3.3.11 Total feed water

The total feed (or total raw water) "*TRW*" fed to the TMDN is the sum of the feed streams entering stage 1 in any unit *i*. Therefore,

$$TRW = \sum_{i} w_{i,1}^{feed} \tag{3.29}$$

Hence, the maximum and minimum amount of water that can be supplied to the entire system is stated as follows:

$$\mathrm{TRW}^{\min} \le TRW \le \mathrm{TRW}^{\max} \tag{3.30}$$

3.3.12 Total permeated water

The total permeated water (*TPW*) is equal to the sum of the permeated water from all units *i* of any stage *k* ($w_{i,k}^{perm}$):

$$TPW = \sum_i \sum_k w_{i,k}^{perm} \tag{3.31}$$

3.3.13 Restriction for the maximum amount of water

The maximum and minimum amount of permeate are bounded as follows:

$$\mathrm{TPW}^{\min} \leq TPW \leq \mathrm{TPW}^{\max} \tag{3.32}$$

Where $\mathrm{TPW}^{\min}$ and $\mathrm{TPW}^{\max}$ are the lower and upper limits for the demanded clean permeate.

3.3.14 Restriction of the concentration in the reject (or brine)

The maximum concentration allowable in the reject must meet the following constraint:

$$z_{i,k}^{rej} \leq \mathrm{z}^{\max} \cdot y_{i,k} \qquad \forall i \in I, \forall k \in K \tag{3.33}$$

$\mathrm{z}^{\max}$ is multiplied by the binary variable $y_{i,k}$ because this constraint only applies when the unit exists.

3.3.15 Total heat consumed

The total heat consumed in the network ($THeat$) accounts for the heat consumed in each stage of the superstructure for each TMD unit ($Q_{i,k}^{Heating}$) as follows:

$$THeat = \sum_i \sum_k Q_{i.k}^{Heating} \tag{3.34}$$

3.3.16 Total membrane area

The total membrane area needed in the desalination units (TMA) is the sum of the areas in each stage in the superstructure for each TMD unit ($A_{m_{i,k}}$) as follows:

$$TMA = \sum_i \sum_k A_{m_{i,k}} \tag{3.35}$$

Where the maximum area in the TMD units is bounded by the maximum available size of a TMD unit as follows:

$$A_{m_{i,k}} \leq \mathrm{A}_{\mathrm{m}}^{\max} \qquad \forall i \in I, \forall k \in K \tag{3.36}$$

3.3.17 Initial data

The concentration in the first stage of the superstructure ($z_{i,1}^{feed}$) is the concentration of the water to be treated. This is a known value for any TMD unit in stage 1. For instance, in the case of the raw feed being seawater, the constraint is given by:

$$z_{i,1}^{feed} = z^{seawater} \qquad \forall i \in I \tag{3.37}$$

Also, the temperature in the first stage of the raw feed water ($t_{i,1}^{in}$) is a known value and this is valid for any TMD unit in stage 1, $t_{i,1}^{in}$ depends on the treated feed. For instance, in the case when the feed is at ambient temperature, the constraint is given by:

$$t_{i,1}^{in} = T^{amb} \qquad \forall i \in I \tag{3.38}$$

3.3.18 Objective function

The total annual cost for the TMDN takes into account the fixed cost for the TMD units as a function of the membrane area (C_{F1}^{TMD}) for TMD modules and as a function of the flow rate of the stream to be fed (C_{F2}^{TMD}) for non-membrane elements, the installation costs of the TMD unit (C_{inst}^{TMD}), and the operating cost for the TMD units (C_{Op1}^{TMD} ; C_{Op2}^{TMD} ; C_{Op3}^{TMD}). The exponent β_k^{TMD} is a factor used to account for the economy of scale. The terms $Cost^{Heating}$ and $Cost^{Cooling}$ are the unit cots for heating and cooling utilities, respectively. Additionally, k_F is the factor used to annualize the investment and H_Y is a factor used to account the operating time per year. It is worth noting that the fixed charge for the involved units is only considered when the units exist through the use of the binary variables ($y_{i,k}$). Thus, the total annual cost is stated as follows:

$$TAC = \left[\begin{array}{c} k_F \sum_i \sum_k \left[\left(C_{inst}^{TMD} \cdot y_{i,k} \right) + \left(C_{F1}^{TMD} \cdot A_{m_{i,k}} \right)^{\beta_2} + \left(C_{F2}^{TMD} \cdot w_{i,k}^{TMD} \right)^{\beta_3} \right] \\ + H_Y \sum_i \sum_k \left[C_{Op1}^{TMD} \cdot y_{i,k} + C_{Op2}^{TMD} \cdot \left(1 - \xi_{i,k} \right) w_{i,k}^{feed} + C_{Op3}^{TMD} \cdot w_{i,k}^{TMD} \right] \\ + H_Y \sum_i \sum_k \left[Cost^{Heating} \cdot Q_{i,k}^{Heating} \right] \end{array} \right] \tag{3.39}$$

Where the fraction of recovery ($\xi_{i,k}$) can be obtained by dividing the permeate water flow rate ($w_{i,k}^{perm}$) by the feed water flow rate at each stage:

$$\xi_{i,k} = \frac{w_{i,k}^{perm}}{w_{i,k}^{feed}} \qquad \forall i \in I, \forall k \in K \tag{3.40}$$

The annual gross profit (AGP) can be calculated as the annual permeate value (APV) minus the total annual cost, according to the following equation:

$$AGP = APV - TAC \tag{3.41}$$

Table 3.1. Data for the examples presented.[13]

Parameter	Units	Value
A_m^{max} = Maximum permissible area in TMD unit	m^2	100 (for Case Study 1) and 30 for Case Study 2
B_{wB} = Temperature independent base value for the permeability	$kg/(m^2 \cdot s \cdot Pa \cdot K^{1.334})$	$7.5x10^{-8}$
C_{F1}^{TMD} = fixed cost of the membrane-related units	$\$/m^2$	58.5
C_{F2}^{TMD} = fixed cost of the non-membrane units	\$/(kg/s)	1,115
C_{inst}^{TMD} = Installation cost of the TMD module	$\$/m^2$	25% of the purchase cost
C_{Op1}^{TMD} = Operational cost related to the TMD module	\$	1,411
C_{Op2}^{TMD} = Operational cost related to the reject processing	\$	43
C_{Op3}^{TMD} = Operational cost related to the feed treatment	\$	1,613
Z^{max} = Maximum permissible concentration	wt%	0.5
β_k^{TMD} = Exponent for area cost of the modules	--	1.0
$\xi_{i,k}$ = Fractional recovery of permeate in TMD unit	--	0.8
δ = Membrane thickness	mm	0.00065

3.4 Case studies

Two case studies are presented to show the applicability of the proposed approach for designing TMDN, the first one corresponds to a seawater desalination process whereas the second one corresponds to treating wastewater from the syrup manufacturing process. **Table 3.1** shows key information for the two case studies.[13] The optimization formulation was

developed based on the aforementioned mathematical problem. The problem was coded using the software GAMS.[37] Where the solver DICOPT were used to solve the associated mixed-integer nonlinear programing. To solve the problem, a computer with an Intel® Core TM i7-4700MQ processor at 2.40GHz and 8 GB of RAM was used. The problem and solution statistics are shown in **Table 3.2**.

Table 3.2. Problem statistics.

Item	Value
Number of continuous variables	1,030
Number of binary variables	25
Number of constraints	964
CPU time (s)	5.56

3.4.1 Case Study 1. Seawater desalination process

Worldwide fresh water demand is rising, largely driven by the increase in the population and living standards, seawater and brackish water desalination have become an alternative for new water supply in coastal areas, especially in areas with stressed and overdrawn fresh water resources.

The proposed optimization model described in section 3 was used to synthesize a TMDN for brackish water desalination on the coast of Saudi Arabia. The feed has 0.1% (1,000 ppm) dissolved NaCl and an initial flow rate of 3456 kg/h. The size of each module is considered with a maximum membrane area of 100 m^2/module. The objective function consists of maximizing the annual gross profit obtained from the sales of permeate minus the total annualized cost of the system. The problem data are given in **Table 3.3**. [13,38]

The optimal solution obtained for the case study is presented as the solution for the first scenario. In addition, nine additional configurations were analyzed to show the advantages of the proposed approach.

Table 3.3. Data for Case Study 1

General data: Desalination[13]		
Concept	Unit	Value
Heating cost	$/10^9 J heating utility	5.00
Cooling cost	$/10^9 J cooling water at 293 K	4.00
Pumping	$/m^3	0.056
Labor	$/m^3	0.030
Cost of permeate	$/m^3	8.00
Initial flow rate	kg/h	3,456
Initial temperature	K	300
Initial concentration	% weight	0.1
Annual operation	h	8,000
Membrane specifications[13,38]		
Membrane thickness	mm	0.65
Membrane cost	$/m^2	90
Maximum membrane area per module	m^2	100
Membrane life time	year	4

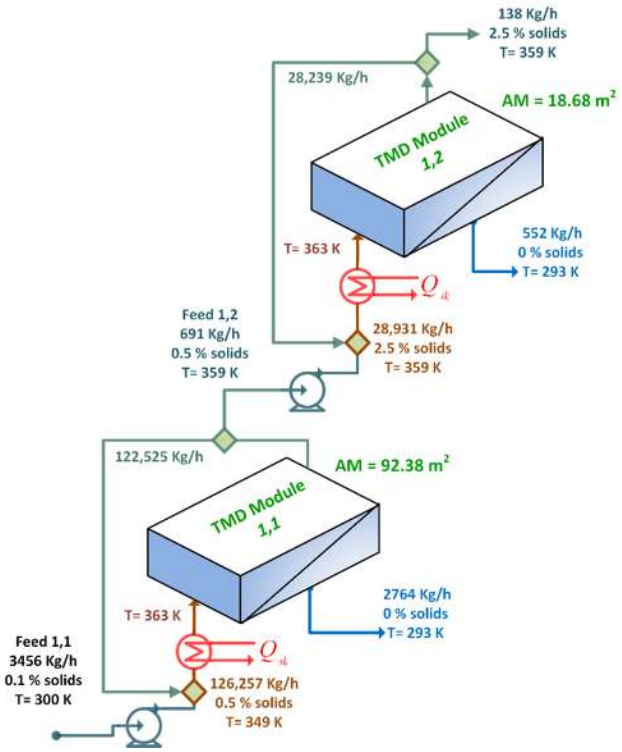

Figure 3.6. Optimal TMDN for Case Study1.

The optimal solution (first scenario) is shown in **Figure 3.6.** It involves two units in series. A total recovery of 95.90% of water as permeate was obtained. The feed temperature for the first unit (1,1) is 300 K and the feed temperature for the second unit (1,2) is 359 K.

The first unit has a membrane area of 92.4 m^2 which represents 83.2% of the total required area of membrane and produces a permeate flow rate of 2,764 kg/h which is 83.4% of the total permeate of the TMDN. The total permeate is 3,316 kg/h, which yields an annual sales revenue of $212,340/y. The total annual cost is $170,347/y and the annual gross profit for the optimal solution is $41,993/y. Unit cost for an optimal solution is 6.3 $\$/m^3$, which is relatively high, however, Elsayed et al. (2014) have been reduced unit cost substantially by coupling with industrial facilities. **Table 3.4** shows the main economic results for the optimal configuration and for other analyzed scenarios.

Table 3.4. Optimal results for Case Study 1 (Scenario 1) and comparison with 11 other scenarios.

		Scenario								
Concept	Unit	Optimal	2	3	4	5	6	7	8	9
Total membrane area	m^2	111.06	92.38	92.38	92.37	115.09	111.03	111.02	111.02	115.05
Number of TMD units	--	2	1	2	3	3	3	4	4	6
Thermal efficiency	--	0.900	0.902	0.902	0.902	0.890	0.900	0.900	0.900	0.880
Total permeate	kg/h	3,316	2,764	2,764	2,763	3,426	3,316	3,315	3,316	3,425
Total feed water	kg/h	3,456	3,456	3,456	3,456	3,456	3,456	3,456	3,456	3,456
Total recovery	%	95.90	80.00	79.97	79.94	98.00	96.00	95.92	96.40	98.60
Total heating cost	$/y	37,633	31,355	31,360	31,344	38,875	37,632	37,616	37,632	38,864
Total annual cost	$/y	170,347	136,644	142,330	146,742	180,665	173,780	178,192	180,398	195,126
Permeate value	$/y	212,340	176,950	176,948	176,948	219,400	212,275	212,275	212,275	219,335
Annual profit	$/y	41,993	40,306	34,617	30,205	38,735	38,495	34,083	31,877	24,209
Unit cost	$\$/m^3$	6.3	6.1	6.4	6.6	6.6	6.5	6.7	6.8	7.1

To show the merits of the optimal solution (Scenario 1), 9 other scenarios are synthesized, analyzed, and compared with the optimal solution. These scenarios are shown by **Figures 3.7-3.11**. Also, the results of these scenarios are shown in **Table 3.4**.

Figure 3.7a shows the scenario 2 considering only one TMD unit, for this case, the total heating cost is $31,355/y, the total permeate is 2,764 Kg/h which has an annual value of $176,950/y. The annual gross profit for this case is $40,306/y which is 4% less than the

optimal solution. **Figure 3.7b** presents scenario 3 considering two TMD units in a parallel arrangement. The total heating cost is $31,360/y and the total permeate is 2,764 Kg/h with an annual value of $176,948/y. The total annual cost for this scenario is $142,330/y and the annual gross profit is $34,617/y which is 17.6% less than the optimal solution. Scenario 4 (see **Figure 3.7c**) shows three TMD units ordered in a parallel arrangement, this change increases the total annual costs up to $146,742/y, which leaves an annual gross profit of $30,205/y that is 28.1% less than the optimal solution.

Scenario 5 presents three units in a series arrangement as shown in **Figure 3.8a**, for this case, the total annual cost is $180,665/y leaving an annual gross profit $38,735/y (7.76% less than the optimal solution). Notice that the total annual cost increases even though the recovery of permeate is higher, this is because of the cost associated with the installation and operation of the three TMD units in a series arrangement. **Figure 3.8b** presents a hybrid configuration between two TMD units in a parallel arrangement and one unit in a series arrangement, the total heating cost is $37,632/y and the total permeate is 3,316 Kg/h with an annual value of $212,275/y. The total annual cost for this scenario is $173,780/y and the annual gross profit is $38,495/y which is 8.3% less than the optimal solution.

Scenario 7 is presented as a hybrid arrangement of three units in parallel and one unit in series that receives the concentrated from the previous stages (see **Figure 3.9**). The total annual costs are $178,192/y, which leaves an annual gross profit of $34,083/y that represents 18.8% less than the optimal solution. In scenario 8 two modules in a parallel arrangement and two units in series arrangement are used (see **Figure 3.10**), having a total annual cost of $180,398/y, where the annual gross profit is $31,877/y which is 24.1% less than the optimal solution.

Finally, scenario 9 presents three TMD units in a parallel arrangement in the first stage, two units in a parallel arrangement in the second stage connected in series arrangement with the units of the previous stage and one unit in the third stage that receives the concentrate of the units of the previous stage as shown in **Figure 3.11**. For this scenario, the total heating cost is $38,864/y and the total permeate is 3,425 kg/h with an annual value of $219,335/y. The total annual cost for this scenario is $195,126/y and the annual gross profit is $24,209/y which is 42.4% less than the optimal solution.

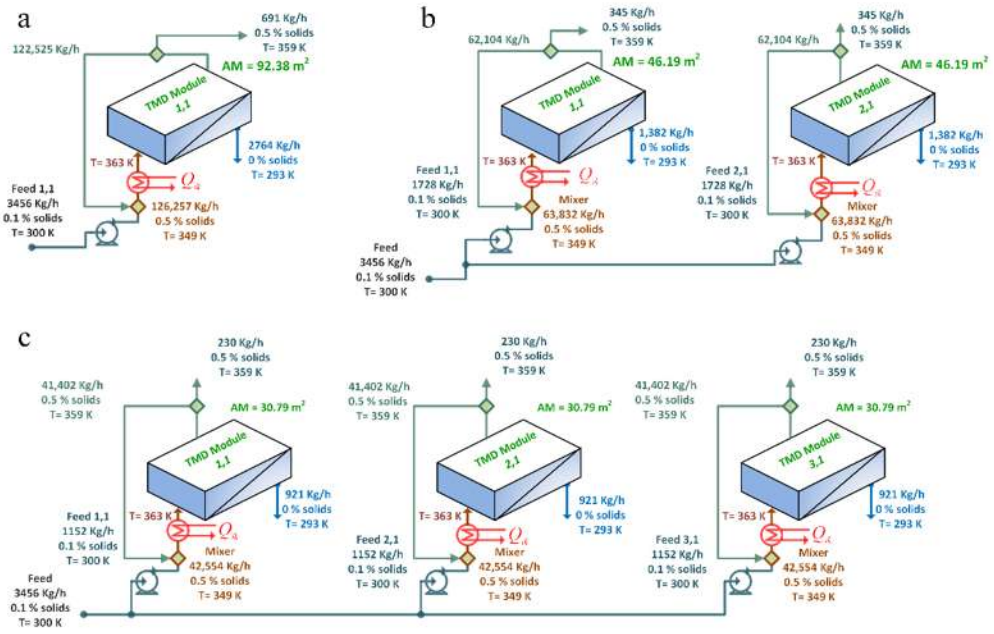

Figure 3.7. TMDN for Case Study 1: (a) Scenario 2, (b) Scenario 3, and (c) Scenario 4.

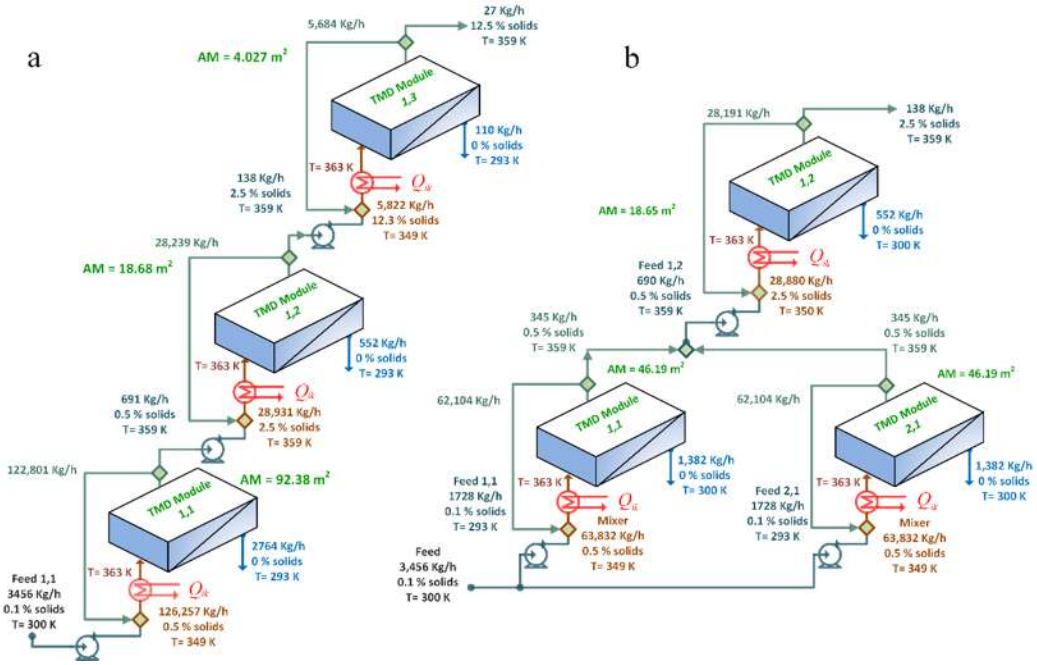

Figure 3.8. TMDN for Case Study 1: (a) Scenario 5 and (b) Scenario 6.

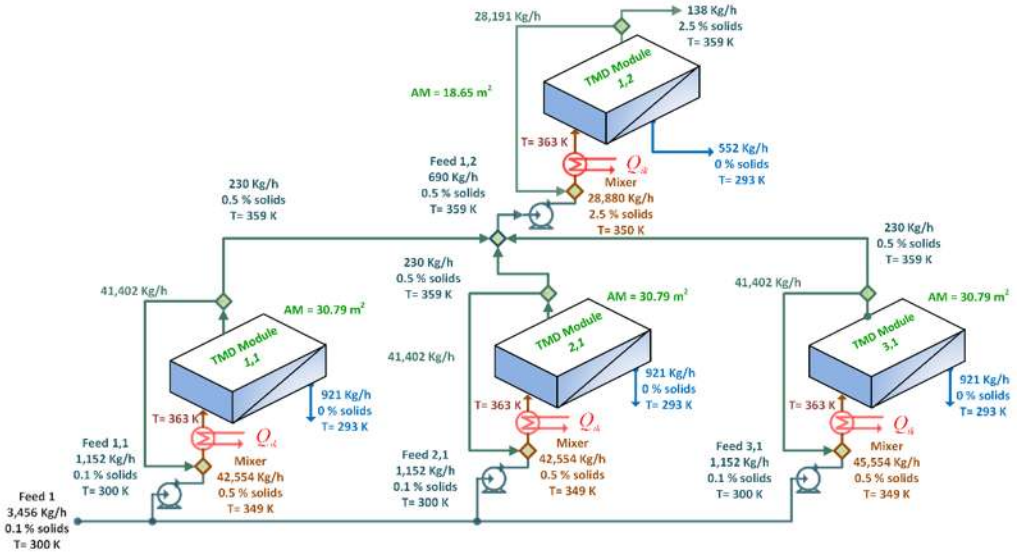

Figure 3.9. TMDN for solution of scenario 7 for Case Study 1.

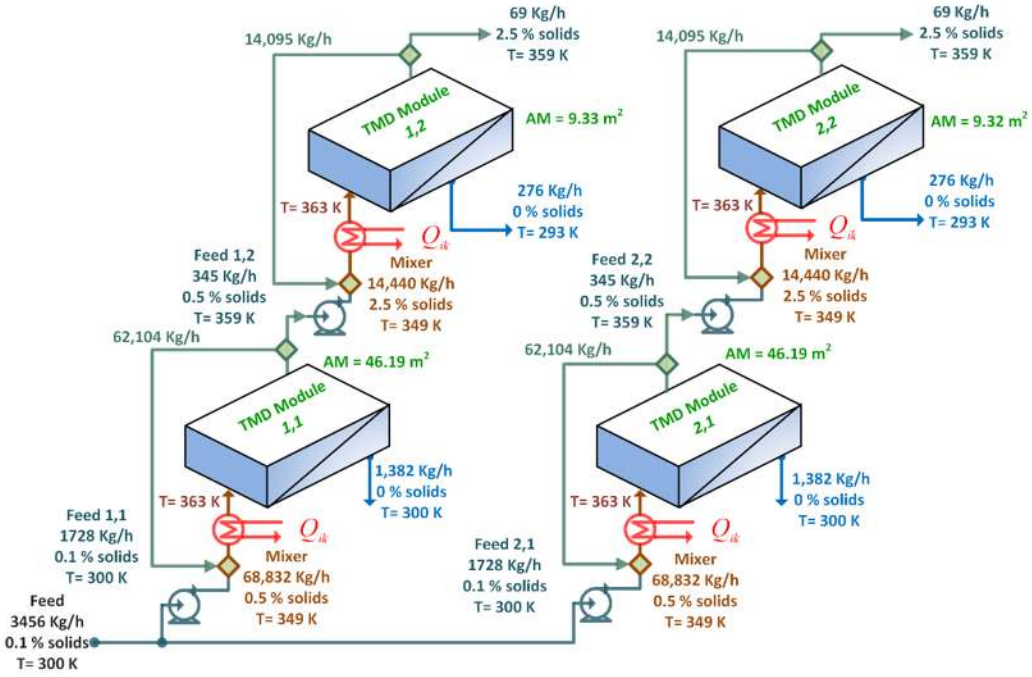

Figure 3.10. TMDN for solution of Scenario 8 of Case Study 1.

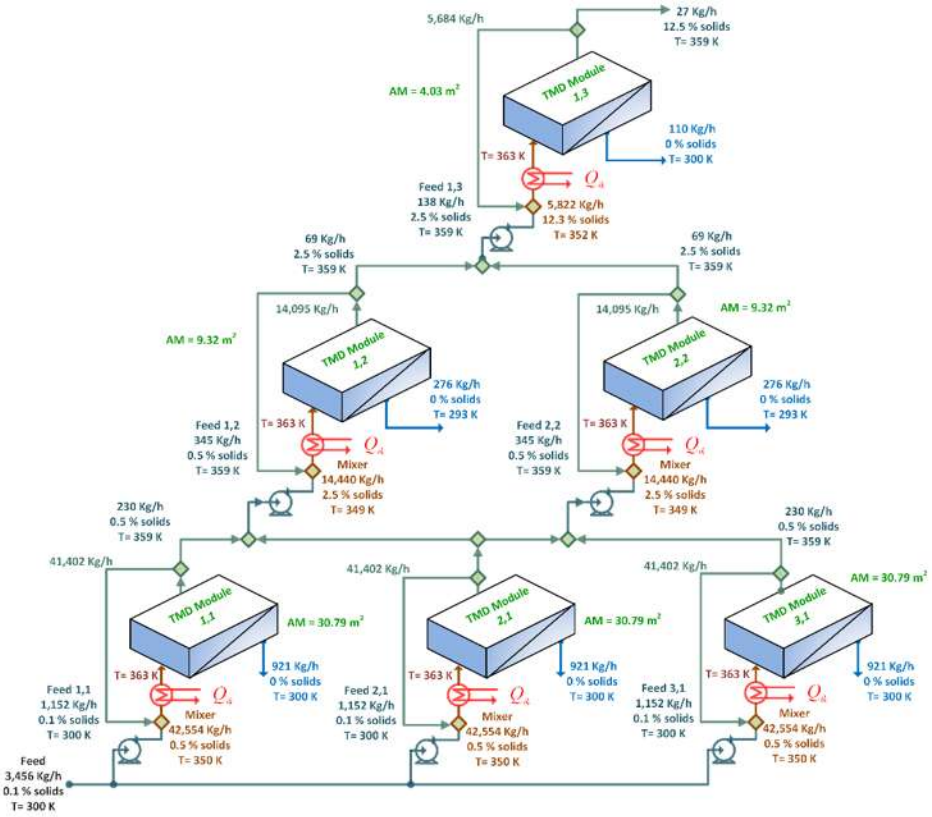

Figure 3.11. TMDN for solution of Scenario 9 for Case Study 1.

3.4.2 Case Study 2: Treating wastewater from the syrup concentration process

TMD technology can be employed in the dextrose syrup manufacturing process for the partial concentration of dextrose syrup. Laboratory tests indicate that water can be removed from the solution up to the extent of 55 % removal. This translates to syrup of 11 % concentration. Also, permeate was found to contain only trace quantities of sugars which allow additional usage of permeate. Since the specifications of commercial sugar syrup dictate a dextrose concentration of about 66 %, conventional evaporation is used for the rest of the concentration task. The flow sheet for the syrup production process proposed by Silayo et al. is shown in **Figure 3.12a**.[39] The objective of this case study is to consider the use of a TMDN for the proposed production process of syrup concentration in conjunction with the evaporator-condenser scheme. A TMDN was synthesized with stream S7 of the system as the feed to the network. The hybrid separation network for the concentration of syrup is shown in **Figure 3.12b**. This hybrid separation scheme leads to significant savings in energy

costs. The feed has 5% (50,000 ppm) of dextrose and an initial flow rate of 648 kg/h. The size of each module is considered a maximum membrane area of 30 m^2/module. The problem data are given in **Table 3.5**.[13,38]

Table 3.5. Data for Case Study 2.

General data: Syrup concentration[13]		
Concept	Unit	Value
Heating cost	$/$10^9$ J heating utility	5.00
Cooling cost	$/$10^9$ J cooling water at 293 K	4.00
Pumping	$/$m^3$	0.056
Labor	$/$m^3$	0.030
Cost of permeate	$/$m^3$	8.00
Feed flow rate	kg/h	648
Initial temperature	K	300
Initial concentration	% weight	5
Annual operation	h	8,000
Membrane specifications[13,38]		
Membrane thickness	mm	0.65
Maximum membrane temperature	K	363
Membrane cost	$/$m^2$	90
Maximum membrane area per module	m^2	30
Membrane life time	year	4

The optimal solution for this Case Study 2 for the syrup concentration process is represented as Scenario 1. For comparison, two additional scenarios are presented.

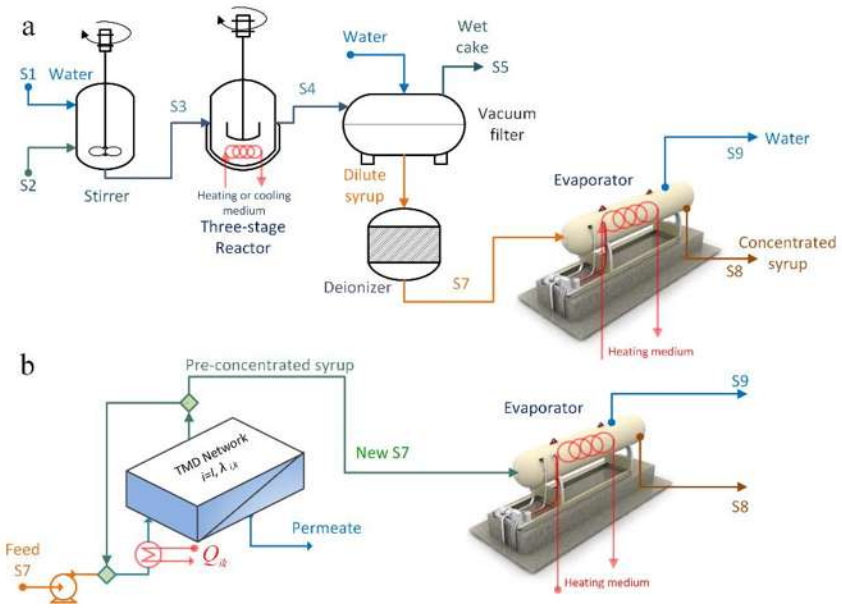

Figure 3.12. (a) Dextrose syrup production process[39] and (b) hybrid TMD-evaporation system for the concentration of dextrose syrup.

The optimal solution for the Case Study 2 represented as Scenario 1 is shown in **Figure 3.13**. For this case, the thermal efficiency is 0.874, the optimal TMD temperature is 363 K, the total recovered permeate is 79% and the feed temperature is 300 K. Notice that in the optimal solution there is no requirement for serial staging because the concentration increases at the end of the first stage at a level higher than the maximum allowable into the membrane. The membrane area for Scenario 1 is 22.542 m^2, the total heating cost is $6,064/y and the permeate flow rate is 518 kg/h, which has a value for permeate of $33,178/y. The total annual cost is $30,589/y and the annual gross profit for the optimal solution is $2,589/y. **Table 3.6** shows the main economic results for the optimal configuration and also for the two other scenarios represented by **Figure 3.14**.

Table 3.6. Results for syrup concentration.

		Scenario		
Concept	Unit	1	2	3
Total membrane area	m^2	22.542	22.542	22.56
Number of TMD units	--	1	2	3
Thermal efficiency	--	0.879	0.874	0.873
Total permeate	kg/h	518	518	518
Total feed water	kg/h	648	648	648
Total heating cost	$/y	6,064	6,064	6,063
Total annual cost	$/y	30,589	35,000	39,411
Permeate value	$/y	33,178	33,178	33,178
Annual profit	$/y	2,589	-1,822	-6,233
Unit cost	$/$m^3$	7.3	8.4	9.5

Scenarios two (see **Figure 3.14a**) and three (see **Figure 3.14b**) have analogous results to scenario one, but there are differences in configuration and in the total costs. In scenario 2 is presented a two TMD units ordered in a parallel arrangement, with a total annual cost of $35,000/y, which leaves economic losses of $1,822/y. On the other hand, in scenario 3 is presented three TMD units in a parallel arrangement, increasing the total annual cost to $39,411/y and economic losses of $6,233/y.

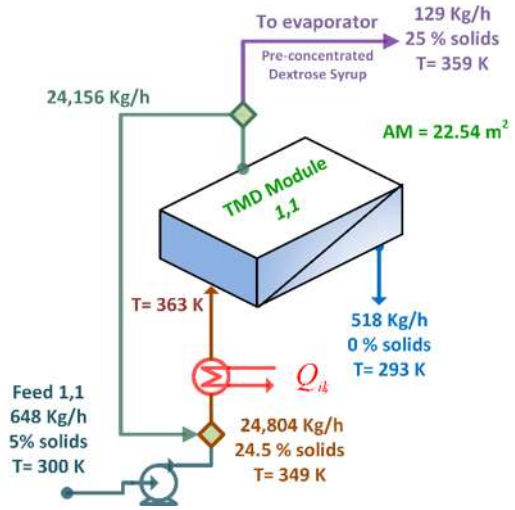

Figure 3.13. TMDN for optimal solution of Scenario 1 of Case Study 2.

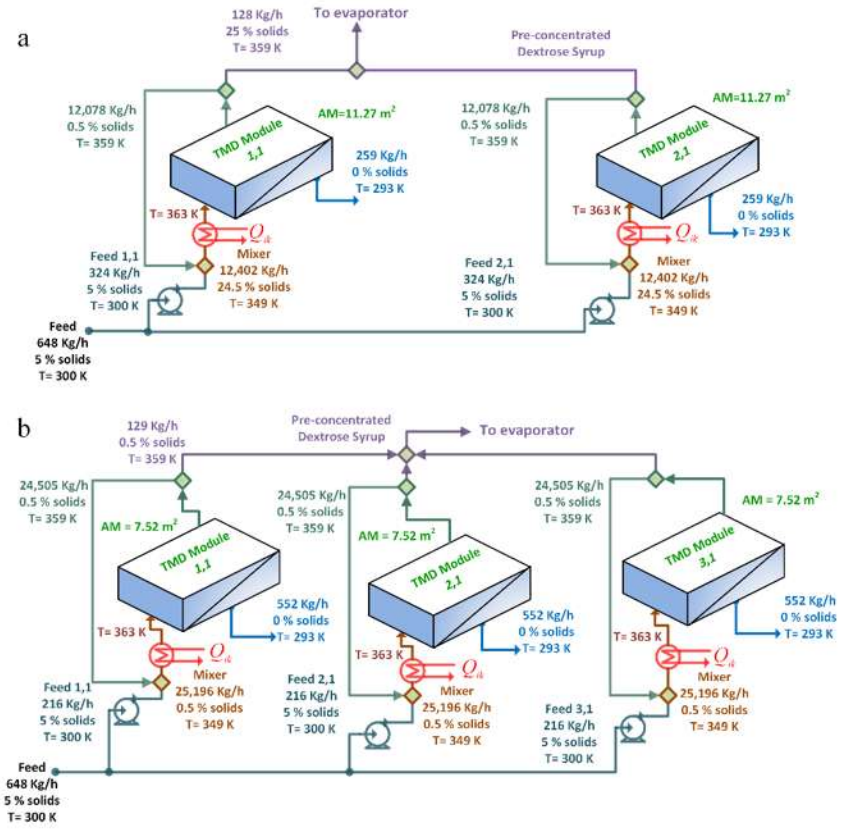

Figure 3.14. TMDN for Case Study 2: (a) Scenario 2 and (b) Scenario 3.

3.5 Conclusions

This chapter has presented an optimization approach for synthesizing a TMDN. A superstructure has been developed to embed network configurations of interest. This superstructure allows various arrangements of TMD modules, pumps, heaters, and condensers. It also accounts for stream recycle and assignment. An optimization formulation has been developed. The proposed model incorporates modeling equations as well as technical and design constraints. The model has been formulated as a mixed-integer nonlinear programming model. The proposed optimization model was applied to two case studies, where the optimal network structure, as well as the operating conditions were determined. The obtained results show that the proposed model yields better results than other configurations. As seen in the results TMD process has been characterized by high unit costs, however, strategies have been applied to the thermal coupling of TMD and processing facilities, this provides a synergistic effect by reducing costs of heating and cooling for the TMD. The on-going and future research should focus on the integration with various desalination processes in order to satisfy various water qualities that reduce the cost of desalination, also it is essential to incorporate clean energy technologies which will have a significant benefit in the desalination cost.

3.6 References

1. Kim, A. S., A two-interface transport model with pore-size distribution for predicting the performance of direct contact membrane distillation (DCMD), *Journal of Membrane Science*, 2013, 428, 410-424.
2. Winter, D., Desalination using membrane distillation: Flux enhancement by feed water deaeration on spiral-wound modules, *Journal of Membrane Science*, 2012, 428-424, 215-224.
3. Lawson, K. W.; Lloyd, D. R., Membrane distillation, *Journal of Membrane Science*, 1997, 124 (1), 1-25.
4. Khayet, M.; Matsuura, T., Membrane distillation: principles and applications (1st edition). Oxford: Elsevier, Inc., 2011.
5. Ibrahim, S. S.; Alsalhy, Q. F., Modeling and simulation for direct contact membrane distillation in hollow fiber modules, *AIChE Journal*, 2013, 59 (2), 589-603.
6. Vatai, G., Separation technologies in the processing of fruit juices, separation, extraction and concentration processes in the food, *Beverage and Nutraceutical Industries*, 2013, 1 (13), 381-395.
7. Cojocaru, C.; Khayet, M., Sweeping gas membrane distillation of sucrose aqueous solutions: Response surface modeling and optimization, *Separation and Purification Technology*, 2011, 81 (1), 12-24.

8. Kozák Á, Békássy-Molnár E, Vatai G. Production of black-currant juice concentrate by using membrane distillation, *Desalination*, 2009, 241 (1-3), 309-314.
9. Adham, S.; Hussain, A.; Matar, J. M., Dores, R.; Janson, A., Application of membrane distillation for desalting brines from thermal desalination plants, *Desalination*. 2013, 314, 101-108.
10. Al-Obaidani, S.; Curcio, E.; Macedonio, F.; Di-Profio, G.; Al-Hinai, H.; Drioli, E., Potential of membrane distillation in seawater desalination: Thermal efficiency, sensitivity study and cost estimation, *Journal of Membrane Science*, 2008, 323, 85-98.
11. Karakulski, K.; Gryta, M.; Morawski, M. A., Membrane processes used for potable water quality improvement, *Desalination*, 2002, 145 (1-3), 315-319.
12. Gryta, M.; Tomaszewska, M.; Morawski, A. W., Water purification by membrane distillation, *Inzynieria Chemiczna I Procesowa*, 2001, 22 (2), 311-322.
13. Elsayed, N. A.; Barrufet, M. A.; El-Halwagi, M. M., Integration of thermal membrane distillation networks with processing facilities, *Industrial and Engineering Chemistry Research*, 2014, 53 (13), 5284-5298.
14. El-Halwagi, M. M., Synthesis of reverse osmosis networks for waste reduction, *AIChE Journal*, 1992, 38 (8), 1185-1198.
15. El-Halwagi, M. M., Optimal-design of membrane-hybrid systems for waste reduction, *Separation Science and Technology*, 1993, 28 (1-3), 283-307.
16. Srinivas, B. K.; El-Halwagi, M. M., Optimal design of pervaporation systems for waste reduction, *Computers and Chemical Engineering*, 1993, 17 (10), 957-970.
17. Crabtree, E. W.; El-Halwagi, M. M.; Dunn, R. F., Synthesis of hybrid gas permeation membrane/condensation systems for pollution prevention, *Journal of the Air and Waste Management Association*, 1998, 48 (7), 616-626.
18. Zhu, M.; El-Halwagi, M. M.; Al-Ahmad, M., Optimal Design and Scheduling of Flexible Reverse Osmosis Networks, *Journal of Membrane Science*, 1997, 129, 161-174.
19. See, H. J.; Vassiliadis, V. S.; Wilson, D. I., Optimization of membrane regeneration scheduling in reverse osmosis networks for seawater desalination, *Desalination*, 1999, 125, 37-54.
20. Qi, R. H.; Henson, M. A., Membrane system design for multicomponent gas mixtures via mixed-integer nonlinear programming, *Computers and Chemical Engineering*, 2000, 24 (12), 2719-2737.
21. Maskan, F.; Wiley, D. E.; Johnston, L. P. M.; Clements, D. J., Optimal design of reverse osmosis module networks, *AIChE Journal*, 2000, 46 (5), 946-954.
22. Kookos, I. K., A targeting approach to the synthesis of membrane networks for gas separations, *Journal of Membrane Science*, 2002, 208 (1-2), 193-202.
23. Marriott, J.; Sorensen, E., The optimal design of membrane systems, *Chemical Engineering Science*, 2003, 58 (22), 4991-5004.
24. Uppaluri, R. V. S.; Linke, P.; Kokossis, A. C., Synthesis and optimization of gas permeation membrane networks, *Industrial and Engineering Chemistry Research*, 2004, 43 (15), 4305-4322.
25. Karuppiah, R.; Bury, S. J.; Vazquez, A.; Poppe, G., Optimal design of reverse osmosis-based water treatment systems, *AIChE Journal*, 2012, 58 (9), 2758-2769.
26. Abejón, R.; Garea, A.; Irabien, A., Optimum design of reverse osmosis systems for hydrogen peroxide ultrapurification, *AIChE Journal*, 2012, 58 (12), 3718-3730.

27. Alnouri, S. Y.; Linke, P., Optimal SWRO desalination network synthesis using multiple water quality parameters, *Journal of Membrane Science*, 2013, 444, 493-512.
28. Alnouri, S. Y.; Linke, P., A systematic approach to optimal membrane network synthesis for seawater desalination, *Journal of Membrane Science*, 2012, 417-418, 96-112.
29. Du, Y.; Xie, L.; Liub, J.; Wang, Y.; Xu, Y.; Wang, S., Multi-objective optimization of reverse osmosis networks by lexicographic optimization and augmented epsilon constraint method, *Desalination*, 2014, 333, 66-81.
30. Almansoori, A.; Saif, Y., Structural optimization of osmosis processes for water and power production in desalination applications, *Desalination*, 2014, 344, 12-27.
31. Saif, Y.; Almansoori, A.; Elkamel, A., Optimal design of Split partial second pass reverse osmosis network for desalination applications, *AIChE Journal*, 2014, 60 (2), 520-532.
32. Dahdah, T. H.; Mitsos, A., Structural optimization of seawater desalination: I. A flexible superstructure and novel MED–MSF configurations, *Desalination*, 2014, 344, 352-265.
33. El-Halwagi, M. M.; Hamad, A. A.; Garrison, G. W., Synthesis of waste interception and allocation networks, *AIChE Journal*, 1996, 42 (11), 3087-3101.
34. Lawson, K. W.; Lloyd, K. R., Membrane distillation, *Journal of Membrane Science*, 1996, 124, 1-25.
35. Martínez-Díez, L.; Vázquez-González, M. I., Temperature polarization in mass transport through hydrophobic porous membranes, *AIChE Journal*, 1996, 42 (7),1844-1852.
36. Khayet, M.; Godino, M. P.; Mengual, J. I., Thermal boundary layers in sweeping gas membrane distillation processes, *AIChE Journal*, 2002, 48 (7), 1488-1497.
37. Brooke, A.; Kendrick, D.; Meeruas, A.; Raman, R., GAMS-language guide, Washington DC: GAMS Development Corporation, 2014.
38. Al-Obaidani, S.; Curcio, E.; Macedonio, F.; Di-Profio, G.; Al-Hinai, H.; Drioli, E., Potential of membrane distillation in seawater desalination: Thermal efficiency, sensitivity, study and cost estimation, *Journal of Membrane Science*, 2008, 323 (1), 85-98.
39. Silayo, V. C.; Lu, J. Y.; Aglan, H. A., Development of a pilot system for converting sweet potato starch into glucose syrup, *Habitation (Elmsford)*, 2003, 9 (1-2), 9-15.

CHAPTER IV

Optimal Design of Water Desalination Systems Involving Waste Heat Recovery

Water desalination appears as an attractive alternative to provide fresh water in several parts of the world. However, this process is very expensive due to the high-energy consumption, and as consequence, significant pollution is produced due to the burning of fossil fuels that yield huge emissions of CO_2. Furthermore, most of the desalination processes yield a lot of waste heat at low temperature, which can be recovered. Therefore, this chapter presents an optimization approach for designing water desalination systems involving heat integration and waste heat recovery to reduce the desalination cost, energy consumption and overall greenhouse gas emissions. The proposed approach accounts for the optimal selection of the existing and emerging desalination technologies, based on the heating and cooling requirements and incorporating waste heat recovery systems. The integration of the proposed systems provides power and thermal energy to the desalination task. Also, the proposed approach includes the optimal selection of fossil fuels, biofuels and solar energy as energy sources. The proposed approach was applied to a case study, and the results show that the system that involves the multiple-effect distillation and thermal membrane distillation shows the best economic and environmental benefits involving water sales, power production, and energy savings.

4.1 Introduction

Despite the effort to improve the desalination technologies, seawater desalination still is an energy-intensive process, and it requires high amounts of fossil fuels, which contribute to the global warming.[1] While some countries have high reserves of oil and gas, others depend on fossil fuel imports to satisfy their energy demands. In addition, the continuous increment in the fossil fuel prices and the environmental restrictions limit the use of this technology.[2] Even so, water desalination still is the best option to satisfy water demands in several water stressed areas around the world. Nevertheless, it is required to propose integrated energy desalination schemes, where the economic, environmental and social objectives are considered.

Many efforts have been developed to improve the water and energy efficiencies in the seawater desalination schemes. In this context, Abduljawad and Ezzeghni developed an optimization approach for multi-stage flash (MSF) desalination systems, they found that the seawater feed temperature has an important effect on the performance of the plant.[3] Khoshgoftar-Manesh et al. proposed an optimization procedure for coupling multi-effect distillation (MED) and reverse osmosis (RO), where a site utility system was integrated and heat and power were produced to run the desalination system, the results showed a series of Pareto solutions for cost of water versus gain output ratio (GOR).[4] Altaee and Zaragoza presented a mathematical model for integrating MSF and forward osmosis (FO) desalination systems, where the concentrated of the MSF unit is sent to the FO unit to improve the process efficiency.[5] Iaquaniello et al. introduced an economic analysis for the integrated MED and RO powered with concentrating solar energy and involving thermal storage, the results showed economic benefits where the lifetime plays an important role.[6] Al-Weshahi et al. presented a parametric study for recovering residual heat from an MSF desalination plant through an organic Rankine cycle (ORC), the results showed attractive solutions.[7] Dahdah and Mitsos proposed a multi-objective optimization model for the simultaneous synthesis of MED and MSF, where the model accounted for both stand-alone or dual purpose desalination (water and power); then this model was extended adding vapor compression (VC) desalination yielding further thermodynamic and economic advantages.[8-9]

Other strategies include heat integration and heat exchanger network (HEN) synthesis,[10-14] these strategies have been applied to the desalination field. Lu et al. published a process integration strategy to reduce the desalination cost, the proposed approach includes low-grade heat integration through HEN synthesis involving thermal membrane distillation (TMD) desalination.[15] Zhou et al. developed a comprehensive mathematical model involving FO and heat recovery, where the results showed the availability to introduce this system in the water treatment scheme.[16] Gabriel et al. presented an optimization procedure involving low heat recovery, in which the proposed model includes water desalination (MED-RO) to produce water, and a turbine network to produce power, the proposed scheme shows important economic benefits related to the water and energy nexus.[17] Zhang et al. presented a framework of low-grade heat integration applied to energy intensive processes.[18]

It should be noticed that the previous works have not considered the existing and emerging desalination process (either thermal or non-thermal) in the same integrated optimization model. Also, the reported approaches have not accounted for the simultaneous optimization for the energy integration with the design and operation of the desalination system. Furthermore, the possibility to incorporate recovered waste heat has not been involved, in which the integration of waste heat recovery systems (i.e., steam Rankine cycle (SRC), absorption refrigeration cycle (AR), ORC and HEN) allows satisfying electrical and thermal requirements of the desalination scheme. It is worth noting that the above-mentioned options may yield attractive solutions (economically and environmentally) for seawater desalination because of the possible reduction of cost and greenhouse gas emissions. Therefore, in this chapter is presented an optimization method for energy integration and waste heat recovery in the desalination field. The proposed method includes MSF, MED and RO desalination systems, as well as the emerging processes of VC desalination and thermal membrane distillation (TMD).

4.2 Problem statement

The proposed approach includes three main optimization stages (see **Figure 4.1**). The first stage (**Figure 4.1a**) considers the optimal selection of the desalination technologies (i.e., multi-stage flash distillation (MSF), multiple-effect distillation (MED), vapor-compression desalination (VC), thermal membrane distillation (TMD) and reverse osmosis(RO)) based

on the energy requirements of the proposed desalination systems. The second stage (**Figure 4.1b**) involves the integration of waste heat recovery systems through heat exchanger networks, this integration includes a steam Rankine cycle, an organic Rankine cycle, and an absorption refrigeration cycle for waste heat recovery to provide power and thermal energy to the desalination system (either thermal or non-thermal). Finally, a multi-objective analysis is performed accounting for environmental, economic and social objectives (**Figure 4.1c**).

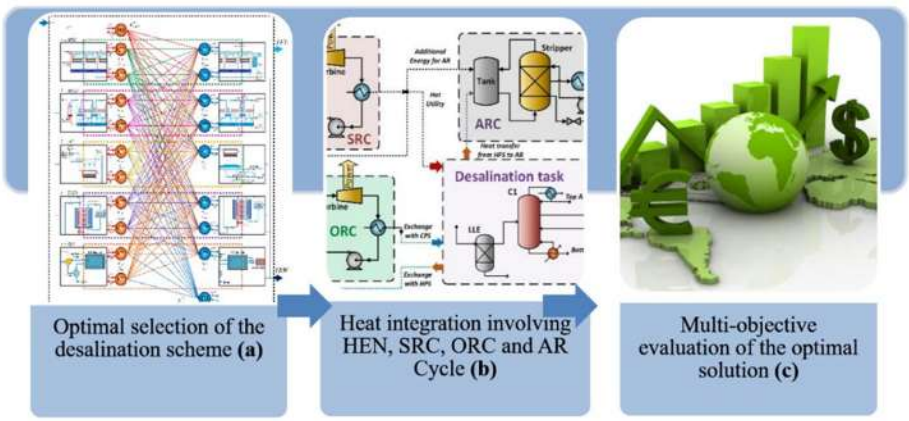

Figure 4.1. Schematic representation of the proposed approach.

The implemented optimization approach can be described as follows. First (see **Figure 4.1a**), there is given the water demand to be satisfied (TFL) as well as the available water desalination systems, which include a set of hot process streams to be cooled (HS) and a set of cold process streams to be heated (CS). Each hot and cold process stream has specific heat capacity and temperatures known with a stream flowrate unknown. Also, there is a set of hot utilities (HU) and a set of cold utilities (CU) with known temperatures. The objective is to determine the heat exchange network that minimizes the total annual cost of the desalination task, including MSF, MED, VC, TMD and RO systems. In addition, some design challenges associated with the selection of the system configuration and other design decisions must be included, which are highlighted as follows:

- The optimal water desalination scheme
- The number of required units and its capacity
- The optimal values for flowrates, heating and cooling duties in each desalination system

- The hot and cold utilities required
- The stream matches and the number of units
- The heat load in each heat exchanger
- The network configuration with flowrates and temperatures for all the streams

Then (see **Figure 4.1b**), the identified hot and cold streams of the desalination task are energetically integrated through heat exchanger networks (HEN) coupling to steam Rankine cycle (SRC), organic Rankine cycle (ORC) and Absorption Refrigeration (AR) cycle (see **Figure 4.2**), where the system can provide power and thermal energy to the desalination task. The model for the HEN synthesis was taken from Lira-Barragan et al., where there is proposed that the hot and cold utilities can be satisfied by the SR, OR and AR Cycles, also the residual energy from hot streams and ORC can be used to run an AR cycle. The model considers that the energy requirements can be provided by solar energy, fossil fuels or biofuels.[19]

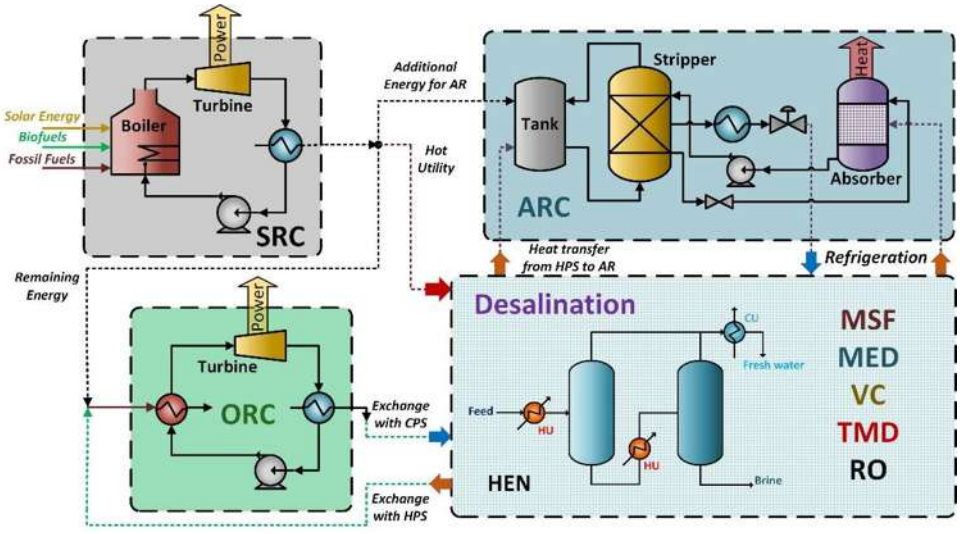

Figure 4.2. Heat integration involving HEN, SRC, ORC, ARC and Desalination.

4.3 Design approach

The model formulation for the optimal selection of the desalination technologies (stage 1) is based on the proposed superstructure shown in **Figure 4.3**. The model considers that the thermal desalination system (MED, MSD, VC and TMD) can give or receive heat from the residual streams of the other desalination systems. In the case of RO, which is not

a thermal-base desalination system, the feed may be used as a cooling utility, this because the RO unit can operate at a maximum temperature of 40 °C, also the recovered water increases in the RO unit when the feed water temperature increases.[20] The model considers that the heating or cooling requirements can be satisfied by utilities. In the model formulation, HS, CS, HU and CU represent hot streams, cold streams, hot utilities and cold utilities, respectively. The index *i* is used for hot streams, *j* represents cold streams, *n* is used to identify hot utilities, *n* for cold utilities, *k* is the temperature intervals and *l* is the desalination systems. This way, the expanded transshipment model by Papoulias and Grossmann was considered to determine the targets for the energy integration.[21,22]

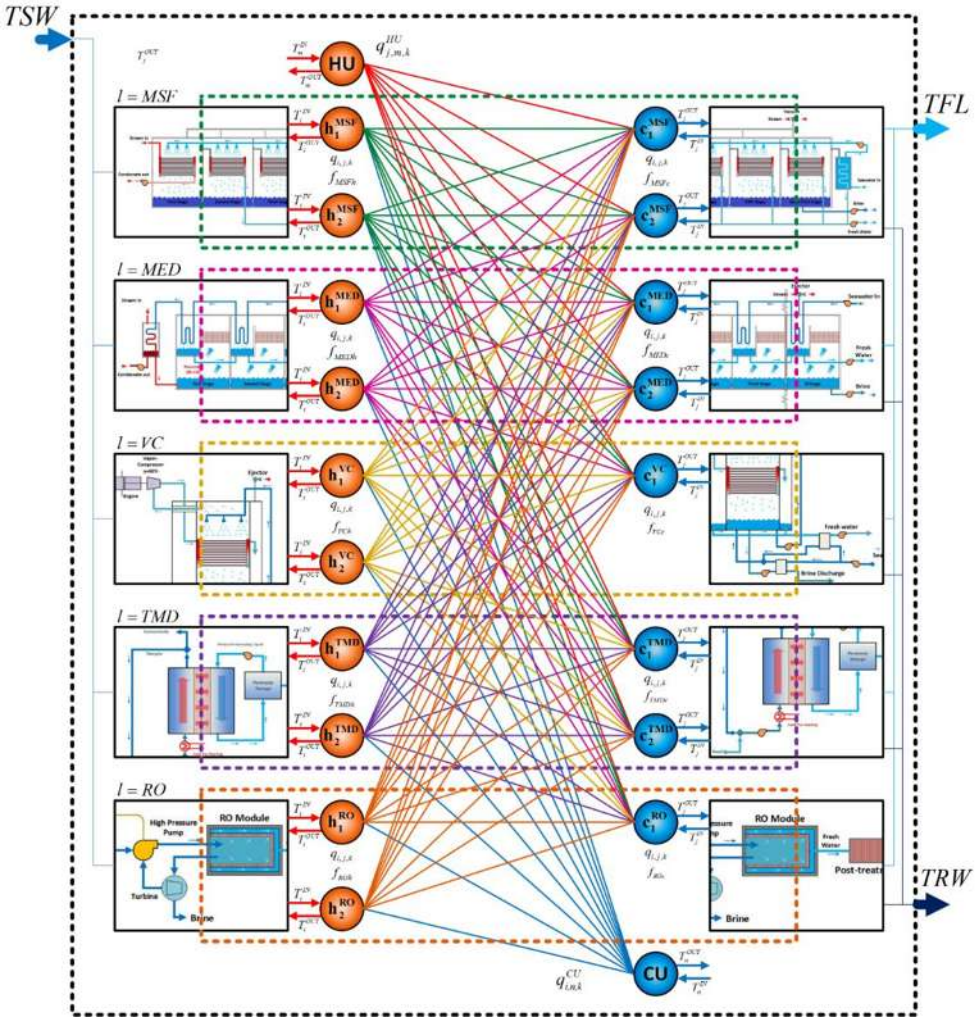

Figure 4.3. Proposed superstructure for designing integrated desalination processes.

4.3.1 Energy balance for hot and cold process streams

The available heat in the hot process stream *i* at any temperature interval *k* is equal to the sum of energy exchanged with any cold process stream *j* and the heat exchanged with the cold utility plus the residual heat of hot stream *i* at interval *k*, minus the residual heat of hot streams from previous temperature interval *k*:

$$q_{i,k}^{HS} = \sum_{j \in CS} q_{i,j,k} + \sum_{n \in CU} q_{i,n,k}^{CU} + r_{i,k} - r_{i,k-1}, \qquad \forall i \in HS; k \in K \tag{4.1}$$

and

$$q_{i,k}^{HS} = f_{i,k}\, \mathrm{Cp}_i \left(\mathrm{T}_{\mathrm{k}}^{\mathrm{in,int}} - \mathrm{T}_{\mathrm{k}}^{\mathrm{out,int}} \right) \qquad \forall i \in HS; k \in K \tag{4.2}$$

where f_i is the total flowrate of the hot process stream, Cp_i is the heat capacity of the hot process stream, $T_{i,k}^{in,int}$ and $T_{i,k}^{out,int}$ are the inlet and outlet temperatures of the hot process streams in interval *k*. The guidelines for partitioning the temperature intervals are based on the works by Papoulias and Grossmann.[21,22]

The hot utility *m* required in the interval *k* is equal to the sum of the heat exchanged with the cold streams, plus the residual heat of hot streams *m* in the temperature interval *k*, minus the residual heat of hot streams from the previous temperature interval *k*:

$$q_{m,k}^{RQ} = \sum_{j \in CS} q_{j,m,k}^{HU} + r_{m,k} - r_{m,k-1}, \qquad \forall m \in HU; k \in K \tag{4.3}$$

The heat required by cold streams *j* in any temperature interval *k* is equal to the sum of the energy exchanged with any hot process stream *i* and the heat exchanged with the hot utility:

$$q_{j,k}^{CS} = \sum_{i \in HS} q_{i,j,k} + \sum_{m \in HU} q_{j,m,k}^{HU} \qquad \forall j \in CS; k \in K \tag{4.4}$$

Where:

$$q_{j,k}^{CS} = f_{j.k}\, \mathrm{Cp}_{\mathrm{j}} \left(\mathrm{T}_{\mathrm{k}}^{\mathrm{in,int}} - \mathrm{T}_{\mathrm{k}}^{\mathrm{out,int}} \right) \qquad \forall j \in CS; k \in K \tag{4.5}$$

f_j is the total flowrate of the cold process stream, Cp_j is the heat capacity of the cold process stream, $T_{j,k}^{in,int}$ and $T_{j,k}^{out,int}$ are the inlet and outlet temperatures of the cold process streams in the interval k.

The total heat load from hot utilities ($THL_{m.k}$) in any temperature interval k is equal to the sum of the heat exchanged with the cold streams:

$$THL_{m,k} = \sum_{j \in CS} q_{j,m,k}^{HU} \qquad \forall m \in HU; k \in K \tag{4.6}$$

Where:

$$THL_{m,k} = f_m \, \mathrm{Cp_m} (\mathrm{T_{m,k}^{in,int}} - \mathrm{T_{m,k}^{out,int}}) \qquad \forall m \in HU; k \in \mathrm{K} \tag{4.7}$$

f_m is the total flowrate of the hot utility, Cp_m is the heat capacity of the hot utility, $T_{m,k}^{in,int}$ and $T_{m,k}^{out,int}$ are the inlet and outlet temperatures of the hot utility in the interval k.

The total heat required by cold utilities ($THR_{m,k}$) is equal to the sum of the heat available in the cold process streams:

$$THR_{n,k} = \sum_{i \in HS} q_{i,n,k}^{CU} \qquad \forall n \in CU; k \in K \tag{4.8}$$

Where:

$$THR_{n,k} = f_n \, \mathrm{Cp_n} (\mathrm{T_{n,k}^{in,int}} - \mathrm{T_{n,k}^{out.int}}) \qquad \forall n \in CU; k \in K \tag{4.9}$$

f_n is the total flowrate of the cold utility, Cp_n is the heat capacity of the cold utility, $T_{n,k}^{in,int}$ and $T_{n,k}^{out,int}$ are the inlet and outlet temperatures of the cold utility in the interval k.

The total utility cost (TUC) involves the factor used to account for the operation time per year ($\mathrm{H_y}$), the heating cost (CUCST), cooling cost (HUCST), the total heat exchanged between cooling utilities ($THR_{n,k}$) and the total heat exchanged between heating utilities ($THL_{m,k}$), as follows:

$$TUC = \mathrm{H_Y} \left[\sum_n \sum_k \mathrm{CUCST}\ THR_{n,k} + \sum_m \sum_k \mathrm{HUCST}\ THL_{m,k} \right] \tag{4.10}$$

4.3.2 Constraints for the feasibility of heat exchange in the superstructure

$$r_{i,'1'} = 0 \qquad \forall i \in HS \tag{4.11}$$

$$r_{i,k} = 0 \qquad \forall i \in HS; \forall k \in K \tag{4.12}$$

$$r_{m,'1'} = 0 \qquad \forall m \in HU \tag{4.13}$$

$$r_{m,k} = 0 \qquad \forall m \in HU; \forall k \in K \tag{4.14}$$

4.3.3 Mass, component and economic balances in the desalination systems

The mass and component balances in desalination systems were stated individually for each desalination system in the next sections. Where the streams were divided as cold (blue lines) and hot streams (red lines), where *l* represents the desalination system.

4.3.4 Model for the MSF system

The MSF feed flow rate (f_{MSFc1}) is a sum between the concentrated brine (f_{MSFh1}) and the fresh water produced (f_{MSFh2}), where f_{MSFh1} and f_{MSFh2} are calculated based on the fresh water recovery fraction of the MSF desalination system. The salinity of seawater can be calculated based on the mass balance of the MSF, in which X_{MSFc1} is the concentration of the feed seawater, X_{MSFh2} is the concentration of the fresh water at the end of the process and X_{MSFh1} is the concentration of the rejected brine. The MSF desalination system has another cold stream that leaves stage 1, which is heated and fed to the stage 1. In this case, the cold stream c_2 (f_{MSFc2}) has an equal flow than the cold stream c_1 (f_{MSFc1}) that is fed to the entire system.

$$l = MSF \left[\begin{array}{l} f_{MSFc1} = f_{MSFh1} + f_{MSFh2} \\ f_{MSFh1} = (1-\theta^{\mathrm{MSF}})\, f_{MSFc1} \\ f_{MSFh2} = \theta^{\mathrm{MSF}} f_{MSFc1} \\ f_{MSFc1}\, \mathrm{X}_{\mathrm{MSFc1}} = f_{MSFh1} x_{MSFh1} + f_{MSFh2}\, \mathrm{X}_{\mathrm{MSFh2}} \\ f_{MSFc2} = f_{MSFc1} \end{array} \right] \tag{4.15}$$

The cost of the MSF desalination system (MSFUC) is based on a fixed cost (MSFFC) multiplied by a binary variable that indicates the existence of the desalination unit (z_1) plus a variable cost (MSFVC) that depends on the production (f_{MSFh2}) capacity of the unit:

$$MSFUC = \mathrm{K_F}\left\{\mathrm{MSFFC}\ \mathrm{z}_l + \left[\, f_{MSFh2}\ \mathrm{MSFVC}\right]^{\beta}\right\} \tag{4.16}$$

The electric power consumption in the MSF unit is equal to an electricity consumption factor multiplied by the water production rate.

$$EPCMSF = \kappa^{MSF} \cdot f_{MSFh2} \tag{4.17}$$

4.3.5 Model for the MED system

The amount of seawater fed to the MED process (f_{MEDc1}) is equal to the desalinated water (f_{MEDh2}) plus the rejected brine (f_{MEDh1}), where f_{MEDh2} and f_{MEDh2} are calculated based on the water recovery fraction of the MED process. The concentration in each stream of the MED system can be calculated based on the mass balance of the MED. Additionally, the MED process feed stream must be heated at the first stage, this stream has been defined as f_{MEDc2} and it has a flow rate equal to the feed stream (f_{MEDc1}).

$$l = MED\left[\begin{array}{l} f_{MEDc1} = f_{MEDh1} + f_{MEDh2} \\ f_{MEDh1} = (1-\theta^{\mathrm{MED}})\, f_{MEDc1} \\ f_{MEDh2} = \theta^{MED} f_{MEDc1} \\ f_{MEDc1}\, \mathrm{X}_{\mathrm{MEDc1}} = f_{MEDh1} x_{MEDh1} + f_{MEDh2}\, \mathrm{X}_{\mathrm{MEDh2}} \\ f_{MEDc2} = f_{MEDc1} \end{array}\right] \tag{4.18}$$

The cost of the MED unit (MEDUC) is based on a unit fixed cost (MEDFC) multiplied by a binary variable for the existence of the desalination unit (z_1) plus a variable cost (MEDCV) that depends on the produced water (f_{MEDh2}):

$$MEDUC = \mathrm{K_F}\left\{\mathrm{MEDFC}\ \mathrm{z}_l + \left[\, f_{MEDh2}\ \mathrm{MEDVC}\right]^{\beta}\right\} \tag{4.19}$$

The electric power consumption in the MED unit is equal to an electricity consumption factor multiplied by the water production rate.

$$EPCMED = \kappa^{MED}\ f_{MEDh2} \tag{4.20}$$

4.3.6 Model for the VC system

The total water fed to the VC module (f_{VCc1}) is equal to the sum of the fresh water obtained (f_{VCh2}) plus the rejected stream (f_{VCh1}), where f_{VCh1} and f_{VCh2} are calculated based on the water recovery fraction of the VC process. The salt content in each stream of the VC system can be calculated using the mass balance of the VC module.

$$l = VC \left[\begin{array}{l} f_{VCc1} = f_{VCh1} + f_{VCh2} \\ f_{VCh1} = (1-\theta^{\mathrm{VC}})\, f_{VCc1} \\ f_{VCh2} = \theta^{\mathrm{VC}}\, f_{VCc1} \\ f_{VCc1}\, \mathrm{X}_{\mathrm{VCc1}} = f_{VCh1} x_{VCh1} + f_{VCh2}\, \mathrm{X}_{\mathrm{VCh2}} \end{array} \right] \tag{4.21}$$

The cost of the VC unit (VCUC) is based on a fixed cost (VCFC) multiplied by a binary variable for the existence of the desalination unit (z_1), plus a variable cost (VCVC) that depends on the water production (f_{VCh2}):

$$VCUC = \mathrm{K_F} \left\{ \mathrm{VCFC} \cdot z_l + \left[f_{VCh2}\, \mathrm{VCVC} \right]^{\beta} \right\} \tag{4.22}$$

The electric power consumption in the VC unit is equal to an electricity consumption factor multiplied by the water production rate (f_{VCh2}):

$$EPCVC = \kappa^{VC} \cdot f_{VCh2} \tag{4.23}$$

4.3.7 Model for the TMD unit

The total water fed to the TMD module (f_{TMDc1}) is the sum of the two streams, fresh water (f_{TMDh2}) and brine (f_{TMDh1}), where f_{TMDh1} and f_{TMDh1} are calculated through the water recovery fraction of the TMD module. The concentration in each stream of the TMD module is calculated using the mass balance in the TMD module. Additionally, the TMD module has a recycle stream that needs to be heated (f_{TMDc2}), this stream is a portion of the recycled brine (f_{TMDh1}).

$$l = TMD \begin{bmatrix} f_{TMDc1} = f_{TMDh1} + f_{TMDh2} \\ f_{TMDh1} = (1-\theta^{\mathrm{TMD}})\, f_{TMDc1} \\ f_{TMDh2} = \theta^{\mathrm{TMD}}\, f_{TMDc1} \\ f_{TMDc1}\, \mathrm{X}_{\mathrm{TMDc1}} = f_{TMDh1} x_{TMDh1} + f_{TMDh2}\, \mathrm{X}_{\mathrm{TMDh2}} \\ f_{TMDc2} = \phi^{TMD} \cdot f_{TMDh1} \end{bmatrix} \tag{4.24}$$

The cost of the TMD module (TMDUC) depends on a fixed cost (TMDFC) multiplied by a binary variable for the existence of the desalination unit (z_1), plus a variable cost (TMDVC) that depends on the water production (f_{TMDh2}):

$$TMDUC = \mathrm{K_F}\left\{\mathrm{TMDFC}\, z_l + \left[f_{TMDh2}\, \mathrm{TMDVC}\right]^{\beta}\right\} \tag{4.25}$$

The electric power consumption in the TMD unit is equal to an electricity consumption factor multiplied by the water production rate (f_{TMDh2}).

$$EPCTMD = \kappa^{\mathrm{TMD}} \cdot f_{TMDh2} \tag{4.26}$$

4.3.8 Model for the RO unit

The total water fed to the RO process (f_{ROc1}) is divided in two streams, the brine (f_{ROh1}) and the fresh water (f_{ROh2}), where f_{ROh1} and f_{ROh2} are calculated based on the water recovery fraction of the TMD module. The concentration in each stream of the RO process can be calculated using the mass balance in the RO unit.

$$l = RO \begin{bmatrix} f_{ROc1} = f_{ROh1} + f_{ROh2} \\ f_{ROh1} = (1-\theta^{\mathrm{RO}})\, f_{ROc1} \\ f_{ROh2} = \theta^{\mathrm{RO}}\, f_{ROc1} \\ f_{ROc1}\, \mathrm{X}_{\mathrm{ROc1}} = f_{ROh1} x_{ROh1} + f_{ROh2}\, \mathrm{X}_{\mathrm{ROh2}} \end{bmatrix} \tag{4.27}$$

The cost of RO unit (ROUC) depends on a fixed cost (ROFC) multiplied by a binary variable for the existence of the desalination unit (z_1), plus a variable cost (ROVC) that depends on the water production (f_{ROh2}):

$$ROUC = \mathrm{K_F}\left\{\mathrm{ROFC}\, z_l + \left[f_{ROh2}\, \mathrm{ROVC}\right]^{\beta}\right\} \tag{4.28}$$

The electric power consumption in the RO unit is equal to an electricity consumption factor times the water production rate (f_{ROh2}):

$$EPCRO = \kappa^{RO} \, f_{ROh2} \tag{4.29}$$

4.3.9 Total mass and cost balances of the desalination network

The total seawater fed to the desalination network is equal to the sum of the stream fed to each existing desalination system, which is stated as follows:

$$TSW = f_{MSFc1} + f_{MEDc1} + f_{VCc1} + f_{TMDc1} + f_{ROc1} \tag{4.30}$$

The total fresh water produced in the desalination network is equal to the sum of the water produced in each existing desalination system, as follows:

$$TFW = f_{MSFh2} + f_{MEDh2} + f_{VCh2} + f_{TMDh2} + f_{ROh2} \tag{4.31}$$

The maximum and minimum limits for the amount of fresh water required are stated as follows:

$$\mathrm{TFW}^{\min} \leq TFW \leq \mathrm{TFW}^{\max} \tag{4.32}$$

Where $\mathrm{TFW}^{\min}$ and $\mathrm{TFW}^{\max}$ are the lower and upper limits for the demanded clean water.

Then, the sales of water are calculated according to the next equation:

$$WaterSales = \mathrm{wC} \cdot TFW \tag{4.33}$$

where wC is the unit water cost.

The total rejected water is equal to the sum of the brine stream in each existing desalination system:

$$TRW = f_{MSFh1} + f_{MEDh1} + f_{VCh1} + f_{TMDh1} + f_{ROh1} \tag{4.34}$$

The total electric consumption of the desalination system is equal to the sum of the electric consumption of each desalination system as follows:

$$EDesTotal = EPCMSF + EPCMED + EPCVC + EPCTMD + EPCRO \tag{4.35}$$

4.3.10 Logical relationships

Logical relationships are required to determine if a potential unit from the superstructure is required in the optimal solution, and these depend on the amount of fed water. Therefore, there are required binary variables to indicate the existence of such units (i.e., the binary variable associated with a given desalination unit is one when the unit exists, otherwise is zero, z_1=Unit existence, {0,1}). This is modeled through the following relationships:

$$f_{MSFc1} \leq \mathrm{W}_l^{\max} z_l \qquad \forall l \in L \tag{4.36}$$

$$f_{MEDc1} \leq \mathrm{W}_l^{\max} z_l \qquad \forall l \in L \tag{4.37}$$

$$f_{VCc1} \leq \mathrm{W}_l^{\max} z_l \qquad \forall l \in L \tag{4.38}$$

$$f_{TMSDc1} \leq \mathrm{W}_l^{\max} z_l \qquad \forall l \in L \tag{4.39}$$

$$f_{ROc1} \leq \mathrm{W}_l^{\max} z_l \qquad \forall l \in L \tag{4.40}$$

Where $\mathrm{W}^{\max}$ is the maximum fed water to the desalination process. To explain previous relationships, when the inlet flow rate to the desalination unit *l* is greater than zero, then the associated binary variable (z_1) must be one. On the other hand, when the binary variable z_1 is zero (i.e., the associated desalination unit does not exist), the fed flow rate must be zero.

Logical relationships are required to determine the existence of a match between hot (*i*) and cold (*j*) streams. This is modeled through the following relationships:

$$\sum_{k \in K} q_{i,j,k} \leq \mathrm{QHCMAX}_{i,j}\, y_{i,j} \qquad \forall i \in HS; \forall j \in CS \tag{4.41}$$

$$\sum_{k \in K} q_{i,n,k} \leq \mathrm{QHWMAX}_{i,n}\, y_{i,n} \qquad \forall i \in HS; \forall n \in CU \tag{4.42}$$

$$\sum_{k \in K} q_{j,m,k} \leq \mathrm{QSCMAX}_{j,m}\, y_{j,m} \qquad \forall j \in CS; \forall m \in HU \tag{4.43}$$

Where $\mathrm{QHCMAX}_{i,j}$ is the maximum allowed heat exchange between *i* and *j*, $\mathrm{QHWMAX}_{i,n}$ is the maximum allowed heat exchange between *i* and *n*, $\mathrm{QSCMAX}_{j,m}$ is the maximum allowed heat exchange between *j* and *m*.

4.3.11 Optimization for the desalination system

The optimal selection of the desalination scheme (**Figure 4.1a**) is solved based on the equations 1 to 43 and taking as an objective function the total annual cost for the heat integrated desalination network (equation 44). This equation involves the cost of the selected desalination systems, MFS (MSFUC), MED (MEDUC), VC (VCUC), TMD (TMDUC) and RO (ROUC), the total electricity consumption cost (*ETotal*), as well as the cost of cooling and heating utilities (TUC):

$$\begin{aligned} TAC = \quad & TUC + MSFUC + MEDUC + VCUC \\ & + TMDUC + ROUC + \mathrm{H_Y} \cdot \mathrm{ECST} \cdot \left[EDesTotal \right] \end{aligned} \tag{4.44}$$

The objective function seeks to minimize the TAC showed in the previous equation, and at the same time, it is needed to minimize the number of units in the heat integration network (SUNITS) as well as the number of units in the desalination network (SDESAL) as follows:

$$SUNITS = \sum_{i \in HS} \sum_{j \in CS} y_{i,j} + \sum_{i \in HS} \sum_{n \in CU} y_{i,n} + \sum_{j \in CS} \sum_{m \in HU} y_{j,m} \tag{4.45}$$

$$SDESAL = \sum_{l} z_l \tag{4.46}$$

4.3.12 HEN integration

The synthesis of the HEN involving SRC, ORC, and ARC (**Figure 4.1b**) was performed using the formulation proposed by Lira-Barragan et al., this formulation was applied to the results obtained in the first stage.[19] This formulation includes some important equations that are described in the following section. The equations to model the SRC include an energy balance for external energy sources, which is stated as follows:

$$Q^{External} = Q_t^{Solar} + \sum_{b \in B} Q_{b,t}^{Biofuels} + \sum_{f \in F} Q_{f,t}^{Fossilfuels}, \qquad \forall t \in T \tag{4.47}$$

where $Q^{External}$ is the energy provided to the SRC system, Q_t^{Solar} is the energy from the solar collector, $Q_{b,t}^{Biofuels}$ is the energy from biofuels and $Q_{b,t}^{Fossilfuels}$ is the energy from fossil fuels.

The power produced by the SRC system ($Power^{src}$) is equal to the total energy from external sources ($Q^{External}$) multiplied by the thermal efficiency factor of the SRC cycle (μ^{src}) as follows:

$$Power^{src} = Q^{External}\,\mu^{\mathrm{src}} \tag{4.48}$$

Then, the heat that cannot be transformed into power (Q^{src_mps}) is sent to the ORC system to produce electricity (Q^{orc_mps}), to the AR system to produce refrigeration (Q^{ar_mps}) or can be sent to the HEN as a hot utility (desalination) (q_j^{lps}), according to the next equation:

$$Q^{src\_mps} = Q^{ar\_mps} + Q^{orc\_mps} + \sum_{j \in CS} q_j^{lps} \tag{4.49}$$

The total energy balance for the SRC system establishes that the total energy from external energy sources is equal to the produced electricity ($Power^{src}$) plus the energy sent to other subsystems (Q^{src_mps}) and the transferred heat to cooling water (Q^{src_cw}).

$$Q^{External} = Power^{src} + Q^{src\_mps} + Q^{src\_cw} \tag{4.50}$$

Since the availability of biofuels depends on the seasonality throughout the year, the following constraint must be included in the model:

$$Q_{b,t}^{Buofuels} \le \mathrm{Heating}_b^{power}\ \mathrm{Avail}_{b,t}^{\max}, \qquad \forall b \in B, t \in T \tag{4.51}$$

where $\mathrm{Heating}_b^{power}$ is the heating power for biofuels and $\mathrm{Avail}_{b,t}^{\max}$ is the maximum availability of biofuels over the time period t.

The equations to model de ORC system include the energy balance where the ORC can receive heat from the SRC system (Q^{orc_mps}) and the energy that can be received from HS ($q_{i,k}^{orc1}$). Then, the power produced in the ORC system ($Power^{orc}$) is obtained considering the efficiency factor of the ORC unit (μ^{orc}) as follows:

$$Power^{orc} = (Q^{orc\_mps} + \sum_{i \in HS} \sum_{k \in K} q_{i,k}^{orc1})\mu^{orc} \tag{4.52}$$

Then, the remaining residual energy (at the condenser of the ORC system) can be used by the CS ($q_{j,k}^{orc2}$) or can be transferred to cold water (Q^{orc_cw}) as follows:

$$Q^{orc\_mps} + \sum_{i \in HS} \sum_{k \in ST} q_{i,k}^{orc1} = Power^{orc} + \sum_{j \in CS} \sum_{k \in K} q_{j,k}^{orc2} + Q^{orc\_cw} \tag{4.53}$$

The AR system is modeled according to the next equation:

$$\frac{\sum_{i\in HS} q_i^{ar2}}{\mathrm{COP}^{ar}} = \sum\sum q_{i,k}^{ar1} + Q^{ar\_mps} \tag{4.54}$$

where the cooling load below the ambient temperature required by the HS ($q_{i,k}^{ar2}$) is supplied by the excess of heat from the HS ($q_{i,k}^{ar1}$) as well as the energy from the SRC system (Q^{ar_mps}). The AR system is modeled based on a COP (coefficient of performance), this value depends on the AR system and it is a factor that can describe the energy conversion from the provided heat and the obtained cooling.

The solar collector is modeled according to the next equations:

$$Q_t^{Solar} \le Q_t^{Useful\_Solar} A_c^{Solar}, \qquad \forall t \in T \tag{4.55}$$

where $Q_t^{Useful\_Solar}$ is the useful solar energy and A_c^{Solar} is the optimal solar collector area.

The economic objective is stated as follows:

$$Max\ Profit = WaterSales + RSP + TCR - CaC - FiC - OC - ESC - TAC \tag{4.56}$$

where the revenues coming from selling power (*RSP*) include the power generated by the SRC and the ORC, minus the power consumed by the desalination system, $\mathrm{Ga}^{\mathrm{Power}}$ corresponds to the gains for selling power, it is determined using the power price ($\mathrm{SuP}^{\mathrm{Power}}$) minus the power production cost (PPCost) as follows:

$$RSP = \mathrm{H_Y}\ \mathrm{Ga}^{\mathrm{Power}} \left[Power^{src} + Power^{orc} - EDesTotal \right] \tag{4.57}$$

$$\mathrm{Ga}^{\mathrm{Power}} = \mathrm{SuP}^{\mathrm{Power}} - \mathrm{PPCost}$$

The tax credit reduction (*TCR*) includes the tax credits for solar energy, biofuels, and fossil fuels, where $\mathrm{R}^{\mathrm{Solar}}$, $\mathrm{R}^{\mathrm{Biofuels}}$ and $\mathrm{R}^{\mathrm{Fossilfuels}}$ represent the unit tax credits, respectively:

$$TRC = \mathrm{H_Y} \left[\mathrm{R}^{\mathrm{Solar}} \sum_{t\in T} Q_t^{Solar} + \mathrm{R}^{\mathrm{Biofuels}} \sum_{t\in T}\sum_{b\in B} Q_{t,f}^{Biofuels} + \mathrm{R}^{\mathrm{Fossilfuels}} \sum_{t\in T}\sum_{f\in F} Q_{t,f}^{Fossilfuels} \right] \tag{4.58}$$

CaC is the capital cost for the AR cycle and the capital cost for the heat exchanger units. FiC represents the fixed cost for all the heat exchanger units required in the optimal solution. OC

corresponds to the operating costs associated with the use of cooling water by the HS, the AR system and the ORC system.[19]

The energy source cost (*ESC*) includes the cost of the consumption of fossil fuels and biofuels, as well as the capital and operating costs for the solar collector:

$$ESC = \mathrm{H_Y}\left[\sum_{f\in F}\left(\mathrm{C_f^{Fossilfuels}}\sum_{t\in T}Q_{f,t}^{Fossilfuels}\right)+\sum_{b\in B}\left(\mathrm{C_b^{Biofuels}}\sum_{t\in T}Q_{b,t}^{Biofuels}\right)\right] + \mathrm{H_Y}\,C_{op}^{Solar}+\mathrm{k_F}\,C_{cap}^{Solar} \tag{4.59}$$

where $\mathrm{C_f^{Fossilfuels}}$ and $\mathrm{C_b^{Biofuels}}$ are the unit costs of fossil fuels and biofuels, C_{op}^{Solar} is the operating cost and C_{cap}^{Solar} is the capital cost for the solar collector.

The environmental objective is carried out through the overall quantification of the greenhouse gas emissions (GHGE), because the fossil fuels and biofuels release carbon dioxide when they are burned (the indexes *b* and *f* represent different types of biofuels and fossil fuels):

$$Min\ NGHGE^{\mathrm{Overall}} = \sum_{t\in T}\sum_{f\in B}\left[\mathrm{GHGE}_f^{\mathrm{Fossil}}\,Q_{f,t}^{\mathrm{Fossil}}\right]+\sum_{t\in T}\sum_{b\in B}\left[\mathrm{GHGE}_b^{\mathrm{Biofuel}}\,Q_{b,t}^{\mathrm{Fossil}}\right] \tag{4.60}$$

The social objective is aimed to account for the maximization of a number of jobs that can be created by the implementation of the project, where the social function consists in maximizing the number of jobs created by the production of fossil fuels, biofuels, and solar collector:

$$Max\ NJOBS^{Overall} = \sum_{t\in T}\sum_{f\in B}\left[\mathrm{NJOB}_f^{\mathrm{Fossil}}\,Q_{f,t}^{\mathrm{Fossil}}\right] + \sum_{t\in T}\sum_{b\in B}\left[\mathrm{NJOB}_b^{\mathrm{Biofuel}}\,Q_{b,t}^{\mathrm{Biofuel}}\right] + \sum_{t\in T}\left[\mathrm{NJOB}^{\mathrm{Solar}}\,Q_t^{\mathrm{Solar}}\right] \tag{4.61}$$

where $\mathrm{NJOB_f^{Fossil}}$, $\mathrm{NJOB_b^{Biofuel}}$ and $\mathrm{NJOB^{Solar}}$ represent the number of jobs generated per kJ provided by fossil fuels, biofuels and the solar collector, respectively.

4.4 Case study

In this chapter, the problem of overexploitation of water in the region of *Costa de Hermosillo* (CH) in the state of Sonora in Mexico was selected as a case study. The CH is one of the most over-exploited aquifers of Mexico, the volume of water extracted is used mainly for crops with high water consumption.[23] The volume of water is mainly used for agricultural purposes in the irrigation district "051 Costa de Hermosillo" (ID051), the ID051 has an annual water extraction of 461 hm^3, it has an estimated natural recharge between 250-320 hm^3 per year, and an annual seawater recharge of 98.4 hm^3, which has caused serious salt pollution of the water.[24] The energy sector in this region also represents a challenge, because it is located near to the Sonoran Desert, where the energy consumption increases in the warmer months due to the use of cooling systems. On the other hand, the radiation levels throughout the year are extremely high, they could be used for the production of heating utilities through the use of solar collectors. This region receives high direct normal irradiation (DNI) values (around 3,000 kWh/m^2).

4.5 Results and discussion

This section presents the results for the heat integration of the desalination processes, an optimal solution is presented as the first scenario and other sets of configurations are analyzed to shown the applicability of the model incorporating different desalination technologies.

The problem was coded in the software GAMS,[49] where the solvers DICOPT, CONOPT, and CPLEX were used to solve the associated mixed-integer nonlinear programming, nonlinear programming, and linear programming problems, respectively. For solving this problem, a computer with an Intel® Core ™ i7-4700MQ processor at 2.40 GHz and 32 GB of RAM was used. The model has 1,174 continuous variables, 266 binary variables, 1,131 constraints and it was solved in 6.34 seconds.

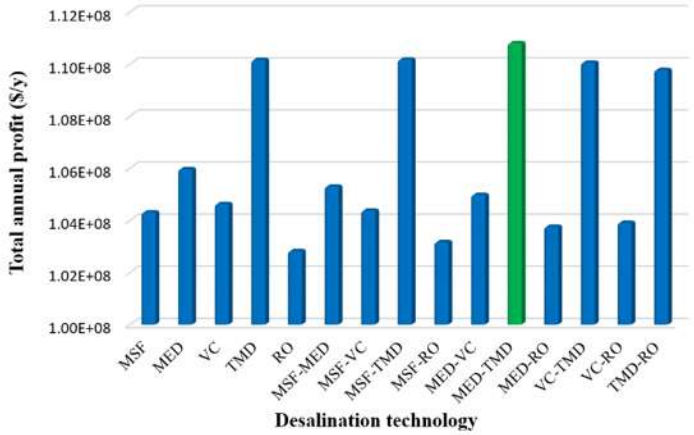

Figure 4.4. Total annual profit for the analyzed configurations.

Figure 4.4 shows the total annual profit for the analyzed configurations, where five configurations are highlighted, these configurations include the TMD desalination system, the integrated MSF-TMD, VC-TMD, TMD-RO and MED-TMD desalination processes, these five configurations have the best annual profit and the results are explained as follows.

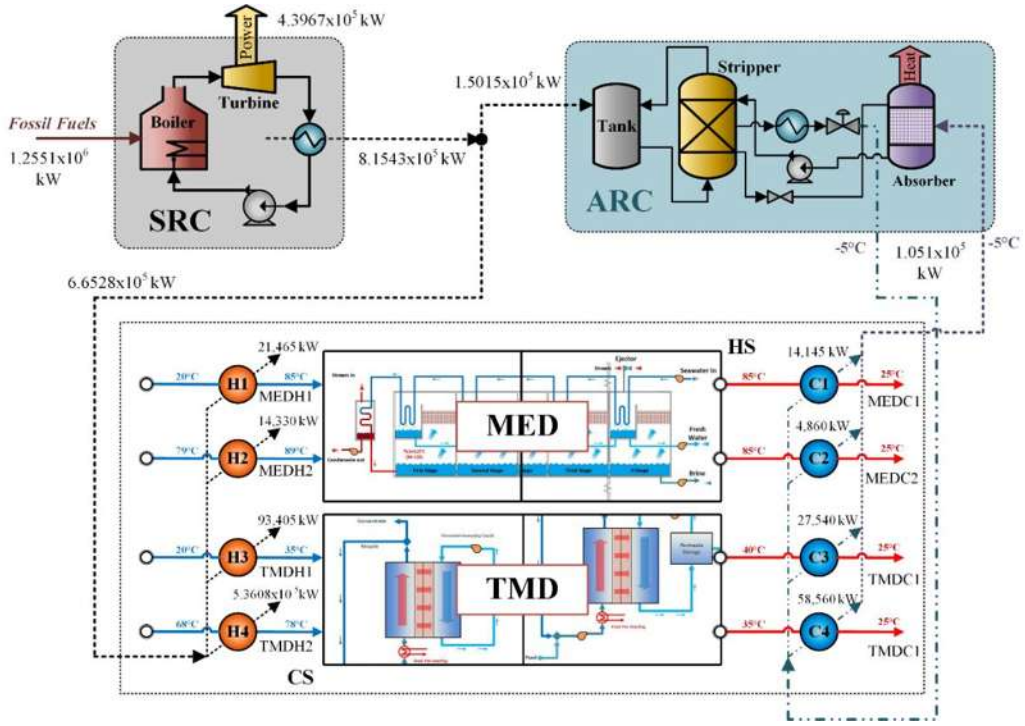

Figure 4.5. Optimal solution for the case study.

Figure 4.5 shows the optimal solution for the case study, which presents two thermally coupled units of MED and TMD, this is because the MED/TMD system shows the best annual profit based on the results showed in **Figure 4.4**. The success of this configuration is mainly caused by the water recovery of the TMD system, this is because the TMD module has a brine recirculation that increases the amount of water on the permeate side, also this stream has a high quantity of heat that can be recovered, which generates a reduction of fuel consumption and the increase of the net annual profit. The optimal configuration shown in **Figure 4.5** includes the SRC system to provide heating to the desalination system as well as the AR cycle to provide cooling utility, in this case, the SRC operates using natural gas and produces $4.3967x10^5$ kW of power, also it provides thermal energy to the AR cycle ($1.5015x10^5$ kW) as well as the desalination process ($6.6528x10^5$ kW). In this case, the AR cycle operates with the H_2O-LiBr system at -5°C. **Figure 4.5** also includes the heat loads for heaters and coolers, **Table 4.1** shows the area of heaters and coolers for the optimal solution. In energy integration, the stream temperatures play an important role, because this energy can be used in the HEN and/or ARC. Moreover, the percentage of recovery of each technology is higher. The success of this configurations is because the use of recovery systems can reduce the energy costs as well as the levels of carbon dioxide. **Table 4.2** shows additional data for the water desalination scheme.

Table 4.1. Area and heat load for heaters and coolers

Heater	Area (m^2)	Heat load (kW)
H1	548	21,465
H2	200	14,330
H3	724	93,405
H4	1541	536,080
Cooler		
C1	104	14,145
C2	85	4,860
C3	508	27,540
C4	3777	58,560

Table 4.2. Additional data for the desalination system for the optimal solution.

		STREAM	ID	T_{IN} (°C)	T_{OUT} (°C)	x	f_l x 10^6 m^3
MED	HPS	Concentrated	MEDH1	40	25	0.055	6.7941
		Fresh W	MEDH2	35	25	0.000	3.5000
	CPS	Feed	MEDC1	20	35	0.036	10.2941
		Add Stream	MEDC2	68	78	---	---
TMD	HPS	Concentrated	TMDH1	85	25	0.112	3.2941
		Fresh W	TMDH2	85	25	0.000	7.0000
	CPS	Feed	TMDC1	20	85	0.036	10.2941
		Add Stream	TMDC2	79	89	---	---

In this case, the MED/TMD configuration has a gross profit of 180.393 MM$/y, which is mainly contributed by 84.44% by the power sales, 14.55% by the water sales and 0.01% by the tax credit reduction. The total annual cost is 69.577 MM$/y, which is constituted mainly by 88.60% by the energy source cost, 7.09% by the desalination cost, also, the total annual cost includes the electricity cost of the desalination unit, the capital cost for the heat exchangers, the fixed cost for the heat exchangers and the operating costs. The results yield a total annual profit of 110.816 MM$/y. In this case, the fuel consumption remains constant through the year and the energy requirements were fulfilled using natural gas, the use of biofuels is negligible due to their high cost and low heating value.

Table 4.3 shows the economic results for the optimal solution and the other analyzed scenarios. In this case, each additional scenario is closer to the optimal solution, this is mainly caused by the integration of the TMD unit in each configuration. The TMD seems the best option to be thermally integrated due to the temperature levels used to run this technology and the amount of residual heat in the recirculated stream. In all the cases, the water sales are 26.25 MM$/y. The performance of the TMD unit reaches a total annual profit of 110.169 MM$/y, which is 0.5% lower than the profit of the optimal solution. The energy source cost is 61.689 MM$/y plus 1.050 MM$/y of the electricity used by the desalination system. The system MSF/TMD has an annual profit of 110.184 MM$/y, which is slightly better than the TMD single unit configuration. The VC/TMD and TMD/RO configurations have annual profits of 110.067 and 109.784 MM$/y, respectively.

Table 4.3. Economic results of the case study.

Concept	Desalination Technology				
	MED/ TMD	**TMD**	**MSF/ TMD**	**VC/TMD**	**TMD/RO**
Water sales (MM$/y)	26.250	26.250	26.250	26.250	26.250
Desalination unit cost (MM$/y)	4.933	3.538	5.506	4.748	5.507
Electricity desalination cost (MM$/y)	1.138	1.050	1.225	2.100	1.400
Power sales (MM$/y)	154.133	154.176	153.051	154.176	153.981
Tax credit reduction (MM$/y)	0.010	0.010	0.010	0.010	0.010
Capital cost for exchanger units (MM$/y)	0.664	1.559	0.620	0.840	0.636
Fixed cost for exchangers (MM$/y)	0.033	0.029	0.033	0.033	0.029
Operating costs (MM$/y)	0.008	1.556	0.200	0.000	0.035
Energy source cost (MM$/y)	61.643	61.689	60.489	61.689	61.481
Fixed cost for desalination (MM$/y)	1.159	0.845	1.054	0.959	1.369
Overall greenhouse gas emissions for the system (10^3 ton CO_2eq/y)	8,767	8,774	8,603	8,774	8,744
Number of jobs created	1123.5	1123.8	1115.6	1120.8	1117.4
TAC (MM$/y)	69.577	70.267	69.127	70.369	70.457
Total annual profit (MM$/y)	110.816	110.169	110.184	110.067	109.784

Additionally, a multi-objective analysis was implemented to propose the best configuration accounting for the environmental impact. In this sense, this analysis involves the reduction of fossil fuel consumption by the increase of the use of biofuels and the possible installation of a solar collector to provide the needed energy. In this case, the Pareto graph involves the maximization of the profit in each analyzed configuration as well as the minimization of the greenhouse gas emissions. **Figure 4.6** shows the results of the multi-objective analysis for each configuration.

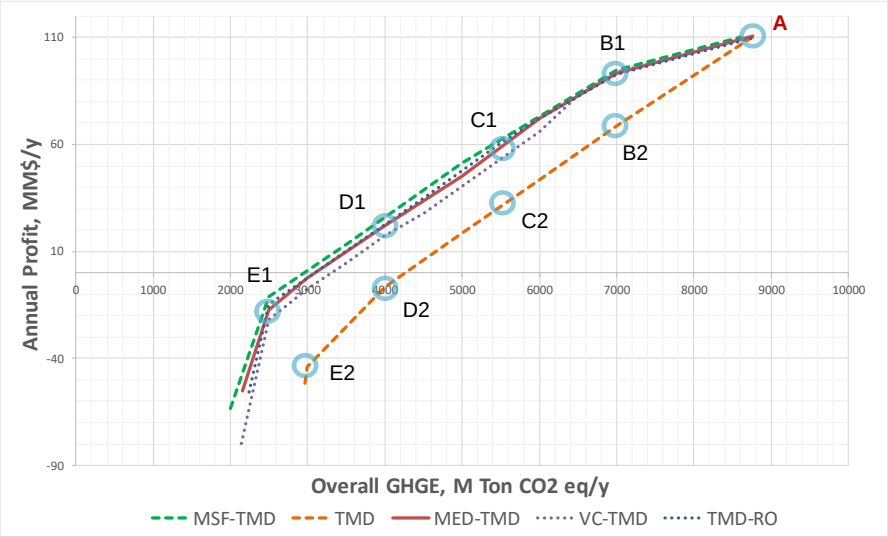

Figure 4.6. Pareto curve for the case study.

In this case, there are identified several solutions where the economic and environmental objectives are compensated. First, point A represents the optimal solution where configuration reached the maximum profit. In this case, the MED/TMD configuration has the best profit over the other proposed configurations, with a total annual profit of 110.816 MM$/y and an overall GHGE of 8,767 M ton CO_2eq/y. Point B1 represents a suboptimal solution, where 7,000 M ton CO_2eq/y are generated, in this case, the integrated MED/TMD, MSF/TMD, VC/TMD and TMD/RO have almost the same behavior, and the MSF/TMD has the best annual profit of 94.853 MM$/y. Also, Point B1 represents the solution where 7,000x10^3 ton CO_2eq/y are generated for a single TMD unit configuration, in this case, the total annual profit is 68.589 MM$/y. The points C and D are additional solutions where the overall GHGE are minimized. An interesting behavior is at the point A, where the integrated MSF/TMD configuration reaches better results than the optimal solution, points E1 and E2 show the solutions where GHGE are 2,500 and 3,000 M ton CO_2eq/y, respectively. In these points E1 and E2, the GHGE are lower than the other points; however, the annual profit is negative.

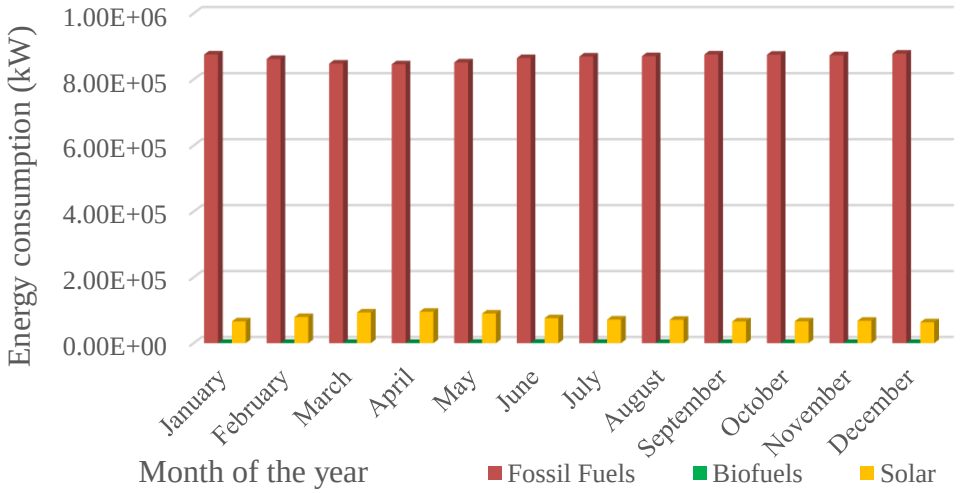

Figure 4.7. Fuel consumption profile through the year for the optimal solution in point E1.

Figure 4.7 shows the fuel consumption profile through the year for the optimal solution of E1 point, where an increase of biofuel consumption and solar technology is observed to reduce the GHGE. **Figure 4.6** also shows the benefit of the heat integration between the desalination systems instead to use one unit separately. **Figure 4.8** shows the profile of the generated jobs, where two mainly points are identified, point A represents the minimum jobs that match with the maximum profit; point B represents the maximum for jobs that matches with the minimum GHGE. Additional solutions are presented, where the number of jobs varies according to the amount of GHGE and the total annual profit.

4.6 Conclusions

This work has presented a multi-objective optimization formulation for designing integrated desalination systems involving solar collectors, absorption refrigeration cycles, and organic Rankine cycles. The proposed method seeks to identify the best configuration to satisfy water and energy demands accounting for thermal and non-thermal desalination technologies. The obtained results have shown interesting benefits since the economic, environmental and social points of view. The thermal membrane distillation system seems to be the best configuration to be integrated thermally, this behavior has been shown in previous works; however, the coupling with common desalination systems as MSF and MED appears to improve the performance of the system. Moreover, much of the success of these configurations is because of the integration of the involved waste heat recovery systems. The

optimal economic solution accounts for the use of natural gas as a primary energy source, this is because its high-energy heating value and cost in comparison with biofuels or solar energy. However, it should be noticed that biofuels and solar energy may help to improve the environmental impact through the reduction of the CO_2 emissions and the proposed approach allows determining compensated solutions between the economic and environmental objectives.

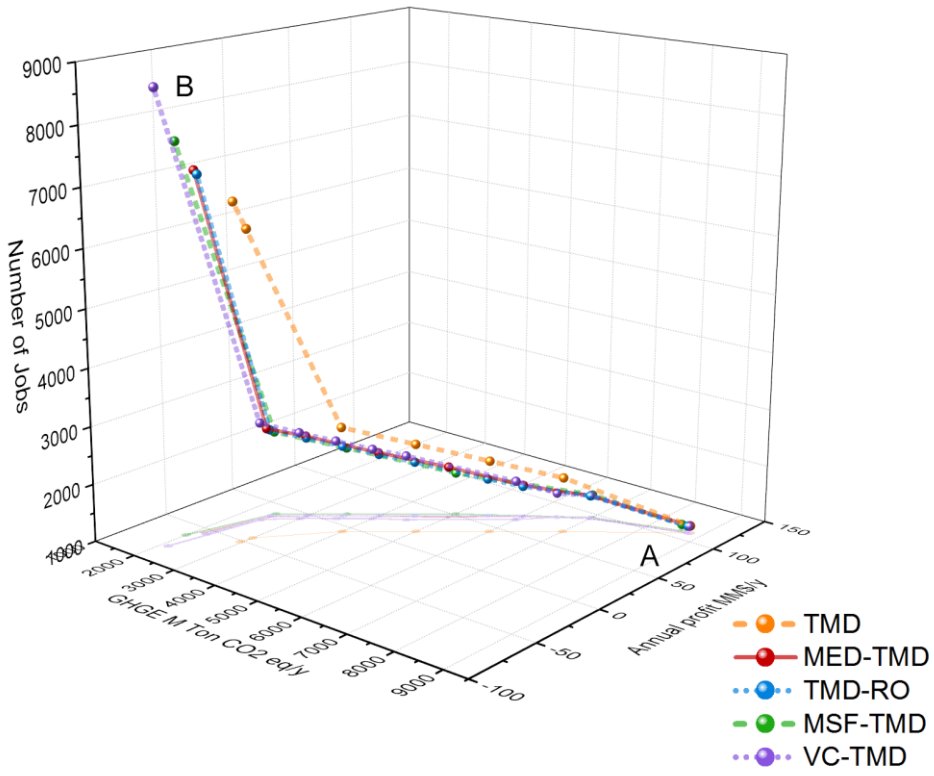

Figure 4.8. Pareto analysis involving the number of generated jobs.

4.7 References

1 Ghaffour, N.; Bundschuh, J.; Mahmoudi, H.; Goosen, M. F. A., Renewable energy-driven desalination technologies: A comprehensive review on challenges and potential applications of integrated systems, *Desalination*, 2015, 356, 94-114.

2 DOE, Department of Energy United States of America. The Water-Energy Nexus: Challenges and Opportunities, Washington, D.C., United States, 2014.

3 Abduljawad, M.; Ezzeghni, U., Optimization of Tajoura MSF desalination plant, *Desalination*, 2010, 254, 23-28.

4 Khoshgoftar-Manesh, M. H.; Ghalami, H.; Amidpour, M.; Hamedi, M. H., Optimal coupling of site utility steam network with MED-RO desalination through total site analysis and exergoeconomic optimization, *Desalination*, 2013, 316, 42-52.

5 Altaee, A.; Zaragoza, G., A conceptual design of low fouling and high recovery FO–MSF desalination plant, *Desalination*, 2014, 343, 2-7.

6 Iaquaniello, G.; Salladini, A.; Mari, A.; Mabrouk, A. A.; Fath, H. E. S., Concentrating solar power (CSP) system integrated with MED–RO hybrid desalination, *Desalination*, 2014, 336, 124-128.

7 Al-Weshahi, M. A.; Anderson, A.; Tian, G., Organic Rankine Cycle recovering stage heat from MSF desalination distillate water, *Appl. Energy*, 2014, 130, 738-747.

8 Dahdah, T. H.; Mitsos, A., Structural optimization of seawater desalination: I. A flexible superstructure and novel MED–MSF configurations, *Desalination*, 2014, 334, 252-265.

9 Dahdah, T. H.; Mitsos, A., Structural optimization of seawater desalination: II novel MED–MSF–TVC configurations, *Desalination*, 2014, 334, 219-227.

10 Rong, B.-G.; Turunen, I., Synthesis of new distillation systems by simultaneous thermal coupling and heat integration, *Ind. Eng. Chem. Res.*, 2006, 45, 3830-3842.

11 Ponce-Ortega, J.; Jiménez-Gutiérrez, M. A.; Grossmann, I. E., Simultaneous retrofit and heat integration of chemical processes, *Ind. Eng. Chem. Res.*, 2008, 47, 5512–5528.

12 George, J.; Sahu, G. C.; Bandyopadhyay, S., Heat integration in process water networks, *Ind. Eng. Chem. Res.*, 2011, 50, 3695–3704.

13 Zhang, B. J.; Luo, X. L.; Chen, Q. L.; Hui, C.-W., Heat integration by multiple hot discharges/feeds between plants, *Ind. Eng. Chem. Res*, 2011, 50, 10744–10754.

14 Lira-Barragán, L. F.; Ponce-Ortega, J. M.; Serna-González, M.; El-Halwagi, M. M., Sustainable integration of trigeneration systems with heat exchanger networks, *Ind. Eng. Chem. Res.*, 2014, 53, 2732−2750.

15 Lu, Y.; Chen, J., Integration design of heat exchanger networks into membrane distillation systems to save energy, *Ind. Eng. Chem. Res*, 2012, 51, 6798−6810.

16 Zhou, X.; Gingerich, D. B.; Mauter, M. S., Water treatment capacity of forward-osmosis systems utilizing power-plant waste heat, *Ind. Eng. Chem. Res*, 2015, 54, 6378−6389.

17 Gabriel, K. J.; El-Halwagi, M. M.; Linke, P., Optimization across the water−energy nexus for integrating heat, power, and water for industrial processes, coupled with hybrid thermal-membrane desalination, *Ind. Eng. Chem. Res*, 2016, 55, 3442−3466.

18 Zhang B. J.; Zhang, Z. L.; Liu, K.; Chen, Q. L., Network modeling and design for low grade heat recovery, refrigeration, and utilization in industrial parks, *Ind. Eng. Chem. Res.*, 2016, 55, 9725−9737.

19 Lira-Barragán, L. F.; Ponce-Ortega, J. M.; Serna-González, M.; El-Halwagi, M. M., Optimal design of process energy systems integrating sustainable considerations, *Energy*, 2014, 76, 139-160.

20 Helal, A. M.; E1-Nashar, A. M.; A1-Katheeri, E. S.; A1-Malek, S. A., Optimal design of hybrid RO/MSF desalination plants Part III: Sensitivity analysis, *Desalination*, 2004, 169, 43-60.

21 Papoulias, S. A.; Grossmann, I. E., A structural optimization approach in process synthesis. Part I: Utility systems, *Comput. Chem. Eng.*, 1983, 7, 695-706.

22 Papoulias, S.A.; Grossmann, I. E., A structural optimization approach in process synthesis. Part II: Heat recovery networks, *Comput. Chem. Eng.*, 1983, 7, 707-721.

23 CONAGUA, National Water Commission. Agricultural Statistics of Irrigation Districts, Mexico City, Mexico, 2014.

24 CEA, Sonora State Water Commission. Water Statistics in the State of Sonora Edition 2008. Hermosillo, Sonora, Mexico, 2008.

25 NREL, National Renewable National Laboratory (U.S. Department of Energy), National Solar Radiation Database, Washington D.C., USA, 2012.

26 Weinstein, L. A.; Loomis, J.; Bhatia, B.; Bierman, D. M.; Wang, E. N.; Chen, G., Concentrating solar power, *Chem. Rev.*, 2015, 115, 12797-12838.

27 Agashichev, S. P.; El-Nashar, A. M., Systemic approach for techno-economic evaluation of triple hybrid (RO, MSF and power-generation) scheme including accounting of CO_2 emission, *Energy*, 2005, 30, 1283-1303.

28 AlMarzooqi, F. A.; Al-Ghaferi, A. A.; Saadat I.; Hilal, N., Application of capacitive deionisation in water desalination: A review, *Desalination*, 2014, 342, 3-15.

29 Al-Karaghouli, A.; Kazmerski, L. L., Energy consumption and water production cost of conventional and renewable-energy-powered desalination processes, *Renew. Sust. Energy Rev*, 2013, 24, 343-356.

30 Ghobeity A.; Mitsos, A., Optimal design and operation of desalination systems: new challenges and recent advances, *Curr. Opin. Chem. Eng.*, 2014, 6, 61-68.

31 Helal, A. M.; Al-Malek, S. A., Design of a solar-assisted mechanical vapor compression (MVC) desalination unit for remote areas in the UAE, *Desalination*, 2006, 197, 273-300.

32 Kim, H. S.; Cheon-NO, H., Thermal coupling of HTGRs and MED desalination plants, and its performance and cost analysis for nuclear desalination, *Desalination*. 2012, 303, 17-22.

33 Mussati, S. F.; Aguirre, P. A.; Scenna, N. J., Improving the efficiency of the MSF once through (MSF-OT) and MSF-mixer (MSF-M) evaporators, *Desalination*, 2004, 166, 141-151.

34 Ng, K. C.; Thu, K.; Oh, S. J.; Ang, L.; Shahzad, M. W.; Ismail, A. B., Recent developments in thermally-driven seawater desalination: Energy efficiency improvement by hybridization of the MED and AD cycles, *Desalination*, 2015, 356, 256-270.

35 Sassi, K. M.; Mujtaba, I. M., Optimal design of reverse osmosis based desalination process with seasonal variation of seawater temperature, *Chem. Eng. Trans.*, 2011, 25, 1055-1060.

36 Sassi, K. M.; Mujtaba, I. M., Optimal design and operation of reverse osmosis desalination process with membrane fouling, *Chem. Eng. J.*, 2011, 171, 582-593.

37 Wang, Y.; Lior, N., Performance analysis of combined humidified gas turbine power generation and multi-effect thermal vapor compression desalination systems — Part 1: The desalination unit and its combination with a steam-injected gas turbine power system, *Desalination*, 2006, 196, 84-104.

38 Mezher, T.; Fath, H.; Abbas, Z.; Khaled, A., Techno-economic assessment and environmental impacts of desalination technologies, *Desalination*, 2011, 266, 263-273.

39 Sharon, H.; Reddy, K. S., A review of solar energy driven desalination technologies. *Renew, Sust. Energy Rev.*, 2015, 41, 1080-1118.

40 Lukic, N.; Diezel, L. L.; Fröba, A. P.; Leipertz, A., Economical aspects of the improvement of a mechanical vapour compression desalination plant by dropwise condensation, *Desalination*, 2010, 264, 173-178.

41 Wittholz, M. K.; O'Neill, B. K.; Colby, C. B.; Lewis D., Estimating the cost of desalination plants using a cost database, *Desalination*, 2008, 229, 10–20.

42 Khayet, M.; Matsuura T., Membrane distillation principles and applications; Economics, energy analysis and costs evaluation in MD. Elsevier, Boston, USA. 2011, 1, 429-452.

43 Al-Sahali, M.; Ettouney, H., Developments in thermal desalination processes:Design, energy, and costing aspects, *Desalination*, 2007, 214, 227–240.
44 Ophir, A.; Gendel, A., Steam driven large multi effect MVC (SD MVC) desalination process for lower energy consumption and desalination costs, *Desalination*, 2007, 205, 224–230.
45 Williams, C. M.; Ghobeity, A.; Pak A. J.; Mitsos, A., Simultaneous optimization of size and short-term operation for an RO plant, *Desalination*, 2012, 301, 42–52.
46 Al-Nory, M. T.; Brodsky, A.; Bozkaya, B.; Graves, S. C., Desalination supply chain decision analysis and optimization, *Desalination*, 2014, 347, 144–157.
47 EIA, Energy Information Administration (U.S.). Independent Statics and Analysis., Washington D.C., USA, 2016.
48 Mago, P. J.; Chamra, L. M.; Somayaji, C., Performance analysis of different working fluids for use in organic Rankine cycles, *J. Power Energy*, 2007, 221, 155-263.
49 Brooke, A.; Kendrick, D.; Meeruas, A.; Raman, R., *GAMS-language guide*, GAMS Development Corporation, Washington DC. 2016.

CHAPTER V

Multi-Objective Optimization of Dual-Purpose Power Plants and Water Distribution Networks

This chapter presents a multi-objective optimization approach for synthesizing water distribution networks involving dual-purpose power plants. The proposed model accounts for environmental, economic and social objectives by accounting for greenhouse gas emissions, jobs, and net profit. The model considers water and energy demands for domestic, agricultural and industrial users. Energy is provided through several alternatives including fossil fuels (i.e. natural gas and oil), biofuels (i.e. biomass, biogas, biodiesel, and bioethanol) and solar energy. Water demands are satisfied by fresh water from dams, lakes, rivers, aquifers and artificial storage tanks. The proposed model is applied to a case study from the Mexican State of Sonora. The results show the viability of the dual-purpose power-water plants, the merits of incorporating solar energy into the system, and the economic, environmental, and social benefits of applying the proposed approach. The optimal solution yields a total annual profit of $MM 1545.9, it generates an overall GHGE of 1.37×10^7 ton CO_2 eq/y and 19,781 jobs.

5.1 Introduction

Water scarcity is one of the main problems around the world. By the year 2030, a global water deficit of 40% is expected due to population growth, migration, urbanization, and industrialization.[1,2] Furthermore, climate change and variability are likely to have a negative impact on fresh water resources. The problem has been experienced most severely in the driest areas of the planet. To address the water shortage problems, several strategies have been proposed.[3] These options include extraction of water from aquifers, inter-state transportation of water and constructions of dams and artificial lakes. Other strategies include the installation of seawater and brackish water desalination plants as well as dual-purpose power plants where water and electricity are simultaneously generated. Currently, more than 86 million m^3 per day of fresh water streams are produced using desalination technologies.[4-6] The International Desalination Association (IDA) reports that there are around 18,000 desalination plants worldwide with most of the installed desalination plants using reverse osmosis (RO) and multi-stage flash (MSF) desalination techniques. It is worth noting that the majority of these plants are coupled with dual-purpose power plants producing simultaneously water and electricity.[3] Coproduction of water and power is a common practice especially in the Middle East and North African (MENA) countries where the lack of fresh water has prompted the installation of large-scale dual-purpose power plants.[4,5] The simultaneous production of water and energy has significant benefits in terms of sustainability, Raluy et al. (2004) reported that a dual-purpose power plant can reduce the overall environmental impact by 75% compared with thermal desalination technologies.[7] More opportunities are possible and the technological innovation is essential in developing new energy-efficient technologies to produce water and energy by reducing the cost and the environmental impact.[8]

Fossil fuels play and important role in power plants, where natural gas and coal remain to be the main sources of energy to produce water and electricity; however, because the used fossil fuels in power plants are responsible for over 65% of the estimated carbon dioxide (CO_2) emissions,[9,10] renewable energy can play an important role in desalination and power generation by reducing the CO_2 emissions that contribute to the global warming and fossil resource depletion.[11] The use and development of renewable energy technologies may provide new pathways for sustainable water and energy production to meet future

demands.[12-15] Several countries (such as Qatar, Egypt, Saudi Arabia, UAE, and Jordan) are developing large solar-powered plants to provide electricity and water.[16,17] Solar energy and biofuels represent great potential alternatives to provide heat. Nonetheless, the use of biofuels and solar technologies should be subjected to techno-economic assessment.

Recently, some approaches have been reported for the proper use of water in industrial parks[18] and refineries.[19] Some others have been proposed to enhance the efficiency of power production and desalination involving renewable energy. Gutierrez-Arriaga et al. developed a multi-objective optimization procedure for designing integrated steam power plants, where economic and environmental objectives were considered.[20] Ianquaniello et al. presented an economic analysis for water desalination (involving MSF and RO) powered by solar energy, this model accounts for energy consumption and greenhouse gas emissions (GHGE), the results showed that the price of water in such systems is close to the price of water produced through conventional fossil-based desalination systems.[21] Liqreina and Qoaider presented a simulation of a concentrating solar power (CSP) in southern Spain, the results showed that the proposed power plant can work better in dry regions.[22] This work was later extended by including an optimization procedure.[23] Fthenakis et al. presented an analysis of RO desalination powered by solar energy (PV), the analysis was performed using small (6,550 m^3/day) and a large (190,000 m^3/day) capacities, the results showed that the PV-RO power plants have the potential to replace 19 million m^3 of diesel fuel per year along with the corresponding reduction in CO_2 emissions.[24] Sankar et al. presented an analysis of integrated solar power and desalination plants, where concentrated solar power plants and biomass can be used, the results showed several savings in internal energy consumption and investment cost.[25] Gorjian and Ghobadian presented a comprehensive analysis for the potential installation of a water desalination plant powered by solar energy with reduction in CO_2 emissions due to the integration of solar energy.[26] Abdelhady et al. developed an optimization approach for the cost-effective conservation of energy and reduction of GHG emissions, the model was applied to an industrial process coupled with cogeneration systems including fossil fuels and solar energy.[27] Palenzuela et al. presented a techno-economic analysis of several seawater desalination systems with concentrated solar power plants applied to the MENA region.[28,29] Diaf et al. proposed a techno-economic analysis for solar

desalination plants based on a multiple tray desalination unit running with solar energy to satisfy small scale water demands.[30]

In addition to the importance of integrating energy and water in developing sustainable development strategies, it is also important to address the water distribution issues through a macroscopic approach. Liu et al. introduced a mixed–integer linear programming (MILP) problem for the management, production, distribution and storage of reclaimed and desalinated water accounting for the location and capacity of the new desalination plant, pipelines, pumping stations, wastewater treatment and reclaimed water plants.[31] Athilan et al. developed a mathematical model to design macroscopic water networks, the model accounted for water sources (seawater, underground water, and desalination plants) and water demands, which allows identifying the location and capacity of new plants. This work was extended later to include monthly demand fluctuations, water storage, and wastewater treatment.[32,33] Napoles-Rivera et al. introduced a mathematical programing formulation for designing water distribution networks considering economic and sustainability aspects, this model includes sources (dams, springs and deep wells) and domestic and agricultural users. Later, this model was extended to include alternative water sources (harvested rainwater), seasonal availability (natural sources), population growth (water demands) and industrial water demands.[34,35] Alnouri et al. presented an energy management approach involving water desalination and power generation where a deterministic MILP problem was used to identify the optimal allocation of desalination plants, capacities, technologies, and energy sources, this model also took into account the variation of water and electricity demands, the results showed significant cost reductions.[36] Gonzalez-Bravo et al. proposed a single objective optimization for the synthesis of water distribution network involving power-desalination plants, the model was applied in a water-stressed region accounting for the water in lakes, dams, aquifers, rivers, as well as the water in existing storage tanks, in this case the authors did not take into account the possibility to integrate multiple fuels as well as the possibility to integrate solar energy to supply the power-desalination plant, since Sonoran desert regions is one of the most solar irradiation areas around the world.[37]

While previous research activities have tackled the problems of design dual-purpose power-water desalination plants and water-management networks separately, there is a need

to address both problems simultaneously and to introduce the use of renewable energy while considering multiple design objectives. This chapter presents a multi-objective optimization model to determine the optimal water distribution network involving dual-purpose power plants powered by renewable energy. The proposed multi-objective optimization model simultaneously addresses economic, environmental, and social objectives.

5.2 Problem statement

The problem statement is descried as follows: Given a macroscopic water distribution problem with:

- Water and electricity demands for domestic users which have seasonal variations through the year.
- Water and electricity demands for industrial users which remain constant through the year.
- Water and electricity demands for agricultural users which depend on the cropping season with seasonal variations through the year.
- The water demands can be satisfied by the existing dams, aquifers, and rivers of each region, the availability of water depends on the natural recharge, precipitation, and extractions.
- The electricity demands can be satisfied by the existing power plants of the region.
- The water and energy demands can be satisfied by the installation of new dual-purpose power plants.
- Overexploited resources (dams, aquifers, and rivers) can be recharged by the water produced in dual-purpose power plants.
- Existing and new storage tanks in the considered regions are also part of the distribution model.
- The energy requirements for the dual-purpose power plants can be satisfied using fossil fuels (i.e. natural gas and oil), biofuels (i.e. biomass, biogas, biodiesel, and bioethanol) and solar energy.
- The use of fossil fuels and biofuels is subject to the maximum availability in each time period.

The main problem consists in finding the optimal water distribution network accounting for economic, environmental and social objectives. The model seeks to satisfy energy and water demands accounting for the net annual profit, as well as the overall greenhouse gas emissions (GHGE). **Figure 5.1** is a schematic representation of the proposed superstructure embedding the potential configurations of the design alternatives.

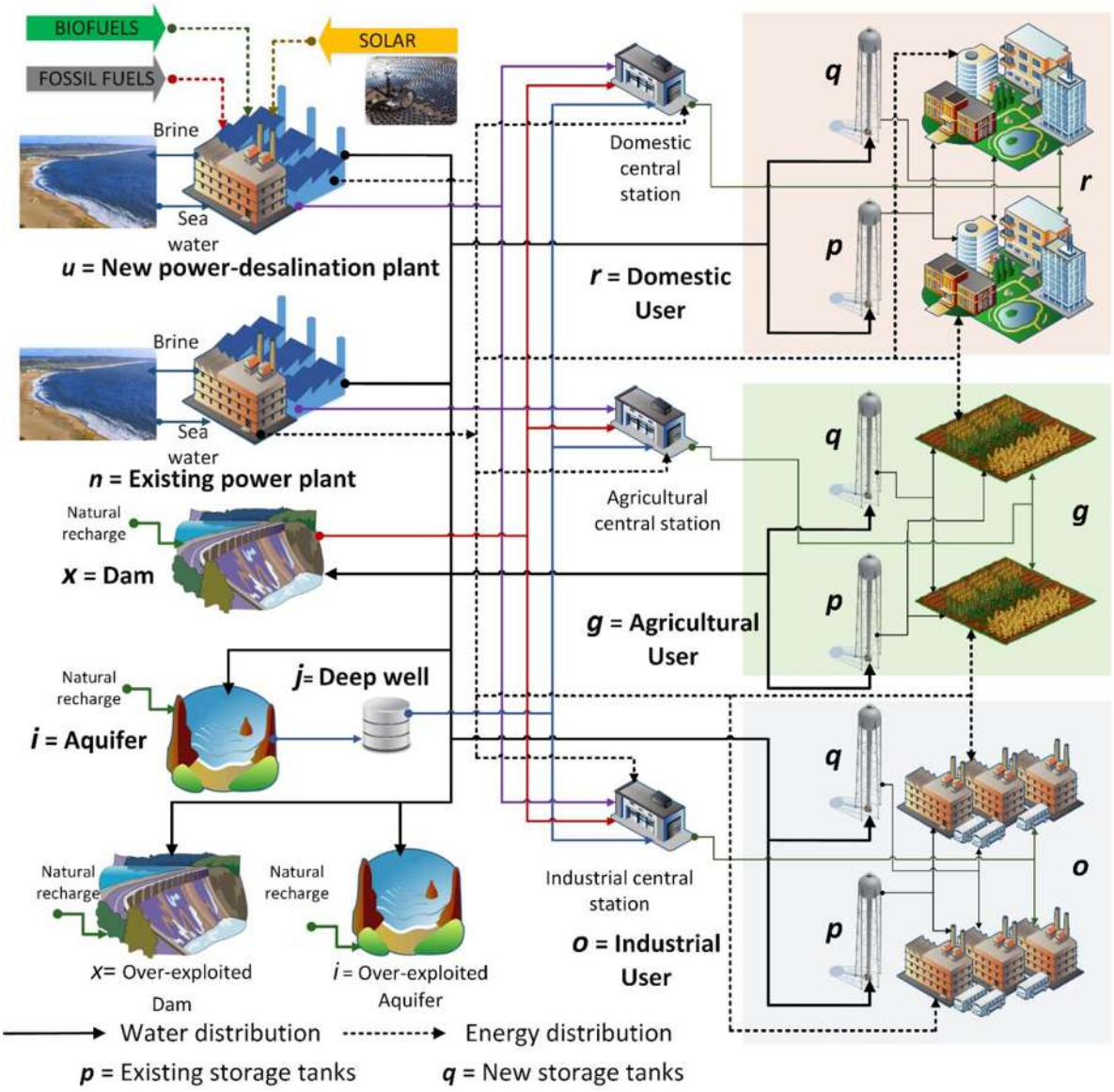

Figure 5.1. Proposed superstructure for water distribution integrated to dual-purpose power plants.

5.3 Mathematical model

The water distribution network can be described by tracking mass, energy, and economic aspects. The mathematical model is based on the superstructure shown in **Figure 5.1**. The water and electricity demands are tracked for domestic users (r), industrial users (o) and agricultural users (g), the water demands can be satisfied by the water volume content in the existing aquifers of the region (i) by extracting water from the existing deep wells in each region (j) and by the existing water in the dams of the region (x). In this case, the model considers the location of existing storage tanks (p) as well as the possible installation of new storage tanks (q). The electricity can be generated in the existing power plants of the region (n) as well as the possible installation of new dual purpose plants (u). The energy requirements of the dual purpose power plant can be fully satisfied using fossil fuels (f), biofuels (b) and/or solar energy. The model is divided in time periods (t) (i.e., months). The proposed model includes linear, nonlinear and logical relationships.

5.3.1 Model for water distribution

The change in the total water volume of an aquifer over a certain time period ($W_{i,t}$ - $W_{i,t-1}$) is equal to the sum of the of water received from existing storage tanks ($s_{p,i,t}^{E,aq}$), new storage tanks ($s_{q,i,t}^{N,aq}$), existing power desalination plants ($B_{n,i,t}^{E,des}$), new power desalination plants ($B_{u,i,t}^{N,des}$), the recharge from agricultural crops ($F_{i,t}^{agr}$) and the natural recharge ($R_{i,t}^{aq}$), minus the water that is sent to deep wells ($a_{i,j,t}^{dw}$):

$$W_{i,t} - W_{i,t-1} = \sum_{p} s_{p,i,t}^{E,aq} + \sum_{q} s_{q,i,t}^{N,aq} + \sum_{n} B_{n,i,t}^{E,des} + \sum_{u} B_{u,i,t}^{N,des} + F_{i,t}^{agr} + R_{i,t}^{aq} - \sum_{j} a_{i,j,t}^{dw}, \qquad \forall i, \in I, \forall t \in T, t \neq 1 \tag{5.1}$$

The water in deep wells ($a_{i,j,t}^{dw}$) is extracted by the distribution stations including domestic stations ($d_{r,j,t}^{dom}$), industrial stations ($d_{g,j,t}^{agr}$) and agricultural stations ($d_{o,j,t}^{ind}$):

$$\sum_{i} a_{i,j,t}^{dw} = \sum_{r} d_{r,j,t}^{dom} + \sum_{g} d_{g,j,t}^{agr} + \sum_{o} d_{o,j,t}^{ind}, \qquad \forall j \in J, \forall t \in T \tag{5.2}$$

Then, the total water in each central station ($h_{i,t}$) is equal to the sum of the water received from existing power desalination plants ($v^{E}_{g,n,t}$), new power desalination plants ($v^{N}_{g,u,t}$), deep wells ($d_{g,j,t}$), and dams ($w_{g,x,t}$).

For domestic stations:

$$h^{dom}_{r,t} = \sum_{n} v^{E,dom}_{r,n,t} + \sum_{u} v^{N,dom}_{r,u,t} + \sum_{j} d^{dom}_{r,j,t} + \sum_{x} w^{dom}_{r,x,t}, \qquad \forall r \in R, \forall t \in T \tag{5.3}$$

For industrial stations:

$$h^{ind}_{o,t} = \sum_{n} v^{E,ind}_{o,n,t} + \sum_{u} v^{N,ind}_{o,u,t} + \sum_{j} d^{ind}_{o,j,t} + \sum_{x} w^{ind}_{o,x,t}, \qquad \forall o \in O, \forall t \in T \tag{5.4}$$

For agricultural stations:

$$h^{agr}_{g,t} = \sum_{n} v^{E,agr}_{g,n,t} + \sum_{u} v^{N,agr}_{g,u,t} + \sum_{j} d^{agr}_{g,j,t} + \sum_{x} w^{agr}_{g,x,t}, \qquad \forall g \in G, \forall t \in T \tag{5.5}$$

The water demands (domdem) can be satisfied by the volume of water in central station ($h_{r,t}$), plus the water in existing storage tanks ($s^{E}_{p,r,t}$) and new storage tanks ($s^{N}_{q,r,t}$).

For domestic users:

$$\mathrm{domdem}_{r,t} = h^{dom}_{r,t} + \sum_{p} s^{E,dom}_{p,r,t} + \sum_{q} s^{N,dom}_{q,r,t}, \qquad \forall r \in R, \forall t \in T \tag{5.6}$$

For industrial users:

$$\mathrm{inddem}_{o,t} = h^{ind}_{o,t} + \sum_{p} s^{E,ind}_{o,p,t} + \sum_{q} s^{N,ind}_{o,q,t}, \qquad \forall o \in O, \forall t \in T \tag{5.7}$$

For agricultural users:

$$\mathrm{agrdem}_{g,t} = h^{agr}_{g,t} + \sum_{p} s^{E,agr}_{g,p,t} + \sum_{q} s^{N,agr}_{g,q,t}, \qquad \forall g \in G, \forall t \in T \tag{5.8}$$

A percentage of the used water for agriculture (pca) seeps into the ground, thus it may recharge the aquifer ($F^{agr}_{i,t}$) as follows:

$$F^{agr}_{i,t} = \sum_{g(i)} pca * \mathrm{agrdem}_{g,i,t} \qquad \forall i \in I, \forall t \in T \tag{5.9}$$

The total water volume in a dam in a certain time period ($M_{x,t}$ - $M_{x,t-1}$) is equal to the sum of the water received from existing power desalination plants ($G^{E,rel}_{n,x,t}$), new power desalination plants ($G^{N,rel}_{u,x,t}$) and the water naturally recharged ($R^{dam}_{x,t}$), minus the water sent to domestic stations ($w^{dom}_{r,x,t}$), industrial stations ($w^{ind}_{o,x,t}$) and agricultural stations ($w^{agr}_{g,x,t}$):

$$M_{x,t} - M_{x,t-1} = \sum_n G^{E,rel}_{n,x,t} + \sum_u G^{N,rel}_{u,x,t} + R^{dam}_{x,t} - \sum_r w^{dom}_{r,x,t} - \sum_g w^{agr}_{g,x,t} - \sum_o w^{ind}_{o,x,t}, \qquad \forall x, \in X, \forall t \in T, t \neq 1 \tag{5.10}$$

The total water volume in existing storage tanks in a certain time period ($S^{E}_{p,t}$ - $S^{E}_{p,t-1}$) is equal to the sum of the water received from existing power desalination plants ($D^{E,Esto}_{n,p,t}$) and new power desalination plants ($D^{N,Esto}_{u,p,t}$), minus the water sent to domestic stations ($s^{E,dom}_{p,r,t}$), industrial stations ($s^{E,ind}_{o,p,t}$), agricultural stations ($s^{E,agr}_{g,p,t}$) and the water sent to aquifers ($s^{E,aq}_{p,i,t}$):

$$S^{E}_{p,t} - S^{E}_{p,t-1} = \sum_n D^{E,Esto}_{n,p,t} + \sum_u D^{N,Esto}_{u,p,t} - \sum_r s^{E,dom}_{p,r,t} - \sum_g s^{E,agr}_{g,p,t} - \sum_o s^{E,ind}_{o,p,t} - \sum_i s^{E,aq}_{p,i,t} \qquad \forall p \in P, \forall t \in T, t \neq 1 \tag{5.11}$$

The total water volume in new storage tanks in a certain time period ($S^{N}_{q,t}$ - $S^{N}_{q,t-1}$) is equal to the sum of the water received from existing power desalination plants ($D^{E,Nsto}_{n,q,t}$) and new power desalination plants ($D^{N,Nsto}_{u,q,t}$), minus the water sent to domestic stations ($s^{N,dom}_{q,r,t}$), industrial stations ($s^{N,ind}_{o,q,t}$), agricultural stations ($s^{N,agr}_{g,q,t}$) and the water sent to aquifers ($s^{N,aq}_{q,i,t}$):

$$S^{N}_{q,t} - S^{N}_{q,t-1} = \sum_n D^{E,Nsto}_{n,q,t} + \sum_u D^{N,Nsto}_{u,q,t} - \sum_r s^{N,dom}_{q,r,t} - \sum_g s^{N,agr}_{g,q,t} - \sum_o s^{N,ind}_{o,q,t} - \sum_i s^{N,aq}_{q,i,t} \qquad \forall q \in Q, \forall t \in T, t \neq 1 \tag{5.12}$$

The amount of seawater extracted from the sea by the existing power desalination plants ($SW^{in,E}_{n,t}$) is equal to the sum of water sent to the existing storage tanks ($D^{E,E\,sto}_{n,p,t}$), new storage tanks ($D^{E,N\,sto}_{n,q,t}$), domestic stations ($v^{E,dom}_{r,n,t}$), industrial stations ($v^{E,ind}_{o,n,t}$) and agricultural

stations ($v_{g,n,t}^{E,agr}$), also the water sent to recharge aquifers ($B_{n,i,t}^{E,des}$), the water sent to recharge dams ($G_{n,x,t}^{E,rel}$) and the water sent to the sea as reject ($b_{n,t}^{E,rej}$):

$$SW_{n,t}^{in,E}(1-\beta)=\sum_{p}D_{n,p,t}^{E,E\,sto}+\sum_{q}D_{n,q,t}^{E,N\,sto}+\sum_{r}v_{r,n,t}^{E,dom}+\sum_{g}v_{g,n,t}^{E,agr}+\sum_{o}v_{o,n,t}^{E,ind}+\sum_{i}B_{n,i,t}^{E,des}+\sum_{x}G_{n,x,t}^{E,rel}+b_{n,t}^{E,rej} \qquad \forall n\in N,\forall t\in T \tag{5.13}$$

The amount of seawater extracted from the sea by the new power desalination plants ($SW_{u,t}^{in,N}$) is equal to the sum of water sent to the existing storage tanks ($D_{u,p,t}^{N,E\,sto}$), new storage tanks ($D_{u,q,t}^{N,N\,sto}$), domestic stations ($v_{r,u,t}^{N,dom}$), industrial stations ($v_{o,u,t}^{N,ind}$) and agricultural stations ($v_{g,u,t}^{N,agr}$), also the water sent to recharge aquifers ($B_{u,i,t}^{N,des}$), the water sent to recharge dams ($G_{u,x,t}^{N,rel}$) and the water sent to the sea as reject ($b_{u,t}^{Nrej}$):

$$SW_{u,t}^{in,N}(1-\beta)=\sum_{p}D_{u,p,t}^{N,Esto}+\sum_{q}D_{u,q,t}^{N,Nsto}+\sum_{r}v_{r,u,t}^{N,dom}+\sum_{g}v_{g,u,t}^{N,agr}+\sum_{o}v_{o,u,t}^{N,ind}+\sum_{i}B_{u,i,t}^{N,des}+\sum_{x}G_{u,x,t}^{N,rel}+b_{u,t}^{N,rej} \qquad \forall u\in U,\forall t\in T$$

(5.14)

The rejected brine can be calculated by multiplying the total seawater by a factor (β) which represents the ratio of brine to seawater flows:

$$b_{n,t}^{E,rej}=b*SW_{u,t}^{in,N}, \qquad \forall u\in U,\forall t\in T \tag{5.15}$$

$$b_{u,t}^{N,rej}=\beta*SW_{u,t}^{in,N}, \qquad \forall u\in U,\forall t\in T \tag{5.16}$$

5.3.2 Model for power production

The total produced power ($TEnergy_t$) is the sum of the energy generated in existing ($Eproduction_{n,t}^{E}$) and new ($Eproduction_{u,t}^{N}$) power desalination plants:

$$TEnergy_t=\sum_{u}Eproduction_{u,t}^{N}+\sum_{n}Eproduction_{n,t}^{E}, \qquad \forall t\in T \tag{5.17}$$

This value is subject to the electricity demands in industrial zones ($E_{o,t}^{ind}$), domestic users ($E_{r,t}^{dom}$) and agricultural regions ($E_{r,t}^{dom}$):

$$TEnergy_t = \sum_r E_{r,t}^{dom} + \sum_g E_{g,t}^{agr} + \sum_o E_{o,t}^{ind} \qquad \forall t \in T \tag{5.18}$$

The energy produced in new power desalination plants is a function of their capacity. This function is represented through multiplying the capacity of the new power desalination plant ($SW_{u,t}^{in,N}$) times a factor (GEP) that represents the energy usage per unit flowrate of incoming seawater:

$$EProduction_{u,t}^{N} = SW_{u,t}^{in,N} \cdot \mathrm{GEP}, \qquad \forall u \in U, \forall t \in T \tag{5.19}$$

5.3.3 Existence of new storage tanks

The existence, location and size of new storage tanks in each region is modeled through binary variables (y_q^{sto}), if the binary variable is equal to one, then the tank is needed, if the binary variable is equal to zero, the tank is not needed, the existence is subject to the maximum capacity of the tank ($\Theta_q^{sto,\max}$) and the minimum capacity of the tank ($\Theta_{\mathrm{q}}^{\mathrm{sto,min}}$):

$$y_q^{sto} \cdot \Theta_{\mathrm{q}}^{\mathrm{sto,min}} \le S_q^{max} \le y_q^{sto} \cdot \Theta_{\mathrm{q}}^{\mathrm{sto,max}} \tag{5.20}$$

The associated installation cost ($InstCost_{q,t}^{sto}$) is a function of a fixed cost of the tank (Z_1), the unit variable cost (Z_2), and a factor used to annualize the inversion (k_{F}). In addition, S_q^{max} represents the maximum capacity for storage tanks:

$$InstCost_q^{sto} = \mathrm{k}_{\mathrm{F}}\left[\mathrm{Z}_1 \cdot y_q^{sto} + \mathrm{Z}_2\left(S_q^{max}\right)^{\alpha}\right], \qquad \forall q \in Q \tag{5.21}$$

Where S_q^{max} is greater than the existing water in the storage tank ($S_{q,t}^{N}$) in any time period t

.

$$S_{q,t}^{N} \le S_q^{max} \qquad q \in Q, t \in T \tag{5.22}$$

Where the storage cost can be calculated by the next equation:

$$StorageCost = H_Y \sum_q InstCost_q^{sto} \tag{5.23}$$

5.3.4 Existence of new power desalination plants

The existence, location, and capacity of the new power desalination plants are modeled through binary variables (y_u^{pdes}). If the binary variable is equal to one, then the power-desalination plant is needed, if the binary variable is equal to zero, the power desalination plant is not needed, also the power-desalination plant has a maximum capacity ($\Theta_u^{pdes,max}$) and a minimum capacity ($\Theta_u^{pdes,min}$):

$$y_u^{pdes} \cdot \Theta_u^{pdes,min} \leq SW_u^{max} \leq y_u^{pdes} \cdot \Theta_u^{pdes,max} \tag{5.24}$$

The installation cost ($InstCost_{u,t}^{pdes}$) is a function of the unit costs (Z_3 and Z_4), the maximum seawater capacity (SW_u^{max}) and a factor used to annualize the inversion (k_F). The operating cost ($OpCost_{u,t}^{pdes}$) is a function of a unit operating cost (Z_5), the total water extracted from the sea ($SW_{u,t}^{in,N}$), the recovery factor ($1-\beta$) and a factor used to account for the operational time per year (H_Y):

$$InstCost_u^{pdes} = k_F\left[Z_3 \cdot y_u^{pdes} + Z_4 \left(SW_u^{max} \right)^{\alpha} \right] \qquad \forall u \in U \tag{5.25}$$

$$OpCost_{u,t}^{pdes} = H_Y\left[Z_5 \left(1-\beta\right) SW_{u,t}^{in,N} \right] \qquad \forall u \in U, \forall t \in T \tag{5.26}$$

Where SW_u^{max} is greater than any possible water in a power-desalination plant ($SW_{q,t}^{N}$) during any time period t.

$$SW_{u,t}^{in,N} \leq SW_u^{max} \qquad u \in U, t \in T \tag{5.27}$$

The operating cost is a function of the total water extracted from the sea ($SW_{n,t}^{in,E}$) multiplying by the total recovery ($1-\beta$) and the operating unit cost (Z_6):

$$OpCost_{n,t}^{E,des} = H_Y\left[Z_6 \left(1-\beta\right) SW_{n,t}^{in,E} \right] \qquad \forall n \in N, \forall t \in T \tag{5.28}$$

H_Y is a factor used to account for the operational time per year.

The installation cost for new power-desalination plants can be calculated as follows:

$$NPDinstcost = \sum_{u} InstCost_{u}^{pdes} \tag{5.29}$$

The operating cost for new power desalination plants can be calculated using the next expression:

$$NPDopcost = \sum_{u}\sum_{t} OpCost_{u,t}^{pdes} \tag{5.30}$$

On the other hand, the total operating cost for existing power-desalination plants can be calculated using the following expression:

$$TEPDopcost = \sum_{n}\sum_{t} TOpCost_{n,t}^{E,des} \tag{5.31}$$

where the total operating cost for the existing power-desalination plant ($TOpCost_{n,t}^{E,des}$) also includes the cost of the fuel consumption.

The total energy requirements ($TER_{u,t}^{N}$) of the new power desalination plants is a function of the total seawater fed. This function has a linear behavior and depends on the capacity of the new power desalination plants ($SW_{u,t}^{in,N}$) multiplied by a factor (FCF):

$$TER_{u,t}^{N} = SW_{u,t}^{in,N} \cdot \mathrm{FCF}, \qquad \forall u \in U, \forall t \in T \tag{5.32}$$

where $TER_{u,t}^{N}$ is equal to the energy obtained by the combustion of fossil fuels ($Q_{f,u,t}^{fossil}$), biofuels ($Q_{b,u,t}^{biofuel}$) and the energy obtained by the solar collector ($Q_{u,t}^{solar}$) during any period *t*.

$$TER_{u,t}^{N} = \sum_{f \in F} Q_{f,u,t}^{fossil} + \sum_{b \in B} Q_{b,u,t}^{biofuel} + Q_{u,t}^{solar}, \qquad \forall u \in U, \forall t \in T \tag{5.33}$$

The total energy cost (TEC^{N}) is obtained by the next equation, where FFC_f and BFC_b are the prices of fossil fuels and biofuels, respectively.

$$NPDenergycost = H_Y \sum_{u}\sum_{t}\left[\sum_{f \in F}\left(\mathrm{FFC}_f \cdot Q_{f,u,t}^{fossil}\right) + \sum_{b \in B}\left(\mathrm{BFC}_b \cdot Q_{b,u,t}^{biofuel}\right)\right] \tag{5.34}$$

The amount of heat to be produced is subject to the availability of biofuels ($\mathrm{AVF}_{f,t}^{\max}$) and fossil fuels ($\mathrm{AVB}_{b,t}^{\max}$) multiplied by its corresponding heating power factor, HPF_f for fossil fuels, and HPB_b for biofuels, according to the next relationships.

For fossil fuels:

$$\sum_u Q_{f.u.t}^{fossil} \le \mathrm{HPF}_f \cdot \mathrm{AVF}_{f,t}^{\max} \qquad \forall f \in F, \forall t \in T \tag{5.35}$$

For biofuels:

$$\sum_u Q_{b.u.t}^{biofuel} \le \mathrm{HPB}_b \cdot \mathrm{AVB}_{b,t}^{\max} \qquad \forall b \in B, \forall t \in T \tag{5.36}$$

5.3.5 Existence of solar collector

The existence, area, and cost of the solar collector are modeled using binary variables (w_u^{solar}). If the binary variable is equal to one, then the solar collector is needed, if the binary variable is equal to zero, the solar collector is not needed, this is activated according to the maximum ($\mathrm{ATot}_u^{\max}$) and minimum collecting area ($\mathrm{ATot}_u^{\min}$):

$$w_u^{solar} \cdot \mathrm{ATot}_u^{\min} \le AREA_u^{solar,max} \le w_u^{solar} \cdot \mathrm{ATot}_u^{\max} \tag{5.37}$$

The capital cost for the solar collector ($SCCost_u^{solar}$) is a function of the unit costs (Z_1^{solar} and Z_2^{solar}), the maximum effective solar collector area ($AREA_u^{solar,max}$), an area factor (γ) and a factor to annualize the inversion ($\mathrm{k_F}$). The operating cost ($OpCost_{u,t}^{solar}$) is a function of a unit operating factor (Z_3^{solar}), the area of the solar collector in each period ($A_{u,t}^{solar}$) and a factor to account for the operational time per year ($\mathrm{H_Y}$):

$$SCCost_u^{solar} = \mathrm{k_F}\left[\mathrm{Z}_1^{solar} \cdot w_u^{solar} + \mathrm{Z}_2^{solar} \left(AREA_u^{solar,max} \right)^{\alpha} \right] \qquad \forall u \in U \tag{5.38}$$

$$SOCost_{u,t}^{solar} = \mathrm{H_Y}\left[\mathrm{Z}_3^{solar} \cdot A_{u,t}^{solar} \right] \qquad \forall u \in U, \forall t \in T \tag{5.39}$$

where $AREA_u^{solar,max}$ is greater than the existing area of the solar collector ($A_{u,t}^{solar}$) in any time period t .

$$A_{u,t}^{solar} \le AREA_{u}^{solar,max} \qquad \forall u \in U, t \in T \tag{5.40}$$

The heating provided by the solar collector ($Q_{u,t}^{solar}$) is obtained multiplying the useful collected energy ($UCE_{u,t}^{solar}$) by the effective area of the solar collector ($A_{u,t}^{solar}$):

$$Q_{u,t}^{solar} = UCE_{u,t}^{solar} \cdot A_{u,t}^{solar} \tag{5.41}$$

The total cost for the solar collector can be calculated using the next expression:

$$SolarCost = \sum_{u} SCCost_{u}^{solar} + \sum_{u}\sum_{t} SOCost_{u,t}^{solar} \tag{5.42}$$

5.3.6 Pumping and piping costs

The water distribution can be calculated using the following equation:

$$\begin{aligned} Piping\ cost = \mathrm{k_F} \Bigg[& \sum_{r} \mathrm{DPC1_r} \cdot y_{r}^{h,dom} + \sum_{p}\sum_{r} \mathrm{DPC2_{p,r}} \cdot y_{p,r}^{sE,dom} + \sum_{q}\sum_{r} \mathrm{DPC3_{q,r}} \cdot y_{q,r}^{sN,dom} \\ & + \sum_{g} \mathrm{APC1_g} \cdot y_{g}^{h,agr} + \sum_{p}\sum_{g} \mathrm{APC2_{p,g}} \cdot y_{g,p}^{sE,agr} + \sum_{q}\sum_{g} \mathrm{APC3_{q,g}} \cdot y_{g,q}^{sN,agr} \\ & + \sum_{o} \mathrm{IPC1_o} \cdot y_{o}^{h,ind} + \sum_{p}\sum_{o} \mathrm{IPC2_{p,o}} \cdot y_{o,p}^{sE,ind} + \sum_{q}\sum_{o} \mathrm{IPC3_{q,o}} \cdot y_{q,o}^{sN,ind} \\ & + \sum_{r}\sum_{j} \mathrm{DPC4_{r,j}} \cdot y_{r,j}^{d,dom} + \sum_{g}\sum_{j} \mathrm{APC4_{g,j}} \cdot y_{g,j}^{d,agr} + \sum_{o}\sum_{j} \mathrm{IPC4_{o,j}} \cdot y_{o,j}^{d,ind} \\ & + \sum_{r}\sum_{x} \mathrm{DPC5_{r,x}} \cdot y_{r,x}^{w,dom} + \sum_{g}\sum_{x} \mathrm{APC5_{g,x}} \cdot y_{g,x}^{w,agr} + \sum_{o}\sum_{x} \mathrm{IPC5_{o,x}} \cdot y_{o,x}^{w,ind} \\ & + \sum_{n}\sum_{i} \mathrm{BPC1_{n,i}} \cdot y_{n,i}^{BE,des} + \sum_{u}\sum_{i} \mathrm{BPC2_{u,i}} \cdot y_{u,i}^{BN,des} + \sum_{r}\sum_{n} \mathrm{DPC6_{r,n}} \cdot y_{r,n}^{vE,dom} \\ & + \sum_{r}\sum_{u} \mathrm{DPC7_{r,u}} \cdot y_{r,u}^{vN,dom} + \sum_{g}\sum_{n} \mathrm{APC6_{g,n}} \cdot y_{g,n}^{vE,agr} + \sum_{g}\sum_{u} \mathrm{APC7_{g,u}} \cdot y_{g,u}^{vN,agr} \\ & + \sum_{o}\sum_{n} \mathrm{IPC6_{o,n}} \cdot y_{o,n}^{vE,ind} + \sum_{o}\sum_{u} \mathrm{IPC7_{o,u}} \cdot y_{o,u}^{vN,ind} + \sum_{n}\sum_{q} \mathrm{EPC1_{n,q}} \cdot y_{n,q}^{DE,Nsto} \\ & + \sum_{n}\sum_{p} \mathrm{EPC2_{n,p}} \cdot y_{n,p}^{DE,Esto} + \sum_{u}\sum_{q} \mathrm{NPC1_{u,q}} \cdot y_{u,q}^{DN,Nsto} + \sum_{u}\sum_{p} \mathrm{NPC2_{u,p}} \cdot y_{u,p}^{DN,Esto} \\ & + \sum_{n}\sum_{x} \mathrm{GPC1_{n,x}} \cdot y_{n,x}^{GE,rel} + \sum_{u}\sum_{x} \mathrm{GPC2_{u,x}} \cdot y_{u,x}^{GN,rel} + \sum_{i}\sum_{j} \mathrm{AQP1_{i,j}} \cdot y_{i,j}^{a,dw} \\ & + \sum_{p}\sum_{i} \mathrm{SPC1_{p,i}} \cdot y_{p,i}^{sE,aq} + \sum_{q}\sum_{i} \mathrm{SPC2_{q,i}} \cdot y_{q,i}^{sN,aq} \Bigg] \end{aligned} \tag{5.43}$$

The piping cost factors are determined by the next equation:

$$PipingCostFactor = k_m LD^m \tag{5.44}$$

where L is the pipe length, D^m is the pipe diameter, k_m and m are pipe cost parameters that depend on the pipe material. Because the diameter of the pipes, the distance from the storage points to final users and height are fixed, then the flow rate determines the piping cost. The existence of the pipe is determined by the binary variable and it is used to activate the pipe cost accounting for the maximum capacity used over all time periods. Maximum values to determine piping cost are described in the supplementary material.

The pumping cost can be calculated using the next expression:

$$\begin{aligned} Pumping\ cost = \mathrm{H_Y} \Bigg[& \sum_{r}\sum_{t} h^{dom}_{r,t}\ \mathrm{PPD1}_{\mathrm{r,t}} + \sum_{p}\sum_{r}\sum_{t} s^{E,dom}_{p,r,t}\ \mathrm{PPD2}_{\mathrm{p,r,t}} + \sum_{q}\sum_{r}\sum_{t} s^{N,dom}_{q,r,t}\ \mathrm{PPD3}_{\mathrm{q,r,t}} \\ & + \sum_{g}\sum_{t} h^{agr}_{g,t}\ \mathrm{PPA1}_{\mathrm{g,t}} + \sum_{g}\sum_{p}\sum_{t} s^{E,agr}_{g,p,t}\ \mathrm{PPA2}_{\mathrm{g,p,t}} + \sum_{q}\sum_{g}\sum_{t} s^{N,agr}_{q,g,t}\ \mathrm{PPA3}_{\mathrm{q,g,t}} \\ & + \sum_{o}\sum_{t} h^{ind}_{o,t}\ \mathrm{PPI1}_{\mathrm{o,t}} + \sum_{o}\sum_{p}\sum_{t} s^{E,ind}_{o,p,t}\ \mathrm{PPI2}_{\mathrm{o,p,t}} + \sum_{q}\sum_{o}\sum_{t} s^{N,ind}_{q,o,t}\ \mathrm{PPI3}_{\mathrm{q,o,t}} \\ & + \sum_{r}\sum_{j}\sum_{t} d^{dom}_{r,j,t}\ \mathrm{PPD4}_{\mathrm{r,j,t}} + \sum_{g}\sum_{j}\sum_{t} d^{agr}_{g,j,t}\ \mathrm{PPA4}_{\mathrm{g,j,t}} + \sum_{o}\sum_{j}\sum_{t} d^{ind}_{o,j,t}\ \mathrm{PPI4}_{\mathrm{o,j,t}} \\ & + \sum_{r}\sum_{x}\sum_{t} w^{dom}_{r,x,t}\ \mathrm{PPD5}_{\mathrm{r,x,t}} + \sum_{g}\sum_{x}\sum_{t} w^{agr}_{g,x,t}\ \mathrm{PPA5}_{\mathrm{g,x,t}} + \sum_{o}\sum_{x}\sum_{t} w^{ind}_{o,x,t}\ \mathrm{PPI5}_{\mathrm{o,x,t}} \\ & + \sum_{n}\sum_{i}\sum_{t} B^{E,des}_{n,i,t}\ \mathrm{PPC1}_{\mathrm{n,i,t}} + \sum_{u}\sum_{i}\sum_{t} B^{N,des}_{u,i,t}\ \mathrm{PPC2}_{\mathrm{u,i,t}} + \sum_{r}\sum_{n}\sum_{t} v^{E,dom}_{r,n,t}\ \mathrm{PPD6}_{\mathrm{r,n,t}} \\ & + \sum_{r}\sum_{u}\sum_{t} v^{N,dom}_{r,u,t}\ \mathrm{PPD7}_{\mathrm{r,u,t}} + \sum_{g}\sum_{n}\sum_{t} v^{E,agr}_{g,n,t}\ \mathrm{PPA6}_{\mathrm{g,n,t}} + \sum_{g}\sum_{u}\sum_{t} v^{N,agr}_{g,u,t}\ \mathrm{PPA7}_{\mathrm{g,u,t}} \\ & + \sum_{o}\sum_{n}\sum_{t} v^{E,ind}_{o,n,t}\ \mathrm{PPI6}_{\mathrm{o,n,t}} + \sum_{o}\sum_{u}\sum_{t} v^{N,ind}_{o,u,t}\ \mathrm{PPI7}_{\mathrm{o,u,t}} + \sum_{n}\sum_{q}\sum_{t} D^{E,Nsto}_{n,q,t}\ \mathrm{PPE1}_{\mathrm{n,q,t}} \\ & + \sum_{n}\sum_{p}\sum_{t} D^{E,Esto}_{n,p,t}\ \mathrm{PPE2}_{\mathrm{n,p,t}} + \sum_{u}\sum_{q}\sum_{t} D^{N,Nsto}_{u,q,t}\ \mathrm{PPN1}_{\mathrm{u,q,t}} + \sum_{u}\sum_{p}\sum_{t} D^{N,Esto}_{u,p,t}\ \mathrm{PPN2}_{\mathrm{u,p,t}} \\ & + \sum_{n}\sum_{x}\sum_{t} G^{E,rel}_{n,x,t}\ \mathrm{PPG1}_{\mathrm{n,x,t}} + \sum_{u}\sum_{x}\sum_{t} G^{N,rel}_{u,x,t}\ \mathrm{PPG2}_{\mathrm{u,x,t}} + \sum_{i}\sum_{j}\sum_{t} a^{dw}_{i,j,t}\ \mathrm{PAQ1}_{\mathrm{i,j,t}} \\ & + \sum_{p}\sum_{i}\sum_{t} s^{E,aq}_{p,i}\ \mathrm{PPS1}_{\mathrm{p,i,t}} + \sum_{q}\sum_{i}\sum_{t} s^{N,aq}_{q,i,t}\ \mathrm{PPS2}_{\mathrm{q,i,t}} \Bigg] \end{aligned} \tag{5.45}$$

The pumping cost factors are determined by the Darcy-Weisbach equation:[38]

$$PumpingCostFactor = \frac{1}{0.0000576}\, f\, \frac{L}{D^5}\, \frac{(\#\text{of hours})(\$/\text{kWh})}{\eta} \tag{5.46}$$

Where f is the friction factor, L is the pipe length, D is the pipe inner diameter and η is the combined pump and motor efficiency. The friction factor is based on the pipe roughness, pipe diameter, and the Reynolds number.

5.3.7 Tax credit reduction

This equation represents the revenues obtained by the reduction in the GHGE as tax credits, this amount is obtained taking into account the GHGE obtained by the combustion of fossil fuels (i.e. natural gas and oil)

$$TRC = H_Y \left[\left(\mathrm{TF}_{\mathrm{CO}_2}^{\mathrm{REF}} - F_{CO_2} \right) \cdot \mathrm{R}_{\mathrm{tax}} \right] \tag{5.47}$$

where $\mathrm{TF}_{\mathrm{CO}_2}^{\mathrm{REF}}$ is the amount of total GHGE when only fossil fuels are used to power the dual purpose power plant and F_{CO_2} is the amount of GHGE when fossil fuels, biofuels or solar technology is used. R_{tax} is the tax credit for CO_2 emissions.

The amount of GHGE are calculated as follows:

$$F_{CO_2} = \sum_f \sum_u \sum_t \left[GHGE_f^{fossil} \cdot Q_{f,u,t}^{fossil} \right] + \sum_b \sum_u \sum_t \left[GHGE_b^{biofuel} \cdot Q_{b,u,t}^{biofuel} \right] \tag{5.49}$$

5.3.8 Objective function

The proposed multi-objective optimization model involves three important aspects. The first one consists in maximizing the gross annual profit, as an economic function. The second one is the minimization of the overall GHGE, as environmental objective. Finally, the third one is the quantification of the jobs generated by the project, as a social objective.

$$\mathrm{OF} = \mathrm{Max}\ \textit{Annual Profit};\ \mathrm{Min}\ \textit{OGHGE};\ \mathrm{Quantifying}\ \textit{ONJobs} \tag{5.50}$$

The economic objective function consists in maximizing the gross annual profit, the function includes water sales, energy sales, and tax credit reduction, minus the total annual cost.

$$Annual\ Profit = Water\ Sales + EnergySales + TCR - TAC \tag{5.51}$$

Where the annual water sales include the water sold to domestic, industrial and agricultural users, and it can be calculated through the next relationship:

$$Water\ Sales = \mathrm{H_Y} \sum_t \left[\begin{array}{l} \left(\sum_r h_{r,t}^{dom} + \sum_p \sum_r s_{p,r,t}^{E,dom} + \sum_q \sum_r s_{q,r,t}^{N,dom} \right) \mathrm{WDC_t} \\ + \left(\sum_g h_{g,t}^{agr} + \sum_g \sum_p s_{g,p,t}^{E,agr} + \sum_q \sum_g s_{q,g,t}^{N,agr} \right) \mathrm{WAC_t} \\ + \left(\sum_o h_{o,t}^{ind} + \sum_o \sum_p s_{o,p,t}^{E,ind} + \sum_q \sum_o s_{q,o,t}^{N,ind} \right) \mathrm{WIC_t} \end{array} \right] \tag{5.52}$$

The energy sales can be calculated using the next equation:

$$Energy\ Sales = \mathrm{H_Y} \sum_t \left[\sum_r E_{r,t}^{dom} \cdot \mathrm{DEC_t} + \sum_g E_{g,t}^{agr} \cdot \mathrm{AEC_t} + \sum_o E_{o,t}^{ind} \cdot \mathrm{IEC_t} \right] \tag{5.53}$$

The total annual cost (TAC) includes the installation ($NPDinstcost$), operating ($NPDopcost$) and energy consumption cost ($NPDenergycost$) for new power-desalination plants, as well as the total operating costs for existing power-desalination plants ($TEPDopcost$), the equation also includes the storage cost ($StorageCost$), piping cost ($PipingCost$), pumping cost ($PumpingCost$) and solar collector cost ($SolarCost$).

$$\begin{aligned} TAC = {} & NPDinstcost + NPDopcost + NPDenergycost + EPDopcost \\ & + StorageCost + PipingCost + PumpingCost + SolarCost \end{aligned} \tag{5.54}$$

The environmental objective function ($OGHGE$) seeks to minimize the overall greenhouse gas emissions, as an indirect environmental impact assessment. The equation takes into account the GHGE for fossil fuels ($GHGE_f^{fossil}$) and biofuels ($GHGE_b^{biofuel}$), the emissions for the solar collector is assumed to be zero, according to the next equation:

$$\begin{aligned} Min\ OGHGE = {} & \sum_f \sum_u \sum_t \left[GHGE_f^{fossil} \cdot Q_{f,u,t}^{fossil} \right] \\ & + \sum_b \sum_u \sum_t \left[GHGE_b^{biofuel} \cdot Q_{b,u,t}^{biofuel} \right] \end{aligned} \tag{5.55}$$

The quantification of jobs ($ONJOBS$) is determined indirectly through the amount of energy used (see Lira-Barragan et al.[39]) based on the JEDI model (Jobs and Economic Development Impact), in which the number of jobs can be obtained per kWh produced by

fossil fuels ($NJOB_f^{fossil}$), biofuels ($NJOB_b^{biofuel}$) and solar energy ($NJOB^{solar}$), this objective can be obtained as follows:

$$\begin{aligned} ONJOBS = & \sum_f \sum_u \sum_t \left[NJOB_f^{fossil} \cdot Q_{f,u,t}^{fossil} \right] \\ & + \sum_b \sum_u \sum_t \left[NJOB_b^{biofuel} \cdot Q_{b,u,t}^{biofuel} \right] \\ & + \sum_u \sum_t \left[NJOB^{solar} \cdot Q_{u,t}^{solar} \right] \end{aligned} \tag{5.56}$$

5.4 Case study

As a case study is addressed the water scarcity problem in Hermosillo Sonora, Mexico (**Figure 5.2**). This problem has been described by Gonzalez-Bravo et al.[37] The city of Hermosillo is located in the Sonoran Desert region where the low rainfall and the increasing demand have led to a shortage of water from lakes, rivers, and aquifers. The most critical situation occurred during 2012 when the Sonoran State Government proposed the construction of an aqueduct that would bring water from El Novillo dam to the inhabitants of the Hermosillo city. Nonetheless, there was insufficient supply from EL Novillo dam because of the water use for agricultural and drinking needs of the inhabitants of the Valle de Yaqui region. This caused conflicts between the people of Hermosillo city and the Valle de Yaqui tribe. The government decided to rule in favor of the inhabitants of the Valle de Yaqui region. Consequently, there is a water shortage in the Hermosillo region.

Figure 5.2 shows a map of the region to be analyzed in the case study. Water demands for domestic and industrial users from Hermosillo city, Obregon city, and Guaymas city are taken into account. The agricultural users involve the irrigation districts 018, 041, 051 and 084. The considered water bodies include the Sonoran River, Yaqui River, and Matape River, also the volume of water content in the "El Novillo" dam, "Alvaro Obregon" dam, "Ignacio R. A." dam, "Abelardo L. R. dam" and "El Molinito dam". The study includes the aquifers of the region, "Costa de Hermosillo", "Guaymas" and "Valle de Yaqui". It should be noted that the "Abelardo L. R." and "El Molinito" dams are drained and the "Costa de Hermosillo", "Guaymas" and "Valle de Yaqui" aquifers are overexploited. Additional information has been presented by Gonzalez-Bravo et al.[37]

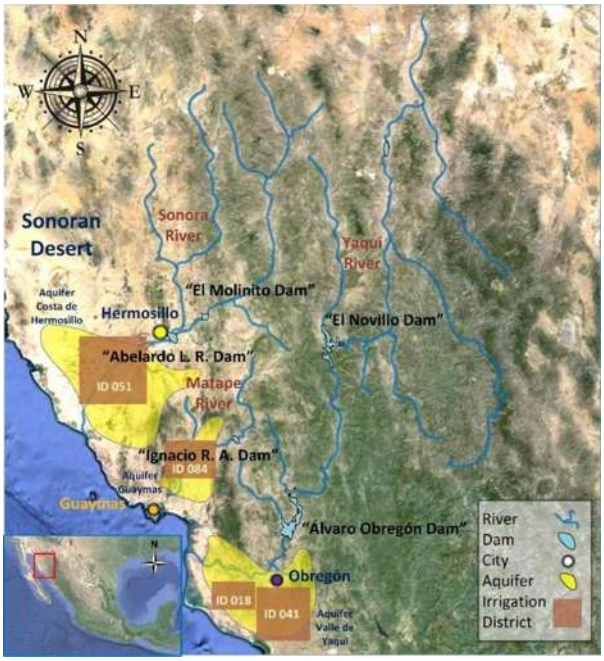

Figure 5.2. Overview of the addressed case study.

The Hermosillo region is near to the Sonoran desert and this represents an attractive location for solar collectors, due to high direct normal irradiation (DNI) values (around 3,000 kWh/m^2) as can be seen in **Figure 5.3**.[40] **Figure 5.4** shows the total energy received by the solar collector and the useful energy in each month based on a solar collector efficiency of 50%.[41] It should be noted in **Figure 5.4** that the highest DNI is always around noon, reaching its extreme between May and August. The solar collector was modeled according to the data reported by Liqreina and Qoaider.[23] For this case, the dual-purpose power plant was modeled using the data reported by a similar facility operated by the Qatar Electricity and Water Company (QEWC).[42] The QEWC is the second largest company producing power and water desalination in the Middle East and North Africa (MENA region). This company generates electricity by 5,432 megawatts and produces 258 million gallons of water per day. The fuels and biofuels taken into account are presented in **Table 5.1**, which contains its heating power, overall GHGE, cost and number of jobs created by each fuel, whereas **Table 5.2** shows the maximum availability in each month for biofuels, this availability depends on the seasonality as well as the production of agricultural waste.[38,43] For the specific case, in Mexico there is no restriction for the availability of fossil fuels to the operation of the dual purpose power plant.

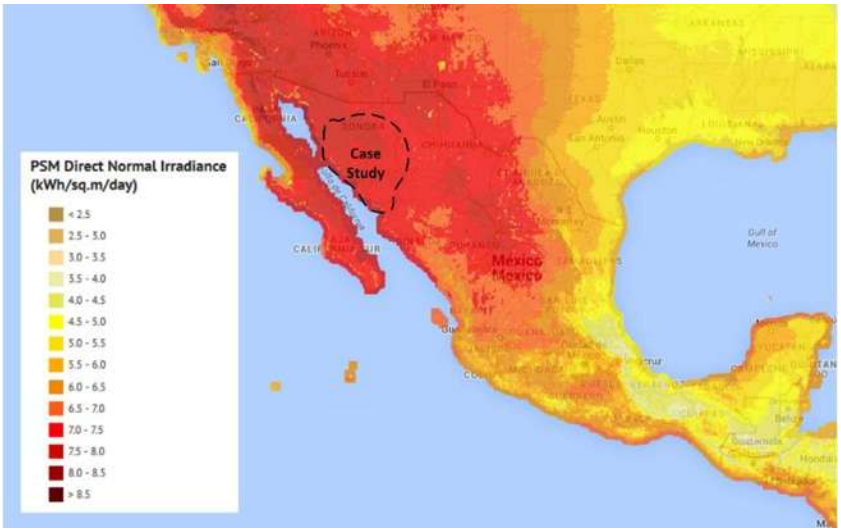

Figure 5.3. DNI irradiation for the case study. [40]

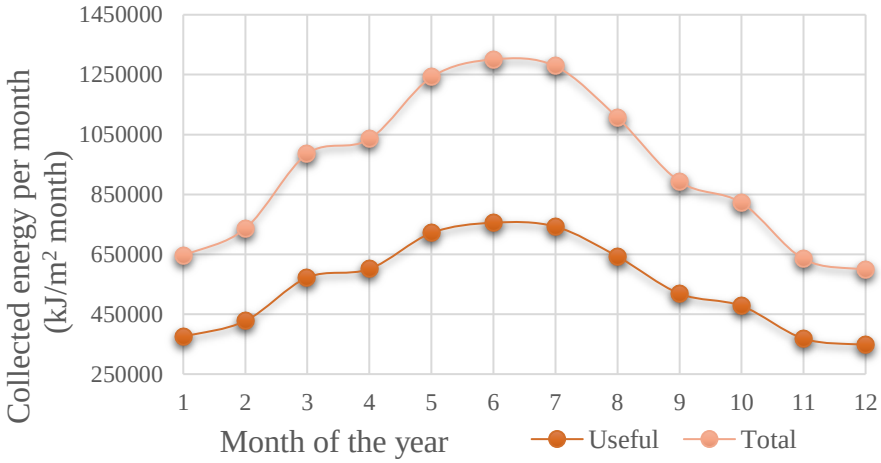

Figure 5.4. Useful collected energy for the case study.[40]

Table 5.1. Data for fossil fuels and biofuels.[38,43]

Fuel	Cost $/MM kJ	Heating Power (kJ/kg)	Overall GHGE (ton CO_2eq/kJ)	Number of jobs (Jobs/kJ)
Fossil				
Oil	26.195	45,200	8.05408×10^{-8}	1.81677×10^{-11}
Natural gas	2.554	54,000	7.90892×10^{-8}	5.25431×10^{-11}
Biofuels				
Biomass	1.980	17,200	2.44307×10^{-8}	6.6964×10^{-8}
Biogas	7.215	52,000	2.68216×10^{-8}	5.25431×10^{-7}
Biodiesel	30.920	40,200	5.13283×10^{-8}	2.46582×10^{-6}
Bioethanol	13.915	29,600	5.8436×10^{-8}	2.87453×10^{-6}

Table 5.2. Maximum availability of fuels and biofuels (kg/month).[38,43]

Fuel/Month	Jan	Feb	Mar	Apr	May	Jun	Jul	Aug	Sep	Oct	Nov	Dec
Biomass	10,000	10,000	40,000	50,000	70,000	150,000	100,000	50,000	40,000	40,000	30,000	20,000
Biogas	5,000	5,000	6,000	6,500	6,500	10,000	10,000	10,000	8,000	7,000	6,000	5,000
Biodiesel	5,000	5,500	6,000	7,000	10,000	10,000	10,000	10,000	9,000	8,000	7,000	6,000
Bioethanol	10,000	11,000	12,000	12,000	15,000	15,000	15,000	15,000	14,000	13,000	11,000	10,000

5.5 Results and discussion

The proposed model was coded in the software GAMS. The solvers DICOPT in conjunction with CONOPT and CPLEX were used to solve it.[44] The model consists of 9,714 equations, 10,058 continuous variables, and 720 binary variables. The model considers three main objectives: Profit, OGHGE, and NJOBS. The model was solved using the constraint method to obtain the Pareto curve taking into account only two objectives (Profit vs OGHGE) because these objectives are to be reconciled. Meanwhile, ONJOBS are evaluated for each point on the Pareto curve.

The results are presented through a Pareto curve (see **Figure 5.6**) where the points A, B, C, D, and E can be identified. Point A represents the optimal results maximizing the Profit, in this case, a total of 1.45 ton CO_2 $x10^7$/y are released, and a total of 10,307 jobs are generated. In this case, the optimal configuration for water and electricity distribution is

presented in **Figure 5.5**. As it was expected, the results are similar to the results presented in Gonzalez-Bravo et al.,[37] in which the dual-purpose power plant is installed in the Hermosillo beach at time period 1, the total amount of water produced in the dual purpose power plant is injected to the "Costa de Hermosillo" aquifer ($402x10^6$ m^3/y), the aquifer also receives water from agricultural users ($4.2x10^6$ m^3/y) and from natural recharge ($250x10^6$ m^3/y). Where the agricultural users extract $416.7x10^6$ m^3/y of water from the aquifer annually. The water for domestic users is taken from the "Costa de Hermosillo" aquifer ($23.95x10^6$ m^3/y), "El Molinito" dam ($1.93x10^6$ m^3/y) and from the "Abelardo L. R." dam ($68.2x10^6$ m^3/y). The water for industrial users is taken from the "El Molinito" dam ($41.4x10^6$ m^3/y). In the case of the Guaymas region, the "Guaymas" aquifer receives water from natural recharge ($78x10^6$ m^3/y) and for agricultural users ($7.4x10^3$ m^3/y). The agricultural users extract water from the "Ignacio L. A." dam ($0.784x10^6$ m^3/y). The domestic demands are supplied with water from the "Guaymas" aquifer ($18.2x10^6$ m^3/y) and from water produced in the Guaymas II power plant ($9.6x10^4$ m^3/y). While industrial demands are supplied with water from the aquifer ($6.9x10^6$ m^3/y). The agricultural users from the irrigation district 041 ($2,106.2x10^4$ m^3/y) and irrigation district 018 ($235x10^4$ m^3/y) in Obregon are supplied by water from the "Alvaro Obregon" dam. Also, domestic users ($50.12x10^4$ m^3/y) and industrial users ($20.7x10^4$ m^3/y) are supplied with water from the "Alvaro Obregon" dam and "El Novillo" dam. Points B, C, D, and E have similar results in the water distribution network. In point A, the new dual-purpose power desalination plant has a maximum capacity of 4,880 MW and $1.4x10^6$ m^3 per day. In this case, the sales of water reach 1,552 MM$/y and the sales of energy are 1346.3 MM$/y. The total annual cost of the plant is 1,237.4 MM$/y, which accounts for the cost of fuels (467.4 MM$/y), the operational cost of a new power desalination plant (592 MM$), piping (1.1 MM$/y) and pumping costs (65.7 MM$/y), and other operational costs of the existing power plants (80 MM$/y).

The economic results are shown in **Figure 5.6**. Point A has an annual net profit of 1,660.9 MM$/y, for this point, the CO_2 emissions are $1.45x10^7$ ton CO_2 eq/y and 10,307 jobs are generated. Point B has an annual net profit of 1,627.9 MM$/y, annual CO_2 emissions of $1.44x10^7$ ton CO_2 eq/y and 10,902 jobs are generated. Point C has a total annual net profit of 1600.8 MM$/y, Point C also has 1.42 $x10^7$ ton CO_2 eq/y and 13,449 jobs are generated. Point D has an annual profit of 1573.5 MM$/y, 1.40 $x10^7$ ton CO_2 eq/y of CO_2 emissions and

16,309 jobs are generated. Point E has an annual net profit of 1545.9 MM$/y, it represents 6% less than the optimal solution of point A, this reduction is mainly due to the fixed cost of the solar collector, which has virtually the same annualized cost as the installation cost of the dual purpose power plant. In point E, there is a reduction of CO_2 emissions of $7.98x10^5$ ton CO_2 eq/y due to the installation of the solar collector. In this case, 19,781 jobs are generated. The capacity of the dual purpose power plant for points B to E has the same capacity of the point A (4,880 MW) however there are small differences in the fuel consumption. **Figure 5.7** shows the annual fuel consumption for each point on the Pareto curve. The total energy requirement in point A is totally fulfilled using natural gas, in this scenario no renewable energy (biofuels or solar energy) was consumed. On the other hand, points B to E also include energy from both biomass and solar. However, the use of biofuels is still very limited for this region due to limited availability of biomass while the use of solar energy is restricted in this case by the capital cost and land requirements.

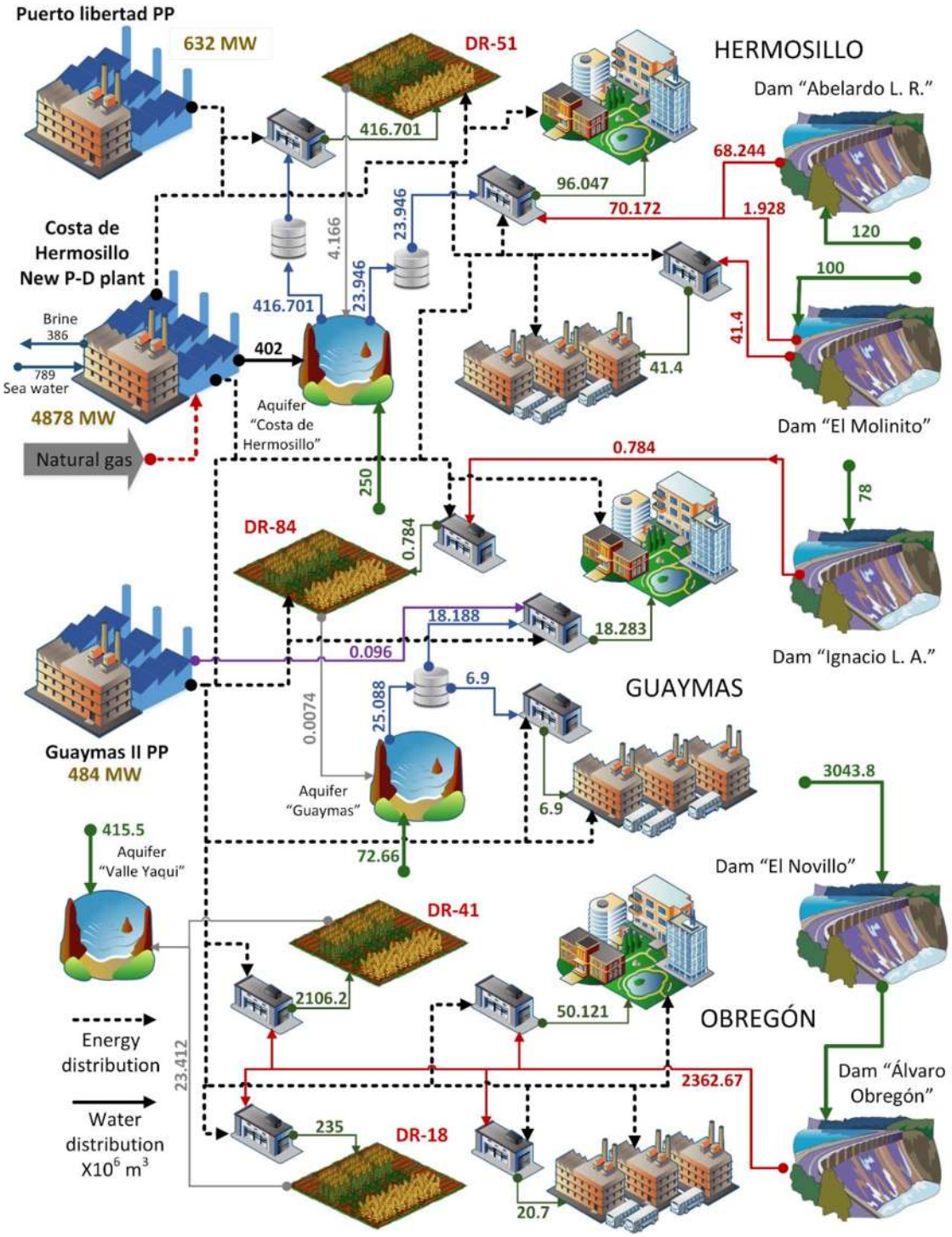

Figure 5.5. Optimal solution for point A.

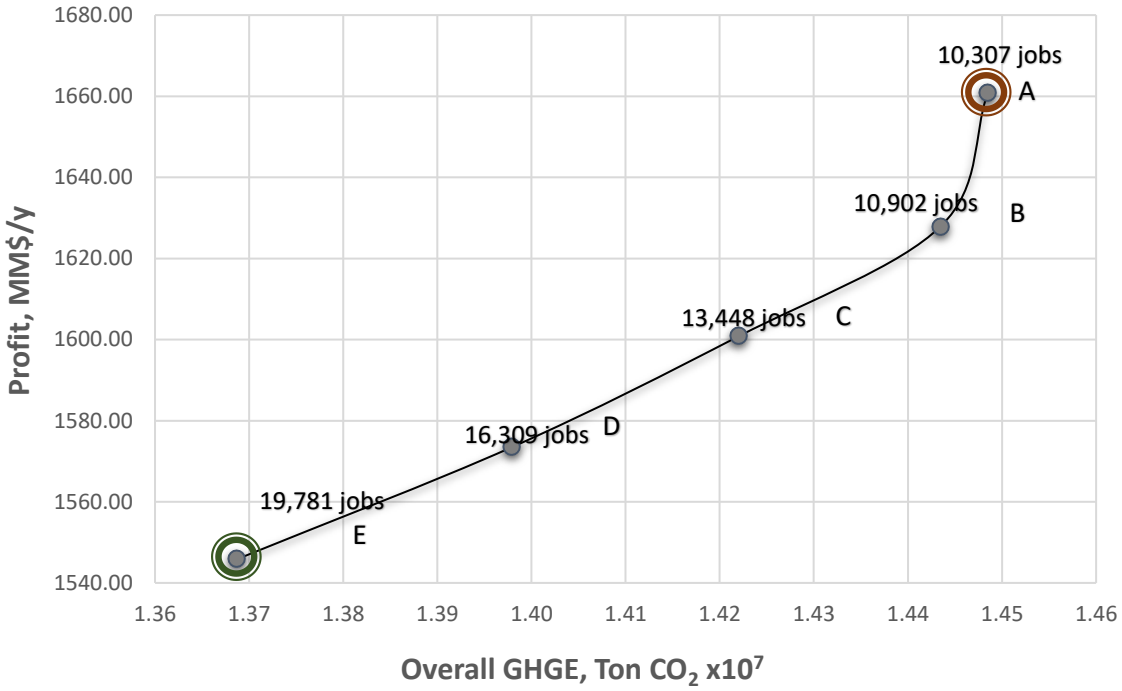

Figure 5.6. Pareto curve for the case study.

In terms of acceptability, the construction of this project would satisfy energy and water requirements of 784,342 inhabitants and 117,360 hectares of crops in the Hermosillo region, the water, and energy requirements of 409.310 inhabitants and 255.672 hectares of crops in the Obregon region, and 149.299 inhabitants and 20.042 hectares of crops in the Guaymas region. The project would also boost the development of 200 relevant companies throughout the region.[45] Is important to analyze the effect of the TCR due to the GHGE, in this case, tax credits of 5$/ton of CO_2 eq., 10$/ton of CO_2 eq., 20$/ton of CO_2 eq. and 30$/ton of CO_2 eq. where evaluated. **Table 5.3** shows the effect over the total annual profit accounting for the TCR, in general, the total annual profit is increased when the TRC is raised, however, in this case, the variation of the profit is only important when the tax credits are over 20$/ton of CO_2 eq. and the overall GHGE are greater than $5x10^5$ ton of CO_2 eq.

Table 5.3. Sensitivity analysis for different values of the tax credit.

	Total Annual Profit				
Scenario	Without TCR	$5/ ton of CO2 equiv	$10/ ton of CO2 equiv	$20/ ton of CO2 equiv	$30/ ton of CO2 equiv
A	1660.9	1660.9	1660.9	1660.9	1660.9
B	1627.9	1628.4	1628.9	1629.9	1631.4
C	1600.8	1602.3	1603.8	1606.8	1611.3
D	1573.5	1576	1578.5	1583.5	1591
E	1545.9	1549.9	1553.9	1561.9	1573.9

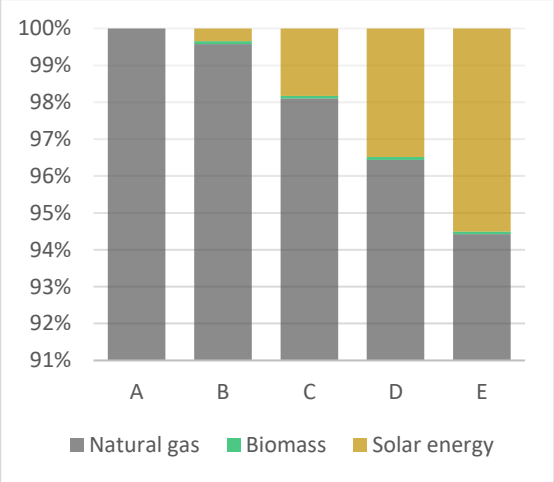

Figure 5.7. Fuel consumption for each Pareto point.

5.6 Conclusions

This chapter has presented a multi-objective mathematical programming model for the optimal design of water distribution networks involving dual-purpose power plants and renewable energy. The considered objectives are the maximization of the net annual profit and the minimization of the overall greenhouse gas emissions while tracking the overall number of new jobs. The optimal water distribution network and the existence of new dual-purpose power plants are determined using binary variables, and the energy requirements are satisfied using fossil fuels, biofuels, and solar energy. The optimal solution is subject to the water and electricity demands of domestic, agricultural and industrial users. A systematic solution approach for this multi-objective optimization model has been presented. The

approach involves the solution of the multi-objective optimization formulation and the construction of a Pareto curve to show the trade-offs of the involved objectives.

The water scarcity problem in the Sonoran Desert in the north-west of Mexico has been considered as a case study. The results show important economic benefits due to the installation of the new dual-purpose power plant Additionally, the integration of renewable energy (biofuels and solar energy) can be an attractive option to satisfy water and energy in water-stressed areas with high solar radiations, however biofuels availability, cost as well as restrictions of land requirements for solar technology still as a disadvantage to compete against fossil fuels. The tradeoffs have been presented and analyzed for the various solution scenarios. Future works must have to take into account strict fluctuation of prices and availability of fossil fuels in a stochastic optimization problem.

5.7 References

1. WWAP, *The United Nations World Water Development Report 2015: Water and Energy*. United Nations World Water Assessment Programme, Paris, France, UNESCO. 2015.
2. Davis, R. J.; Kim, Y.; Logan, B. E., Increasing desalination by mitigating anolyte pH imbalance using catholyte effluent addition in a multi-anode bench scale microbial desalination cell, *ACS Sustainable Chem. Eng*., 2013, 1, 1200−1206.
3. IRENA, *Water Desalination Using Renewable Energy: Technology Brief*., International Renewable Energy Agency, Abu Dhabi, United Arab Emirates. 2012.
4. Almansoori, A.; Saif, Y., Structural optimization of osmosis processes for water and power production in desalination applications, *Desalination*, 2014, 344, 12-27.
5. Esfahani, I. J.; Kim, J. T.; Yoo, C. K., A Cost approach for optimization of a combined power and thermal desalination system through exergy and environmental analysis, *Industrial & Engineering Chemistry Research*, 2013, 52 (32), 11099-11110.
6. Zhang, S.; Zhang, Y.; Chung, T.-S, Facile preparation of antifouling hollow fiber membranes for sustainable osmotic power generation, *ACS Sustainable Chem. Eng*., 2016, 4, 1154−1160.
7. Raluy, R. G.; Serra, L.; Uche, J.; Valero, A., Lifecycle assessment of desalination technologies integrated with energy production systems, *Desalination*, 2004, 167, 445-458.
8. Shaffer, D. L.; Chavez, L. H. A.; Ben-Sasson, M.; Castrillón S. R.-V.; Yip, N. Y.; Elimelech, M., Desalination and reuse of high-salinity shale gas produced water: drivers, technologies, and future directions, *Environmental Science and technology*, 2013, 47, 9569-9583.
9. Gutiérrez-Arriaga, C. G.; Serna-González, M.; Ponce-Ortega, J. M.; El-Halwagi, M. M., Sustainable integration of algal biodiesel production with steam electric power plants for greenhouse gas mitigation, *ACS Sustainable Chem. Eng*., 2014, 2, 1388−1403.

10. Tavakkoli, S.; Lokare, O. R.; Vidic, R. D.; Khanna, V., Systems-level analysis of waste heat recovery opportunities from natural gas compressor stations in the United States, *ACS Sustainable Chem. Eng*., 2016, 4, 3618−3626.
11. Sternberg, A.; Bardow, A., Life Cycle Assessment of power-to-gas: Syngas vs methane, *ACS Sustainable Chem. Eng.*, 2016, 4 (8), 4156-4165.
12. Miller, S.; Shemer, H.; Semiat, R., Energy and environmental issues in desalination, *Desalination*, 2015, 366, 2-8.
13. Lueken, C.; Cohen, G. E.; Apt, J., Costs of solar and wind power variability for reducing CO_2 emissions, *Environmental Science & Technology*, 2012, 46, 9761-9767.
14. Ravi, S.; Lobell, D. B.; Field, C. B., Tradeoffs and synergies between biofuel production and large solar infrastructure in deserts, *Environmental Science and technology*, 2014, 48, 3021-3030.
15. Börjesson, K.; Lennartson, A.; Moth-Poulsen, K., Efficiency limit of molecular solar thermal energy collecting devices, *ACS Sustainable Chem. Eng*., 2013, 1, 585−590.
16. Mabrouk, A. A.; Fat, H. E. S., Techno-economic analysis of hybrid high performance MSF desalination plant with NF membrane, *Desalination and Water Treatment*, 2012, 51 (4-6), 844-856.
17. Mabrouk, A. A.; Fat, H. E. S., Experimental study of high performance hybrid NF-MSF desalination pilot test unit driven by renewable energy, *Desalination and Water Treatment*, 2013, 51 (37-39), 6895-6904.
18. López-Díaz, D. C.; Lira-Barragán, L. F.; Rubio-Castro, E.; Ponce-Ortega, J. M.; El-Halwagi, M. M., Synthesis of eco-industrial parks interacting with a surrounding watershed, *ACS Sustainable Chem. Eng.*, 2015, 3, 1564−1578.
19. Tovar-Facio, J.; Lira-Barragán, L. F.; Nápoles-Rivera, F.; Bamufleh, H. S.; Ponce-Ortega, J. M.; El-Halwagi, M. M., Optimal synthesis of refinery property-based water networks with electrocoagulation treatment systems, *ACS Sustainable Chem. Eng*., 2016, 4, 147−158.
20. Gutierrez-Arriaga, C. G.; Serna-Gonzalez, M.; Ponce-Ortega, J. M.; El-Halwagi, M. M., Multi-objective optimization of steam power plants for sustainable generation of electricity, *Clean Technologies and Environmental Policy*, 2013, 15, 551-566.
21. Iaquaniello, G.; Salladini, A.; Mari, A.; Mabrouk, A. A.; Fath, H. E. S., Concentrating solar power (CSP) system integrated with MED–RO hybrid desalination, *Desalination*, 2014, 336, 121–128.
22. Liqreina, A.; Qoaider, L., Dry cooling of concentrating solar power (CSP) plants, an economic competitive option for the desert regions of the MENA region, *Solar Energy*, 2014, 103, 417–424.
23. Liqreina, A.; Qoaider, L., Optimization of dry-cooled parabolic trough (CSP) plants for the desert regions of the Middle East and North Africa (MENA), *Solar Energy*, 2015, 122, 976–985.
24. Fthenakis, V.; Atia, A. A.; Morin, O.; Bkayrat, R.; Sinha P., New prospects for PV powered water desalination plants: Case studies in Saudi Arabia, *Progress in Photovoltaics: Research and Applications*, 2015, DOI: 10.1002/pip.2572.
25. Sankar, D.; Deepa, N.; Rajagopal, S.; Karthik, K. M., Solar power and desalination plant for carbon black industry: Improvised techniques, *Solar Energy*, 2015, 119, 243–250.

26. Gorjian, S.; Ghobadian, B., Solar desalination: A sustainable solution to water crisis in Iran, *Renewable and Sustainable Energy Reviews*, 2015, 48, 571-584.
27. Abdelhady, F.; Bamufleh, H.; El-Halwagi, M. M.; Ponce-Ortega, J. M., Optimal design and integration of solar thermal collection, storage, and dispatch with process cogeneration systems, *Chemical Engineering Science*, 2015, 136, 158-167.
28. Palenzuela, P.; Alarcón-Padilla, D. C.; Zaragoza, G.; Blanco, J., Comparison between CSP+MED and CSP+RO in Mediterranean area and MENA region: Techno-economic analysis, *Energy Procedia*, 2015, 69, 1938-1947.
29. Palenzuela, P.; Alarcón-Padilla, D. C.; Zaragoza, G., Large-scale solar desalination by combination with CSP: Techno-economic analysis of different options for the Mediterranean Sea and the Arabian Gulf, *Desalination*, 2015, 366, 130-138.
30. Diaf, A.; Cherfa, A.; Karadaniz, L.; Tigrine, Z., A technical–economical study of solar desalination, *Desalination*, 2016, 377, 123–127.
31. Liu, S.; Konstantopoulou, F.; Gikas, P.; Papageorgiou, L. G., A mixed integer optimization approach for integrated water resources management, *Computers and Chemical Engineering*, 2011, 35 (5), 858-875.
32. Atilhan, S.; Linke, P.; Abdel-Wahab, A., A systems integration approach to the design of regional water desalination and supply networks, *International Journal of Process Systems Engineering*, 2011, 1 (2), 125-135.
33. Atilhan, S.; Mahfouz, A.; Batchelor, B.; Linke, P.; Abdel-Wahab, A.: Nápoles-Rivera, F.; Jiménez-Gutiérrez, A.; El-Halwagi, M. M., A systems-integration approach to the optimization of macroscopic water desalination and distribution networks: a general framework applied to Qatar's water resources, *Clean Technologies and Environmental Policy*, 2012, 14 (2), 161-171.
34. Nápoles-Rivera, F.; Serna-González, M.; El-Halwagi, M. M.; Ponce-Ortega, J. M., Sustainable water management for macroscopic systems, *Journal of Cleaner Production*, 2013, 47, 102-117.
35. Nápoles-Rivera, F.; Rojas-Torres, M. G.; Ponce-Ortega, J. M.; Serna-González, M.; El-Halwagi, M. M., Optimal design of macroscopic water networks under parametric uncertainty, *Journal of Cleaner Production*, 2015, 88, 172-184.
36. Alnouri, S. Y.; Linke, P.; El-Halwagi, M. M., A synthesis approach for industrial city water reuse networks considering central and distributed treatment systems, *Journal of Cleaner Production*, 2015, 89, 231-250.
37. González-Bravo, R.; Nápoles-Rivera, F.; Ponce-Ortega, J. M.; El-Halwagi, M. M., Involving integrated seawater desalination-power plants in the optimal design of water distribution networks, *Resources, Conservation and Recycling*, 2015, 104, 181–193.
38. Swamee, P. K.; Sharma, A. K., Design of Water Supply Pipe Networks, Wiley-Interscience, 2008, 1, 13-16.
39. Lira-Barragan, L. F.; Ponce-Ortega, J. M.; Serna-González, M.; El-Halwagi, M. M., Synthesis of integrated absorption refrigeration systems involving economic and environmental objectives and quantifying social benefits, *Applied Thermal Engineering*, 2013, 52, 402-419.
40. NREL, *National Solar Radiation Database*, National Renewable National Laboratory (U.S. Department of Energy), Washington DC. 2012.
41. Weinstein, L. A.; Loomis, J.; Bhatia, B.; Bierman, D. M.; Wang, E. N.; Chen, G., Concentrating solar power, *Chemical Reviews*, 2015, 115, 12797-12838.

42. QEWC, *Qatar Electricity and Water Company Annual Report*, Qatar Electricity and Water Company, Doha, Qatar. 2014.
43. EIA, U.S., *Independent Statics and Analysis*, Energy Information Administration, Washington DC. 2016.
44. Brooke, A.; Kendrick, D.; Meeruas, A.; Raman, R., *GAMS-language guide*, GAMS Development Corporation, Washington DC. 2016.
45. INEGI, Consultation System for Census Information, *National Institute of Statistics and Geography*, México. 2012, Available at. http://gaia.inegi.org.mx/scince2/viewer.html

CHAPTER VI

Defining Priorities in the Design of Power and Water Distribution Networks

This chapter presents an approach for designing power and water distribution networks involving the sizing, geographic location, as well as the economic, environmental and social impacts, and taking into account the multiplicity of criteria for the stakeholders involved in the development of operational policies and new facilities. In this chapter is presented a method for defining solutions concerning to the design of power and water distribution networks based on a multi-stakeholder environment. A multi-objective optimization model, considering economic, environmental and social factors, is used for illustrating how the different criteria, about priorities of the stakeholders, affect the design of the system and how to propose a solution for achieving a tradeoff between the multiple stakeholders. The proposed method was applied to an electric and water stressed scheme in the north of Mexico, the results show that the minimization of the dissatisfaction of the involved systems can provide an optimal solution that meets the objectives of all stakeholders.

6.1 Introduction

Energy and water are very important resources for the development of the modern society. The growth of the urban areas, agricultural crops, and industrial facilities has increased the use of both resources.[1] The distribution problems have increased significantly because of the availability of water and the current scheme of water and power distribution (centralized distribution).[2] The development of liberalized electricity and water markets impels the design of new strategies,[3] taking into account economic, environmental and social aspects.[4] In the case of water, the first problem is the allocation of water resources. The natural sources of fresh water are limited and the access is restricted by factors such as political issues,[5] transportation cost, treatment,[6] lack of adequate pricing policy on water supply,[7] exploitation limits,[8] policies based on rationalization of resources[9] and scarcity.[10] Due to these factors, the current water distribution systems have to consider the external consumption. Usually, water is transported from a source in remote areas. This way, the problems involved in the design of water distribution networks have different dimensions. The economic dimension of water distribution networks has been addressed considering aspects as cost of treatment intended for human consumption[11] or for sanitary use,[12] cost of pipelines,[13] maintenance of the network,[14] pumping,[15] efficiency in energy consumption,[16] cost of utilities[17] and cost of extraction.[18] The environmental dimension has considered the life cycle assessment analysis,[19] emissions generated by the system[20] and reducing water losses.[21] The social dimension has focused on improving the behavior of the final user,[22] final usage[23] and conflicts in the distribution between different communities and users.[24]

The design of power distribution networks has similar problems to the water distribution networks. The economic dimension of the design has considered sizing the system,[25] reducing energy losses in distributed generation,[26] and transmission based on centralized generation,[27] increasing the generation efficiency,[28] maximizing the profit,[29] improving the fuel consumption[30] and the maintenance of the transportation lines.[31] The environmental dimension has focused on the emissions,[32] life cycle assessment[33] and water consumption.[34] The social impact involves the response of the system to the behavior of the end user[35] and the economic benefit to local communities.[36] The study of power distribution networks has been applied by many authors, in which the prices of electricity consumption and the future growth have an important role in the decisions making, these strategies have

been applied in the electricity sector in Italy,[37] Hong Kong,[38] Japan,[39] Denmark[40] and Hungary.[41]

Other strategies have been introduced to analyze the use of desalination systems to provide fresh water in water-stressed areas.[42] In this context, macroscopic water networks have been incorporated to involve seawater, groundwater and desalination plants in the system.[43] Furthermore, other approaches considered the monthly fluctuating demands in designing macroscopic water networks.[44] Nowadays, the integration of renewable energy based on existing desalination technologies is very important,[45] involving small and large power capacities[46] and also to reduce the CO_2 emissions.[47] It should be noticed that the integration of desalination and power production is a good option to reduce the desalination cost.[48] Power-desalination schemes have been widely used in cities of the middle east, in which the production of water and electricity have the advantage of reducing the environmental impact and energy consumption.[49] The integration of power-desalination systems in the synthesis of water distribution networks represents an attractive option to satisfy water demands in arid regions.[50]

Due to the high impact of these projects is important to assess the effect of each part, which implies that the optimal solution must satisfy each stakeholder. These multiple objectives in the design of water and energy distribution networks have increased the complexity of the design process. The decision-makers have different criteria about the objectives. Most of the investors have preferences for the economic benefits,[51] the communities and government have focused on the environmental impact and social benefits of the new systems.[52] Sometimes, these actors show different interest levels about the design objectives according to with local or personal priorities and perspectives about the project. These different criteria have led to conflicts between the different stakeholders. A compensated solution or a multi-objective analysis is not enough in these cases. When the problem implicates an interesting conflict between all the stakeholders involved, the analysis considering the Pareto optimal solutions, using the own criteria of the designer based on a multi-objective approach, could be not enough for sensitizing to the actors about the effects of their priorities in the final configuration of the system. Then, it is not possible to provide an effective framework for discussing solution paths to the conflict and to propose a compromise solution that could reach the satisfaction between all the part-takers. Therefore,

a tool that can show the impact of the priorities stablished by the stakeholders in the design can help to solve the conflicts or show different impacts in the design caused by the different levels and preferences in the priorities and it can lead to a dialogue between the part-takers in the final decision about the system.[53]

In this chapter is presented a method for designing water and energy distribution networks considering the multi-stakeholder environment. Economic, environmental and social objectives are considered for defining the priorities of the stakeholders. The proposed solution approach takes into account different levels or weights in the preferences about the objectives of the stakeholders. Finally, an approach for trading-off the different criteria is introduce as well as the levels of dissatisfaction of the stakeholders with this configuration in the design of the system.

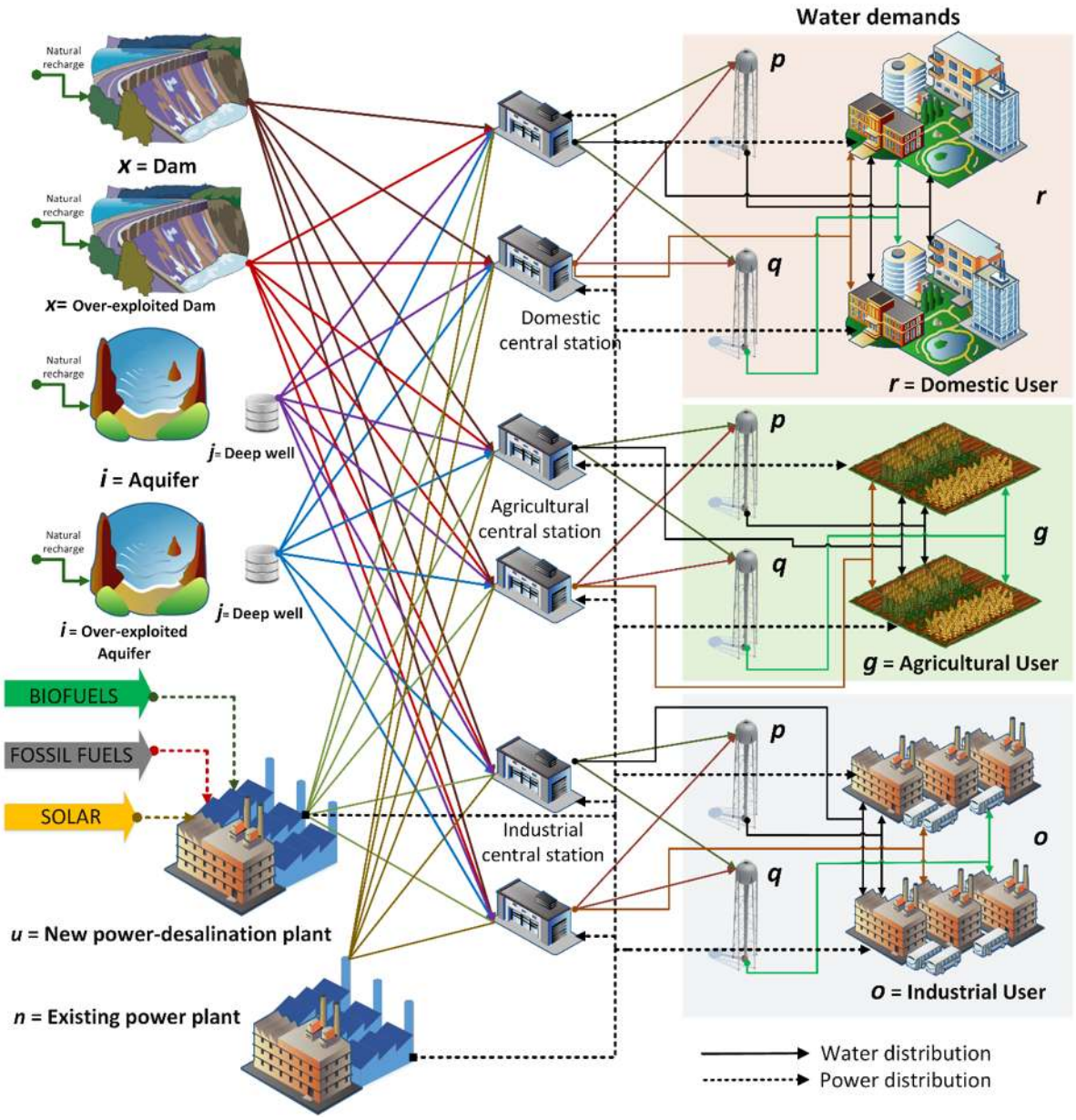

Figure 6.1. Proposed superstructure for water and power distribution networks.

6.2 Mathematical model

The mathematical formulation for synthesizing power and water distribution networks is based on the superstructure shown in **Figure 6.1**. In this figure, there are defined the water and electricity demands for domestic users (r), industrial users (o) and agricultural users (g), in which the water demands can be supplied by the existing water in the aquifers (i), by extracting water from the existing deep wells in each region (j) and also

the water in dams (x). Here, there is considered the location of existing storage tanks (p) as well as the installation of new storage tanks (p), if it is necessary, in which the storage tanks, represent the artificial storage for water either new or existing On the other hand, the energy demand is satisfied by the electricity produced in the existing power plants (n) as well as the possible installation of new power-desalination plants (u), where the fuel requirements of the dual-purpose power plant can be fully satisfied using fossil fuels (f), biofuels (b) and/or solar energy.

The proposed mathematical model includes accumulation balances in aquifers, mass balances in deep wells, equations to account the water demand for domestic, industrial and agricultural users, as well as accumulation balances in dams, new and existing storage tanks, also the mass balances of the existing and new power and desalination plants. The electricity production is performed using energy balances of the existing and new power and desalination plants, these equations account for the energy demands of domestic, industrial and agricultural users. The formulation includes binary variables to determine the existence of new storage tanks as well as the existence of new power and desalination plants, where the operations include fixed and variable costs, the formulation also includes pumping and piping costs.

6.2.1 Objective functions

In this case, it is needed a multi-objective optimization problem, this formulation includes the maximization of the gross annual profit (economic objective) and the maximization of the jobs generated by the project (social objective), also the formulation accounts for the minimization of the overall green house gas emissions (GHGE) as environmental objective.

$$\text{OF} = \text{Max } AnnualProfit; \text{Min } OGHGE; \text{Max } ONJobs \tag{6.1}$$

The multi-stakeholder decision problem implies the priorities of investors ($AnnualProfit$), environmental damage ($OGHGE$) and the social acceptability ($ONJobs$). Where the economic objective includes the maximization of water sales, power sales, tax

credit reduction at the minimum total annual cost of the power and water distribution network, according to the next equation:

$$Annual\ Profit = Water\ Sales + PowerSales + TCR - TAC \tag{6.2}$$

where, the water sales involves the water consumed by the domestic, industrial, and agricultural users:

$$Water\ Sales = \mathrm{H_Y} \sum_t \left[\begin{array}{l} \left(\sum_r h_{r,t}^{dom} + \sum_p \sum_r s_{p,r,t}^{E,dom} + \sum_q \sum_r s_{q,r,t}^{N,dom} \right) \mathrm{WDC_t} \\ + \left(\sum_g h_{g,t}^{agr} + \sum_g \sum_p s_{g,p,t}^{E,agr} + \sum_q \sum_g s_{q,g,t}^{N,agr} \right) \mathrm{WAC_t} \\ + \left(\sum_o h_{o,t}^{ind} + \sum_o \sum_p s_{o,p,t}^{E,ind} + \sum_q \sum_o s_{q,o,t}^{N,ind} \right) \mathrm{WIC_t} \end{array} \right] \tag{6.3}$$

The power sales are defined as the electricity consumed by domestic, industrial and agricultural users:

$$PowerSales = H_Y \sum_t \left[\sum_r E_{r,t}^{dom} \cdot \mathrm{DEC}_t + \sum_g E_{g,t}^{agr} \cdot \mathrm{AEC}_t + \sum_o E_{o,t}^{ind} \cdot \mathrm{IEC}_t \right] \tag{6.4}$$

The total annual cost (TAC) accounts for the installation ($NPDinstcost$), operating ($NPDopcost$) and energy consumption costs ($NPDenergycost$) for new power-desalination plants, the equation also includes the total operating costs for existing power-desalination plants ($TEPDopcost$), storage cost ($Storage\,Cost$), piping cost ($Piping\,Cost$), pumping cost ($Pumping\,Cost$) and solar collector cost ($SolarCost$).

$$\begin{aligned} TAC = {} & NPDinstcost + NPDopcost + NPDenergycost + EPDopcost \\ & + Storage\,Cost + Piping\,Cost + Pumping\,Cost + SolarCost \end{aligned} \tag{6.5}$$

The social objective seeks to maximize the generation of external jobs ($ONJobs$), where the number of jobs can be determined according to the kilowatt hour produced by fossil fuels ($NJOB_f^{fossil}$), biofuels ($NJOB_b^{biofuel}$), and solar energy ($NJOB^{solar}$):

$$ONJOBS = \sum_{f}\sum_{u}\sum_{t}\left[NJOB_{f}^{fossil}\cdot Q_{f,u,t}^{fossil}\right] + \sum_{b}\sum_{u}\sum_{t}\left[NJOB_{b}^{biofuel}\cdot Q_{b,u,t}^{biofuel}\right] + \sum_{u}\sum_{t}\left[NJOB^{solar}\cdot Q_{u,t}^{solar}\right] \quad (6.6)$$

where the amount of heat produced depends on the monthly availability of fossil fuels ($\mathrm{AVB}_{b,t}^{\max}$) and biofuels ($\mathrm{AVF}_{f,t}^{\max}$) multiplied by their heating power value, HPF_f for fossil fuels, and HPB_b for biofuels:

$$Q_{f.t}^{fossil} \le \mathrm{HPF}_f \cdot \mathrm{AVF}_{f,t}^{\max} \qquad \forall f \in F, \forall t \in T \quad (6.7)$$

$$Q_{b.t}^{biofuel} \le \mathrm{HPB}_b \cdot \mathrm{AVB}_{b,t}^{\max} \qquad \forall b \in B, \forall t \in T \quad (6.8)$$

The energy obtained by the solar collector ($Q_{u,t}^{solar}$) is equal to the usefully collected energy ($UCE_{u,t}^{solar}$) multiplied by the effective area of the solar collector ($A_{u,t}^{solar}$):

$$Q_{u,t}^{solar} = UCE_{u,t}^{solar}\cdot A_{u,t}^{solar}, \qquad \forall u \in U, \forall t \in T \quad (6.9)$$

The environmental objective function accounts for the overall GHGE, as an indirect measure of environmental impact, this function involves the GHGE emitted by fossil fuels ($GHGE_f^{fossil}$) and biofuels ($GHGE_b^{biofuel}$), and the emissions for the solar collector are assumed as zero:

$$Min\,OGHGE = \sum_{f}\sum_{u}\sum_{t}\left[GHGE_{f}^{fossil}\cdot Q_{f,u,t}^{fossil}\right] + \sum_{b}\sum_{u}\sum_{t}\left[GHGE_{b}^{biofuel}\cdot Q_{b,u,t}^{biofuel}\right] \quad (6.10)$$

6.2.2 Multi-stakeholder decision-making model

The multi-objective solution must be selected from the Pareto set, in this sense, the multi-stakeholder strategy uses the coordinates of the utopia point (UP), this point represents the lower bounds (LB) of the proposed objective functions ($AnnualProfit^{LB}$; $OGHGE^{LB}$; $ONJOBS^{LB}$); on the other hand, the upper bounds (UB) ($AnnualProfit^{UB}$; $OGHGE^{UB}$;

$ONJOBS^{UB}$) represent the Nadir solution (NS). In this case, these objectives are opposites, then by scaling the objective functions using the UP and NS, the following equations to solve the optimization problem are obtained:

Economic objective function:

$$\varphi = \frac{AnnualProfit^{UB} - AnnualProfit}{AnnualProfit^{UB} - AnnualProfit^{LB}} \tag{6.11}$$

Social objective function:

$$\psi = \frac{ONJOBS^{UB} - ONJOBS}{ONJOBS^{UB} - ONJOBS^{LB}} \tag{6.12}$$

Environmental objective function:

$$\tau = \frac{OGHGE - OGHGE^{LB}}{OGHGE^{UB} - OGHGE^{LB}} \tag{6.13}$$

Is important to notice that the compromise solution is to reduce the absolute distance between the proposed points and the objective functions (UB and LB points), the main idea is to obtain an optimal value satisfying all parts, and this solution must be a Pareto optimal solution. Then, the compromise solution (CS) is stated as follows:

$$\min CS = \varphi + \psi + \tau \tag{6.14}$$

The objective function values have been scaled; then, their values lie in the interval [0,1]:

$$0 \le \varphi \le 1 \tag{6.15}$$

$$0 \le \psi \le 1 \tag{6.16}$$

$$0 \le \tau \le 1 \tag{6.17}$$

By assigning weights to the CS function and taking into account k number of stakeholders, where each stakeholder has an individual solution (FS_k) that represents a different configuration of the system according to the weight assigned to the different

objectives. These weights represent the levels of preference of the stakeholder over the objective functions. In this way, it is possible to formulate different solutions according to the individual priorities of the stakeholders:

$$FS_k = w_k^{eco}\varphi_k + w_k^{soc}\psi_k + w_k^{envi}\tau_k, \qquad \forall k \in K$$

(6.18)

Then average solution (AF) to account the weighting of all stakeholders is given by:

$$AF = \frac{\sum_{k=1}^{k} FS_k}{k} \tag{6.19}$$

Finally, the compensated solution of the problem seeks to minimize the average of the dissatisfactions and the main objective function is stated as follows:

$$\min \left| CS - FS \right| \tag{6.20}$$

This solution represents a point in the Pareto curve that is compensative with the priorities of all the stakeholders. It is expected that the final configuration of the system prioritizes the objectives with a significant weight in the preferences of the established set of stakeholders.

6.3 Case study

The case study involves one of the most critical situations of power and water supply in the north part of Mexico, in the zone near to the Sonoran Desert. This region has one of the highest electricity consumption of the country; this is because there are severe weather changes because of the proximity to the Sonoran Desert. Also, there is an unequal distribution of water resources, which has generated a competition between the domestic sector and the agricultural sector, the main reason has been the lack of rain and prolonged drought and strong population growth in the region. This has generated a strong overexploitation of groundwater and surface water, which has led to problems among the inhabitants of the driest regions by the dispute of this resource. **Figure 6.2** shows an overview of the analyzed problem. **Figure 6.3** shows the description of the involved domestic, industrial and agricultural users presented in the case study, as well as the involved natural sources, existing

power plants and the possible location of new power desalination plants. A deep description of the problem was described by Gonzalez-Bravo et al.[40]

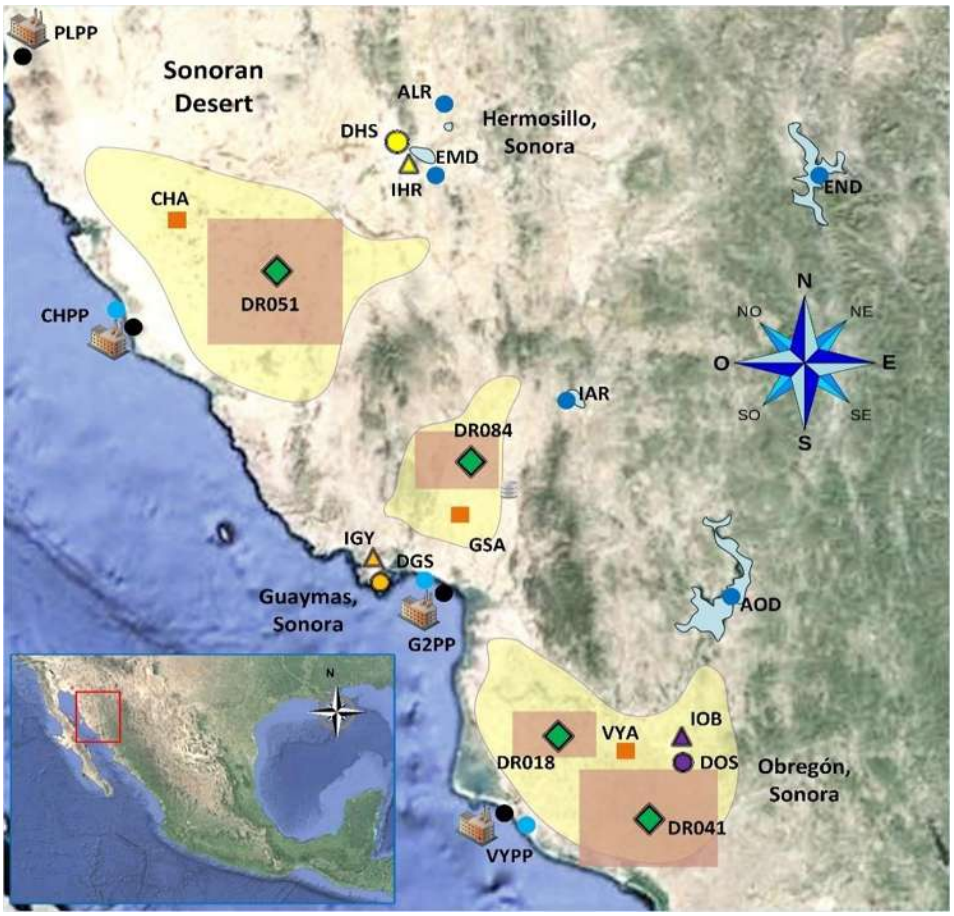

Figure 6.2. Location for the case study.

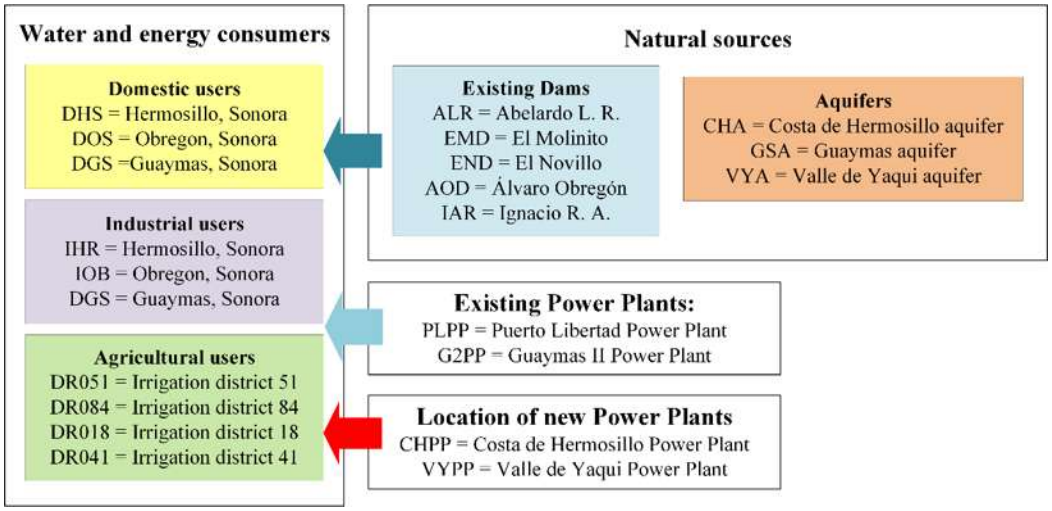

Figure 6.3. Description of the involved users and sources for the case study.

This problem involves the water and electricity demands for three cities, Hermosillo, Guaymas and Obregon in the Mexican state of Sonora. **Figure 6.4** shows the electricity demands for domestic, agricultural and industrial users of the involved cities. Domestic demands have variations through the year with peaks in the hottest months, while industrial and agricultural demands remain constant through the year. **Figure 6.5** shows the water demands for domestic, agricultural and industrial users, in this case, the consumption of water decreases in the hottest months due to the low rainfall, also the consumption of agricultural users depends on the crop as well as the irrigation season though the year. It is worth to notice that in this region there is an irregular distribution of water resources,[54] agriculture spends 93% of total available water, while 5% corresponds to the domestic sector, 1% to the industrial sector and 1% to the livestock sector and others.[55]

In this case, the energy requirements for power and water production (power-desalination plant) can be supplied by the fossil fuels, biofuels, and solar energy. The data for fossil fuels and biofuels are shown in **Table 6.1**, which shows the heating power, overall GHGE, unit costs and the number of jobs generated by each fuel.[56] The generated data are determined indirectly for the production of fossil fuels, biofuels and the operation of the solar collector using the JEDI model (jobs and economic development impact) for quantifying the number of jobs generated per kilojoule produced by each energy source.[57] **Table 6.2** shows the maximum availability in each month for biofuels,[58] which depends on of the availability of biomass in the region. On the other hand, the Sonoran Desert is an attractive location for solar technology, it has high direct normal irradiation (DNI) values as shown in **Figure 6.6**.[59] **Figure 6.6** also shows monthly useful collected energy based on a solar collector efficiency of 55%, in which there are maximum peaks of DNI between May and August. The power-desalination plant is modeled using data obtained from the Qatar Electricity and Water Company report,[60] this company generates 5,432 megawatts and produces 258 million gallons of water per day.

The addressed problem involves three points of view. First, the society requires meeting the demands for water and energy, on the other hand, the environment has been affected by overexploitation of water resources due to the extreme conditions of the region. Finally, the investors prefer to get the economic benefit, no matter the society demands and

the environmental depletion. These conditions lead to the development of different criteria with different levels, or weights, of importance over the objective functions that are showed in **Table 6.3**.

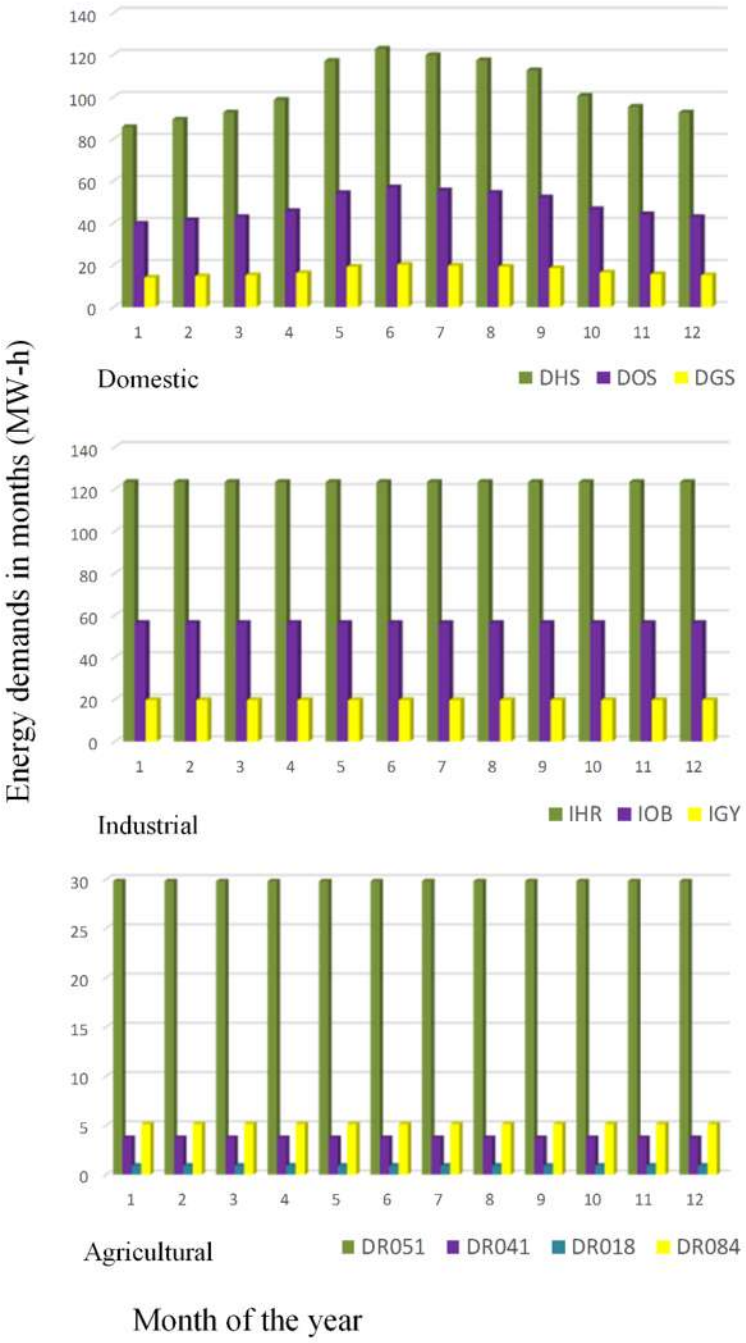

Figure 6.4. Electricity demands of the case study.

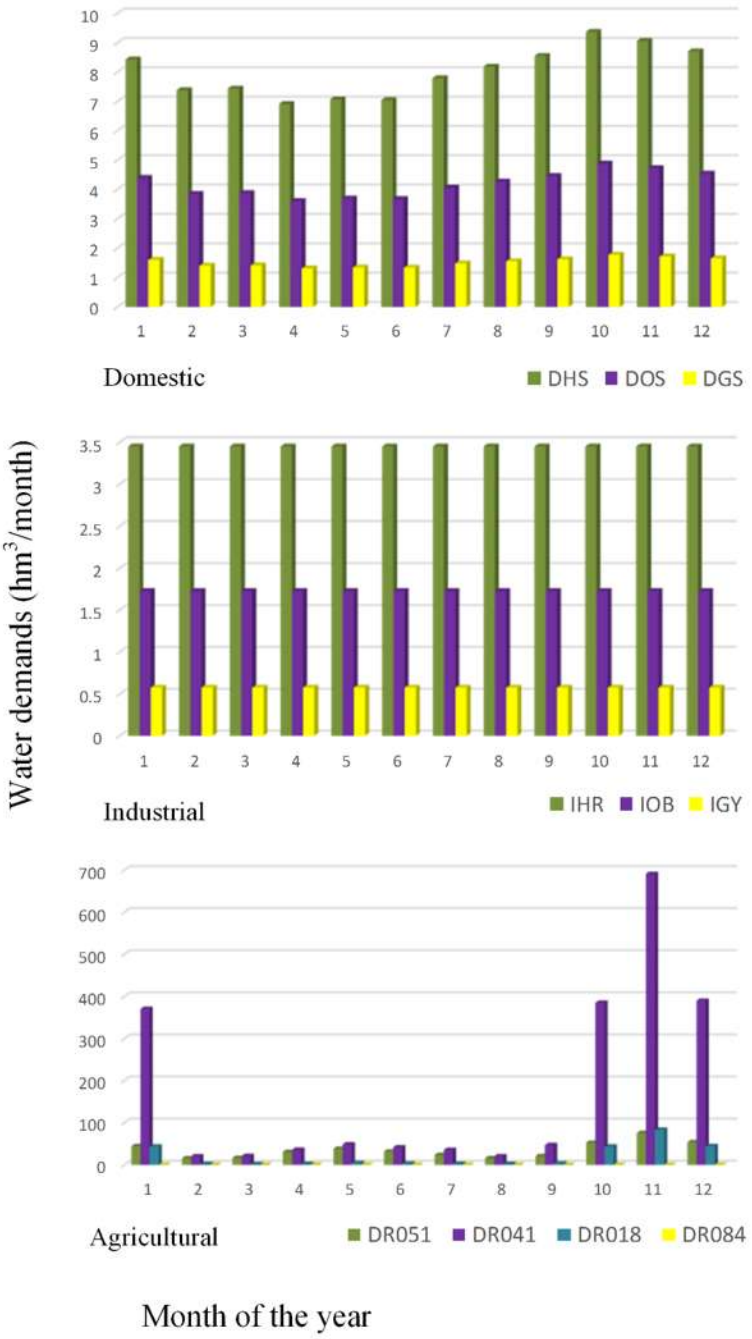

Figure 6.5. Water demands for the case study.

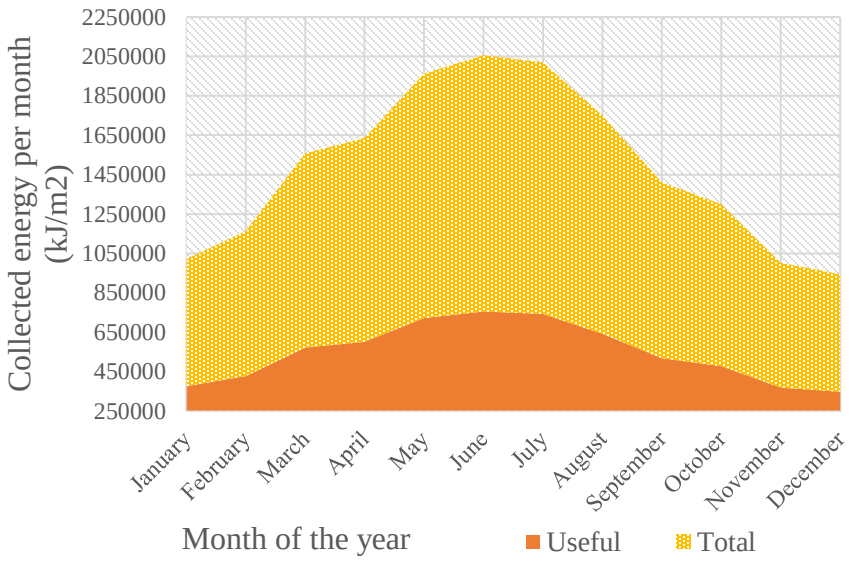

Figure 6.6. Useful collected energy for the case study.[59]

Table 6.1. Data for fossil fuels and biofuels.[57,58]

Fuel	Cost $/MM kJ	Heating Power (kJ/Kg)	Overall GHGE (ton CO_2eq/kJ)	Number of jobs (Jobs/kJ)
Fossil				
Oil	26.195	45,200	8.05408×10^{-8}	1.81677×10^{-11}
Coal	1.741	35,000	2.21357×10^{-8}	1.06281×10^{-11}
Natural gas	2.554	54,000	7.90892×10^{-8}	5.25431×10^{-11}
Biofuels				
Biomass	1.980	17,200	2.44307×10^{-8}	6.6964×10^{-8}
Biogas	7.215	52,000	2.68216×10^{-8}	5.25431×10^{-7}
Biodiesel	30.920	40,200	5.13283×10^{-8}	2.46582×10^{-6}
Bioethanol	13.915	29,600	5.8436×10^{-8}	2.87453×10^{-6}

Table 6.2. Maximum availability of fuels and biofuels (kg/month).[57]

Fuel/Month	Jan	Feb	Mar	Apr	May	Jun	Jul	Aug	Sep	Oct	Nov	Dec
Biomass	10,000	10,000	40,000	50,000	70,000	150,000	100,000	50,000	40,000	40,000	30,000	20,000
Biogas	5,000	5,000	6,000	6,500	6,500	10,000	10,000	10,000	8,000	7,000	6,000	5,000
Biodiesel	5,000	5,500	6,000	7,000	10,000	10,000	10,000	10,000	9,000	8,000	7,000	6,000
Bioethanol	10,000	11,000	12,000	12,000	15,000	15,000	15,000	15,000	14,000	13,000	11,000	10,000

6.4 Results and discussion

The proposed model was coded in the software GAMS and it was solved using the solver BARON.[61] The model consists of 9,724 equations, 10,062 continuous variables, and 720 binary variables, where the average CPU time was 13,116 s in a computer with an i7 Intel core processor at 3.20 GHz and 32 GB of RAM. The model was solved using the multi-stakeholder theory to find the solution that minimizes the dissatisfaction of the involved objective functions. The model involves opposite goals, the economic objective function seeks to maximize the total annual profit, as well as the social objective function which seeks to maximize the number of jobs generated by the project, and on the other hand, the environmental objective function seeks to minimize the overall GHGE.

The electric and water demands for domestic, industrial and agricultural users were met based on the proposed model, taking into consideration the information provided in the case study. Twenty stakeholders with different criteria about the priorities in the design objectives were considered and the results are shown in **Figure 6.7**, and the results for each stakeholder are presented in **Table 6.3**. These criteria reflect the main levels of preference and priorities over the objective functions of the stakeholders involved in the decisions about the design of the system presented. As most of the multi-objective problems, it is possible to show different Pareto optimal solutions exploring the generated Pareto surface, but the main interest is to provide the discussion framework for defining the effects of the priorities, see equation (18), and to propose a compromise solution that reduces the levels of dissatisfaction between all the different stakeholders, in this way is possible to reduce the levels of conflict in the final configuration of the system, see equation (20). The number of stakeholders is defined by the total of decision-makers involved in the conflict and the final decision about the definitive. It means that it is possible to consider just a single actor who defines the priorities of the system or a defined number of criteria. In this case, the twenty stakeholders considered reflecting the main levels of preference over the objective functions.

Figure 6.7 shows the Utopia point (UP), which represents the desired values of the considered objective functions. This UP is located on 46,050 jobs generated by the project, which represents the maximum number of the jobs generated by the project, and also represents the 100% of satisfaction of the social objective. The net profit at the UP is 1660.93

MM$/y, which represents the maximum economic benefit of the project and overall, and represents the 100% of satisfaction of the economic objective, in this point (UP), the GHGE of 1.3551 x10^7 ton CO_2 eq/y are obtained, which are the minimum value of GHGE emitted to the environment, and this point represents the 100% satisfaction of environmental objective.

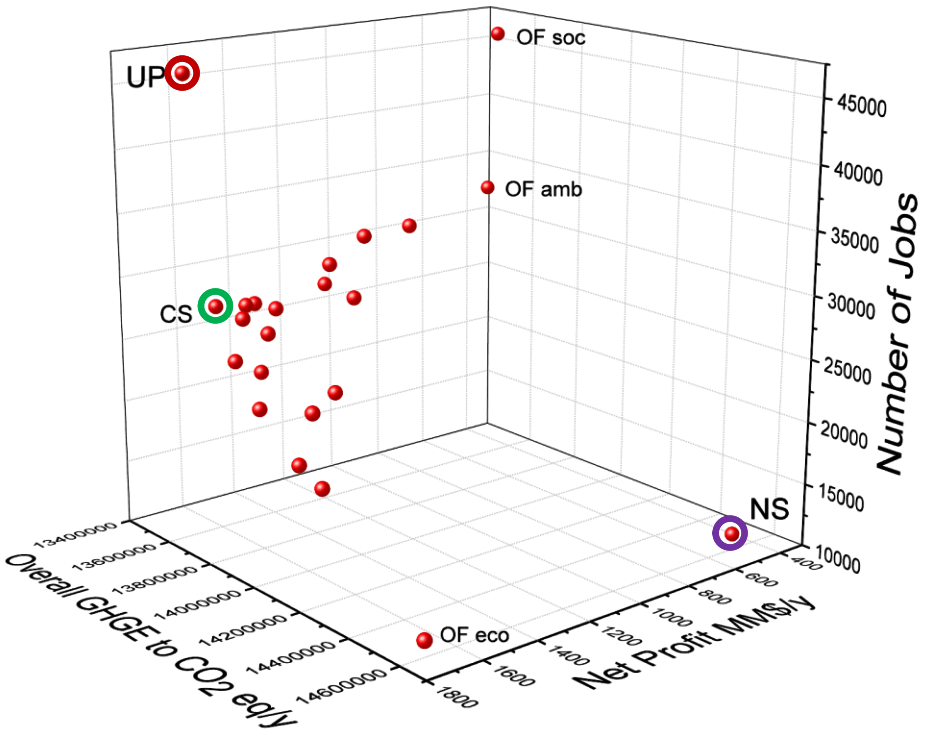

Figure 6.7. Solution for different sets of stakeholders.

It should be noted that the UP is infeasible because is outside of the feasible region, however, it is very important to locate this point because it helps us to obtain the feasible solution which minimizes the dissatisfaction of all stakeholders. The Nadir solution (NS) represents the undesired values of the considered objective functions, it is located on 10,307 jobs, a net profit of 424.27 MM$/y and 1.4544x$10^7$ ton CO_2 eq/y, these three points represent the total dissatisfaction of the involved stakeholders. The compromise solution is denoted as CS and it is located on 28,146 jobs, a total net profit of 1610.936 MM$/y and 1.3609 x$10^7$ ton CO_2 eq/y, this point represent the solution which minimizes the overall dissatisfaction of all stakeholders. Also, it is important to note that almost all the solutions obtained by the proposed stakeholders are around the optimal economic value and the minimum overall

GHGE. In which the profit decreases at the same time that the solar field is installed and the use of biofuels are increased. This means that the number of jobs generated by the project is the variable that is more sensitive to the slight changes in each configuration, this is also supported by the values (*CS-FS*) obtained in **Table 6.3**, where the dissatisfactions of the involved goals increase according to the weight assigned to the social objective. In this case, the social objective is the less favored by the construction of the project.

Table 6.3. Solutions for water and energy distribution network problem.

Stakeholders	w^{eco}	w^{amb}	w^{soc}	OF *eco* (MM$/y)	OF *amb* (ton CO_2 eq/y)	OF *soc* (jobs)	*CS* value	*CS-FS* Dissatisfaction
0	1	1	1	1,660.93	1.3559 x10^7	28,495	0.509	--
1	1	0	0	1,660.93	1.4544 x10^7	10,307	0	0.000747
2	0	1	0	456.20	1.3551 x10^7	33,046	0	0.010889
3	0	0	1	424.27	1.3559 x10^7	46,050	0	0.503714
4	0.33	0.33	0.33	1,460.93	1.3963 x10^7	23,041	0.169	0.170069
5	0.5	0.5	0	1,660.93	1.4039 x10^7	19,046	0.084	0.005818
6	0	0.5	0.5	1,302.27	1.3759 x10^7	31,069	0.256	0.257302
7	0.5	0	0.5	1,660.93	1.4137 x10^7	18,055	0.179	0.252231
8	0.7	0.3	0	1,600.93	1.3869 x10^7	22,081	0.054	0.003790
9	0.3	0.7	0	1,540.93	1.3729 x10^7	23,384	0.074	0.007846
10	0	0.3	0.7	1,300.27	1.3863 x10^7	29,056	0.321	0.355867
11	0.7	0	0.3	1,660.93	1.3762 x10^7	25,055	0.107	0.151637
12	0.3	0	0.7	1,490.93	1.3641 x10^7	28,046	0.251	0.352824
13	0.15	0.7	0.15	1,187.56	1.3664E+07	28,046	0.595	0.083291
14	0.7	0.15	0.15	1,569.23	1.3741E+07	28,632	0.076	0.077713
15	0.15	0.15	0.7	1,025.32	1.3865E+07	33,286	0.283	0.354345
16	0.2	0.2	0.6	1,203.54	1.3841E+07	33,145	0.262	0.304556
17	0.2	0.6	0.2	1,520.36	1.3776E+07	28,632	0.112	0.107426
18	0.6	0.2	0.2	1,660.00	1.3825E+07	28,632	0.102	0.103369
19	0.35	0.35	0.3	1,570.00	1.3896E+07	27,046	0.155	0.155187
20	0.8	0.1	0.1	1,660.21	1.4143E+07	23,511	0.051	0.052058
Utopia point				1,660.93	1.3551 x10^7	46,050	UP	
Nadir solution				424.27	1.4544 x10^7	10,307	NS	
Compromise solution				1,610.01	1.3609 x10^7	28,146	CS	

Is important to note that the social objective (number of jobs) has a high sensitiveness in each configuration, **Figure 6.8** shows the variation of net profit accounting for the fuel prices. Nowadays, fuel prices have high fluctuations during the year, which may affect the net profit of the year, principally natural gas prices.

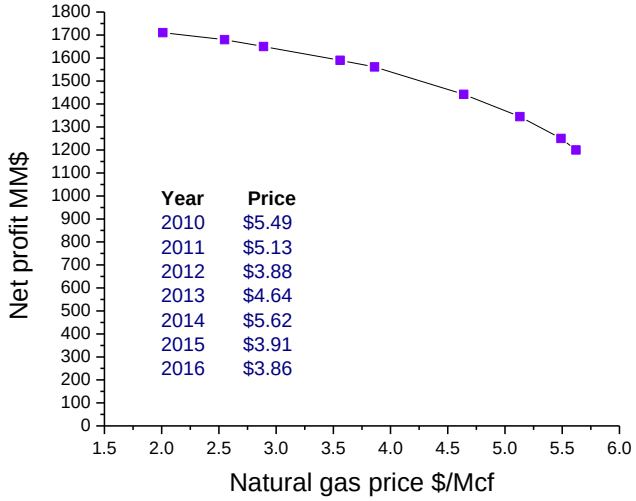

Figure 6.8. Variation of net profit accounting for fuel prices.

Figure 6.9 shows the power and water distribution network for the optimal economic solution (OF eco). This solution represents the 100% of satisfaction to the investors. The figure represents the synthesized power and water network at minimum cost, where there is obtained a net annual profit of 1660.93 MM$/y, with 10,307 jobs generated by the project, and 1.4544 x10^7 ton CO_2 eq/y. In this case, the total amount of water produced in the power-desalination plant is injected to the CHA aquifer. The water demands for domestic and industrial users in Hermosillo city are satisfied by water from the Costa de Hermosillo aquifer as well as water extracted from the EMD and ALD dams, the total amount of water to the DR051 users is extracted from the CHA aquifer. The water demands for Guaymas city are satisfied from the GSA aquifer, while the water demands for DR084 users are satisfied using water from the IAD dam. The water from the END and AOD dams are enough to satisfy the water demands of users of Obregon city as well as the volume of water used by the DR041 and DR018 users. The electricity demands for domestic, industrial and agricultural users are totally fulfilled by the installation of a power-desalination plant with a total capacity of 4,880 MW in Costa de Hermosillo (CHPP) plus the electricity generated in the existing power plants in the region (PLPP and G2PP). In this case, the total energy requirement of the power-desalination plant is satisfied using natural gas as shown in **Figure 6.13a**.

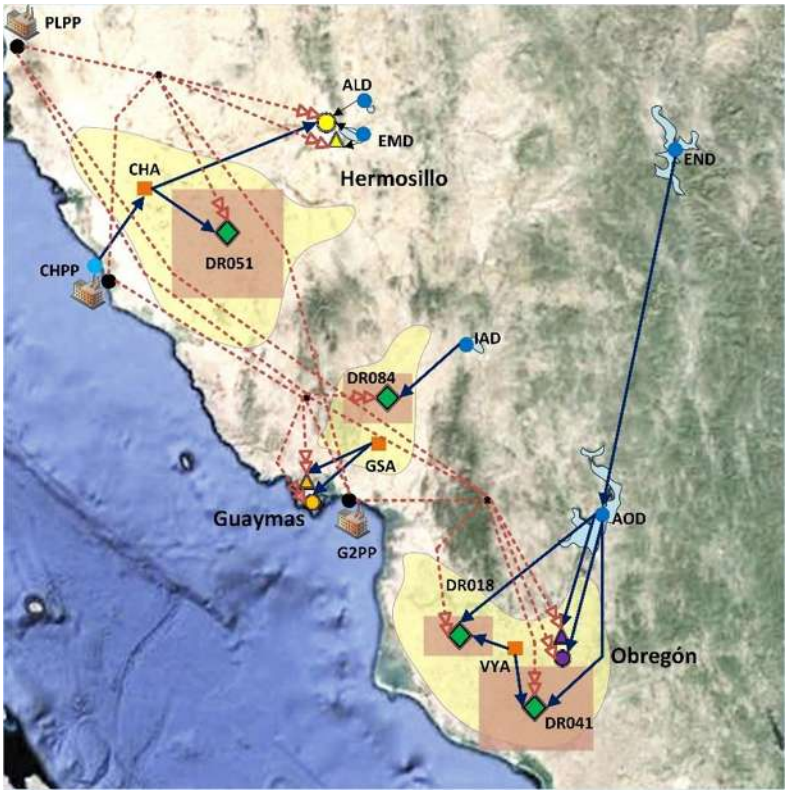

Figure 6.9. Optimal economic solution for the case study.

Figure 6.10 shows the power and water distribution network for the optimal social solution (OF soc). This solution represents the 100% of satisfaction for the inhabitants of the region. In this case, 46,050 jobs are generated, and 1.3559 x10^7 ton CO_2 eq/y are emitted, a total annual profit of 424.27 MM$/y is obtained, this value differs from the optimal economic solution because of the installation of two power-desalination plants, the first one in Costa de Hermosillo (CHPP) with a total capacity of 2,548 MW and the other one in the Valle de Yaqui region (VYPP) with a total capacity of 2,332 MW. The total energy requirement of the power-desalination plant is satisfied using natural gas, biofuels, and solar energy, the fuel consumption profile is shown in **Figure 6.13b**. The results show that the use of biofuels and solar energy increases considerably the number of jobs. On the other hand, the obtained water-energy network satisfies the total demands of the region, however, there are additional pipes to send water to the Hermosillo region from the END dam. These variations have increased the number of jobs generated by the project.

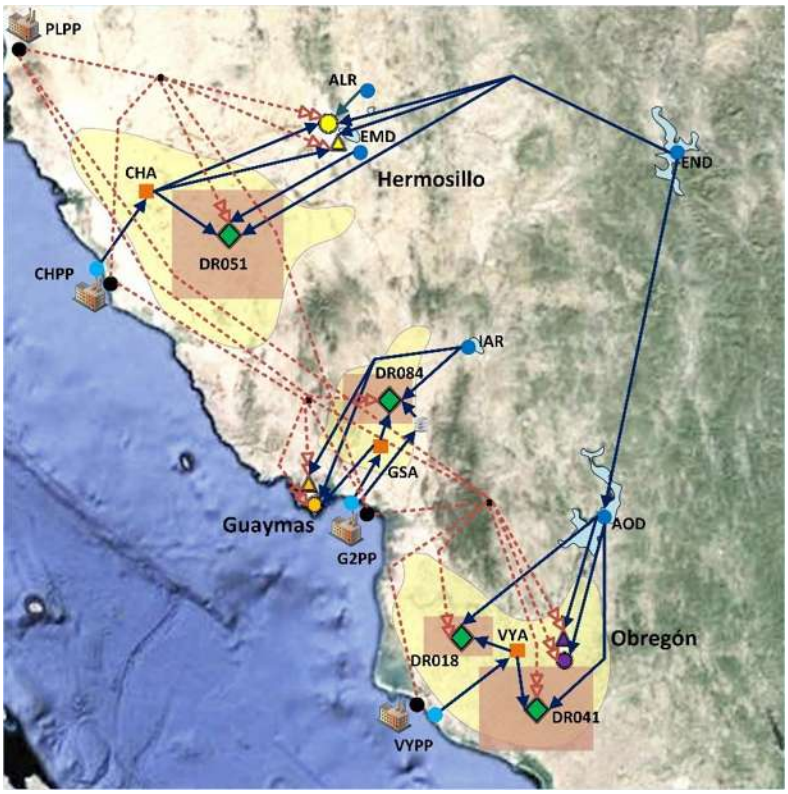

Figure 6.10. Optimal social solution for the case study.

Figure 6.11 shows the water and energy distribution network for the optimal environmental solution (OF amb). This solution represents the optimal solution that minimizes the environmental impact. In this case, a total annual profit of 456.20 MM$/y is obtained and 33,046 jobs are generated, in this case, the emissions of CO2 eq/y are 1.3551 $x10^7$. The water-energy distribution network is similar to the distribution obtained in the optimal economic solution, however, in this case, the maximum solar area and the maximum available biofuels have been used to supply the power-desalination plant, this has reduced the amount of CO_2 eq emitted to the air. The total energy requirement of the power-desalination plant is shown in **Figure 6.13c.**

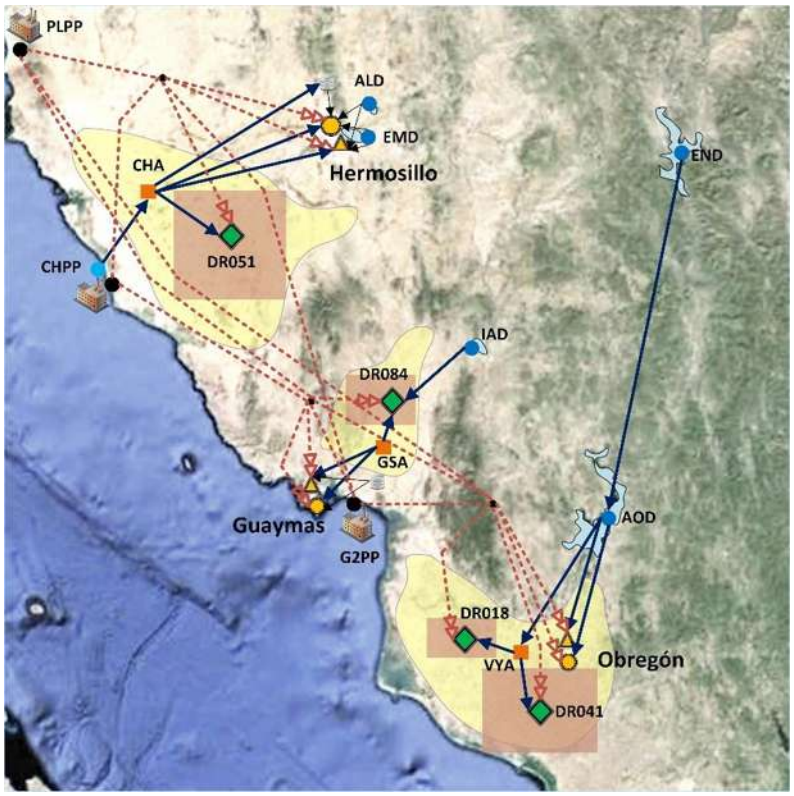

Figure 6.11. Optimal environmental solution for the case study.

Figure 6.12 shows the solution that minimizes the dissatisfaction for the involved objective functions, the water-energy distribution network is similar to the one obtained using the environmental and economic objectives, there are minimal changes in the water distribution network, this is because the solution is closer to the region in the graph (**Figure 6.7**) that represents the minimum GHGE and the maximum net profit. In this case, a total annual profit of 1,489.33 MM$/y is obtained, 26,046 jobs are generated and a total of 1.3679 $x10^7$ ton of CO2 eq/y are emitted, this solution represents a feasible solution on the Pareto curve. The total energy requirement of the power-desalination plant is shown in **Figure 6.13d.**

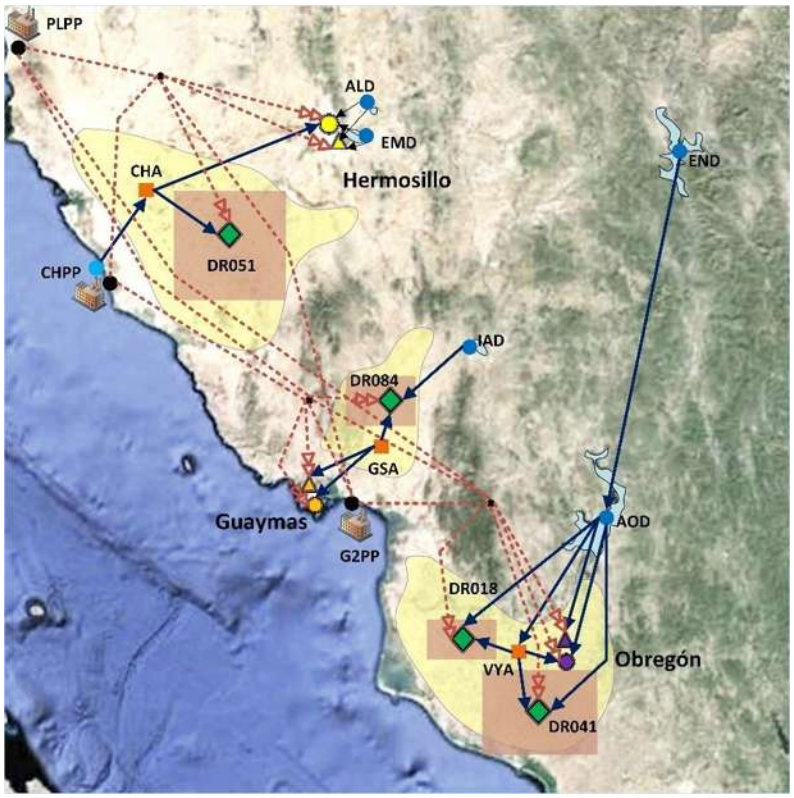

Figure 6.12. Minimization of dissatisfactions for the case study.

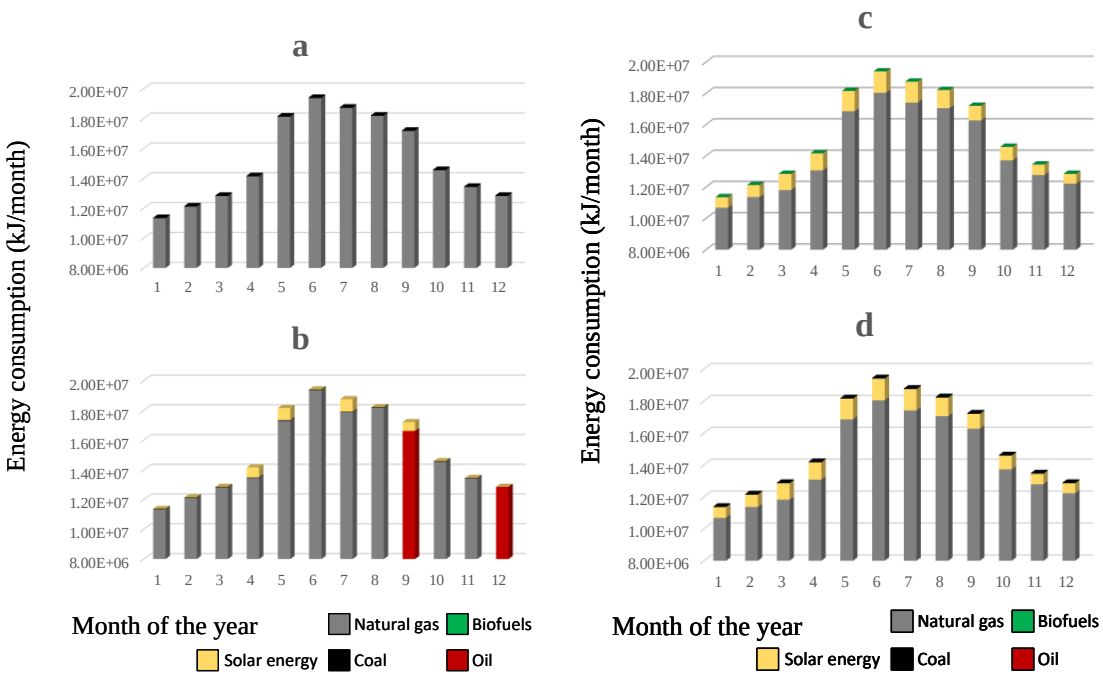

Figure 6.13. Total energy consumption.

6.5 Conclusions

This chapter has presented a method for applying the multi-stakeholder environment into the synthesis of water and energy distribution networks. The considered objectives take into account the economic, environmental and social impacts in the development of operational policies and new facilities. The proposed mathematical model takes into account water and energy demands of a water and energy stressed scheme, in which those demands can be satisfied by the existing natural sources of the region (water content in aquifers and dams) as well as the possibility to produce water and energy by the installation of power-desalination plants. The proposed method identifies the optimal solution that minimizes the dissatisfaction levels of the involved stakeholders. This formulation was applied to the water scarcity problem in the northwest of Mexico (Hermosillo, Guaymas, and Obregon), in which the results show important economic, environmental and social benefits that satisfy the inhabitants of the region, the possible investors and taking into account the environmental impact. It is worth to notice that despite that the objective functions are contradictories, feasible solutions that satisfy the involved stakeholders can be obtained using the proposed method.

6.6 References

1. Griggs, D.; Stafford-Smith, M.; Gaffney, O.; Rockström, J.; Öhman, M. C.; Shyamsundar, P.; Noble, I., Policy: Sustainable development goals for people and planet, *Nature*, 2013, 495 (7441), 305-307.
2. Ibarra-Yunez, A., Energy reform in Mexico: Imperfect unbundling in the electricity sector, *Utilities Policy*, 2015; 35: 19-27.
3. Foley, A. M.; Ó-Gallachóir, B. P.; Hur, J,; Baldick, R.; McKeogh, E. J., A strategic review of electricity systems models, *Energy*, 2010, 35, 4522-4530.
4. Jano-Ito, M. A.; Crawford-Brown, D., Investment decisions considering economic, environmental and social factors: An actors' perspective for the electricity sector of Mexico, *Energy*, 2017, 121, 92-106.
5. Hall, D.; Lobina, E.; Motte, R. D. L., Public resistance to privatization in water and energy, *Development in Practice*, 2005, 15 (3-4), 286-301.
6. Lee, E. J.; Schwab, K. J., Deficiencies in drinking water distribution systems in developing countries, *Journal of Water and Health*, 2005, 3 (2), 109-127.
7. Rogers, P.; De-Silva, R.; Bhatia, R., Water is an economic good: How to use prices to promote equity, efficiency, and sustainability, *Water Policy*, 2002, 4 (1), 1-17.
8. Xia, J.; Zhang, L.; Liu, C.; Yu, J., Towards better water security in North China, *Water Resources Management*, 2007, 21 (1), 233-247.

9. Pereira, L. S.; Oweis, T.; Zairi, A., Irrigation management under water scarcity, *Agricultural Water Management*, 2002, 57 (3), 175-206.
10. Vairavamoorthy, K.; Gorantiwar, S. D.; Pathirana, A., Managing urban water supplies in developing countries–Climate change and water scarcity scenarios, *Physics and Chemistry of the Earth*, Parts A/B/C, 2008, 33(5), 330-339.
11. Worm, G. I. M.; Van der Helm, A. W. C.; Lapikas, T.; Van Schagen, K. M.; Rietveld, L. C., Integration of models, data management, interfaces, and training support in a drinking water treatment plant simulator, *Environmental Modelling and Software*, 2010, 25 (5), 677-683.
12. Islam, N.; Sadiq, R.; Rodriguez, M. J., Optimizing booster chlorination in water distribution networks: a water quality index approach, *Environmental Monitoring and Assessment*, 2013, 185 (10), 8035-8050.
13. Cisty, M., Hybrid genetic algorithm and linear programming method for least-cost design of water distribution systems, *Water Resources Management*, 2010, 24 (1), 1-24.
14. Piratla, K. R.; Ariaratnam, S. T., Criticality analysis of water distribution pipelines, *Journal of Pipeline Systems Engineering and Practice*, 2011, 2 (3), 91-101.
15. Pulido-Calvo, I.; Gutiérrez-Estrada, J. C., Selection and operation of pumping stations of water distribution systems, *Environmental Research Journal*, Nova Science Publishers, 2011, 5 (3), 1-20.
16. Vilanova, M. R. N.; Balestieri, J. A. P., Energy and hydraulic efficiency in conventional water supply systems, *Renewable and Sustainable Energy Reviews*, 2014, 30, 701-714.
17. Venkatesh, G., rattebø, H., Energy consumption, costs, and environmental impacts for urban water cycle services: a case study of Oslo (Norway), *Energy*, 2011, 36 (2), 792-800.
18. De Corte, A.; Sörensen, K., Optimization of gravity-fed water distribution network design: A critical review, *European Journal of Operational Research*, 2013, 228 (1), 1-10.
19. Xue, X.; Schoen, M. E.; Ma, X. C.; Hawkins, T. R.; Ashbolt, N. J.; Cashdollar, J.; Garland, J., Critical insights for a sustainability framework to address integrated community water services: Technical metrics and approaches, *Water Research*, 2015, 77, 155-169.
20. Lim, S. R.; Kim, Y. R.; Woo, S. H.; Park, D.; Park, J. M., System optimization for eco-design by using monetization of environmental impacts: a strategy to convert bi-objective to single-objective problems, *Journal of Cleaner Production*, 2013, 39, 303-311.
21. Xu, Q.; Liu, R,; Chen, Q.; Li, R., Review on water leakage control in distribution networks and the associated environmental benefits, *Journal of Environmental Sciences*, 2014, 26 (5), 955-961.
22. Alcocer-Yamanaka, V. H.; Tzatchkov, V. G.; Arreguin-Cortes, F. I., Modeling of drinking water distribution networks using stochastic demand, *Water Resources Management*, 2012, 26 (7), 1779-1792.
23. Diao, K.; Zhou, Y.; Rauch, W., Automated creation of district metered area boundaries in water distribution systems, *Journal of Water Resources Planning and Management*, 2012, 139 (2), 184-190.

24. Kanta, L.; Zechman, E., Complex adaptive systems framework to assess supply-side and demand-side management for urban water resources, *Journal of Water Resources Planning and Management*, 2013,140 (1), 75-85.
25. Ghosh, S.; Ghoshal, S. P.; Ghosh, S., Optimal sizing, and placement of distributed generation in a network system, *International Journal of Electrical Power and Energy Systems*, 2010, 32 (8), 849-856.
26. Marnay, C.; Lai, J., Serving electricity and heat requirements efficiently and with appropriate energy quality via microgrids, *The Electricity Journal*, 2012, 25 (8), 7-15.
27. Schaber, K.; Steinke, F.; Mühlich, P.; Hamacher, T., Parametric study of variable renewable energy integration in Europe: Advantages and costs of transmission grid extensions, *Energy Policy*, 2012, 42, 498-508.
28. Bracco, S.; Dentici, G.; Siri, S., Economic and environmental optimization model for the design and the operation of a combined heat and power distributed generation system in an urban area, *Energy*, 2013, 55, 1014-1024.
29. Vespucc, M. T.; Innorta, M.; Cervigni, G., A mixed integer linear programming model of a zonal electricity market with a dominant producer, *Energy Economics*, 2013, 35, 35-41.
30. Munir, S. M.; Manan, Z. A.; Alwi, S. R. W., Holistic carbon planning for industrial parks: a waste-to-resources process integration approach, *Journal of Cleaner Production*, 2012, 33, 74-85.
31. Mendoza, J. E.; López, M. E.; Fingerhuth, S. C.; Peña, H. E.; Salinas, C. A., Low voltage distribution planning considering micro-distributed generation, *Electric Power Systems Research*, 2013, 103, 233-240.
32. Yang, J.; Guo, J.; Ma, S., Low-carbon city logistics distribution network design with resource deployment, *Journal of Cleaner Production*, 2016, 119, 223-228.
33. Turconi, R.; Tonini, D.; Nielsen, C. F.; Simonsen, C. G.; Astrup, T., Environmental impacts of future low-carbon electricity systems: detailed life cycle assessment of a Danish case study, *Applied Energy*, 2014, 132, 66-73.
34. Lubega, W. N.; Farid, A. M., Quantitative engineering systems modeling and analysis of the energy–water nexus, *Applied Energy*, 2014, 135, 142-157.
35. Siano, P.; Sarno, D., Assessing the benefits of residential demand response in a real-time distribution energy market, *Applied Energy*, 2016, 161, 533-551.
36. Koirala, B. P.; Koliou, E.; Friege, J.; Hakvoort, R. A.; Herder, P. M., Energetic communities for community energy: A review of key issues and trends shaping integrated community energy systems, *Renewable and Sustainable Energy Reviews*, 2016, 56, 722-744.
37. Bianco, V.; Manca, O.; Nardini, S., Electricity consumption forecasting in Italy using linear regression models, *Energy*, 2009, 34, 1413-1421.
38. Ma, T.; Østergaard, P. A.; Lund, H.; Yang, H.; Lu, L., An energy system model for Hong Kong in 2020, *Energy*, 2014, 68, 301-310.
39. Zhang, Q.; Ishihara, K. N.; Mclellan, B. C.; Tezuka, T., Scenario analysis on future electricity supply and demand in Japan, *Energy*, 2012, 38, 376-385.
40. Lund, H.; Mathiesen, B. V., Energy system analysis of 100% renewable energy systems - The case of Denmark in years 2030 and 2050, *Energy*, 2009, 34, 524-531.
41. Sáfián, F., Modelling the Hungarian energy system - The first step towards sustainable energy planning, *Energy*, 2014, 69, 58-66.

42. Liu, S.; Konstantopoulou, F.; Gikas, P.; Papageorgiou, L. G., A mixed integer optimization approach for integrated water resources management, *Computers and Chemical Engineering*, 2011, 35 (5), 858-875.
43. Atilhan, S.; Linke, P.; Abdel-Wahab, A., A systems integration approach to the design of regional water desalination and supply networks. *International Journal of Process Systems Engineering*, 2011, 1 (2), 125-135.
44. Atilhan, S.; Mahfouz, A; Batchelor, B.; Linke, P.; Abdel-Wahab, A.; Nápoles-Rivera, F.; Jiménez-Gutiérrez, A.; El-Halwagi, M. M., A systems-integration approach to the optimization of macroscopic water desalination and distribution networks: a general framework applied to Qatar's water resources, *Clean Technologies and Environmental Policy*, 2012, 14 (2), 161-171.
45. Diaf, A.; Cherfa, A.; Karadaniz, L.; Tigrine, Z., A technical–economical study of solar desalination, *Desalination*, 2016, 377, 123–127.
46. Fthenakis, V.; Atia, A. A.; Morin, O.; Bkayrat, R.; Sinha, P., New prospects for PV powered water desalination plants: Case studies in Saudi Arabia, *Progress in Photovoltaics: Research and Applications*, 2016, 24, 543-550.
47. Gorjian, S.; Ghobadian, B., Solar desalination: A sustainable solution to water crisis in Iran, *Renewable and Sustainable Energy Reviews*, 2015, 48, 571-584.
48. Alnouri, S. Y.; Linke, P.; El-Halwagi, M. M., A synthesis approach for industrial city water reuse networks considering central and distributed treatment systems, *Journal of Cleaner Production*, 2015, 89, 231-250.
49. Raluy, R. G.; Serra, L.; Uche, J.; Valero, A., Lifecycle assessment of desalination technologies integrated with energy production systems, *Desalination*, 2004, 167, 445-458.
50. González-Bravo, R.; Nápoles-Rivera, F.; Ponce-Ortega, J. M.; El-Halwagi, M. M., Involving integrated seawater desalination-power plants in the optimal design of water distribution networks, Resources, *Conservation and Recycling*, 2015, 104, 181–193.
51. Harrison, J. S.; Wicks, A. C., Stakeholder theory, value, and firm performance, *Business Ethics Quarterly*, 2013, 23 (01), 97-124.
52. Bovaird, T., Attributing outcomes to social policy interventions–'Gold standard' or 'fool's gold' in public policy and management?, *Social Policy and Administration*, 2014, 48 (1), 1-23.
53. Dowling, A. W.; Ruiz-Mercado, G.; Zavala, V. M., A framework for multi-stakeholder decision-making and conflict resolution, *Computers and Chemical Engineering*, 2016, 90, 136-150.
54. CEA, 2008. Sonora State Water Commission. Water Statistics in the State of Sonora. Available at. http://www.ceasonora.gob.mx/archivos/admin/file/Estadisticas Agua_Sonora_ed2008.pdf (Accessed September 2016)
55. CONAGUA, National Water Commission. Statistics on water in Mexico. (2013). Available at. http://www.conagua.gob.mx/CONAGUA07/Noticias/SGP-2-14Web.pdf (Accessed September 2016)
56. Lira-Barragan, L. F.; Ponce-Ortega, J. M.; Serna-González, M.; El-Halwagi, M. M., Optimal design of process energy systems integrating sustainable considerations, *Energy*, 2014, 76, 139-160.

57. Lira-Barragan, L. F.; Ponce-Ortega, J. M,; Serna-González, M.; El-Halwagi, M. M., Sustainable integration of trigeneration systems with heat exchanger networks, *Energy*, 2014, 53, 2732-2750.
58. EIA, U.S., Independent Statics, and Analysis, Energy Information Administration, Washington DC, 2016.
59. NREL, National Solar Radiation Database, National Renewable National Laboratory (U.S. Department of Energy), Washington DC., 2012.
60. QEWC, Qatar Electricity and Water Company Annual Report, Qatar Electricity and Water Company, Doha, Qatar, 2014.
61. Brooke, A.; Kendrick, D.; Meeruas, A.; Raman, R., GAMS-language guide, GAMS Development Corporation, Washington DC, 2016.

List of Tables:

Caption for Figures:

Chapter I

Chapter II

Chapter III

Chapter IV

■Nomenclature Chapter II

Indexes.

i	Hot stream
j	Cold stream
k	Index stage
i'	Subset for hot process streams
j'	Subset for cold process streams
NOK	Total number of stages

Sets.

CS	Cold streams
HS	Hot streams
SN	Stage number
cu	Cold utilities
hu	Hot utilities

Parameters.

B_{wB}	Temperature independent base value for the permeability, kg/(m^2·s·Pa·K$^{1.334}$)
$C_{i,j}^{exc}$	Area cost coefficient for intermediate heat exchangers, \$/m^2
C_{i}^{cu}	Area cost coefficient for cooling utilities, \$/m^2
C_{j}^{hu}	Area cost coefficient for heating utilities, \$/m^2
$C_{F_{i,j,k}}^{exc}$	Unit fixed cost for the heat exchangers between process streams, \$
C_{Fi}^{cu}	Unit fixed cost for coolers, \$
C_{Fj}^{hu}	Unit fixed cost for heaters, \$
C_{F}^{TMD}	Unit capital cost of the membrane, \$/m^2
C_{nm}^{TMD}	Unit non-membrane capital cost, \$/(kg/s)
C_{op}^{TMD}	Unit operating cost for the TMD module, \$/kg
CCU	Unit cost of cold utility, \$/kJ
CHU	Unit cost of hot utility, \$/kJ
Cp_{feed}	Specific heat capacity for the feed stream, kJ/(kg·K)
H_Y	Operating time for the plant per year, s/y
H_i	Fouling heat transfer coefficient for hot stream *i*, kW/(m^2·K)
H_j	Fouling heat transfer coefficient for cold stream *j*, kW/(m^2·K)
H_{cu}	Fouling heat transfer coefficient for cooling utilities, kW/(m^2·K)
H_{hu}	Fouling heat transfer coefficient for heating utilities, kW/(m^2·K)
K_F	Factor used to annualize the capital cost

K_m	Thermal conductivity of the membrane, kW/(m·K)
P_m	Air pressure in the membrane pores, Pa
PM_{NaCl}	Molecular weight for NaCl, g/mol
PM_{wt}	Molecular weight for water, g/mol
$Q_{i,j}^{MAX}$	Upper bound for heat exchanged for match (*i*, *j*), kJ/s
Q_i^{MAX}	Upper bound for heat exchanged for hot streams, kJ/s
Q_j^{MAX}	Upper bound for heat exchanged for cold streams, kJ/s
r	Pore radius, m
R	Universal gas constant, J/mol K
T_{feed}^{S}	Supply temperature of raw water feed stream to TMD, K
T_{bbrine}	Temperature of the brine, K
T_{perm}^{out}	Temperature of the permeate, K
T_i^{OUT}	Target temperature for hot stream, K
T_j^{OUT}	Target temperature for cold stream, K
T_{OUT}^{cu}	Outlet temperature for the cold utility, K
T_{OUT}^{hu}	Outlet temperature for the hot utility, K
V_{perm}	Value per kg of permeate, $/kg
V_{ww}^{Annual}	Income for wastewater treatment, $/kg
V_{ww}	Unit income for waste water treatment, $/kg
W_{ww}	Wastewater flow rate, kg/s
W_{feed}^{raw}	Raw feed flow, kg/s
y_{feed}^{raw}	Mass fraction of impurities in the raw water
y_{brine}	Mass fraction in brine stream
ΔT_{min}	Minimum approach temperature difference, K
$\Delta T_{i,j}^{MAX}$	Upper bound for temperature difference for match (*i*, *j*), K
ΔT_i^{MAX}	Upper bound for temperature difference for hot streams, K
ΔT_j^{MAX}	Upper bound for temperature difference for cold streams, K
δ	Membrane thickness, m
ξ	Water recovery for TMD module
θ	Temperature polarization coefficient
π	3.141516.
τ	Pore tortuosity

Positive variables.

A_m	Membrane area, m^2
AFC^{TMD}	Capital cost for the TMD unit, $
AOC^{TMD}	Operating cost of TMD unit, $/s
b_w	Membrane permeability, kg/(m^2·Pa)
$dt_{i,j,k}$	Temperature approach difference for match (*i*, *j*) at stage *k*, K
dt_i^{cu}	Temperature approach difference for match between hot stream *i* and a cold utility, K
dt_j^{hu}	Temperature approach difference for match between hot stream *j* and a hot utility, K
$deltat$	Temperature difference on both sides of the membrane, K
fCp_i	Heat capacity flow rate for hot stream *i*, kJ/(s·K)
fCp_j	Heat capacity flow rate for cold stream *j*, kJ/(s·K)
j_w	Water flux across the membrane, kg/(m^2·s)
p_{wfeed}^{vap}	Water vapor pressure of the feed, Pa
p_{wperm}^{vap}	Water vapor pressure of the permeate, Pa
$q_{i,j,k}$	Heat exchanged between hot process stream *i* and cold process stream *j* in stage *k*, kJ/s
q_i^{cu}	Heat exchanged between cold utility and hot stream *i*, kJ/s
q_j^{hu}	Heat exchanged between hot utility and hot stream *j*, kJ/s
q_{cond}	Heat lost per unit area of the membrane, kJ/s·m^2
q_{vap}	Rate of heat used in vaporizing the flux per unit area of the membrane, kJ/s·m^2
TAC	Total annual cost, $/y
$t_{i,k}$	Temperature of hot stream *i* at the stage *k*, K
$t_{j,k}$	Temperature of cold stream *j* at the stage *k*, K
t_{bfeed}	Temperature of the feed in the bulk, K
t_{bperm}	Temperature of the permeate in the bulk, K
t_{feed}^{TMD}	Supply temperature of the TMD unit, K
t_m	Average temperature, K
t_{mbrine}	Temperature of the brine at the TMD unit, K
t_{mfeed}	Temperature of the feed at the membrane, K

t_{mperm}	Temperature of the permeate at the membrane, K
t_i^{IN}	Inlet temperature for hot stream *i*, K
$t_{i'}^{IN}$	Inlet temperature for subset of hot process streams *i'*, K
t_i^{OUT}	Outlet temperature for hot stream *i*, K
t_j^{IN}	Inlet temperature for cold stream *j*, K
$t_{j'}^{IN}$	Inlet temperature for subset of cold process streams *j'*, K
t_j^{OUT}	Outlet temperature for cold stream *j*, K
V_{perm}^{Annual}	Annual value of permeate, $/y
w_{brine}^{TMD}	Flow rate of the brine, kg/s
w_{perm}^{TMD}	Flow rate of the permeate, kg/s
w_{feed}^{TMD}	TMD feed flow rate, kg/s
x_{NaCl}	Mole fraction of NaCl in feed
x_{wfeed}	Mole fraction of water in feed
y_{feed}^{TMD}	Mass fraction of the feed in TMD
Δh_{vw}	Latent heat of vaporization for water, kJ/kg
β	Exponent for area cost
φ	Small number
υ	Ratio of recycled reject to raw feed, kg recycled reject/kg raw feed
$\eta_{Conduction}$	Heat loss owing to conduction in the membrane
$\eta_{Thermal}$	Overall thermal efficiency of TMD module
γ_{wfeed}	Activity coefficient of the water in feed

Binary variables.

$z_{i,j,k}$	Binary variables for the existence of intermediate heat exchanger units
z_i^{cu}	Binary variables for the existence of heat exchanger units for the HS
z_j^{hu}	Binary variables for the existence of heat exchanger units for the CS

Free Variables.

$Profit$	Total profit in heat network exchange TMD system, $/y

■Nomenclature Chapter III

Indexes.

i	Units connected in parallel
i'	Subsequent line for i
k	Units connected in series

Parameters.

A_m^{max}	Maximum permissible area in TMD unit, m^2
B_{wB}	Temperature independent base value for the permeability, $kg/(m^2 \cdot s \cdot Pa \cdot K^{1.334})$
C_{F1}^{TMD}	Fixed cost of the TMD module, $\$/m^2$
C_{F2}^{TMD}	Fixed cost of the TMD module, \$/(kg/s)
C_{inst}^{TMD}	Installation cost of the TMD module, $\$/m^2$
C_{Op}^{TMD}	Operational cost of the TMD module, \$
$Cost^{Heating}$	Cost of heat utility, \$/kW
$Cost^{Cooling}$	Cost of cold utility, \$/kW
$Cp_{i,k}^{feed}$	Specific heat capacity for the feed stream, kJ/(kg·K)
$Cp_{i,k}^{rej}$	Specific heat capacity for the rejected stream, kJ/(kg·K)
$Cp_{i,k}^{TMD}$	Specific heat capacity for the stream fed the TMD unit, kJ/(kg·K)
H_Y	Operating hours for the plant per year
K_F	Factor used to annualize the capital cost
PM_{NaCl}	Molecular weight of NaCl
PM_{wt}	Molecular weight of water
TPW^{min}	Minimum amount of total permeate water, kg/s
TPW^{max}	Maximum amount of total permeate water, kg/s
TRW^{min}	Minimum amount of total feed water, kg/s
TRW^{max}	Maximum amount of total feed water, kg/s
T^{amb}	Seawater temperature, K
W^{min}	Minimum amount of feed water flow rate in the TMD unit, kg/s
W^{max}	Maximum amount of feed water flow rate in the TMD unit, kg/s
$z_{i,k}^{perm}$	Mass concentration of permeate
z^{max}	Maximum mass concentration of permeate permissible
$z^{seawater}$	Seawater concentration

Greek symbols

β_k^{TMD}	Exponent for area cost
δ	Membrane thickness, mm

$\xi_{i,k}$ Fraction recovery in TMD unit

Positive variables.

$A_{m_{i,k}}$ Membrane area, m^2

AGP Annual gross profit, $/y

APV Annual permeate value, $/y

$b_{w_{i,k}}$ Membrane permeability, kg/(m^2·Pa)

$f_{i,i',k}$ Flow rate in the subsequent lines, kg/s

$j_{w_{i,k}}$ Water flux across the membrane, kg/(m^2·s)

$k_{m_{i,k}}$ Thermal conductivity of the membrane, kW/(m·K)

$p^{vap}_{wfeed_{i,k}}$ Water vapor pressure of the feed, Pa

$p^{vap}_{wperm_{i.k}}$ Water vapor pressure of the permeate, Pa

$Q^{Heating}_{i,k}$ Heat consumed in the heater unit, kJ/s

$t^{rej}_{i,k}$ Temperature of the concentrate, K

$t^{in}_{i,k}$ Inlet temperature, K

$t^{mix}_{i,k}$ Outlet temperature of the recycle mixer, K

$t_{m_{i,k}}$ Average temperature in TMD unit, K

$t_{mfeed_{i,k}}$ Temperature of the feed at the membrane, K

$t_{mperm_{i,k}}$ Temperature of the permeate at the membrane, K

$t^{perm}_{i,k}$ Temperature of the permeate in the bulk, K

$t^{TMD}_{i,k}$ Feed temperature at bulk in TMD module, K

$THeat$ Total heat consumed, kW

TMA Total membrane area, m^2

TPW Total permeate water, kg/s

TRW Total raw water feed, kg/s

$w^{conc}_{i,k}$ Flow rate of the concentrate, kg/s

$w^{feed}_{i,k}$ Flow rate of the raw feed, kg/s

$w^{perm}_{i,k}$ Flow rate of the permeate, kg/s

$w^{recycle}_{i,k}$ Flow rate of the recycle, kg/s

$w^{rej}_{i,k}$ Flow rate of the rejected flow, kg/s

$w^{TMD}_{i,k}$ Feed flow rate of the TMD unit, kg/s

$x_{wfeed_{i,k}}$ Molar fraction of water in feed

$x_{NaCl_{i,k}}$ Molar fraction of NaCl in feed

$z^{rej}_{i,k}$ Mass concentration in concentrate

$z_{i,k}^{feed}$	Mass concentration in raw feed
$z_{i,k}^{TMD}$	Mass fraction in TMD unit feed
Δh_{vw}	Latent heat of vaporization for water, kJ/kg
$\gamma_{wfeed_{i,k}}$	Activity coefficient of the water in feed
$\theta_{i,k}$	Temperature polarization coefficient
$\eta_{i,k}$	Overall thermal efficiency of TMD module

Binary variables.

$y_{i,k}$	Binary variables for the existence of TMD units

Free Variables.

TAC	Total annual cost, $/y

■Nomenclature Chapter IV

Scripts

b	Biofuel
f	Fossil fuel
i	Hot stream
j	Cold stream
k	Temperature interval
m	Heating utilities
n	Cooling utilities
l	Desalination system

Parameters

$Avail^{max}$	Maximum availability, kg/month
$C^{Fossilfuels}$	Unit cost of fossil fuels, $/kJ
$C^{Biofuels}$	Unit cost of biofuels, $/kJ
C^{Solar}	Cost of solar collector, $/y
Cp_i	Specific heat capacity for hot stream, kJ/(kg·K)
Cp_j	Specific heat capacity for cold stream, kJ/(kg·K)
Cp_m	Specific heat capacity for hot utility, kJ/(kg·K)
Cp_n	Specific heat capacity for cold utility, kJ/(kg·K)
COP	Coefficient of performance
CuCST	Unit cost of cold utility, $/J
D_t	Time conversion factor, s/month
ECST	Electricity cost, $/kW
Ga^{Power}	Gains for selling power, $/kW
GHGE	Unitary greenhouse gas emissions, ton CO_2 eq/kJ
H_Y	Operating hours for the plant per year, h/y
$Heating^{Power}$	Heating power, kJ/kg
HUCST	Unit cost of hot utility, $/J
K_F	Factor used to annualize the capital cost, 1/y
MEDFC	Fixed cost for MED process, $/y
MEDVC	Variable cost for MED Process, $/y
MSFFC	Fixed cost for MSF process, $/y
MSFVC	Variable cost for MSF process, $/y
PPCost	Power production cost, $/kW
$QHCMAX_{i,j}$	Upper bound for heat exchanged for match (*i*, *j*), kJ/s
$QHWMAX_{i,n}$	Upper bound for heat exchanged for hot streams, kJ/s
$QSCMAX_{j,m}$	Upper bound for heat exchanged for cold streams, kJ/s
R	Unit tax credit reduction factor, $/kJ
ROFC	Fixed cost for RO module, $/y
ROVC	Variable cost for RO module, $/y
SuP^{Power}	Unitary price for the power, $/kW
$T_{i,k}^{out,int}$	Outlet temperature for hot stream *i* in interval *k*, K

$T_{j,k}^{out,int}$	Outlet temperature for cold stream *j* in interval *k*, K
$T_{m,k}^{out,int}$	Outlet temperature for hot utility *m* in interval *k*, K
$T_{n,k}^{out,int}$	Outlet temperature for cold utility *n* in interval *k*, K
$T_{i,k}^{in,int}$	Inlet temperature for hot stream *i* in interval *k*, K
$T_{j,k}^{in,int}$	Inlet temperature for cold stream *j* in interval *k*, K
$T_{m,k}^{in,int}$	Inlet temperature for hot utility *m* in interval *k*, K
$T_{n,k}^{in,int}$	Inlet temperature for cold utility *n* in interval *k*, K
TFW^{max}	Maximum fresh water demand, kg/s
TFW^{min}	Minimum fresh water demand, kg/s
TMDFC	Fixed cost for TMD module, $/y
TMDVC	Variable cost for TMD module, $/y
VCFC	Fixed cost for VC process, $/y
VCVC	Variable cost for VC process, $/y
W_l^{min}	Minimum raw feed flow, kg/s
X	Mass fraction of NaCl in feed
β	Exponent for area cost
ϕ	Recycle ratio
κ	Electric power consumption factor
θ	Desalination system recovery fraction
μ	Efficiency factor

Positive variables

A^{Solar}	Solar collector area, m^2
CaC	Capital cost for HEN, $/y
EDesTotal	Total electric consumption by the desalination system, kW
EPCMSF	Electric power consumption in MSF, kW
EPCMED	Electric power consumption in MED, kW
EPCRO	Electric power consumption in RO, kW
EPCTMD	Electric power consumption in TMD, kW
EPCVC	Electric power consumption in VC, kW
ESC	Energy sources cost for HEN, $/y
$f_{i,k}$	Flow rate of hot stream *i* in interval *k*, kg/s
$f_{j,k}$	Flow rate of cold stream *j* in interval *k*, kg/s
$f_{m,k}$	Flow rate of hot utility *m* in interval *k*, kg/s
$f_{n,k}$	Flow rate of cold utility *n* in interval *k*, kg/s
f_{MEDc}	Flow rate of cold stream in MED unit, kg/s
f_{MEDh}	Flow rate of hot stream in MED unit, kg/s
f_{MSFc}	Flow rate of cold stream in MSF unit, kg/s
f_{MSFh}	Flow rate of hot stream in MSF unit, kg/s
f_{ROc}	Flow rate of cold stream in RO module, kg/s
f_{ROh}	Flow rate of hot stream in RO module, kg/s
f_{TMDc}	Flow rate of cold stream in TMD module, kg/s
f_{TMDh}	Flow rate of hot stream in TMD module, kg/s
f_{VCc}	Flow rate of cold stream in VC unit, kg/s
f_{VCh}	Flow rate of hot stream in VC unit, kg/s
FiC	Fixed cost for HEN, $/y
MEDUC	Cost of MED desalination system, $/y

MSFUC	Cost of MSF desalination system, $/y
NJOB	Unitary number of jobs generated, jobs/kJ
OC	Operating cost for HEN, $/y
Power	Power output, kW
q	Heat transferred in the heat exchanger units, kJ/s
$q_{i,j,k}$	Heat exchanged between hot stream i and cold stream j in interval k, kJ/s
$q_{i,n,k}^{CU}$	Heat exchanged between cold utility and hot stream i in interval k, kJ/s
$q_{j,m,k}^{HU}$	Heat exchanged between hot utility and cold stream j in interval k, kJ/s
$q_{i,k}^{HS}$	Heat available in hot stream i over any temperature interval k, kJ/s
$q_{m,k}^{RO}$	Heat utility required in interval k, kJ/s
$q_{j,k}^{CS}$	Heat required by cold streams j in interval k, kJ/s
Q	Heat exchanged between the energy subsystems in HEN, kJ/s
$Q^{External}$	Total energy from external sources, kJ/s
Q^{Useful_Solar}	Useful solar energy, kJ/m^2 month
ROUC	Cost of RO desalination system, $/y
RSP	Revenues coming from selling power, $/y
$r_{i,k}$	Residual heat of a hot stream i in interval k, kJ/s
$r_{m,k}$	Residual heat of hot utility m in interval k, kJ/s
T_{IN}	Inlet temperature, °C
T_{OUT}	Outlet temperature, °C
TAC	Total annual cost of the desalination system, $/y
TCR	Tax credit reduction, $/y
TFW	Total fresh water produced, kg/s
$THL_{m,k}$	Total heat load from hot utilities in interval k, kJ/s
$THR_{n,k}$	Total heat required from cold utilities in interval k, kJ/s
TMDUC	Cost of TMD desalination system, $/y
TRW	Total rejected brine, kg/s
TSW	Total seawater fed, kg/s
TUC	Total utility cost, $/y
VCUC	Cost of VC desalination system, $/y
x	Mass fraction of salt content

Binary variables

$y_{i,j}$	Binary variables for match between i and j
$y_{i,n}$	Binary variables for match between i and n
$y_{i,m}$	Binary variables for match between j and m
Z_1	Binary variables for the existence of desalination units

Free variables

NGHGE	Greenhouse gas emissions, ton CO_2 eq/y
NJOBS	Number of jobs generated, jobs
Profit	Total annual profit, $/y
SUNITS	Number of units in the in the heat integration
SDESAL	Number of units in the desalination network

■Nomenclature Chapter V

Subscripts

b	Biofuels
f	Fossil fuels
g	Location of agricultural users
i	Existing aquifer
j	Deep wells
n	Location of existing power-desalination plants
o	Location of industrial users
p	Location of existing water storage tanks
q	Possible location of new water storage tanks
r	Location of domestic users
t	Distribution time in months
u	Possible location of new power-desalination plants
x	Existing dam as natural resources

Positive variable

$a_{i,j,t}^{dw}$	Water sent to the deep wells from aquifers, m^3 $x10^6$/year
$Annual\ Profit$	Annual profit from water sales, \$ $x10^6$
$AREA_u^{solar,max}$	Maximum effective solar collector area, m^2
$A_{u,t}^{solar}$	Effective solar collector area, m^2
$b_{n,t}^{E,rej}$	Water sent to the sea as reject from existing power-desalination plants, m^3 $x10^6$/year
$b_{u,t}^{N,rej}$	Water sent to the sea as reject from new power-desalination plants, m^3 $x10^6$/year
$B_{n,i,t}^{E,des}$	Water received from existing power-desalination plants, m^3 $x10^6$/year
$B_{u,i,t}^{N,des}$	Water received from new power-desalination plants, m^3 $x10^6$/year
$d_{r,j,t}^{dom}$	Water distributed in central stations from deep wells (domestic), m^3 $x10^6$/year
$d_{g,j,t}^{agr}$	Water distributed in central stations from deep wells (agricultural), m^3 $x10^6$/year
$d_{o,j,t}^{ind}$	Water distributed in central stations from deep wells (industrial), m^3 $x10^6$/year
$D_{n,p,t}^{E,Esto}$	Water received in storage tanks from existing power-desalination plants, m^3 $x10^6$/year
$D_{u,p,t}^{N,Esto}$	Water received in storage tanks from new power-desalination plants, m^3 $x10^6$/year

$E_{r,t}^{dom}$	Energy demand by domestic users, kW x10^6
$E_{g,t}^{agr}$	Energy demand by agricultural users, kW x10^6
$E_{o,t}^{ind}$	Energy demand by industrial users, kW x10^6
$EnergySales$	Energy sales from power-desalination plants, $ x10^6
$Eproduction_{n,t}^{E}$	Energy produced in existing power-desalination plants, kW x10^6
$TEPDopcost$	Total operational cost for existing power-desalination plants, $ x10^6
$Eproduction_{u,t}^{N}$	Energy produced in new power-desalination plants, kW x10^6
$F_{i,t}^{agr}$	Aquifer recharge from agricultural users, m^3 x10^6/year
F_{CO_2}	Amount of GHGE emitted in the dual purpose power plant, ton of CO_2 eq.
$G_{n,x,t}^{E,rel}$	Water received in dams from existing power-desalination plants, m^3 x10^6/year
$G_{u,x,t}^{N,rel}$	Water received in dams from new power-desalination plants, m^3 x10^6/year
$h_{r,t}^{dom}$	Water in domestic central station, m^3 x10^6/year
$h_{g,t}^{agr}$	Water in agricultural central station, m^3 x10^6/year
$h_{o,t}^{ind}$	Water in industrial central station, m^3 x10^6/year
H_Y	Operating hours for the plant per year, h/year
$InstCost_{q}^{sto}$	Storage installation cost, $ x10^6
$InstCost_{u}^{pdes}$	Installation cost (new power-desalination plants), $ x10^6
K_F	Factor used to annualize the inversion, $year^{-1}$
$M_{x,t}$	Water in dam, m^3 x10^6/year
$NPDinstcost$	Installation cost for new power-desalination plants, $ x10^6
$NPDopcost$	Operational cost for new power-desalination plants, $ x10^6
$OpCost_{u,t}^{pdes}$	Operational cost (new power-desalination plants), $ x10^6
$TOpCost_{n,t}^{E,des}$	Total operational cost (existing power-desalination plants), $ x10^6
pca	Percentage of water that seeps into the ground
$PipingCost$	Piping cost, $ x10^6
$PumpingCost$	Pumping cost, $ x10^6
Q	Heat, kJx10^6/year
$R_{i,t}^{aq}$	Natural recharge of water, m^3x10^6/year
$SolarCost$	Total solar collector cost, $ x10^6
$SCCost_{u}^{solar}$	Capital cost of solar collector, $ x10^6
$SOCost_{u,t}^{solar}$	Operating cost of solar collector, $ x10^6
$s_{p,i,t}^{E,aq}$	Water received from existing storage tanks, m^3 x10^6/year
$s_{q,i,t}^{N,aq}$	Water received from new storage tanks, m^3 x10^6/year
$s_{p,r,t}^{E,dom}$	Water received from existing storage tanks (domestic), m^3 x10^6/year

$s_{q,r,t}^{N,dom}$ Water received from new storage tanks (domestic), m^3 x10^6/year

$s_{g,p,t}^{E,agr}$ Water received from existing storage tanks (agricultural), m^3 x10^6/year

$s_{g,q,t}^{N,agr}$ Water received from new storage tanks (agricultural), m^3 x10^6/year

$s_{o,p,t}^{E,ind}$ Water received from existing storage tanks (industrial), m^3 x10^6/year

$s_{o,q,t}^{N,ind}$ Water received from new storage tanks (industrial), m^3 x10^6/year

$S_{p,t}^{E}$ Water in existing storage tanks, m^3 x10^6/year

$S_{q,t}^{N}$ Water in new storage tanks, m^3 x10^6/year

S_{q}^{max} Maximum storage value, m^3 x10^6

$StorageCost$ Storage cost, \$ x10^6

SW_{u}^{max} Maximum seawater consumption, m^3 x10^6/year

$SW_{n,t}^{in,E}$ The total water extracted from the sea for existing power-desalination plants, m^3 x10^6/year

$SW_{u,t}^{in,N}$ The total water extracted from the sea for new power-desalination plants, m^3 x10^6/year

TAC Total annual cost, \$ x10^6

TEC^{N} Total energy cost, \$ x10^6

$TEnergy_{t}$ Total energy produced, kW x10^6

$TER_{u,t}$ Total energy requirement, kJ x10^6

TRC Tax credit reduction, \$ x10^6

$v_{r,n,t}^{E,dom}$ Water received in central stations from existing power-desalination plants (domestic), m^3 x10^6/year

$v_{g,n,t}^{E,agr}$ Water received in central stations from existing power-desalination plants (agricultural), m^3 x10^6/year

$v_{o,n,t}^{E,ind}$ Water received in central stations from existing power-desalination plants (industrial), m^3 x10^6/year

$v_{r,u,t}^{N,dom}$ Water received in central stations from new power-desalination plants (domestic), m^3 x10^6/year

$v_{g,u,t}^{N,agr}$ Water received in central stations from new power-desalination plants (agricultural), m^3 x10^6/year

$v_{o,u,t}^{N,ind}$ Water received in central stations from new power-desalination plants (domestic), m^3 x10^6/year

$Water\ Sales$ Water sales from power-desalination plants, \$ x10^6

$W_{i,t}^{aq}$ Water in aquifer, m^3 x10^6/year

$w_{r,x,t}^{dom}$ Water received in central stations from dams (domestic), m^3 x10^6/year

$w_{g,x,t}^{agr}$ Water received in central stations from dams (agricultural), m^3 x10^6/year

$w_{o,x,t}^{ind}$ Water received in central stations from dams (industrial), m^3 x10^6/year

Parameters

AEC_t	Agricultural energy cost, \$ $x10^6$/kW $x10^6$
APC	Agricultural piping cost, \$ $x10^6/m^3$ $x10^6$
AQP	Deep well piping cost, \$ $x10^6$/ $x10^6$ m^3
$agrdem_{g,t}$	Water requirements of agricultural users, m^3/year
$ATot^{min}$	Minimum available area of solar collector, m^2
$ATot^{min}$	Maximum available area of solar collector, m^2
AVF^{max}	Maximum amount available for fossil fuels, kg $x10^6$/month
AVB^{max}	Maximum amount available for biofuels, kg $x10^6$/month
BPC	Aquifer recharge piping cost, \$ $x10^6$/ $x10^6 m^3$
BFC	Biofuel cost, \$ $x10^6$/ kJ$x10^6$
DEC_t	Unit domestic energy cost, \$ $x10^6$/kW $x10^6$
DPC	Unit domestic piping cost, \$ $x10^6/m^3$ $x10^6$
$domdem_{r,t}$	Water requirements of domestic users, m^3/year
EPC	Storage recharge piping cost (existing P-D plant), \$ $x10^6$/ $x10^6 m^3$
FCF	Fuel consumption factor, kJ $x10^6/m^3$ $x10^6$
FFC	Fossil fuel cost, \$ $x10^6$/ kJ$x10^6$
GEP	Energy generation factor, kW $x10^6/m^3$ $x10^6$
GPC	Unit dam recharge piping cost, \$ $x10^6$/ $x10^6 m^3$
HPF_f	Heating power for fossil fuels, kJ $x10^6$/kg $x10^6$
HPB_b	Heating power for biofuels, kJ $x10^6$/kg $x10^6$
IEC_t	Unit industrial energy cost, \$ $x10^6$/kW $x10^6$
IPC	Unit industrial piping cost, \$ $x10^6$/ $x10^6 m^3$
$inddem_{o,t}$	Water requirements of industrial users, m^3/year
NPC	Unit storage recharge piping cost (new power-desalination plant), \$ $x10^6$/ $x10^6 m^3$
PPA	Unit agricultural pumping cost, \$ $x10^6/m^3$ $x10^6$
PAQ	Unit deep well pumping cost, \$ $x10^6/m^3$ $x10^6$
PPC	Unit aquifer recharge pumping cost, \$ $x10^6/m^3$ $x10^6$
PPD	Unit domestic pumping cost, \$ $x10^6/m^3$ $x10^6$
PPE	Unit storage recharge piping cost (existing power-desalination plant), \$ $x10^6/m^3$ $x10^6$
PPG	Unit dam recharge pumping cost, \$ $x10^6/m^3$ $x10^6$
PPI	Unit industrial pumping cost, \$ $x10^6/m^3$ $x10^6$
PPN	Unit storage recharge piping cost (new power-desalination plants), \$ $x10^6/m^3$ $x10^6$
PPS	Unit storage pumping cost, \$ $x10^6/m^3$ $x10^6$
R_{tax}	Tax credit for CO_2, \$ $x10^6$/ton of CO_2 eq.
SPC	Unit storage piping cost, \$ $x10^6$/ $x10^6 m^3$
$SW_{u,t}^{N,max}$	Maximum value of seawater extracted from the sea, m^3 $x10^6$/year

$TF'^{REF}_{CO_2}$ Total GHGE when only fossil fuels are used, ton of CO_2 eq.

$UCE^{solar}_{u,t}$ Useful collected energy, kJ $x10^6/m^2$ month

WAC_t Unit cost of water for agricultural use, \$ $x10^6/m^3$ $x10^6$

WDC_t Unit cost of water for domestic use, \$ $x10^6/m^3$ $x10^6$

WIC_t Unit cost of water for industrial use, \$ $x10^6/m^3$ $x10^6$

Z_1 Unit fixed cost of the tank, \$ $x10^6$

Z_2 Unit fixed cost of the tank, \$ $x10^6$

Z_3 Unit fixed cost of new power-desalination plants, \$ $x10^6$

Z_4 Unit fixed cost of new power-desalination plants, \$ $x10^6$

Z_5 Unit fixed cost of new power-desalination plants, \$ $x10^6$

Z_6 Unit fixed cost of new power-desalination plants, \$ $x10^6$

Z^{solar} Unitary cost of solar collector, \$ $x10^6$

α Economic scale factor

β Reject factor of power-desalination plants

$\Theta^{sto,max}_q$ Maximum capacity of the tank, m^3 $x10^6$

$\Theta^{sto,min}_q$ Minimum capacity of the tank, m^3 $x10^6$

$\Theta^{pdes,max}_u$ Maximum capacity of new power-desalination plants, m^3 $x10^6$/year

$\Theta^{pdes,min}_u$ Minimum capacity of the new power-desalination plants, m^3 $x10^6$/year

Binary variables

w^{solar}_u Existence of a solar collector

y^{sto}_q Existence of a storage tanks

y^{pdes}_u Existence of power-desalination plants

■Nomenclature Chapter V

Subscripts

b	Biofuels
f	Fossil fuels
g	Location of agricultural users
i	Existing aquifer
j	Deep wells
n	Location of existing power-desalination plants
o	Location of industrial users
p	Location of existing water storage tanks
q	Possible location of new water storage tanks
r	Location of domestic users
t	Distribution time in months
u	Possible location of new power-desalination plants
x	Existing dam as natural resources
k	Number of stakeholders

Positive variable

$Annual\ Profit$	Annual profit from water sales, \$ x10^6
$A_{u,t}^{solar}$	Effective solar collector area, m^2
AF	Average solution
CS	Compromise solution
$E_{r,t}^{dom}$	Energy demand by domestic users, kW x10^6
$E_{g,t}^{agr}$	Energy demand by agricultural users, kW x10^6
$E_{o,t}^{ind}$	Energy demand by industrial users, kW x10^6
$EnergySales$	Energy sales from power-desalination plants, \$ x10^6
FS	Stakeholder solution
$h_{r,t}^{dom}$	Water in domestic central station, m^3 x10^6/year
$h_{g,t}^{agr}$	Water in agricultural central station, m^3 x10^6/year
$h_{o,t}^{ind}$	Water in industrial central station, m^3 x10^6/year
H_Y	Operating hours for the plant per year, h/year
$ONJobs$	Total number of jobs
$OGHGE$	Overall greenhouse gas emissions, ton CO_2 eq/y x10^7
Q	Heat, kJx10^6/year
$s_{p,r,t}^{E,dom}$	Water received from existing storage tanks (domestic), m^3 x10^6/year
$s_{q,r,t}^{N,dom}$	Water received from new storage tanks (domestic), m^3 x10^6/year

$s_{g,p,t}^{E,agr}$	Water received from existing storage tanks (agricultural), m^3 $x10^6$/year
$s_{g,q,t}^{N,agr}$	Water received from new storage tanks (agricultural), m^3 $x10^6$/year
$s_{o,p,t}^{E,ind}$	Water received from existing storage tanks (industrial), m^3 $x10^6$/year
$s_{o,q,t}^{N,ind}$	Water received from new storage tanks (industrial), m^3 $x10^6$/year
TAC	Total annual cost, \$ $x10^6$
TRC	Tax credit reduction, \$ $x10^6$
Water Sales	Water sales from power-desalination plants, \$ $x10^6$
φ	Normalized economic function
ψ	Normalized social function
τ	Normalized objective function

Parameters

AEC_t	Agricultural energy cost, \$ $x10^6$/kW $x10^6$
AVF^{max}	Maximum amount available for fossil fuels, kg $x10^6$/month
AVB^{max}	Maximum amount available for biofuels, kg $x10^6$/month
DEC_t	Unit domestic energy cost, \$ $x10^6$/kW $x10^6$
GHGE	Greenhouse gas emission factor, ton CO_2 eq/y/ kJ $x10^6$
HPF_f	Heating power for fossil fuels, kJ $x10^6$/kg $x10^6$
HPB_b	Heating power for biofuels, kJ $x10^6$/kg $x10^6$
IEC_t	Unit industrial energy cost, \$ $x10^6$/kW $x10^6$
NJOB	Factor for number of jobs, jobs/kW$x10^6$
$UCE_{u,t}^{solar}$	Useful collected energy, kJ $x10^6$/m^2 month
w	Stakeholder weight factor
WAC_t	Unit cost of water for agricultural use, \$ $x10^6$/m^3 $x10^6$
WDC_t	Unit cost of water for domestic use, \$ $x10^6$/m^3 $x10^6$
WIC_t	Unit cost of water for industrial use, \$ $x10^6$/m^3 $x10^6$